AD_____

Award Number:  W81XWH-07-1-0FÍÎ

TITLE: Væ‡*^cǎ*ÁÞ^˘¦[]ǎ‚ÏË/‡‚ÁÚ¦[•ææ^ÁÔæ‚&^¦ÁÓ[}^ÁT^ææææ‹ã

PRINCIPAL INVESTIGATOR:  Ö¦ĚÁÖæˇ‡‚*ÁÝ˘

CONTRACTING ORGANIZATION:  Ò[¦¦^ÁW}ã̃^¦•ã̂
OE‡‡æ}‡æ‚ĚÁÕOEÁH€HGGÁ

REPORT DATE:  Œ}¦ã̃ÁG€FF

TYPE OF REPORT:  Øã̇æ‡

PREPARED FOR:  U.S. Army Medical Research and Materiel Command
Fort Detrick, Maryland  21702-5012

DISTRIBUTION STATEMENT:  Approved for public release; distribution unlimited

The views, opinions and/or findings contained in this report are those of the author(s) and should not be construed as an official Department of the Army position, policy or decision unless so designated by other documentation.

# REPORT DOCUMENTATION PAGE

*Form Approved*
*OMB No. 0704-0188*

| 1. REPORT DATE *(DD-MM-YYYY)* 01-04-2011 | 2. REPORT TYPE Final | 3. DATES COVERED *(From - To)* 1 APR 2007 - 31 MAR 2011 |
|---|---|---|
| **4. TITLE AND SUBTITLE** Targeting Neuropilin-1 in Prostate Cancer Bone Metastasis | | **5a. CONTRACT NUMBER** |
| | | **5b. GRANT NUMBER** W81XWH-07-1-0156 |
| | | **5c. PROGRAM ELEMENT NUMBER** |
| **6. AUTHOR(S)** Dr. Daqing Wu  E-Mail: dwu2@emory.edu | | **5d. PROJECT NUMBER** |
| | | **5e. TASK NUMBER** |
| | | **5f. WORK UNIT NUMBER** |
| **7. PERFORMING ORGANIZATION NAME(S) AND ADDRESS(ES)** Emory University Atlanta, GA 30322 | | **8. PERFORMING ORGANIZATION REPORT NUMBER** |
| **9. SPONSORING / MONITORING AGENCY NAME(S) AND ADDRESS(ES)** U.S. Army Medical Research and Materiel Command Fort Detrick, Maryland 21702-5012 | | **10. SPONSOR/MONITOR'S ACRONYM(S)** |
| | | **11. SPONSOR/MONITOR'S REPORT NUMBER(S)** |

**12. DISTRIBUTION / AVAILABILITY STATEMENT**
Approved for Public Release; Distribution Unlimited

**13. SUPPLEMENTARY NOTES**

**14. ABSTRACT**
Abstract on next page.

**15. SUBJECT TERMS**

prostate cancer, bone metastasis, neuropilin-1, CREB, VEGF, c-Met, Stat3, Mcl-1

| 16. SECURITY CLASSIFICATION OF: | | | 17. LIMITATION OF ABSTRACT | 18. NUMBER OF PAGES | 19a. NAME OF RESPONSIBLE PERSON USAMRMC |
|---|---|---|---|---|---|
| **a. REPORT** U | **b. ABSTRACT** U | **c. THIS PAGE** U | UU | 195 | **19b. TELEPHONE NUMBER** *(include area code)* |

Standard Form 298 (Rev. 8-98)
Prescribed by ANSI Std. Z39.18

# 14. ABSTRACT

The role of neuropilin-1 (NRP1) in the progression of human prostate cancer (PCa) remains unclear. This New Investigator Award is to investigate the signaling mechanism and targeting potential of NRP1 in PCa bone metastasis. During the entire period of award performance, we accomplished three major tasks: 1) Molecular mechanism of NRP1 signaling in bone metastatic PCa cells. We elucidated a novel signaling mechanism by which bone metastatic PCa cells acquire survival advantages through the induction of VEGF via a CREB-HIF-1-dependent pathway, which subsequently activates autocrine signaling by inducing NRP1-c-MET signaling and upregulates Mcl-1 expression via Stat3. We identified Mcl-1 as a convergent molecular target of VEGF and PDGF signaling in bone metastatic PCa cells. 2) Clinical significance of NRP1 signaling components in human PCa bone metastasis. We validated the clinical importance of our findings in human PCa bone metastasis. Expression of the key signaling components, including p-CREB, VEGF, NRP1, p-c-MET and Mcl-1, was found to be significantly associated with PCa bone metastasis. 3) Targeting NRP1 signaling in bone metastatic PCa cells. We explored the targeting potential of the NRP1-Mcl-1 signaling pathway in treating PCa bone metastasis. Several strategies (including siRNA, shRNA, monoclonal antibody and small molecule agents) were developed to effectively induce apoptosis and tumor regression in pre-clinical models of PCa metastasis.

This project has resulted in 6 peer-reviewed publications, 1 manuscript under review and 3 meeting abstracts.

**Table of Contents**

## Introduction

Overexpression of neuropilin-1 (NRP1), a "co-receptor" of vascular endothelial growth factor (VEGF), has been implicated in the progression of prostate cancer (PCa) and other solid tumors. However, the signaling mechanism of NRP1 in cancer cells lacking the "classic" receptors (VEGFRs), and the clinical significance of NRP1 signaling in PCa, remain largely unknown. This New Investigator Award is to investigate the signaling mechanism and targeting potential of NRP1 in PCa bone metastasis. Three tasks are proposed:

1) To investigate a crucial role of NRP1 signaling in the survival of bone metastatic PCa cells;

2) To evaluate the clinical significance of NRP1 signaling in human PCa bone metastasis;

3) To explore therapeutic strategies for interrupting the NRP1 signaling to inhibit PCa growth and colonization in bone.

Our major findings and accomplishments during the entire funding period are described in detail below.

## Body

### A. Molecular mechanism of NRP1 signaling in bone metastatic PCa cells

**In this task, we characterized the regulatory mechanism for VEGF expression, and NRP1-mediated VEGF signaling components in PCa cells. We demonstrated that: 1) cAMP-responsive element-binding protein (CREB) is a novel regulator of VEGF expression in bone metastatic PCa cells. CREB may regulate VEGF transcription via a hypoxia-inducible factor-1α (HIF-1α)-dependent mechanism in normoxic conditions. 2) VEGF-NRP1 signaling confers PCa cells resistance to apoptosis and supports tumor growth by inducing expression of myeloid cell leukemia-1 (Mcl-1) via c-MET-dependent activation of Src kinases and signal transducers and activators of transcription 3 (Stat3).**

1. Elucidation of a novel regulatory mechanism for VEGF expression in bone metastatic PCa cells

We elucidated a novel signaling mechanism by which bone metastatic PCa cells acquire survival advantages through the induction of VEGF via a CREB-HIF-1-dependent pathway.

*1.1. CREB activation is associated with bone metastatic potential and EMT in PCa cells*

We used a human PCa ARCaP progression model with epithelial-to-mesenchymal transition (EMT) properties to investigate the roles of CREB in PCa bone metastasis. An ARCaP subclone, ARCaP$_E$, has a relatively low propensity for bone metastasis (12.5%) after intracardiac injection, whereas ARCaP$_M$, a bone metastatic derivative of ARCaP closely associated with ARCaP$_E$, has dramatically greater bone metastatic potential (100%) and significantly shorter latency.
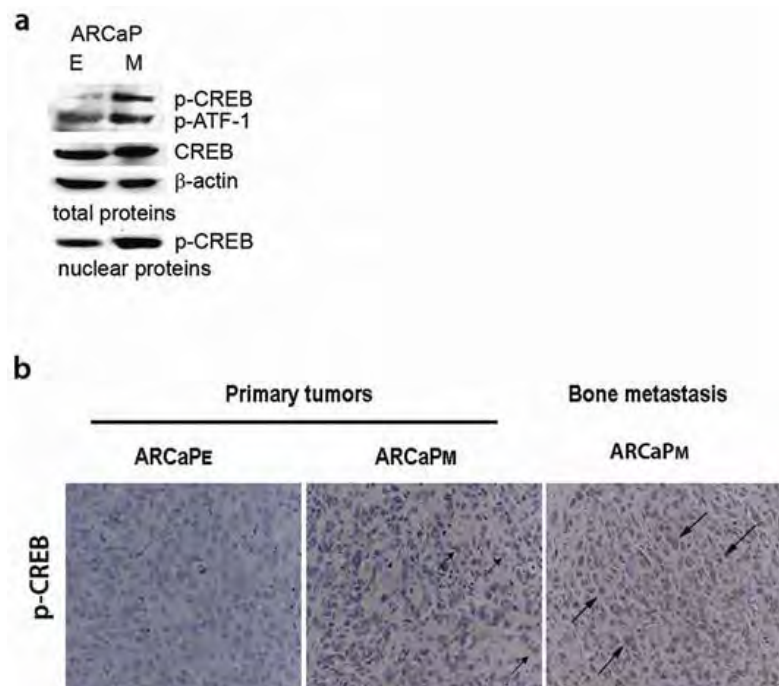


**Figure 1. CREB phosphorylation is associated with bone-metastatic potential and EMT.** a) Western blot analysis demonstrated increased expression of p-CREB in whole-cell lysates and nuclear portions of ARCaPM cells. b) IHC staining of p-CREB increased in primary tumor specimens of ARCaPM and increased further in ARCaPM bone metastatic tissue specimens.

Western blot analysis (Fig.1a) showed a slight increase in CREB expression in ARCaP$_M$ total lysates, with significantly elevated activated CREB. Phosphorylation of CREB (p-CREB) proteins was more abundant in the ARCaP$_M$ nucleus, indicating activation of CREB-dependent transcription. The association of p-CREB expression with increased bone metastatic potential was confirmed in tumor tissues from ARCaP primary and bone metastasis specimens (Fig.1b).

## 1.2. Activation of CREB induces VEGF transcription in ARCaP cells

We examined differential expression of VEGF transcripts in normoxic ARCaP cells. Reverse transcription-PCR (RT-PCR) analysis showed elevated endogenous mRNA levels of both VEGF$_{121}$ and VEGF$_{165}$ in ARCaP$_M$ cells (Fig.2a). ELISA of ARCaP conditioned medium (CM) confirmed a 2-fold increase in total VEGF secretion by ARCaPM when compared to ARCaP$_E$ cells (Fig.2b), indicating that VEGF upregulation occurred in normoxic PCa cells and this increased secretion may be associated with EMT and the invasiveness of PCa cells.
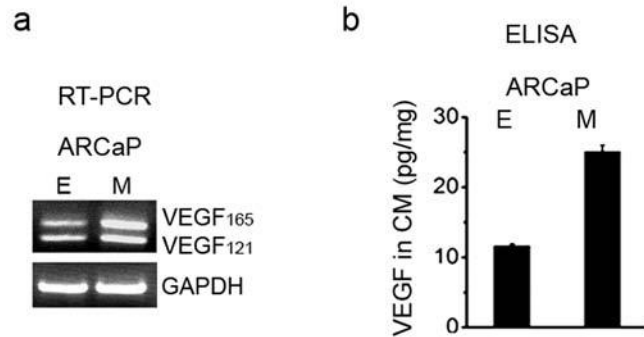


**Figure 2. VEGF up-regulation is associated with bone-metastatic potential and EMT.** (a) Expression of VEGF isoforms VEGF165 and VEGF121 was increased in ARCaPM cells in normoxia. (b) VEGF secretion increased in ARCaPM CM ($p < 0.01$). Relative VEGF levels were normalized by dividing VEGF concentrations (pg/ml) by total protein concentrations (mg/ml) in CM.

Pharmacological and gene transfer experiments in ARCaPE cells explored whether CREB activation is responsible for VEGF expression in PCa cells. Treatment with adenylate cyclase activator forskolin (FSK) rapidly increased VEGF mRNA levels, with more significant induction of VEGF$_{165}$ than VEGF$_{121}$ (Fig.3a). Conversely, a PKA selective inhibitor, H89, reduced VEGF mRNA levels. VEGF ELISA in ARCaP$_E$ CM confirmed these results; VEGF secretion was induced by FSK and inhibited by H89 (Fig.3b). VEGF expression may be controlled by PKA-CREB signaling in normoxic PCa cells.

ARCaP$_E$ cells were transiently transfected with expression vectors for wild-type CREB (WTCREB), a dominant negative mutant of CREB (KCREB), using empty vector (pCMV) as the control. KCREB forms an inactive dimer with CREB, blocking its ability to bind cAMP-response element (CRE) without interfering with CREB phosphorylation. Western blot analysis confirmed



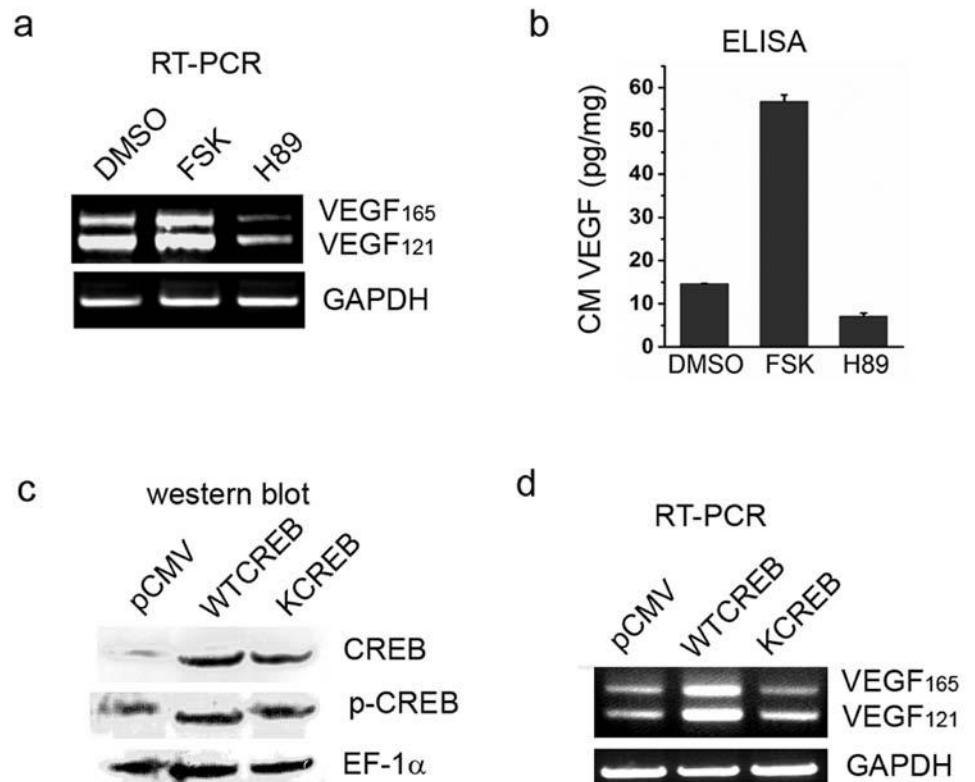**Figure 3. CREB regulates VEGF transcription in ARCaP cells.** (a) FSK treatment (10 μM; 4 h) induced and H89 (5 μM) inhibited VEGF transcription in ARCaPE cells. (b) FSK treatment (2 d) induced and H89 inhibited VEGF secretion in ARCaPE CM. (c) Transient expression (72 h) of pCMV (vector), WTCREB or KCREB in ARCaPE cells. (d) Ectopic expression (72 h) of WTCREB induced and KCREB inhibited VEGF transcription in ARCaPE cells.

expression of WTCREB or KCREB. p-CREB expression was significantly higher in WTCREB-transfected ARCaP$_E$ cells and slightly increased in KCREB-transfected cells (Fig.3c). RT-PCR analysis showed that mRNA levels of VEGF$_{165}$ and VEGF$_{121}$ were remarkably enhanced by WTCREB but inhibited by KCREB (Fig.3d), suggesting that CREB could regulate VEGF transcription in ARCaP cells.

*1.3. HIF-1α is required for CREB regulation of VEGF in ARCaP cells*

We investigated whether p-CREB directly interacts with putative CRE site(s) within VEGF promoter to regulate VEGF transcription. We performed computational analysis on the 5'-flanking sequence of the human VEGF gene and identified a putative CRE site was located about 5 kb upstream from the transcriptional start site, with one base variation (TGAGGTCA) (Fig.4a). We used a pVEGF-KpnI plasmid for a reporter assay, with a 2.65 kb fragment of VEGF promoter including a 47-bp HRE sequence (-985 to -939 bp) but not the putative CRE motif (Fig.4a). Luciferase activity showed that WTCREB increased and KCREB inhibited VEGF reporter activity (Fig.4b), confirming that CREB induces VEGF transcription in normoxic PCa cells and suggesting the putative CRE site may be dispensable for CREB induction of VEGF.



**Figure 4. HIF-1α is required for CREB regulation of VEGF transcription in normoxia.** (a) Schematic description of the human VEGF 5'-flanking region. The locations of HRE and a putative CRE site are shown relative to the transcriptional initiation site in human VEGF gene. (b) pVEGF-KpnI reporter activity was induced by transient expression (48 h) of WTCREB but inhibited by KCREB in ARCaPE cells. (c) HIF-1α expression was increased in total lysates and nucleus of ARCaPM cells. (d) HIF-1α siRNA transfection (48 h) reduced HIF-1α expression in ARCaPE cells. FSK (10 µM; 2 h) induced VEGF transcription in ARCaPE cells transfected with control siRNA (48 h), but not in HIF-1α siRNA-treated cells.

CREB may rely on HIF-1α to regulate VEGF expression in PCa cells, since higher basal HIF-1α expression was found in ARCaP$_M$ cells compared to normoxic ARCaP$_E$ cells (Fig.4c). ARCaP$_M$ also expresses more p-CREB and VEGF (Fig.1a, Fig.2). HIF-1α small interfering RNA (siRNA) experiments tested whether HIF-1α-dependent gene transcription is involved in CREB regulation of VEGF transcription. HIF-1α siRNA inhibited endogenous HIF-1α expression in ARCaP$_E$ cells. FSK could stimulate VEGF transcription in control- siRNA- but not HIF-1α-siRNA-transfected ARCaP$_E$ cells (Fig.4d). These data suggest that HIF-1α and CREB activation are essential to promote VEGF expression in PCa cells.
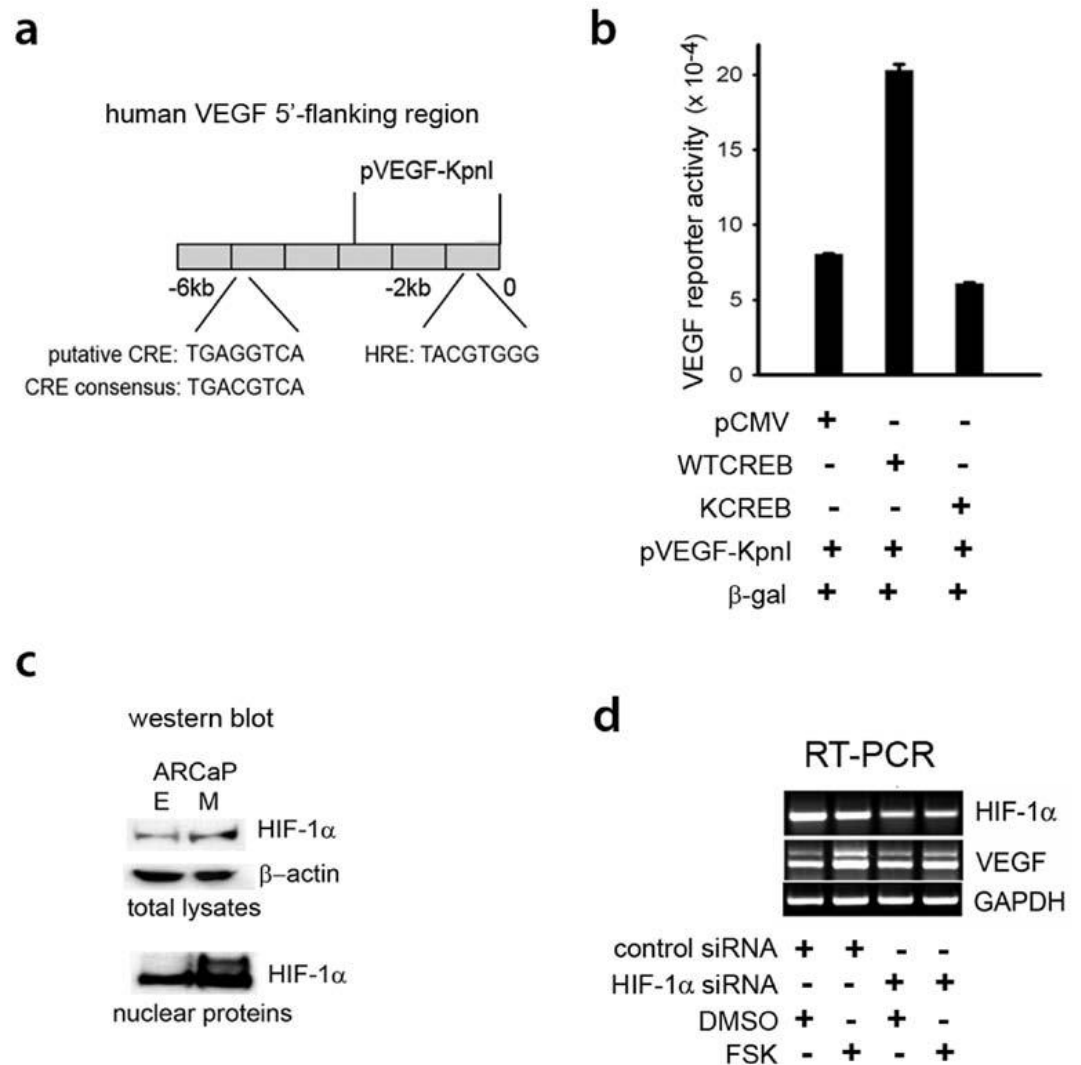
## 1.4. Activation of CREB recruits HIF-1α and facilitates its binding to VEGF promoter region

To examine whether activated CREB induced intracellular translocation of HIF-1α, ARCaP$_E$ nuclear proteins were extracted after FSK treatment (10 µM) at various time periods. Western blot analysis showed dynamic changes in expression of several CREB-interacting transcription factors in the nucleus (Fig.5a). CREB activation seems to be accompanied by a dynamic change in nuclear accumulation of HIF-1α, CBP and p300, which may form a transcriptional complex induced by hypoxia or FSK to regulate VEGF promoter activity and HIF-1α-dependent transcription.

To determine whether CREB activation induces HIF-1α binding to HRE, we used ELISA to quantify HIF-1α activation and binding to HRE in ARCaP$_E$ cells (Fig.5b). The data suggest that CREB activation by FSK induced specific interaction between the ARCaP$_E$ nuclear transcription complex which comprised of CREB/HIF-1α and the HRE consensus.

We investigated whether CREB activation promoted specific binding of HIF-1α to VEGF promoter by chromatin immunoprecipitation (ChIP) assay. Activation of CREB signaling by FSK showed a considerable increase in HIF-1α binding with the HRE region in ARCaP$_E$ cells, but not in KCREB-transfected ARCaP$_E$ cells (Fig.5c), demonstrating that CREB activation facilitates association of HIF-1α with VEGF promoter. Further supporting this model, HIF-1α reporter activity was significantly induced in WTCREB-transfected, but not in KCREB-transfected cells in the pHIF1-luc reporter assay (Fig.5d).



**Figure 5. Activation of CREB may induce a HIF-1α-dependent transcriptional complex on VEGF promoter.** (a) FSK (10 µM) induced rapid nuclear translocation of p-CREB, HIF-1α, CBP and p300 in ARCaPE cells. (b) Transcription factor ELISA assay demonstrated that FSK (10 µM) induced specific binding of ARCaPE nuclear extracts to the HRE consensus in a time-dependent manner, which was inhibited by wild-type HRE oligonucleotide, but not by mutated oligonucleotide. *COS nu .prot:* CoCl2-treated COS-7 nuclear extract (5µg); *wt. oligo*: wile-type HRE consensus; *mut. oligo*: mutated HRE consensus; *nu. prot*: ARCaPE nuclear proteins. (c) ChIP assay demonstrated that FSK treatment (10 µM) induced specific binding of HIF-1α to the HRE site within the VEGF promoter in ARCaPE cells, but not in KCREB-transfected cells. (d) Transient expression of WTCREB induced, but KCREB inhibited, HIF-1α reporter activity in ARCaPE cells.

**In summary, these results elucidated a novel regulatory mechanism of VEGF expression in bone metastatic PCa cells (Fig.6). This signaling pathway was independently supported by our other studies in PCa and renal cancer cells.** For detailed description, please refer to our publications (1-3) (Appendices 1-3).

## 2. Elucidation of NRP1 downstream signaling in bone metastatic PCa cells

We elucidated a novel mechanism by which VEGF regulates Mcl-1 expression through NRP1-dependent activation of c-MET signaling, which may contribute to PCa bone metastasis.
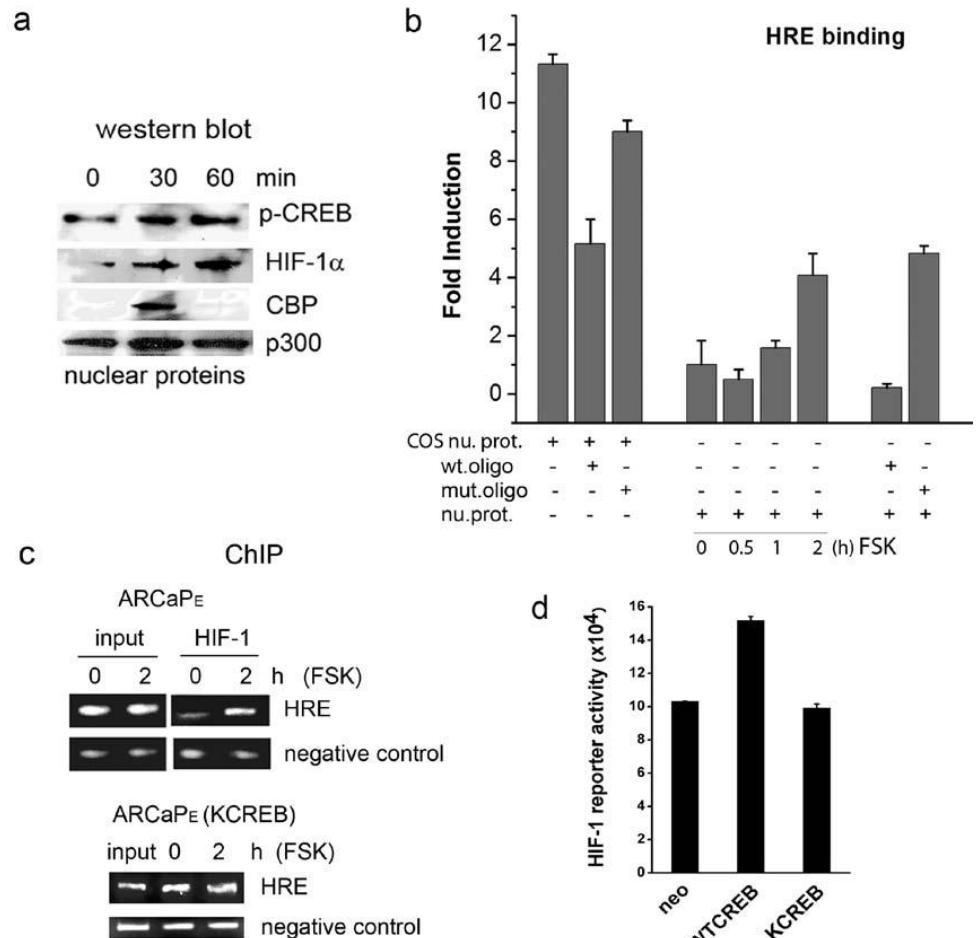
## 2.1. Mcl-1 is a survival factor in human PCa cells

We developed a new model for the study of PCa bone metastasis. The ARCaP$_M$-C2 subclone, derived from metastatic bone tissues after two rounds of intracardiac injection of ARCaP$_M$ cells in athymic mice, forms predictable metastases to bone, adrenal gland and other soft tissue with higher propensity and shorter latency (Fig. 7a). RT-PCR and immunoblotting analyses found that Mcl-1 was substantially expressed by ARCaP$_M$ cells, and further increased in ARCaP$_M$-C2 cells (Fig. 7b). Similarly, increased Mcl-1 expression was observed in metastatic C4-2 and C4-2B cells when compared to their parental, androgen-dependent human PCa cell line LNCaP. These results suggested a possible association between Mcl-1 expression and invasive phenotypes of PCa cells.



**Figure 6. Proposed model for CREB regulation of VEGF expression.** CBP or p300 may be scaffold proteins for p-CREB and HIF-1$\alpha$ to form a transcriptional complex on VEGF promoter in response to CREB activation (Wu et al., Oncogene, 2007).

To examine the function of Mcl-1 in PCa cell survival, a Mcl-1 siRNA was transfected into ARCaP$_M$ cells. siRNA treatment effectively inhibited Mcl-1 expression and significantly reduced cell viability by ~36% after 72h (Fig. 7c). Annexin V staining by fluorescence-activated cell sorting (FACS) analysis showed that the Mcl-1 siRNA induced apoptosis in 24.4±2.3% of ARCaP$_M$ cells (Fig.7d). These results indicated that Mcl-1 may be an important survival factor in PCa cells.

## 2.2. VEGF regulates Mcl-1 expression in human PCa cells

RT-PCR assay that could differentiate mRNA expression of VEGF$_{165}$ and VEGF$_{121}$ isoforms was performed in ARCaP$_M$ and ARCaP$_M$-C2 cells, showing a significant increase in the expression of both VEGF isoforms in ARCaP$_M$-C2 cells, as confirmed at protein level by ELISA. Similarly, C4-2 cells express higher levels of VEGF when compared to LNCaP cells (Fig.8a). These data suggested that VEGF expression is elevated in metastatic PCa cells.

Intriguingly, VEGF$_{165}$ was found to rapidly induce Mcl-1 mRNA expression in a dose- and time-dependent manner, with the maximum accumulation of Mcl-1 mRNA after 2 h-incubation at the concentration of 10 ng/ml. Western blot analysis confirmed a remarkable increase of Mcl-1 protein in ARCaP$_M$ cells and LNCaP cells treated with VEGF$_{165}$ (Fig.8b). Conversely, when ARCaP$_M$ cells were transfected with a VEGF siRNA nucleotide that selectively inhibited expression of VEGF$_{165}$ but not VEGF$_{121}$, expression of Mcl-1, but not Bcl-2, was reduced after 72 h (Fig. 8c). These results indicated that VEGF$_{165}$ may specifically regulate Mcl-1 expression in PCa cells.
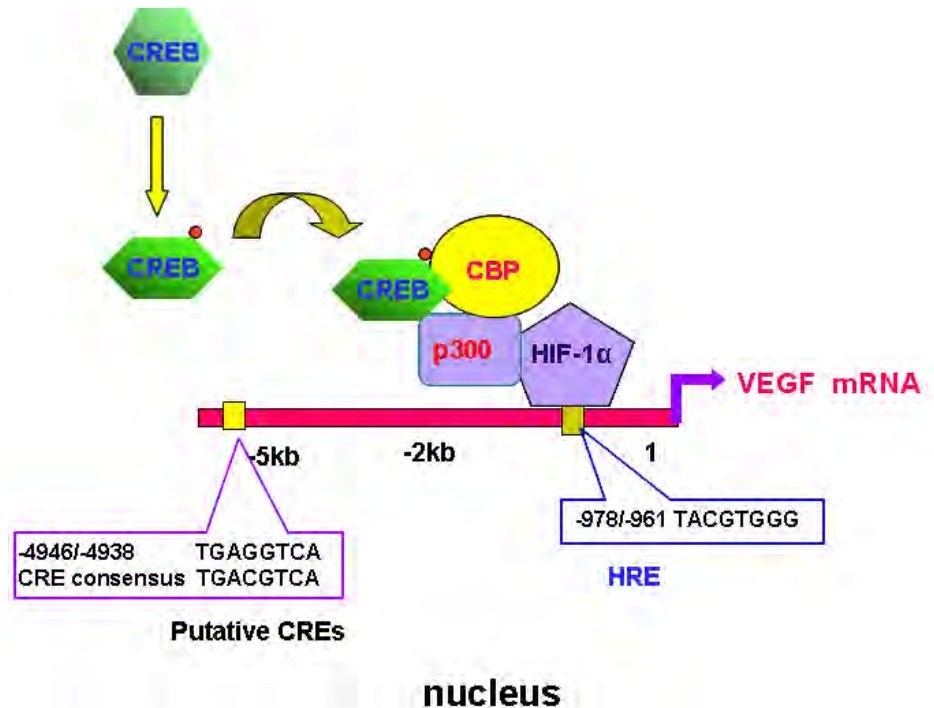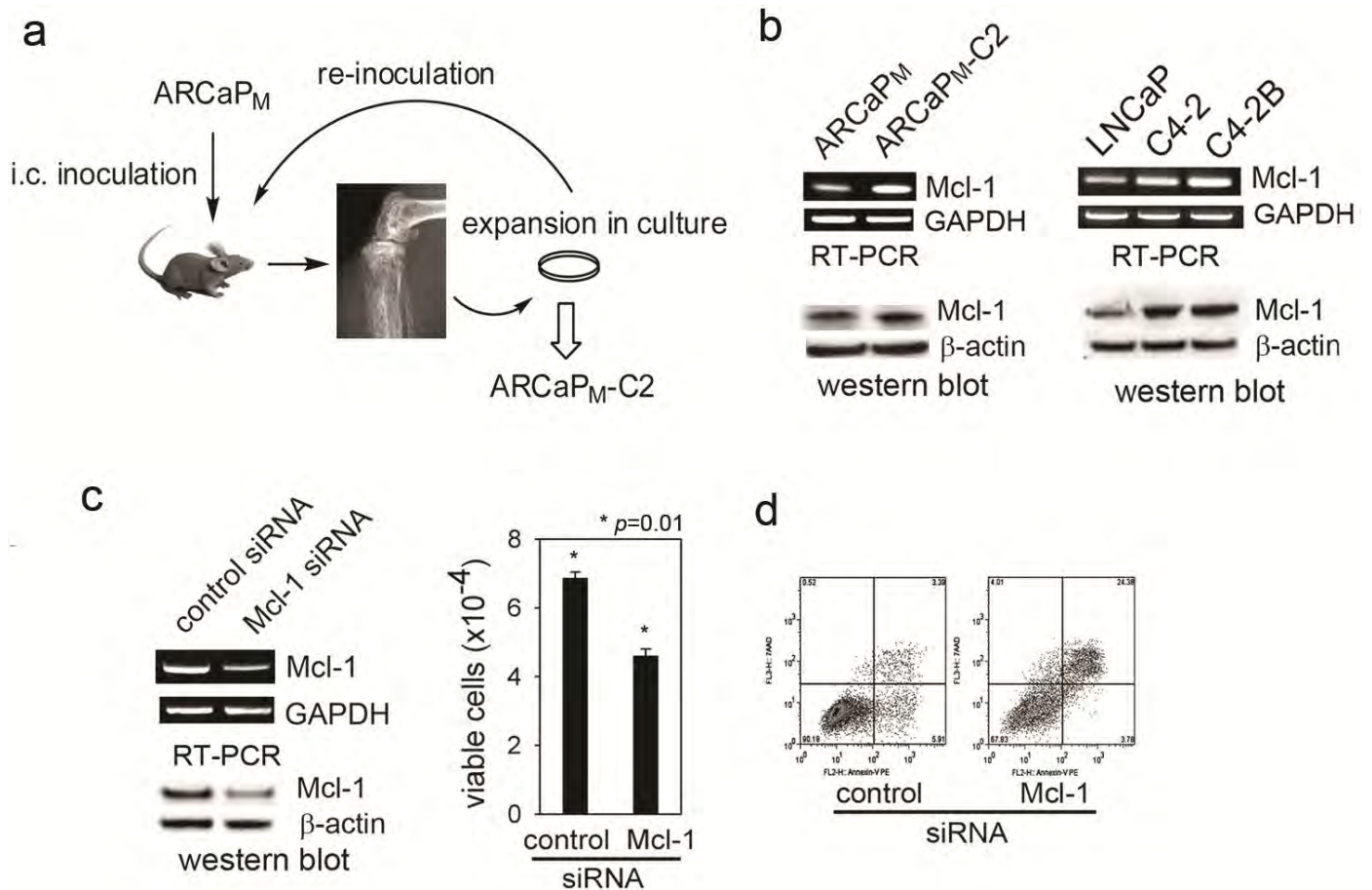
**Figure 7. Mcl-1 is a survival factor in human PCa cells.** (a) Intracardiac (i.c) injection of ARCaP$_M$ cells in athymic mice resulted in metastases to bone and soft tissues. The ARCaP$_M$-C2 subclone was derived from metastatic bone tissues after two rounds of intracardiac inoculation of ARCaP$_M$ cells. (b) Endogenous Mcl-1 expression in the ARCaP$_M$ model was examined by RT-PCR and western blotting analyses. (c) Effect of Mcl-1 siRNA on ARCaP$_M$ cell viability. Subconfluent ARCaP$_M$ cells on a 6-well plate were transiently transfected with Mcl-1 siRNA (30 nM) for 72 h. Endogenous expression of Mcl-1 at the mRNA and protein levels, and cell viability of ARCaP$_M$ cells as counted with trypan blue staining, were significantly inhibited by Mcl-1 siRNA treatment compared to the control. (d) Effects of Mcl-1 siRNA on ARCaP$_M$ cell apoptosis. Subconfluent ARCaP$_M$ cells were transfected with Mcl-1 siRNA or control siRNA for 72h, expression of annexin V was measured by FACS.
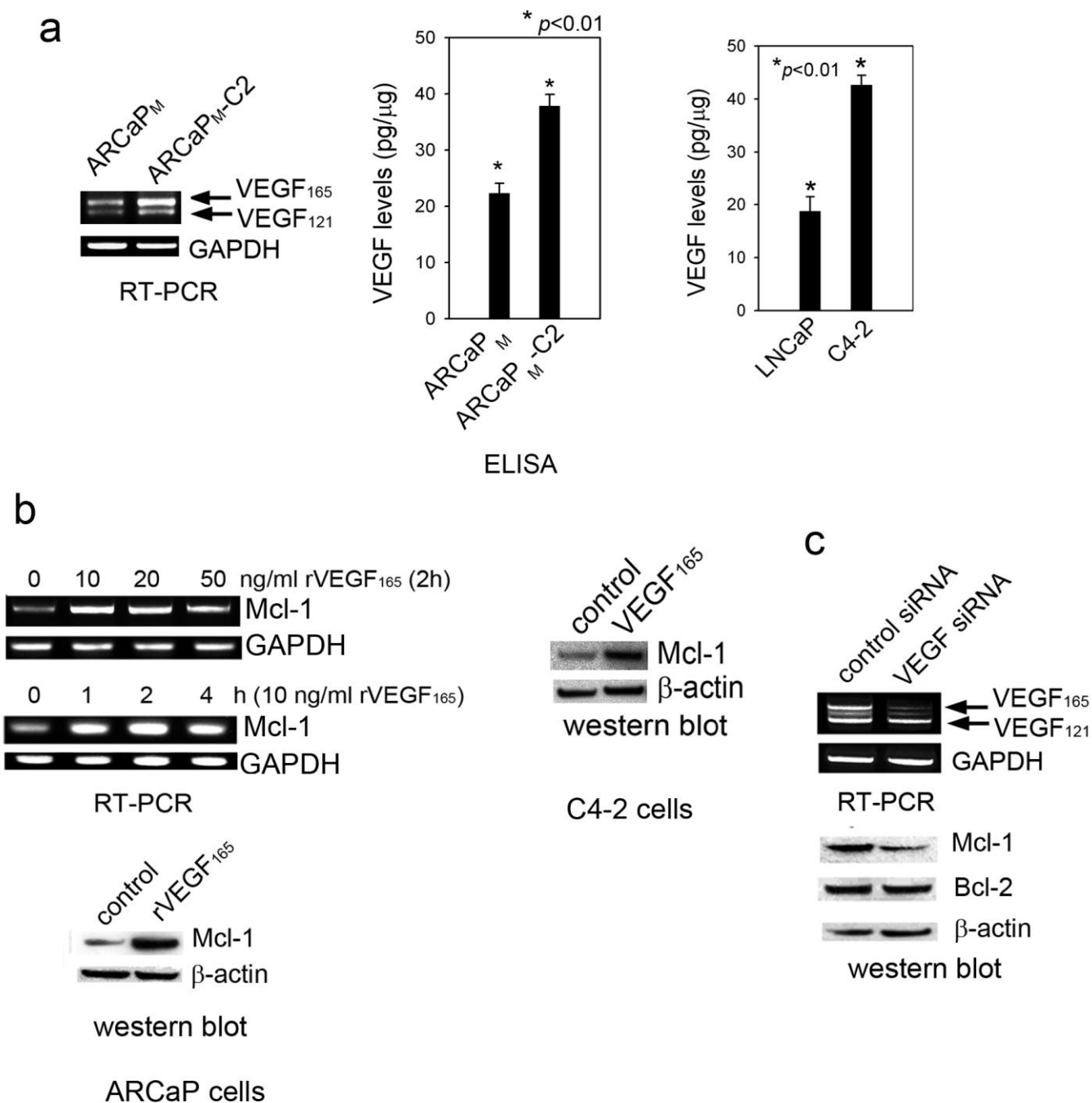
**Figure 8. VEGF$_{165}$ regulates Mcl-1 expression in PCa cells.** (a) VEGF expression in ARCaP$_M$-ARCaP$_M$-C2 and LNCaP-C4-2 models. (b) VEGF$_{165}$ effects on Mcl-1 expression in ARCaP$_M$ and LNCaP cells. Cells were treated with VEGF$_{165}$ at indicated concentrations and times, and Mcl-1 mRNA expression was measured. For immunoblotting, ARCaP$_M$ cells were incubated with VEGF$_{165}$ (10 ng/ml) for 72h. (d) Effects of VEGF siRNA on Mcl-1 expression. ARCaP$_M$ cells were transfected with VEGF siRNA or control siRNA (80 nM) for 72 h.

## 2.3. NRP1 regulates both basal expression and VEGF induction of Mcl-1 in PCa cells

Expression of VEGF-Rs was examined in several PCa cell lines with human umbilical vein endothelial cells (HUVEC) as a positive control (Fig. 9a). VEGF-R1 was undetectable in PCa cells. Only very low expression of

VEGF-R2 could be observed in ARCaP$_M$-C2 cells. However, NRP1 was ubiquitously expressed in PCa cells at a level comparable to that in HUVEC, and higher in metastatic ARCaP$_M$-C2, PC3, C4-2 and C4-2B cells. NRP2, the "co-receptor" for VEGF-C, was not detected in PCa cells. These data implied that NRP1 may be the major receptor mediating VEGF effects in PCa cells.

The role of NRP1 in the regulation of Mcl-1 expression was investigated. Compared to the control, ectopic expression of NRP1 resulted in increased Mcl-1 at both the mRNA and protein levels (Fig.9b). Conversely, transfection with a NRP1 siRNA specifically inhibited NRP1 and reduced endogenous Mcl-1 expression in ARCaP$_M$ cells (Fig. 9c). These data indicated that NRP1 may be required and sufficient for basal expression of Mcl-1 in PCa cells. Further, Fig. 9d showed that expression of NRP1 siRNA, but not control siRNA, abrogated VEGF$_{165}$ induction of Mcl-1 in ARCaP$_M$ cells. These data indicated an indispensible role of NRP1 in mediating VEGF$_{165}$ induction of Mcl-1 in PCa cells.

*2.4. c-MET signaling is required for VEGF regulation of Mcl-1 in PCa cells*

We demonstrated that c-MET is involved in VEGF regulation of Mcl-1 in PCa cells. A c-MET siRNA construct was transfected into ARCaP$_M$ cells, which effectively inhibited endogenous c-MET (Fig.10a). c-MET siRNA treatment reduced Mcl-1 protein expression, suggesting that c-MET is involved in maintaining basal expression of Mcl-1 in PCa cells. Interestingly, however, recombinant HGF treatment did not significantly affect Mcl-1 expression at either RNA or protein levels (Fig.10b), indicating that HGF-dependent activation of c-MET signaling is not sufficient to induce Mcl-1 expression in these cells.

We further investigated whether c-MET signaling is required for VEGF$_{165}$ induction of Mcl-1. VEGF$_{165}$ only induced Mcl-1 expression in ARCaP$_M$ cells transfected with control siRNA, not in those expressing c-MET siRNA (Fig.10c). PHA-665752, a c-MET selective inhibitor, was used to treat ARCaP$_M$ cells prior to addition of VEGF$_{165}$. PHA-665752 significantly attenuated VEGF$_{165}$ induction of Mcl-1in ARCaP$_M$ cells
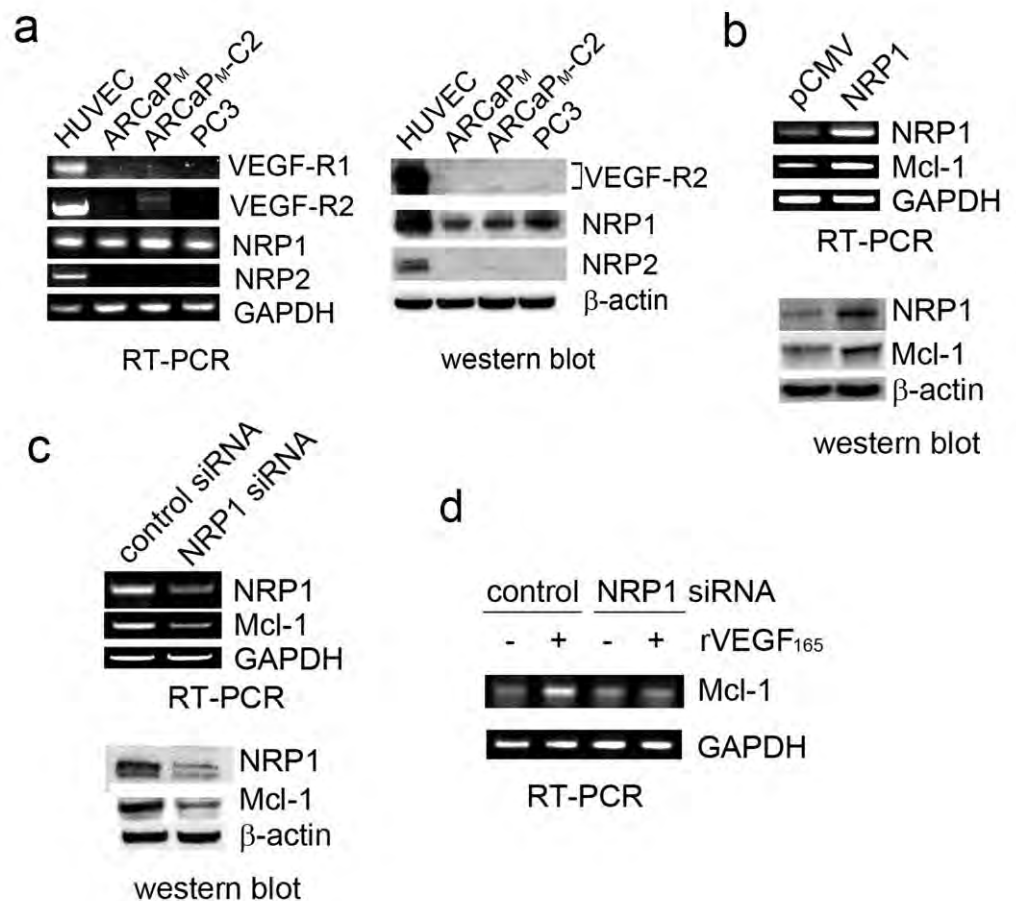


**Figure 9. NRP1 is required for basal expression and VEGF$_{165}$ induction of Mcl-1 in ARCaP$_M$ cells.** (a) Expression of VEGF-Rs in PCa cells and HUVEC. (b) Effect of ectopic expression of NRP1 on Mcl-1 basal level. Subconfluent ARCaP$_M$ cells on 6-well plates were transfected with pCMV-NRP1 or pCMV-XL4 (16 µg) for 48h (for RT-PCR) or 72h (for immunoblotting). (c) Effects of NRP1 siRNA on Mcl-1 basal expression. ARCaP$_M$ cells were transfected with NRP1 siRNA or control siRNA (60 nM) for 48h (for RT-PCR) or 72h (for immunoblotting). (d) Effects of NRP1 siRNA on VEGF$_{165}$ induction of Mcl-1. ARCaP$_M$ cells were transfected with NRP1 siRNA or control siRNA for 48 h, respectively. Cells were then serum-starved overnight, and treated with VEGF$_{165}$ (10 ng/ml) or PBS for 2h.

(Fig.10d). These data indicated that c-MET signaling is required for VEGF regulation of Mcl-1 in PCa cells.

## 2.5. VEGF induces c-MET activation by a NRP1-dependent mechanism in PCa cells

We showed that $VEGF_{165}$ could induce c-MET activation through NRP1. $ARCaP_M$ cells were transiently transfected with NRP1 siRNA or control siRNA before $VEGF_{165}$ treatment. $VEGF_{165}$ induced rapid phosphorylation of c-MET at Tyr1230/1234/1235 residues in $ARCaP_M$ cells transfected with control siRNA, but this effect was significantly attenuated by expression of NRP1 siRNA. Expression of total c-MET protein was not affected by siRNA treatment (Fig.11a).

An immunoprecipitation assay was performed in $ARCaP_M$ cells treated with $VEGF_{165}$ for varying times,



**Figure 10. c-MET signaling is required for $VEGF_{165}$ induction of Mcl-1 in $ARCaP_M$ cells.** (a) Effects of c-MET inhibition on Mcl-1 expression. $ARCaP_M$ cells were transfected with c-MET siRNA or control siRNA (30 nM) for 72h. (b) Effects of recombinant HGF treatment (10 ng/ml) on Mcl-1 expression at RNA (0, 2, 4 and 6 h) and protein levels (72h). (c) $ARCaP_M$ cells were transfected with c-MET siRNA or control siRNA for 48 h, serum-starved overnight, and treated with $VEGF_{165}$ (10 ng/ml) for 2h. (d) $ARCaP_M$ cells were treated with PHA-665752 (0.5 µM) or dimethyl sulfoxide (DMSO) for 2h, before treatment with $VEGF_{165}$ (10 ng/ml) or PBS for 2h.

which demonstrated that VEGF can promote the physical association between NRP1 and c-MET, and activation (phosphorylation) of c-MET (p-c-MET) (Fig.11b). Confocal microscopy (Fig.11c) independently supported a mechanism that NRP1 may be constitutively associated with c-MET on plasma membrane. Upon $VEGF_{165}$ binding, NRP1 may further recruit c-MET and facilitate its activation, subsequently transmitting $VEGF_{165}$ signal (Fig.12).

## 2.6. Src kinases and Stat3 mediate VEGF induction of Mcl-1

We demonstrated that the Src kinase-Stat3 pathway is a downstream component in NRP1 signaling in $ARCaP_M$ cells (Figure 13a). Expression of NRP1 siRNA in $ARCaP_M$ cells significantly inhibited phosphorylation of Src kinases at Tyr416 (p-Src), as well as activation of Stat3 at Tyr705 (p-Stat3), without altering expression of endogenous Src kinases and Stat3.

$VEGF_{165}$ rapidly induced expression of both p-Src (Tyr416) and p-Stat3 (Tyr705) in a time-dependent manner in $ARCaP_M$ cells. Significantly, $VEGF_{165}$ promoted rapid intracellular translocation of p-Stat3 (Tyr705) from the cytoplasm to the nucleus, indicating activation of Stat3-dependent gene expression. By contrast, nuclear presence of p-Stat3 (Ser727), which has been associated with HGF-induced Mcl-1 expression in primary human hepatocytes, was not affected (Fig.13b). These data indicated that Src kinase-Stat3 pathway activation may be an important event following $VEGF_{165}$ stimulation.

We assessed the role of Src kinase-Stat3 signaling in $VEGF_{165}$ regulation of Mcl-1. PP2, a selective inhibitor of Src kinases, was used to treat $ARCaP_M$ cells before $VEGF_{165}$ stimulation. PP2 treatment effectively abrogated $VEGF_{165}$ induction of Mcl-1 (Fig.13c). Similarly, Mcl-1 mRNA expression was rapidly induced by $VEGF_{165}$ in $ARCaP_M$ cells transfected with control siRNA, but not in the cells expressing Stat3 siRNA (Fig.13d). Collectively these data suggested that Src kinase-Stat3 signaling may be required for VEGF induction of Mcl-1 in PCa cells (Fig.12).
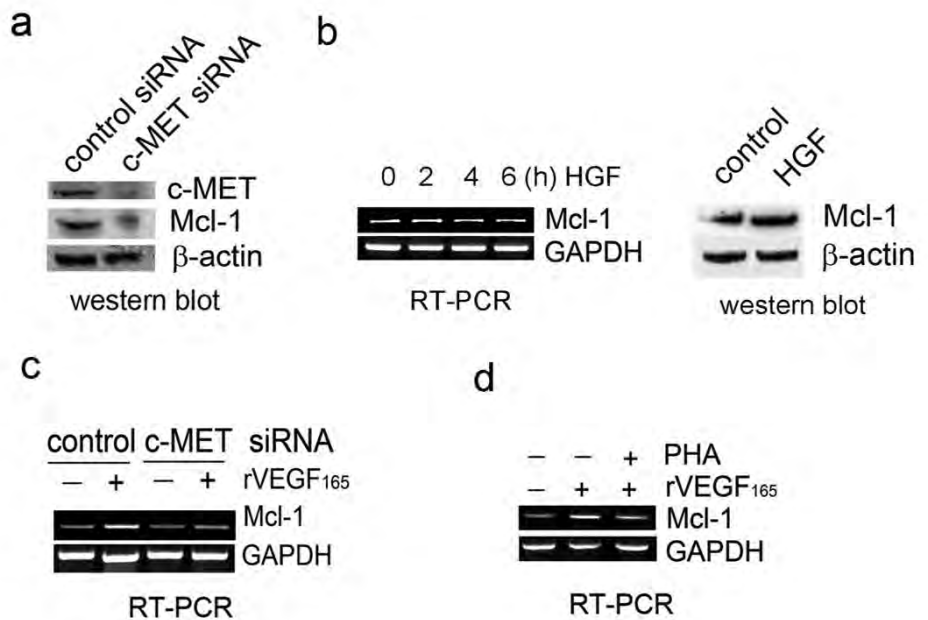
**Figure 11. VEGF$_{165}$ induces c-MET activation through a NRP1-dependent mechanism.** (a) Effects of NRP1 depletion on VEGF$_{165}$-mediated c-MET phosphorylation. ARCaP$_M$ cells were transfected with NRP1 siRNA or control siRNA for 48h, serum-starved overnight, then treated with VEGF$_{165}$ (10 ng/ml) for 60 min. (b) Immunoprecipitation assay of NRP1-c-MET interaction. Serum-starved ARCaP$_M$ cells were treated with VEGF$_{165}$ (10 ng/ml) for the indicated times, and immunoprecipitated with anti-NRP1 (upper), or anti-c-MET (low) antibody. (c) Co-localization of NRP1 and c-MET or p-c-MET. Serum-starved ARCaP$_M$ cells were treated with VEGF$_{165}$ (10ng/ml) or PBS for the indicated times. Immunofluorescence staining of NRP1, c-MET or p-c-MET was performed and visualized by confocal microscopy. Arrows indicate co-localization of NRP1 and c-MET or p-c-MET.

**In summary, we demonstrated that activation of VEGF-NRP1-c-MET signaling is responsible for Mcl-1 expression, which may confer survival advantages allowing PCa cells to evade apoptosis and progress towards invasive states (Figure 12).** For detailed description, please refer to our recent publication (4) (Appendix 4).

3. Mcl-1 is a convergent target gene of VEGF and platelet-derived growth factor (PDGF) signaling in bone metastatic PCa cells.

We demonstrated PDGF-BB could significantly activate Mcl-1 expression at mRNA level, which may contribute to PCa bone metastasis.

*3.1. PDGF-BB induces Mcl-1 expression and antagonizes apoptosis in PCa cells*

PDGF-BB was found to significantly induce
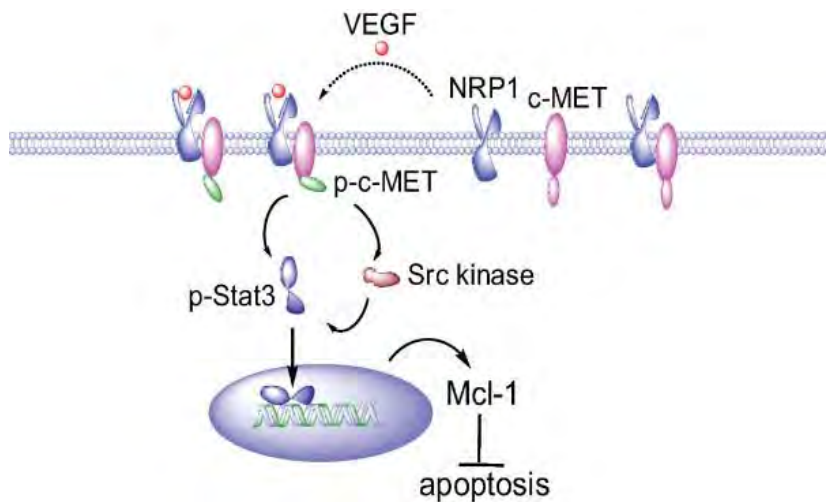


**Figure 12. A proposed model for VEGF$_{165}$ regulation of Mcl-1 in PCa cells**. NRP1 may be constitutively associated with c-MET on plasma membrane. VEGF$_{165}$ engagement recruits c-MET into the protein complex and promotes its interaction with NRP1, thereby enhancing phosphorylation of c-MET. Src kinase-Stat3 signaling is subsequently activated, resulting in nuclear translocation of p-Stat3 and activation of Mcl-1 expression. Increased intracellular Mcl-1 protects PCa cells from apoptosis (Zhang et al., Mol. Cancer., 2010).
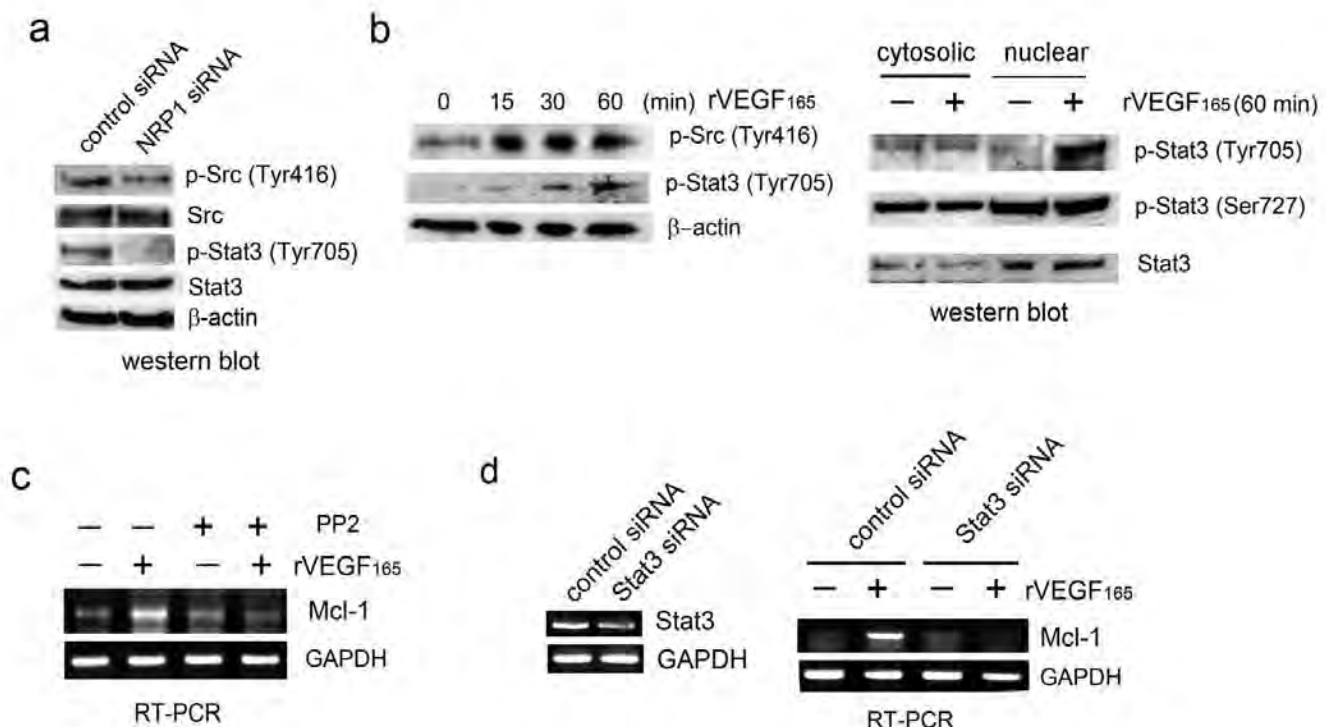


**Figure 13. Src kinase-Stat3 signaling mediates VEGF$_{165}$ induction of Mcl-1 expression in ARCaP$_M$ cells.** (a) Effects of NRP1 inhibition on phosphorylation of Src kinases and Stat3. ARCaP$_M$ cells were transfected with NRP1 siRNA or control siRNA for 72 h. (b) Effects of VEGF$_{165}$ on the phosphorylation of Src kinases and Stat3. ARCaP$_M$ cells were treated with VEGF$_{165}$ (10 ng/ml) for the indicated time, and immunoblotting was performed on total lysates (left) and nuclear extracts and cytoplasmic proteins (right). (c) Effects of Src kinases on VEGF$_{165}$ regulation of Mcl-1. ARCaP$_M$ cells were treated with PP2 (10 µM) or DMSO for 2h before treatment with VEGF$_{165}$ or PBS. (d) Effects of Stat3 depletion on VEGF$_{165}$ induction of Mcl-1. ARCaP$_M$ cells were transfected with Stat3 siRNA or control siRNA (80 nM) for 48h, serum-starved overnight, then treated with VEGF$_{165}$ (10 ng/ml) or PBS for 2h.

Mcl-1 expression in PCa cells (Fig. 14a). Treatment with recombinant human PDGF-BB increased Mcl-1 mRNA in a dose- and time-dependent manner. Western blot analysis confirmed the inductive effects of PDGF-BB on Mcl-1 expression at protein level. These data identified PDGF-BB as a novel regulator of Mcl-1 expression, which could provide a survival mechanism to protect PCa cells from apoptosis. Indeed, addition of PDGF-BB in PCa cell cultures effectively antagonized the cytotoxicity of docetaxel (Fig.14b).
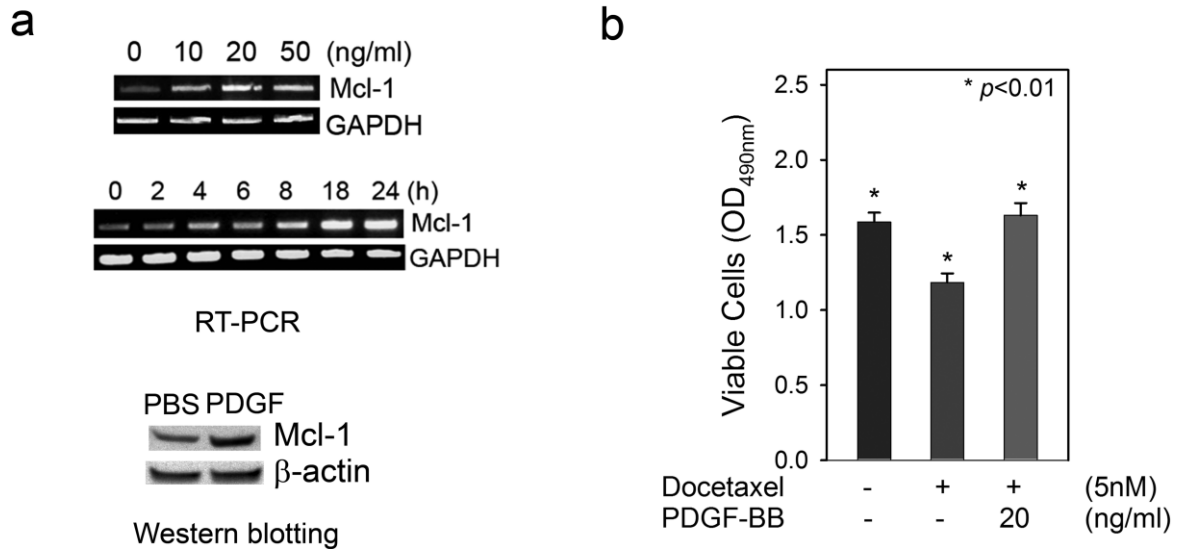
**Fig. 14. PDGF-BB upregulates Mcl-1 and protects PCa cells from apoptosis.** (a) Upper and middle panels: The dose- and time-dependent effects of PDGF-BB on Mcl-1mRNA expression in ARCaP$_M$ cells; bottom panel: The effects of PDGF-BB treatment (20ng/ml, 72 h) on Mcl-1 protein expression in ARCaP$_M$ cells. (b) The effects of exogenous PDGF-BB on the cytotoxicity of docetaxel in ARCaP$_M$ cells, as determined by the MTS assay.

### 3.2. An autocrine PDGFR signaling mediates PDGF-BB regulation of Mcl-1 in PCa cells
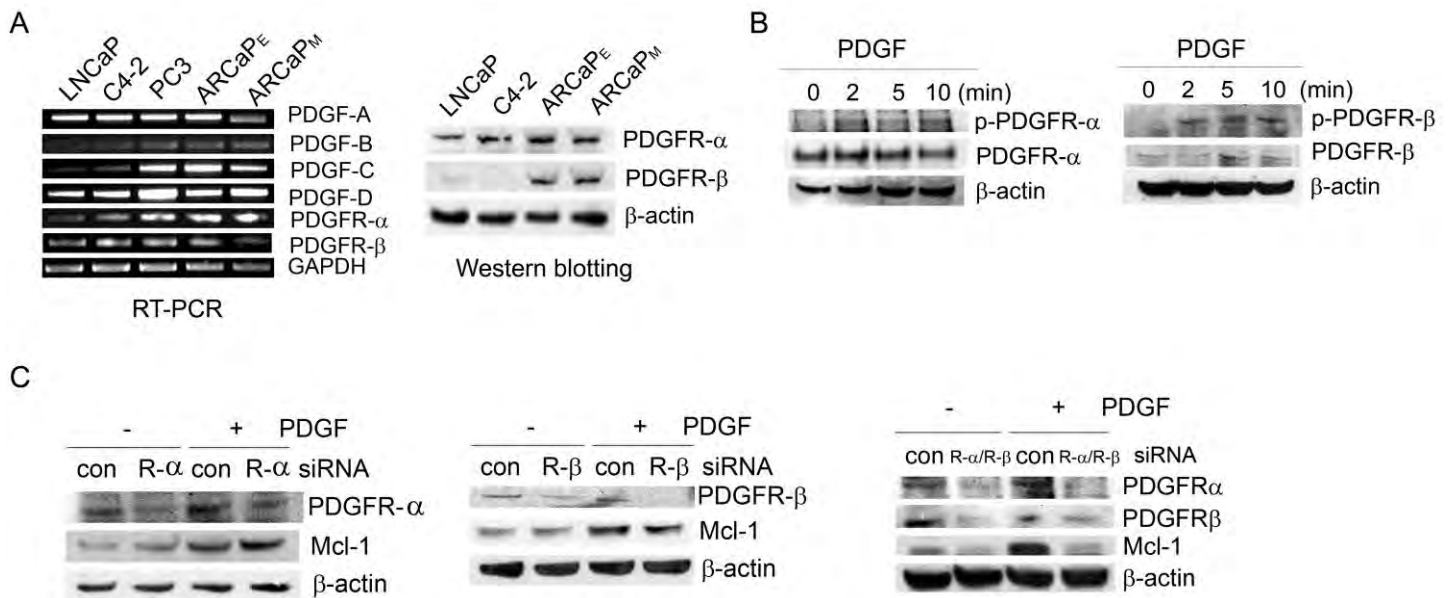
**Figure. 15. Activation of the PDGFR signaling is required for Mcl-1 expression in PCa cells.** (A) Expression profile of PDGFR signaling components in PCa cells, as analyzed by RT-PCR and Western blotting. (B) The effects of PDGF-BB (20 ng/ml) on the phosphorylation of PDGFR-α and -β in ARCaP$_M$ cells. (C) The effects of depleting PDGFR-α or/and -β on Mcl-1 protein expression in ARCaP$_M$ cells. The cells were transfected with either isotype-specific siRNAs targeting PDGFR-α (left panel, 30 nM) or PDGFR- β (central panel, 100 nM), or a mixture of PDGFR-α and -β siRNAs (right panel) for 48 h, serum-starved overnight, and incubated in the presence or absence of PDGF-BB (20 ng/ml) for 72 h.

RT-PCR analyses showed that the PDGF isoforms were differentially expressed at mRNA level. Interestingly, PDGFR-α mRNAs appeared to be substantially expressed in PCa cells, which was confirmed at protein level by Western blot analysis. In contrary, though PDGFR-β mRNAs were detected by RT-PCR in most PCa cell lines, immunoblotting analysis could only confirm protein expression in ARCaP$_E$ and ARCaP$_M$ cells (Fig.15a). Taken together, these data suggested a functional PDGF autocrine signaling in certain PCa cells.



**Figure 16. β-catenin mediates PDGF regulation of Mcl-1 expression in PCa cells.** (A) Expression profile of β-catenin-TCF signaling components in PCa cells. (B) TCF reporter activity in the LNCaP-C4-2 and ARCaP$_E$-ARCaP$_M$ cells. (C) Upper panel: The effects of PDGF-BB (20 ng/ml) on the nuclear translocation of β-catenin in ARCaP$_M$ cells; Bottom panel: The effects of PDGF-BB (20 ng/ml) on TCF reporter activity in the presence (100 nM) or absence of AG-17. (D) The effects of ectopic expression of β-catenin (72 h) on Mcl-1 expression at both mRNA and protein levels. (E) The effects of β-catenin depletion on PDGF-BB regulation of Mcl-1 expression in ARCaP$_M$ cells. The cells were transfected with β-catenin siRNA or control siRNA (30 nM) for 48 h, serum-starved overnight, and incubated in the presence or absence of PDGF-BB (20 ng/ml) for 72 h. (F) The effects of β-catenin depletion on Mcl-1 reporter activity in ARCaP$_M$ cells. The cells were transfected with β-catenin or control siRNA (30 nM) for 48 h, and further transfected with a human Mcl-1 reporter for 24 h. Following serum starvation overnight, the cells were incubated in the presence or absence of PDGF-BB (20 ng/ml) for 48 h.

13

**Figure 17. PDGF-BB activates the c-Abl-p68-β-catenin signaling cascade in PCa cells.** (A) Expression of c-Abl and p68 in PCa cells. (B) The effects of PDGF-BB (20 ng/ml) on the phosphorylation of c-Abl and p68, and the expression of β-catenin in the p68 immunoprecipitates in ARCaP$_M$ cells. (C) The effects of PDGF-BB (20 ng/ml) on the nuclear translocation of p68 in ARCaP$_M$ cells. (D) Confocal microscopy analysis of the effects of PDGF-BB on the co-localization of β-catenin and p68 in the nucleus in a time course experiment in ARCaP$_M$ cells. (E) The effects of p68 depletion on PDGF regulation of Mcl-1 in ARCaP$_M$ cells. The cells were transfected with p68 or control siRNA (30 nM) for 48 h, serum-starved overnight, and incubated in the presence or absence of PDGF-BB (20 ng/ml) for 72 h. (F) The effects of p68 depletion on Mcl-1 reporter activity in ARCaP$_M$ cells. The cells were transfected with p68 or control siRNA (30 nM) for 48 h, and further transfected with human Mcl-1 reporter for 24 h. Following serum starvation overnight, the cells were incubated in the presence or absence of PDGF-BB (20 ng/ml) for 48 h.
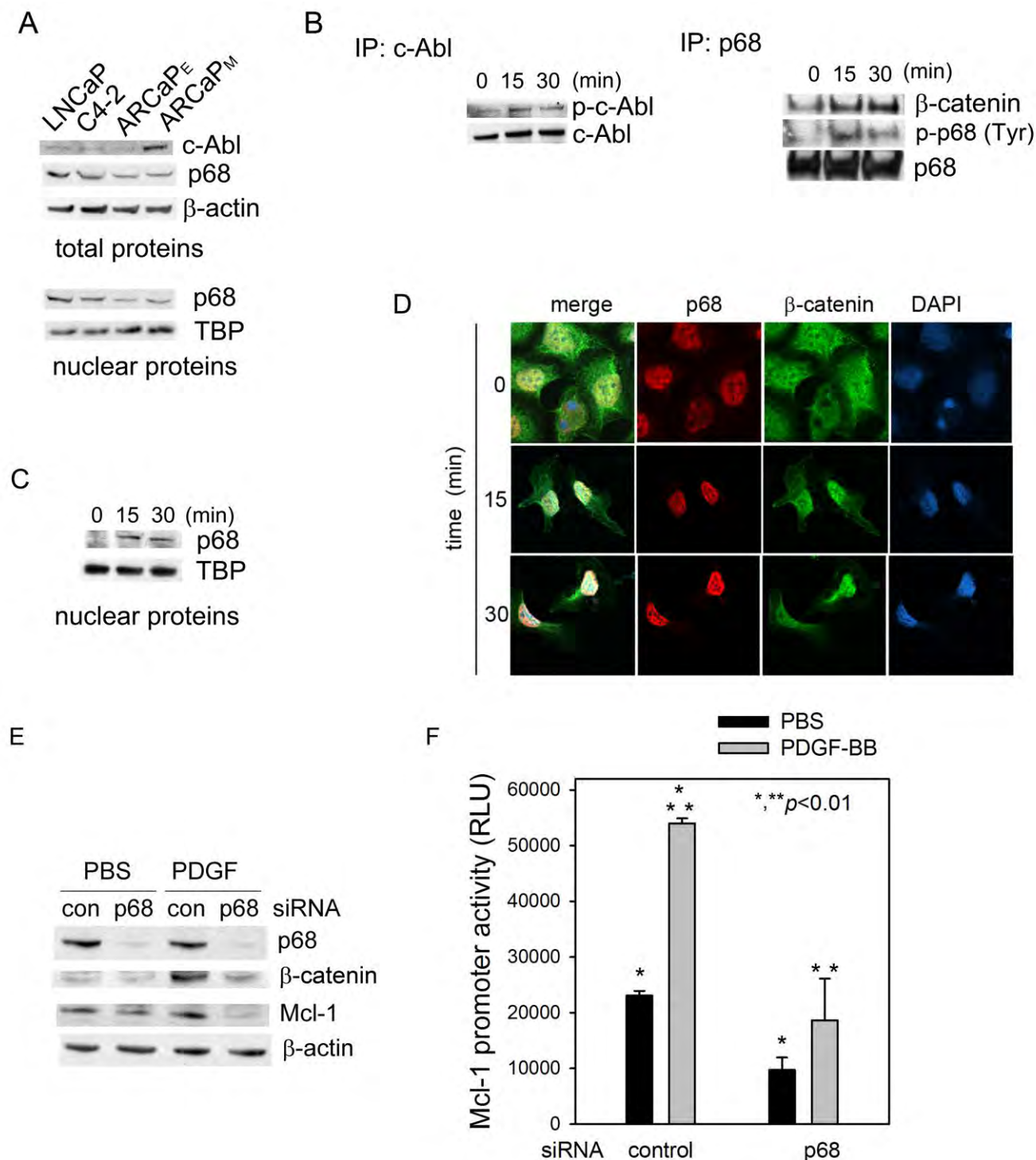
14

Both PDGFR-α and -β were highly expressed in bone metastatic ARCaP$_M$ cells, and rapidly phosphorylated in a time-dependent manner in response to the stimulation of exogenous PDGF-BB (Fig.15b). Interesting, depletion of either PDGFR-α or -β by isoform-specific siRNA did not block the inductive effect of PDGF-BB on Mcl-1 expression (Fig.15c, left and central panels), suggesting that activation of either receptors may be sufficient for the upregulation of Mcl-1. Supporting this hypothesis, transient transfection with a mixture of siRNAs targeting both PDGFR-α and -β inhibited the basal expression of Mcl-1, and abrogated PDGF-BB induction of Mcl-1 ARCaP$_M$ cells (Fig.15c, right panel).
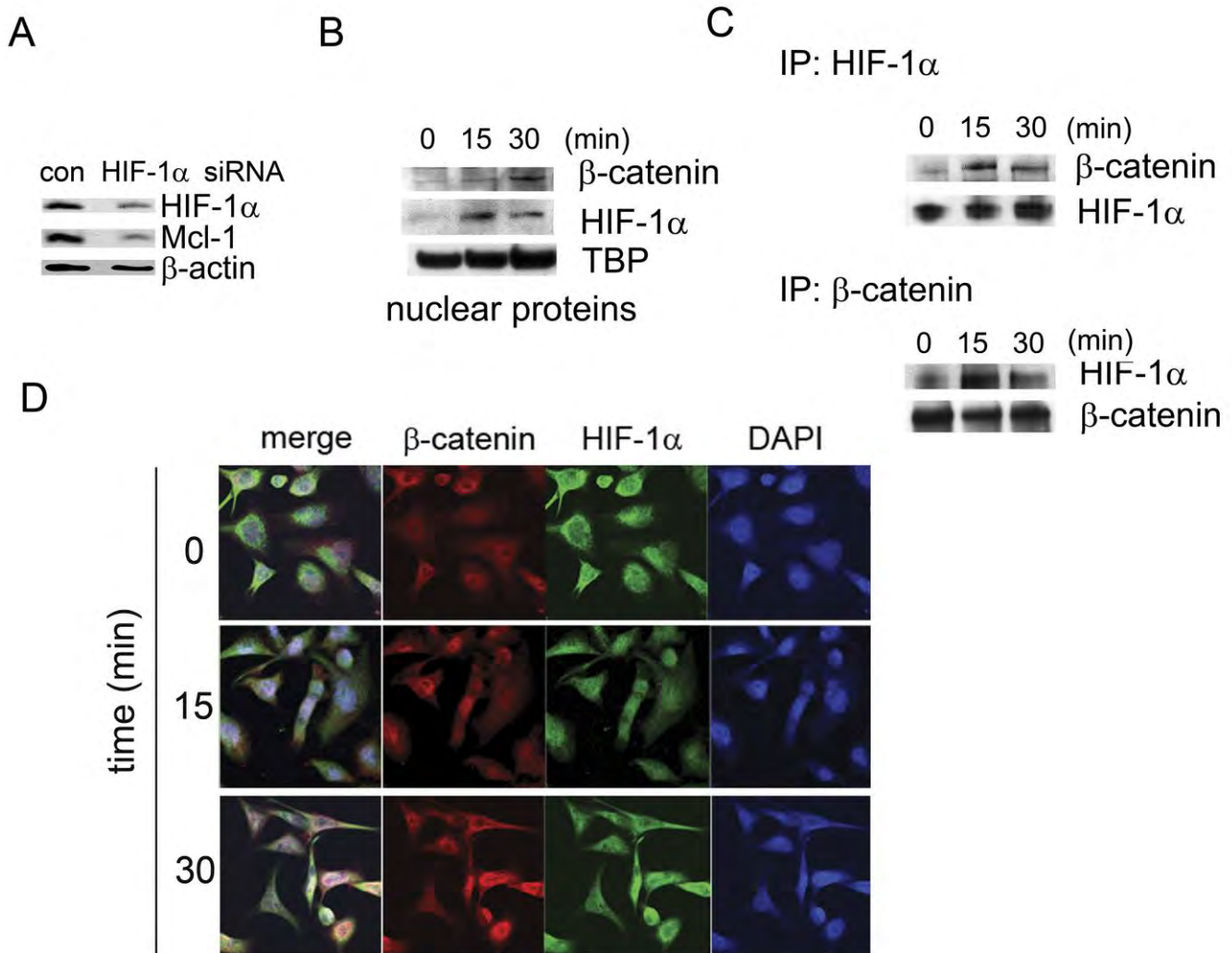


**Figure 18. PDGF-BB promotes protein interaction between β-catenin and HIF-1α in PCa cells.** (A) The effects of HIF-1α depletion on Mcl-1 expression in ARCaP$_M$ cells. The cells were transfected with HIF-1α or control siRNA (30 nM) for 72 h, and analyzed for Mcl-1 expression by immunoblotting. (B) Western blot analysis of the effects of PDGF-BB (20 ng/ml) on the nuclear translocation of β-catenin and HIF-1α in ARCaP$_M$ cells. (C) Co-immunoprecipitation assays of the effects of PDGF-BB (20 ng/ml) on the interaction between β-catenin and HIF-1α in the nucleus in ARCaP$_M$ cells. (D) Confocal microscopy of the effects of PDGF-BB (20 ng/ml) on the co-localization of β-catenin and HIF-1α in the nucleus in ARCaP$_M$ cells.

## 3.3. β-catenin mediates PDGF regulation of Mcl-1 expression in PCa cells

Western blot analysis found that β-catenin and TCF4, a major β-catenin-interacting transcription factor, were differentially expressed in PCa cells (Fig.16a), suggesting a functional β-catenin-TCF4 signaling in these cells. In fact, an artificial TCF promoter was activated in both the LNCaP-C4-2 and ARCaP$_E$-ARCaP$_M$ cell lineages,

and the reporter activities appeared to be associated with increased *in vivo* metastatic potential in C4-2 and ARCaP$_M$ cells (Fig.16b).

Upon PDGF-BB treatment, the nuclear presence of β-catenin was rapidly increased in ARCaP$_M$ cells (Fig.16c, upper panel). Consistently, TCF reporter activity was also significantly increased following PDGF-BB stimulation, which was attenuated by the pre-treatment with AG-17 (Fig.16c, bottom panel). These data indicated that PDGF-BB activated β-catenin signaling in a PDGFR-dependent manner.

To investigate the role of β-catenin in the regulation of Mcl-1 expression, ARCaP$_M$ cells were transiently transfected with a construct expressing wild-type β-catenin. RT-PCR and Western blot analyses showed that ectopic epression of β-catenin increseased Mcl-1 at both mRNA and protein levels (Fig.16d). In contrary, β-catenin depletion using a siRNA pool efficiently inhibited both the basal expression of Mcl-1 and its induction by PDGF-BB (Fig.16e). Consistently, whereas PDGF-BB significantly induced the luciferase activity of a full-length human Mcl-1 promoter in ARCaP$_M$ cells transfected with non-targeting control siRNAs, this effect was abrogated by transient depletion of endogeneous β-catenin (Fig.16f). These results suggested that activation of β-catenin signaling may be sufficient and required for Mcl-1 expression in PCa cells.
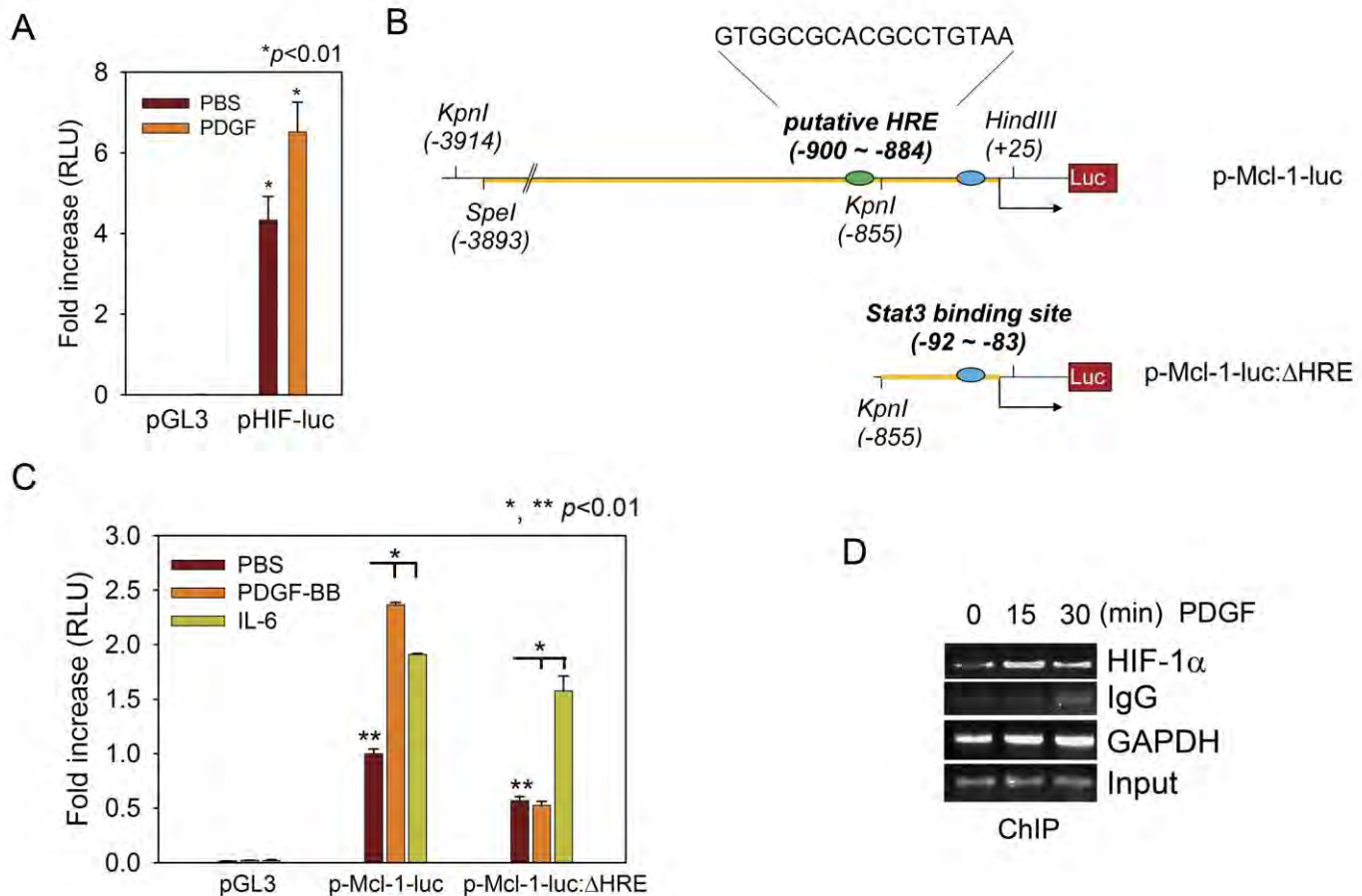


**Figure 19. A putative HRE site is required for PDGF-BB activation of Mcl-1 promoter.** (A) The effects of PDGF-BB on the HIF-1 reporter activity in ARCaP$_M$ cells. The cells were transiently transfected with HIF-1 reporter or pGL3 for 24 h, serum-starved and incubated in the presence or absence of PDGF-BB (20 ng/ml) for 48 h. (B) Schematic diagram of human Mcl-1 promoter and its deletion mutation at the putative HRE site. (C) The effects of deleting the putative HRE site on PDGF regulation of Mcl-1 promoter activity in ARCaP$_M$ cells. IL-6 (200 ng/ml) was included as the positive control. (D) ChIP assay of the effects of PDGF-BB treatment (20 ng/ml) on HIF-1α binding to human Mcl-1 promoter region in ARCaP$_M$ cells.

## 3.4. PDGF activates p68-β-catenin signaling in PCa cells

Western blot analyses found that c-Abl and p68 were differentially expressed in PCa cells (Fig.17a). Upon PDGF-BB treatment, tyrosine phosphorylation of c-Abl and p68 were rapidly activated, as evidenced by immunoprecipitation-immunoblotting assays (Fig.17b). Importantly, the presence of β-catenin in p68 immunoprecipitates was also increased in a time-dependent manner, suggesting an enhanced physical association between β-catenin and p68 proteins. In fact, PDGF-BB induced rapid nuclear translocation of p68 (Fig.17c), which was associated with increased co-localization of p68 and β-catenin in the nucleus (Fig.17d). These data indicated that PDGF-BB could activate the c-Abl-p68 cascade and subsequent β-catenin signaling in PCa cells.

As shown in Figure 17e, depletion of p68 inhibited endogeneous β-catenin and effectively attenuated PDGF-BB induction of Mcl-1 protein. Consistently, Mcl-1 promoter activity was significantly inhibited by the treatment with p68 siRNA in ARCaP$_M$ cells, either with or without the presence of PDGF-BB in the cultures (Fig.17f). These data indicated an indispensible function of p68 in the regulation of Mcl-1 in PCa cells.

## 3.5. PDGF-BB promotes protein interaction between β-catenin and HIF-1α in PCa cells

Transfection of a HIF-1α-specific siRNA significantly reduced Mcl-1 protein expression in ARCaP$_M$ cells (Fig.18a), suggesting that HIF-1α may be required for Mcl-1 regulation in PCa cells. Western blot analysis found that both HIF-1α and β-catenin were rapidly increased in the nucleus (Fig.18b). A co-immunoprecipitation assay showed that in response to PDGF-BB stimulation, nuclear presence of β-catenin and HIF-1α was increased (Fig.18c). The enhanced co-localization of β-catenin and HIF-1α proteins was further demonstrated by confocal microscopy, which appeared to acheive the maximum intensity at 30 min upon PDGF-BB stimulation (Fig.18d). These results indicated that in repsonse to PDGF-BB stimulation, β-catenin physically interacts with HIF-1α in the nucleus, which may lead to the activation of Mcl-1 transcription in PCa cells.
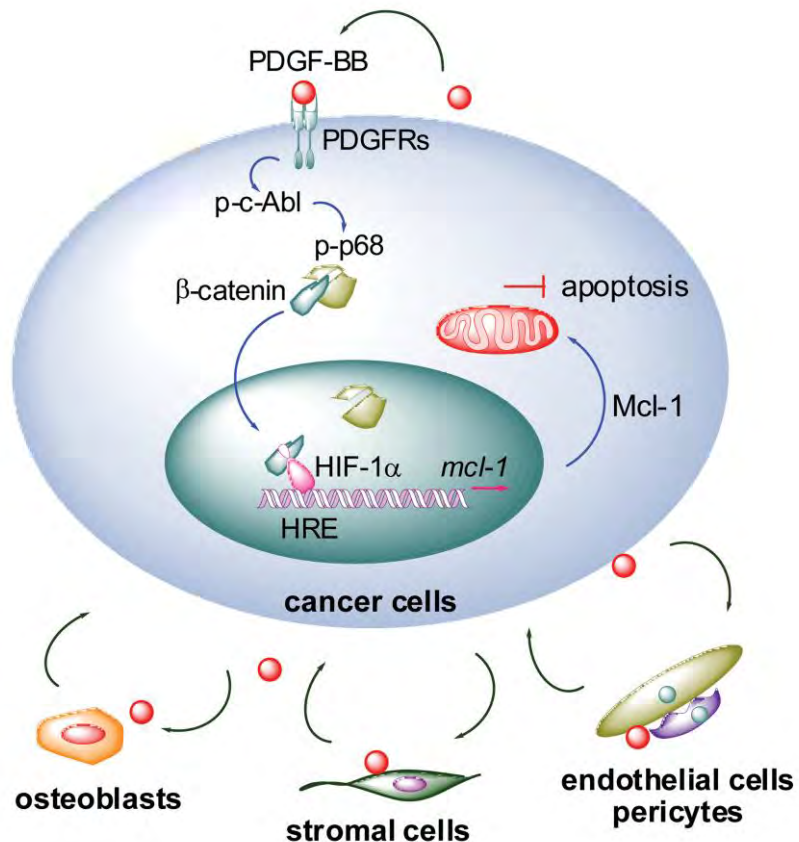


**Figure 20. A proposed model for PDGF-BB regulation of Mcl-1 expression in PCa cells.** The engagement of PDGF-BB to PDGFR dimers activates the c-Abl-p68 cascade, which subsequently stablizes β-catenin and promotes its nuclear translocation. In the nucleus, interaction between β-catenin and HIF-1α increases the binding of HIF-1α to the HRE site within Mcl-1 promoter, thereby activating the transcription of Mcl-1 gene. Upregulation of Mcl-1 antagonizes apoptotic signals and confers survival advantages to metastatic PCa cells. Furthermore, tumor-derived and locally expressed PDGF may mediate the interactions between PCa and bone microenvironment. Co-targeting the PDGF signaling in PCa cells (autocrine) and microenvironment (paracrine) could provide a new strategy to disrupt the "vicious cycle" and efficaciously treat metastatic PCa.

### 3.6. A putative HRE motif is required for PDGF-BB activation of Mcl-1 promoter

In ARCaP$_M$ cells, PDGF-BB treatment significantly increased luciferase expression driven by an artificial HRE promoter (pHIF-luc) (Fig.19a). Interestingly, a putative HRE motif was identified within human Mcl-1 promoter region, which is located between -900 and -884 nucleotides at the 5'-upstream of transcription start site. We characterized a deletion mutant of the putative HRE motif using human Mcl-1 promoter region as the template (Fig.19b). The resulting reporter construct (p-Mcl-1-Luc: ΔHRE), or the luciferase reporter driven by the full-length Mcl-1 promoter (p-Mcl-1-Luc), was transiently expressed in ARCaP$_M$ cells respectively, and treated with PDGF-BB or PBS. IL-6, which has been shown to activate Mcl-1 transcription in PCa and cholangiocarcinoma cells through a signal transducer and activator of transcription 3 (Stat3)-dependent mechanism, was included as the positive control. Luciferase activity assay showed that PDGF-BB induced the activation of p-Mcl-1-Luc promoter to a greater degree than IL-6 in ARCaP$_M$ cells. Significantly, deletion of the HRE motif not only reduced the basal activity of Mcl-1 promoter, but also abrogated the inductive effects of PDGF-BB on reporter activity. In contrary, p-Mcl-1-Luc: ΔHRE, containing a Stat3-binding sequence at position between -92 and -83, remained activated upon IL-6 treatment (Fig.19c). These data indicated that the putative HRE cis-element is required for PDGF-BB activation of Mcl-1 expression in PCa cells. Finally, we investigated whether PDGF-BB promoted specific binding of HIF-1α to Mcl-1promoter by ChIP assay. Fractionated chromatin from controls and PDGF-BB-treated ARCaP$_M$ cells was immunoprecipitated with HIF-1α antibody or control IgG. From the isolated DNA, a 151-bp region was amplified by PCR. Upon PDGF-BB stimulation, a considerable increase in HIF-1α binding with the HRE region in was observed (Fig.19d), demonstrating that PDGF-BB could facilitate association of HIF-1α with Mcl-1 promoter, thereby activating its expression.

**In summary, we demonstrated that PDGF-Mcl-1 signaling is a crucial survival mechanism in bone metastatic PCa cells (Figure 20), indicating that interruption of the PDGF-Mcl-1 survival signal may provide a novel strategy for treating PCa metastasis.** For detailed description, please refer to our manuscript under review (Appendix 5).

**B. Clinical significance of NRP1 signaling components in human PCa bone metastasis**

**We used human PCa specimens (tissue and blood samples) as "gold standard" to evaluate the clinical importance of the NRP1 signaling components in PCa metastasis. This task was in collaboration with Drs. Haiyen Zhau (who relocated to Cedars-Sinai Medical Center at LA in 2009) and Adeboye Osunkoya (Emory University School of Medicine, Department of Pathology).**

<u>1. CREB activation is associated with human PCa bone metastasis</u>

To investigate the clinicopathologic significance of CREB, we analyzed the IHC protein expression of p-CREB in primary and bone metatstatic PCa tissue. We defined well-differentiated PCa as Gleason score ≤6 and poorly-differentiated PCa as Gleason score ≥8. In all specimens, activated CREB or nuclear localization of p-CREB expression was undetectable in normal/benign glands (0/5; Fig.21a) or well-differentiated cancer (0/5; Fig.21b) but was positively associated with poorly-differentiated cancers (5/5; Fig.21c).All seven PCa bone metastatic tissue specimens were positive for p-CREB (Fig.21d).



**Figure 21. CREB phosphorylation positively correlates to clinical PCa progression.** IHC analysis of p-CREB expression in PCa tumor specimens. P-CREB expression (arrows) was seen in poorly-differentiated primary tumors and bone-metastatic tumors, but not in normal/benign prostatic glands or well-differentiated primary tumors.

<u>2. Serum levels of VEGF in PCa patients positively correlate with bone metastasis</u>

A double-blind study measured VEGF levels in sera from 31 patients with non-metastatic PCa versus 24 patients with bone-metastatic PCa. ELISA results indicate a statistically significant difference between the two

groups (p=0.0013). The mean serum level of VEGF in patients with non-bone metastatic PCa was 207.8 pg/ml (27.3 - 613.6 pg/ml) and 397.4 pg/ml in patients with bone metastasis (135.6 - 1,083.7 pg/ml) (Fig.22), suggesting that serum VEGF positively correlates with bone-metastatic status. In this study, the average serum prostate-specific antigen (PSA) levels of these two groups of patients were 3.1 ng/ml (incomplete data, n=19; serum PSA in 8 patients was less than 0.1 ng/ml) and 358.1 ng/ml (n=24), respectively (p=0.004).
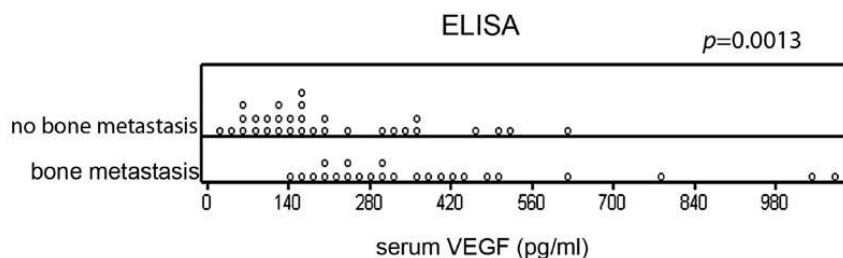


**Figure 22. Serum VEGF levels are associated with PCa bone metastasis.** Dotplot analysis showed there is a statistically significant difference between serum VEGF levels in patients with non-bone metastatic tumors (n=31) and with bone metastasis (n=24).
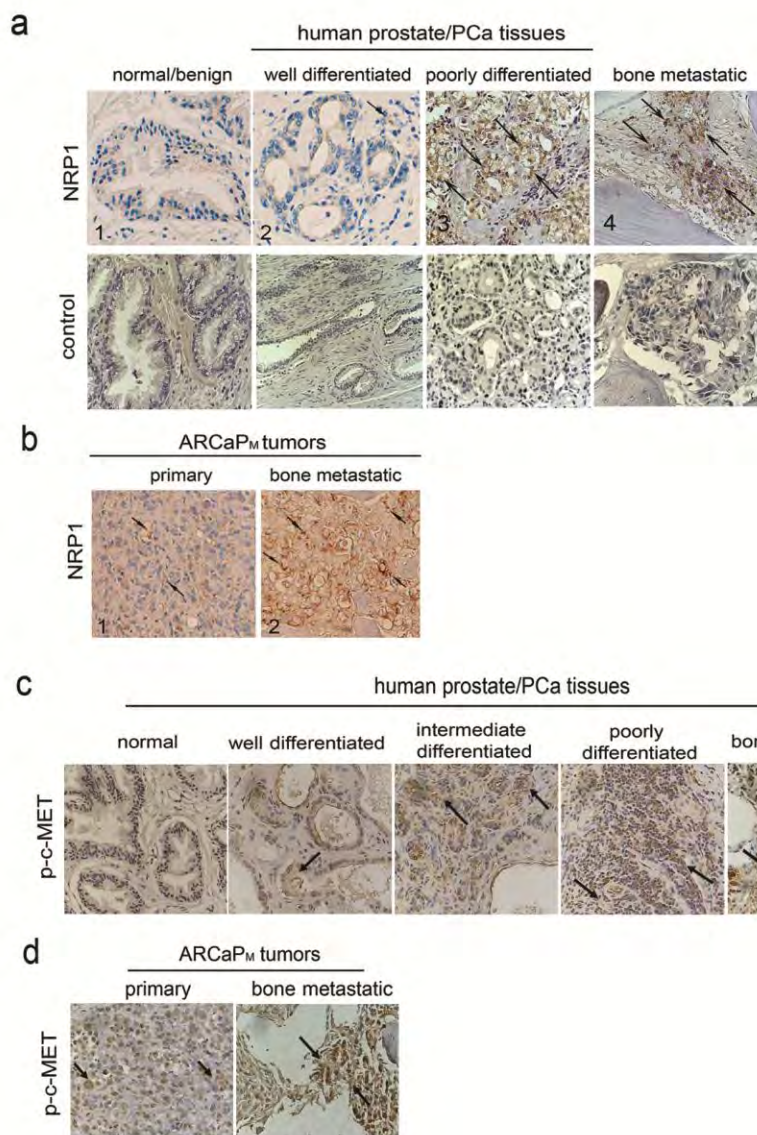


**Figure 23. Expression of NRP1 and p-c-MET is associated with bone metastatic status of human PCa specimens and the ARCaP$_M$ model.** IHC analyses of NRP1 expression in human normal/benign, cancerous and metastatic prostatic tissue specimens (a) and primary and bone metastatic tissue specimens from ARCaP$_M$ model (b), and of p-c-MET expression in human PCa progression (c) and ARCaP$_M$ xenografts (d). Arrows indicate positively-stained cells.

3. NRP1 overexpression and c-MET activation are positively associated with human PCa progression and bone metastasis

To validate the clinical significance of NRP1-c-MET signaling in PCa progression, and avoid the potential bias from using human PCa cell lines, IHC analyses were performed to determine the expression of NRP1 and p-c-MET in human PCa tissue specimens. Prostatic tissue specimens of normal/benign glands, primary and bone metastatic tumors were analyzed. NRP1 expression was increased from normal/benign glands (0/5) or well-differentiated cancer (1/5) to poorly-differentiated cancers (5/5) and bone metastatic tissues (5/5) (Fig.23a). NRP1 staining was also determined in tumor specimens from the ARCaP$_M$ xenograft model in which ARCaP$_M$ cells were inoculated into athymic mice orthotopically, resulting in skeletal metastases with a short latency. Consistently, NRP1 expression was significantly greater in bone metastatic tumors than in primary tumors (Fig.23b).

We and others have reported that c-MET overexpression is positively associated with PCa progression. As shown in Fig.23c, p-c-MET was expressed at a low level in normal human prostatic tissue, but increased significantly from well-differentiated and intermediate to poorly-differentiated primary PCa. Importantly, bone metastatic PCa specimens displayed a higher expression of p-c-MET than primary PCa. p-c-MET expression was also remarkably increased in bone metastatic ARCaP$_M$ tumors (Fig.23d).

4. Elevated Mcl-1 expression is associated with PCa progress and bone metastasis

IHC analyses were performed to determine the expression of Mcl-1 in a human PCa tissue microarray with matched normal adjacent tissue and bone metastatic bone specimens (Fig.24). We defined tumors with Gleason score 2-6 as well-differentiated (n=2), Gleason score 7 as intermediately-differentiated (n=26) and Gleason score 8-10 as poorly-differentiated (n=43). Mcl-1 immunointensity was increased from normal tissues to well-differentiated cancer and further elevated in high grade PCa, although the difference between Mcl-1 intensity in intermediate- and poorly-differentiated cancers was not statistically significant ($p = 0.93$). Intriguingly, Mcl-1 staining in bone metastatic tumors (n=6) was remarkably increased compared to that in either intermediate- or poorly-differentiated PCa ($p < 0.002$). These data correlated elevated Mcl-1 expression to clinical PCa progression, particularly bone metastasis.



**Figure 24.** IHC staining of Mcl-1 in human PCa tissue microarray consisting of normal adjacent tissues, primary PCa and bone metastases.
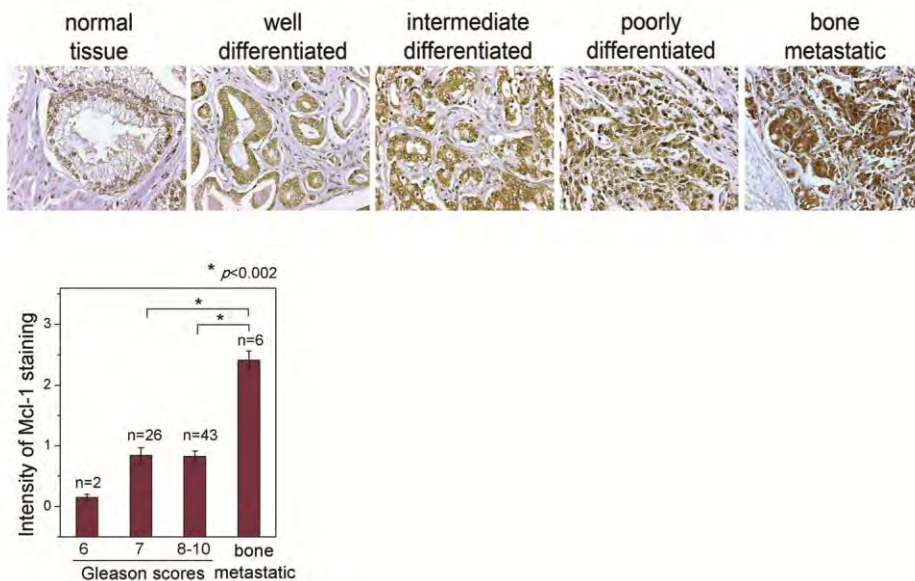
**In summary, we validated the clinical significance of the following VEGF-NRP1 signaling components in human PCa bone metastasis: 1) CREB phosphorylation positively correlates to clinical PCa bone metastasis; 2) serum VEGF was significantly elevated in PCa patients with bone metastasis compared to that in those with non-metastatic PCa; 3) Mcl-1 expression is positively associated with PCa progression, particularly bone metastasis.** For detailed description, please refer to our publications (1, 4) (Appendices 1 and 4).

## C. Targeting NRP1 signaling in bone metastatic PCa cells

**We explored the targeting potential of the NRP1-Mcl-1 signaling pathway in treating PCa bone metastasis. Several strategies (including siRNA, shRNA, monoclonal antibody and small molecule agents) were developed to effectively induce apoptosis and tumor regression in pre-clinical models of PCa metastasis.**

1. Inhibition of NRP1-Mcl-1 signaling induces PCa cell apoptosis.

Treatment with siRNAs for NRP1 or Mcl-1 effectively inhibited cell proliferation by 37% or 48% after a 3-day culture, respectively (Fig.25a). Annexin-V staining showed that the two siRNA constructs respectively induced apoptosis in 14.8% or 24.4% of ARCaPM cells (Fig.25b). Cleavage of caspase 3 and PARP increased in ARCaPM cells following treatments with NRP1 or Mcl-1 siRNAs (Fig.25c), indicating that the NRP1-Mcl-1 pathway is a survival mechanism in metastatic PCa cells.
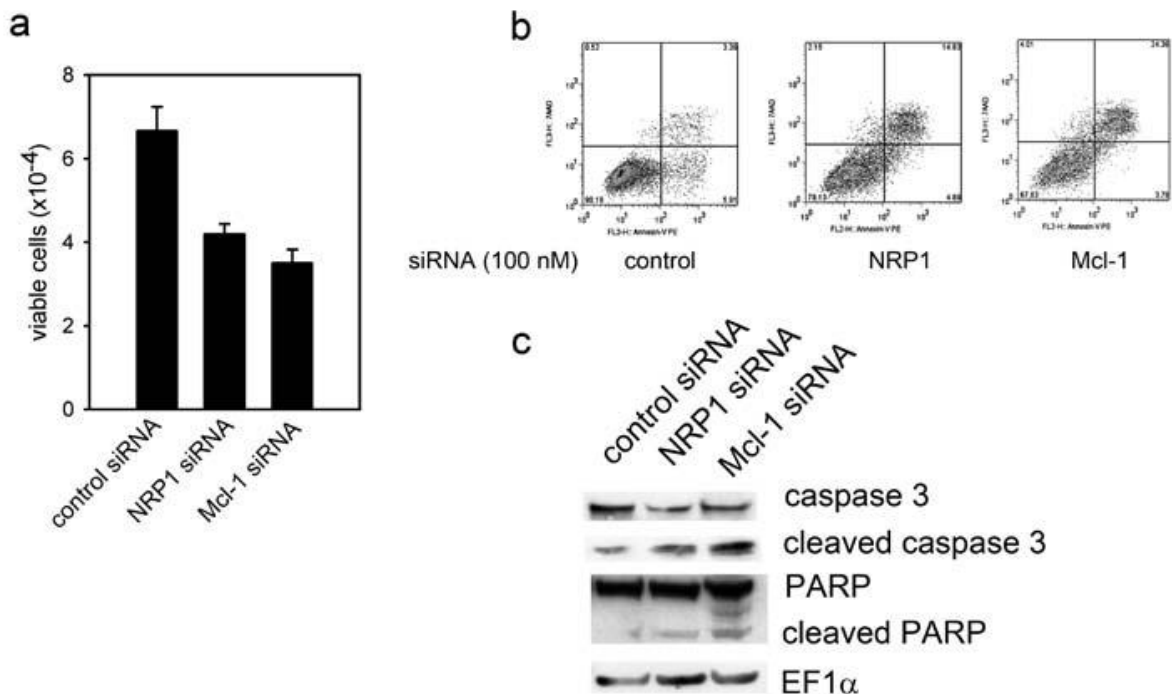


**Figure 25. Blockade of NRP1-Mcl-1 signaling induces apoptosis in ARCaPM cells.** (a) Treatment with NRP1 or Mcl-1 siRNA induced cell death after 72 h. (b) Annexin-V analysis of apoptotic ARCaPM cells after transfection with NRP1 or Mcl-1 siRNA (72 h). (c) NRP1 or Mcl-1 siRNA treatment increased cleavage of caspase 3 and PARP.
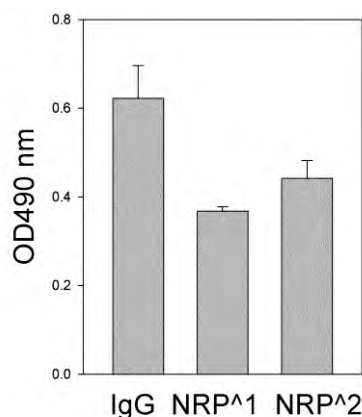


**Figure 26. Genentech NRP1 antibodies inhibited proliferation of ARCaP$_M$ cells.**

**Figure 27. Expression of shRNA (no. 1 and 3) stably inhibited NRP1 expression in ARCaP$_M$ cells.** pRS, control vector.

21

## 2. Genentech NRP1 monoclonal antibodies moderately inhibited proliferation of bone metastatic PCa cells

In collaboration with Genentech, we evaluated the in vitro effects of two NRP1 monoclonal antibodies on the proliferation of ARCaP$_M$ cells. Figure 26 showed that at the concentration of 20 µg/ml, both antibodies inhibited proliferation moderately, with a higher degree when NRP1^1 was used. We will test the in vivo effects of these antibodies with the intention of co-targeting tumor and vasculature to achieve more efficacious inhibition of tumor growth in animal models.

## 3. Establishment of ARCaP$_M$ cells stably expressing NRP1 short-hairpin RNA (shRNA)

To explore the targeting potential of NRP1 in treating PCa bone metastasis, we established two sublines of ARCaP$_M$ that express specific shRNA against human NRP1 (obtained from Origene, Inc.), which could be used in experimental models of PCa bone metastasis (Fig.27).

## 4. Small-molecule blockade of PDGF-Mcl-1 signaling induces apoptosis in bone metastatic PCa cells

In bone metastatic PCa cells, treatment with AG-17 (Tyrphostin), a selective pharmacological inhibitor of PDGFRs, reduced Mcl-1 expression at both mRNA and protein levels and markably increased cleavage of PARP. These effects were attenuated by the presence of PDGF-BB in cultures (Fig.28a). Consistently, AG-17 treatment at low doses (such as 100 nM) effectively induced apoptosis in ARCaP$_E$ and ARCaP$_M$ cells (Fig.28b), indicating a pivotal role of PDGFR signaling in the survival of PCa cells. We are testing the in vivo efficiacy of AG-17 in retarding PCa growth in mouse bone.

**In summary, we explored several independent approaches, including shRNA, monoclonal antibody and small-molecule agents, to specifically and effectively target the NRP1-Mcl-1 survival axis in bone metastatic PCa cells.**
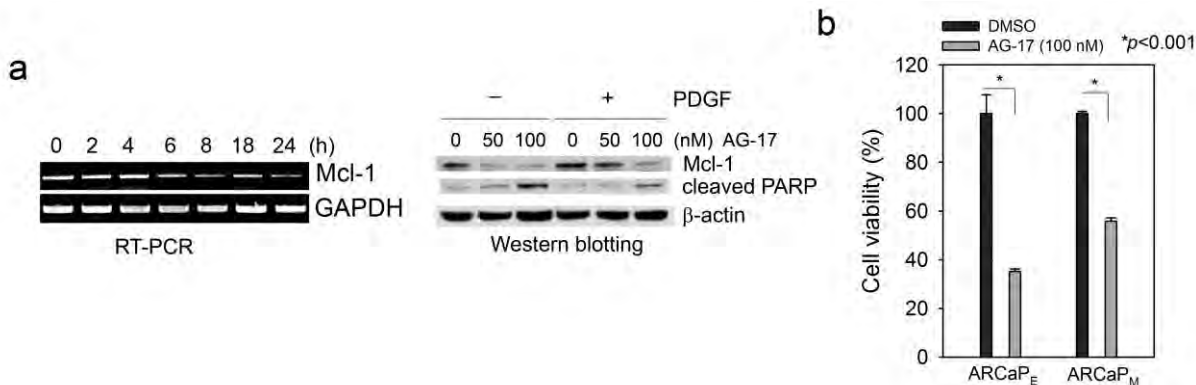


**Figure 28. AG-17 inhibition of Mcl-1 induces apoptosis in bone metastatic PCa cells.** (a) Upper panel: The time-dependent effects of AG-17 (100 nM) on Mcl-1 mRNA expression in ARCaP$_M$ cells; bottom panel: The effects of AG-17 treatment on the expression of Mcl-1 and cleaved PARP in the presence (20 ng/ml) or absence of PDGF-BB (20 ng/ml) in ARCaP$_M$ cells. (b) The effects of AG-17 treatment (100 nM, 72 h) on the viability of ARCaP$_E$ and ARCaP$_M$ cells.

**Key Research Accomplishments**

During the entire period of award performance, our key research accomplishments are:

**1. Elucidation of NRP1 signaling mechanism in bone metastatic PCa cells**. We characterized the regulatory mechanism for VEGF expression, and NRP1-mediated VEGF signaling components in PCa cells. We demonstrated that:

a) CREB is a novel regulator of VEGF expression in bone metastatic PCa cells. CREB may regulate VEGF transcription via a HIF-1α-dependent mechanism in normoxic conditions.
 b) VEGF-NRP1 signaling confers PCa cells resistance to apoptosis and supports tumor growth by inducing expression of Mcl-1 via c-MET-dependent activation of Src kinases and Stat3
c) We identified Mcl-1 as a convergent molecular target of VEGF and PDGF signaling in bone metastatic PCa cells.

**2. Validation of clinical significance of NRP1 signaling components in human PCa bone metastasis**. We validated the clinical significance of the CREB-VEGF-NRP1 signaling components in human PCa bone metastasis. We demonstrated that:

 a) CREB phosphorylation positively correlates to clinical PCa bone metastasis;
b) Serum VEGF was significantly elevated in PCa patients with bone metastasis compared to that in those with non-metastatic PCa;
c) Mcl-1 expression is positively associated with PCa progression, particularly bone metastasis.

**3. Exploration of novel approaches for targeting NRP1 signaling in bone metastatic PCa cells.** We explored the targeting potential of the NRP1-Mcl-1 signaling pathway in treating PCa bone metastasis. Several strategies (including siRNA, shRNA, monoclonal antibody and small molecule agents) were developed to effectively induce apoptosis and tumor regression in pre-clinical models of PCa metastasis.  We demonstrated that:

a) Inhibition of NRP1-Mcl-1 signaling induces PCa cell apoptosis;
b) Genentech NRP1 monoclonal antibodies moderately inhibited proliferation of bone metastatic PCa cells;
c) A small-molecule agent AG-17 blockade of PDGF-Mcl-1 signaling induces apoptosis in bone metastatic PCa cells;
d) We establishment of ARCaP$_M$ cells stably expressing NRP1 shRNA for *in vivo* testing.

**Reportable Outcomes**

**1. Publication/manuscript/abstract**

During the supporting period (04/01/2007-03/31/2011), this project has resulted in 6 peer-reviewed publications, 1 manuscript under review and 3 meeting abstracts (please see the Appendices).

<u>Publications</u>

**Research Papers**

Wu, D., Zhau, H.E., Huang, W.C., Iqbal, S., Habib, F.K., Sartor, O., Cvitanovic, L., Marshall, F.F., Xu, Z., and Chung, L.W. 2007. cAMP-responsive element-binding protein regulates vascular endothelial growth factor expression: implication in human prostate cancer bone metastasis. *Oncogene* 26:5070-5077 (Appendix 1). http://www.ncbi.nlm.nih.gov/pubmed/17310988.

Zhang, S., Zhau, H.E., Osunkoya, A.O., Iqbal, S., Yang, X., Fan, S., Chen, Z., Wang, R., Marshall, F.F., Chung, L.W., et al. 2010. Vascular endothelial growth factor regulates myeloid cell leukemia-1 expression through neuropilin-1-dependent activation of c-MET signaling in human prostate cancer cells. *Mol Cancer* 9:9 (Appendix 4). http://www.ncbi.nlm.nih.gov/pubmed/20085644.

Iqbal S, Zhang S, Driss A, Liu Z-R, Zhau HE, Kucuk O, Chung LWK, Wu D.2011. Platelet-derived growth factor upregulates myeloid cell leukemia-1 through activation of β-catenin and hypoxia-inducible factor-1α-dependent signaling in human bone metastatic prostate cancer cells. *PLoS ONE (manuscript in review)* (Appendix 5).

Seo S, Gera L, Zhau HE, Qian W, Iqbal S, Johnson NA, Zhang S, Zayzafoon M, Stewart J, Wang R, Chung LWK, Wu D. 2008. BKM1740, an acyl-tyrosine bisphosphonate amide derivative, inhibits the bone metastatic growth of human prostate cancer cells by inducing apoptosis. *Clin Cancer Res.,* 14, 6198-6206 (Appendix 6). http://www.ncbi.nlm.nih.gov/pubmed?term=bkm1740.

Zhang S, Zhau HE, Wang X, Osunkoya AO, Chen Z, Iqbal S, Müller S, Chen Z, Josson S, Coleman IM, Nelson PS, Wang R, Shin DM, Marshall FF, Kucuk O, Chung LWK, Wu D. 2011. EPLIN downregulation promotes epithelial-mesenchymal transition and correlates with lymph node metastasis in human prostate cancer. *Oncogene (Epub ahead of print)* (Appendix 7). http://www.ncbi.nlm.nih.gov/pubmed/21625216.

**Reviews**

Sung SY, Hsieh CL, Wu D, Chung LW, Johnstone PA. 2007. Tumor microenvironment promotes cancer progression, metastasis, and therapeutic resistance. *Curr Probl Cancer* 31:36-100 (Appendix 8). http://www.ncbi.nlm.nih.gov/pubmed/17362788

Chung LWK, Huang W-C, Sung S-Y, Wu D, Odero-Marah V and Zhau HE. 2007. Cancer-host interactions: a paradigm shift brings new understanding and new opportunities. In Prostate Cancer: Biology, Genetics and the New Therapeutics (2nd edition) (Chung LWK, Isaacs WB and Simons JW, eds), Humana, Totowa, NJ, 73-86.

<u>Abstract</u>

Wu D, Iqbal S, Seo S, Zhau HE, Chung LWK. Vascular endothelial growth factor (VEGF) is a survival factor in metastatic human prostate cancer cells via induction of myeloid cell leukemia-1 (Mcl-1). American Association for Cancer Research Annual Meeting, Los Angeles, CA, 2007.

Zhang S, Zhau HE, Iqbal S, Chung LWK, Wu D. Vascular endothelial growth factor regulates myeloid cell leukemia-1 expression through neuropilin-1-dependent activation of c-MET signaling in metastatic human prostate cancer cells. American Association for Cancer Research Annual Meeting, Denver, CO, 2009.

Iqbal S, Zhang S, Driss A, Liu Z-R, Zhau HE, Chung LWK, Wu D. Platelet-derived growth factor upregulates myeloid cell leukemia-1 through activation of β-catenin and hypoxia-inducible factor-1α-dependent signaling in human bone metastatic prostate cancer cells. DoD IMPaCT meeting, Orlando, FL, 2011.

## 2. Cell lines and animal models

ARCaP$_M$-C2 cells with high *in vivo* bone metastatic propensity (Zhang et al., Mol. Cancer).
ARCaP$_E$ cells stably expressing NRP1 or pcDNA3.1.
ARCaP$_M$ cells stably expressing NRP1 shRNA.

## 3. New collaborations

We collaborated with Genentech, Inc., in the evaluation of a NRP1 mAb in inhibiting the growth of bone metastatic PCa. We also established new collaboration with Dr. Adeboye Osunkoya at the Department of Pathology, Emory University School of Medicine, in evaluating the expression of VEGF-NRP1 signaling components in human PCa tissues.

## 4. Personnel

> Daqing Wu, Ph.D., Emory University
> Shumin Zhang, Ph.D., Emory University
> Haiyen E. Zhau, Ph.D., Cedars-Sinai Medical Center

## Conclusion

In this DoD PCRP New Investigator Award project, we accomplished three major goals: 1) elucidation of the NRP1 signaling mechanism in bone metastatic PCa cells; 2) evaluation of the clinical significance of NRP1 signaling components in human PCa bone metastasis; and 3) development of novel strategies targeting NRP1 signaling for the treatment of PCa bone metastasis. Our studies provided important evidence supporting a pivotal role of NRP1 in bone metastatic PCa. Interruption of this survival mechanism, thereby, may provide a new strategy to efficiently treat PCa bone metastasis.

# References

1.     Wu, D., Zhau, H.E., Huang, W.C., Iqbal, S., Habib, F.K., Sartor, O., Cvitanovic, L., Marshall, F.F., Xu, Z., and Chung, L.W. 2007. cAMP-responsive element-binding protein regulates vascular endothelial growth factor expression: implication in human prostate cancer bone metastasis. *Oncogene* 26:5070-5077.

2.     Huang, W.C., Wu, D., Xie, Z., Zhau, H.E., Nomura, T., Zayzafoon, M., Pohl, J., Hsieh, C.L., Weitzmann, M.N., Farach-Carson, M.C., et al. 2006. beta2-microglobulin is a signaling and growth-promoting factor for human prostate cancer bone metastasis. *Cancer Res* 66:9108-9116.

3.     Nomura, T., Huang, W.C., Zhau, H.E., Wu, D., Xie, Z., Mimata, H., Zayzafoon, M., Young, A.N., Marshall, F.F., Weitzmann, M.N., et al. 2006. Beta2-microglobulin promotes the growth of human renal cell carcinoma through the activation of the protein kinase A, cyclic AMP-responsive element-binding protein, and vascular endothelial growth factor axis. *Clin Cancer Res* 12:7294-7305.

4.     Zhang, S., Zhau, H.E., Osunkoya, A.O., Iqbal, S., Yang, X., Fan, S., Chen, Z., Wang, R., Marshall, F.F., Chung, L.W., et al. 2010. Vascular endothelial growth factor regulates myeloid cell leukemia-1 expression through neuropilin-1-dependent activation of c-MET signaling in human prostate cancer cells. *Mol Cancer* 9:9.

**Appendices**

1. Wu, D., Zhau, H.E., Huang, W.C., Iqbal, S., Habib, F.K., Sartor, O., Cvitanovic, L., Marshall, F.F., Xu, Z., and Chung, L.W. 2007. cAMP-responsive element-binding protein regulates vascular endothelial growth factor expression: implication in human prostate cancer bone metastasis. *Oncogene* 26:5070-5077. http://www.ncbi.nlm.nih.gov/pubmed/17310988.

2. Huang, W.C., Wu, D., Xie, Z., Zhau, H.E., Nomura, T., Zayzafoon, M., Pohl, J., Hsieh, C.L., Weitzmann, M.N., Farach-Carson, M.C., et al. 2006. beta2-microglobulin is a signaling and growth-promoting factor for human prostate cancer bone metastasis. *Cancer Res* 66:9108-9116 . http://www.ncbi.nlm.nih.gov/pubmed/16982753.

3. Nomura, T., Huang, W.C., Zhau, H.E., Wu, D., Xie, Z., Mimata, H., Zayzafoon, M., Young, A.N., Marshall, F.F., Weitzmann, M.N., et al. 2006. Beta2-microglobulin promotes the growth of human renal cell carcinoma through the activation of the protein kinase A, cyclic AMP-responsive element-binding protein, and vascular endothelial growth factor axis. *Clin Cancer Res* 12:7294-7305. http://www.ncbi.nlm.nih.gov/pubmed/17189401.

4. Zhang, S., Zhau, H.E., Osunkoya, A.O., Iqbal, S., Yang, X., Fan, S., Chen, Z., Wang, R., Marshall, F.F., Chung, L.W., et al. 2010. Vascular endothelial growth factor regulates myeloid cell leukemia-1 expression through neuropilin-1-dependent activation of c-MET signaling in human prostate cancer cells. *Mol Cancer* 9:9. http://www.ncbi.nlm.nih.gov/pubmed/20085644.

5. Iqbal S, Zhang S, Driss A, Liu Z-R, Zhau HE, Kucuk O, Chung LWK, Wu D.2011.  Platelet-derived growth factor upregulates myeloid cell leukemia-1 through activation of β-catenin and hypoxia-inducible factor-1α-dependent signaling in human bone metastatic prostate cancer cells. *PLoS ONE (in review)*.

6. Seo S, Gera L, Zhau HE, Qian W, Iqbal S, Johnson NA, Zhang S, Zayzafoon M, Stewart J, Wang R, Chung LWK, Wu D. 2008. BKM1740, an acyl-tyrosine bisphosphonate amide derivative, inhibits the bone metastatic growth of human prostate cancer cells by inducing apoptosis. *Clin Cancer Res.,* 14, 6198-6206. http://www.ncbi.nlm.nih.gov/pubmed?term=bkm1740.

7. Zhang S, Zhau HE, Wang X, Osunkoya AO, Chen Z, Iqbal S, Müller S, Chen Z, Josson S, Coleman IM, Nelson PS, Wang R, Shin DM, Marshall FF, Kucuk O, Chung LWK, Wu D. 2011. EPLIN downregulation promotes epithelial-mesenchymal transition and correlates with lymph node metastasis in human prostate cancer. *Oncogene (Epub ahead of print)*. http://www.ncbi.nlm.nih.gov/pubmed/21625216.

8. Sung SY, Hsieh CL, Wu D, Chung LW, Johnstone PA. 2007. Tumor microenvironment promotes cancer progression, metastasis, and therapeutic resistance. *Curr Probl Cancer* 31:36-100. http://www.ncbi.nlm.nih.gov/pubmed/17362788

npg

ORIGINAL ARTICLE

# cAMP-responsive element-binding protein regulates vascular endothelial growth factor expression: implication in human prostate cancer bone metastasis

D Wu[1], HE Zhau[1], W-C Huang[1], S Iqbal[1], FK Habib[2], O Sartor[3], L Cvitanovic[4], FF Marshall[1], Z Xu[1] and LWK Chung[1]

[1]Molecular Urology and Therapeutics Program, Department of Urology and Winship Cancer Institute, Emory University School of Medicine, Atlanta, GA, USA; [2]Prostate Research Group, Division of Oncology, School of Molecular and Clinical Medicine, Western General Hospital, Edinburgh, UK; [3]Lank Center for Genitourinary Oncology, Dana-Farber Cancer Institute, Harvard Medical School, Boston, MA, USA and [4]The Stanley Scott Cancer Center at LSU Health Sciences Center, New Orleans, LA, USA

**Aberrant expression of vascular endothelial growth factor (VEGF) is associated with human prostate cancer (PCa) metastasis and poor clinical outcome. We found that both phosphorylation of cyclic AMP-responsive element-binding protein (CREB) and VEGF levels were significantly elevated in patient bone metastatic PCa specimens. A PCa ARCaP progression model demonstrating epithelial-to-mesenchymal transition exhibited increased CREB phosphorylation and VEGF expression as ARCaP cells became progressively more mesenchymal and bone-metastatic. Activation of CREB induced, whereas inhibition of CREB blocked, VEGF expression in ARCaP cells. CREB may regulate VEGF transcription *via* a hypoxia-inducible factor-dependent mechanism in normoxic conditions. Activation of CREB signaling is involved in the coordinated regulation of VEGF and may pre-dispose to PCa bone metastasis.**

## Introduction

Cyclic AMP (cAMP)-responsive element-binding protein (CREB) signaling is implicated in tumor progression, stimulating growth, conferring apoptotic resistance and supporting angiogenesis (Abramovitch *et al.*, 2004; Kinjo *et al.*, 2005). In human prostate cancer (PCa), CREB may promote acquisition of neuroendocrine differentiation, associated with androgen-independent progression (Chen *et al.*, 1999; Deeble *et al.*, 2001). Previous studies from our laboratory and others indicated that CREB signaling regulated osteomimicry in PCa bone metastasis, conferring tumor survival and growth advantages in the bone microenvironment (Huang *et al.*, 2006). Our results demonstrated that $\beta$-2 microglobulin activation of protein kinase A (PKA)-CREB signaling resulted in increased expression of osteocalcin and bone sialoprotein and conferred explosive PCa growth in bone. This communication seeks to demonstrate a functional link between CREB activation and vascular endothelial growth factor (VEGF) expression in PCa bone metastasis.

Increased plasma levels of VEGF correlate with clinical lymph node and skeletal metastasis in PCa (Duque *et al.*, 1999; George *et al.*, 2001; Chen *et al.*, 2004). Overexpression of VEGF and its receptors is associated with increased tumor vascularity, metastasis, chemoresistance and poor prognosis (Ferrer *et al.*, 1998). VEGF may affect bone remodeling and facilitate nesting of metastatic cancer cells, crucial for tropism during bone metastasis (Kitagawa *et al.*, 2005). VEGF-induced activation of VEGFR-1 may promote tumor progression by inducing epithelial-to-mesenchymal transition (EMT) (Yang *et al.*, 2006), tumor cell migration, invasion and metastasis (Huber *et al.*, 2005).

VEGF expression is regulated by several factors (Ferrara *et al.*, 2003). Hypoxia is a major modulator. Hypoxia inducible factor-1 (HIF-1) is a key regulator of transcriptional response to hypoxia, binding the hypoxia-response elements (HREs) within VEGF promoter, and activation of VEGF promoter activity (Forsythe *et al.*, 1996). Optimal control of VEGF expression requires the assembly of a transcriptional complex dynamically coordinated by HIF-$1\alpha$ and its co-activators, including CREB-binding protein (CBP)/p300 (Arany *et al.*, 1996; Niu *et al.*, 2002; Ziel *et al.*, 2004). In this study, we demonstrate that CREB may be crucial for promoting PCa bone metastasis, inducing VEGF expression via HIF-1-dependent signaling.

## Results

### Expression of activated CREB in human PCa tissue specimens

To investigate the clinicopathologic significance of CREB, we analysed the immunohistochemical (IHC) protein expression of phosphorylated CREB (p-CREB) in primary and bone metatstatic PCa tissue. We defined well-differentiated PCa as Gleason score $\leqslant 6$ and poorly-differentiated PCa as Gleason score $\geqslant 8$. In all specimens, activated CREB or nuclear localization of p-CREB expression was undetectable in normal/benign glands (0/5; Figure 1a) or well-differentiated cancer (0/5; Figure 1b) but was positively associated with poorly-differentiated cancers (5/5; Figure 1c). All seven PCa bone metastatic tissue specimens were positive for p-CREB (Figure 1d).

### CREB activation is associated with bone metastatic potential and EMT

We used a human PCa ARCaP progression model with EMT properties (Zhau et al., 1996; Xu et al., 2006) to investigate the roles of CREB in PCa bone metastasis. An ARCaP subclone, ARCaP$_E$, has a relatively low propensity for bone metastasis (12.5%) after intracardiac injection, whereas ARCaP$_M$, a bone metastatic derivative of ARCaP closely associated with ARCaP$_E$, has dramatically greater bone metastatic potential (100%) and significantly shorter latency.

Western blot analysis (Figure 2a) showed a slight increase in CREB expression in ARCaP$_M$ total lysates, with significantly elevated activated CREB. Phosphorylation of activating transcription factor-1, a member of the CREB transcription factor family, was also elevated



**Figure 1** CREB phosphorylation positively correlates to clinical PCa progression. IHC analysis of p-CREB expression in PCa tumor specimens. p-CREB expression (arrows) was seen in poorly-differentiated primary tumors and bone-metastatic tumors, but not in normal/benign prostatic glands or well-differentiated primary tumors.

in ARCaP$_M$ cells. p-CREB proteins were more abundant in the ARCaP$_M$ nucleus, indicating activation of CREB-dependent transcription. The association of p-CREB expression with increased bone metastatic potential was confirmed in tumor tissues from ARCaP primary and bone metastasis specimens (Figure 2b).

### Serum levels of VEGF in PCa patients positively correlate with bone metastasis

A double-blind study measured VEGF levels in sera from 31 patients with non-metastatic PCa versus 24 patients with bone-metastatic PCa. Enzyme-linked immunosorbent assay (ELISA) results indicate a statistically significant difference between the two groups ($P = 0.0013$). The mean serum level of VEGF in patients with non-bone metastatic PCa was 207.8 pg/ml (27.3–613.6 pg/ml) and 397.4 pg/ml in patients with bone metastasis (135.6–1,083.7 pg/ml) (Figure 3), suggesting that serum VEGF positively correlates with bone-metastatic status. In this study, the average serum prostate-specific antigen (PSA) levels of these two groups of patients were 3.1 ng/ml (incomplete data, $n = 19$; serum PSA in eight patients was less than 0.1 ng/ml) and 358.1 ng/ml, ($n = 24$), respectively ($P = 0.004$). However, the possible effects of treatment on serum VEGF in patients with bone metastasis were not determined.

### Activation of CREB induces VEGF transcription in ARCaP cells

We examined differential expression of VEGF transcripts in normoxic ARCaP cells. The human VEGF gene consists of eight exons, and alternative exon splicing generates at least four isoforms: VEGF$_{121}$, VEGF$_{165}$, VEGF$_{189}$ and VEGF$_{206}$. VEGF$_{165}$ is the predominant isoform, with optimal bioavailability and is responsible for VEGF biological potency (Ferrara et al., 2003). Reverse transcription–polymerase chain reaction (RT–PCR) analysis showed elevated endogenous mRNA levels of both VEGF$_{121}$ and VEGF$_{165}$ in ARCaP$_M$ cells (Figure 4a). ELISA of ARCaP-conditioned medium (CM) confirmed a two-fold increase in total VEGF secretion by ARCaP$_M$ when compared to ARCaP$_E$ cells (Figure 4b), indicating that VEGF upregulation occurred in normoxic PCa cells and this increased secretion may be associated with EMT and the invasiveness of PCa cells.

Pharmacological and gene transfer experiments in ARCaP$_E$ cells explored whether CREB activation is responsible for VEGF expression in PCa cells. Treatment with adenylate cyclase activator forskolin (FSK) rapidly increased VEGF mRNA levels, with more significant induction of VEGF$_{165}$ than VEGF$_{121}$ (Figure 5a). Conversely, a PKA selective inhibitor, H89, reduced VEGF mRNA levels. VEGF ELISA in ARCaP$_E$ CM confirmed these results; VEGF secretion was induced by FSK and inhibited by H89 (Figure 5b). VEGF expression may be controlled by PKA–CREB signaling in normoxic PCa cells.
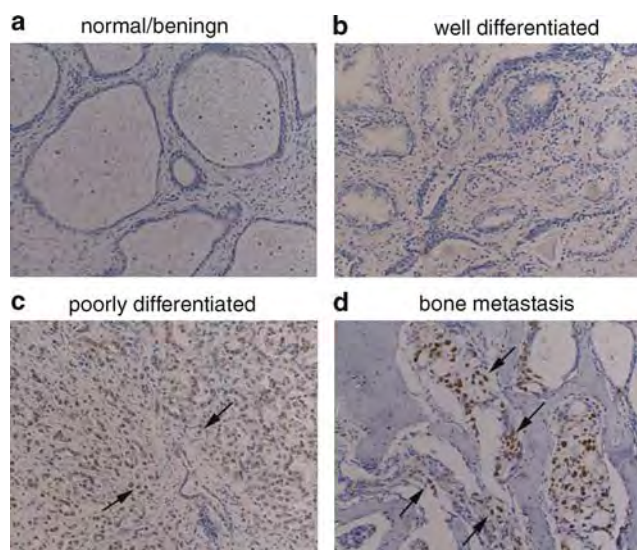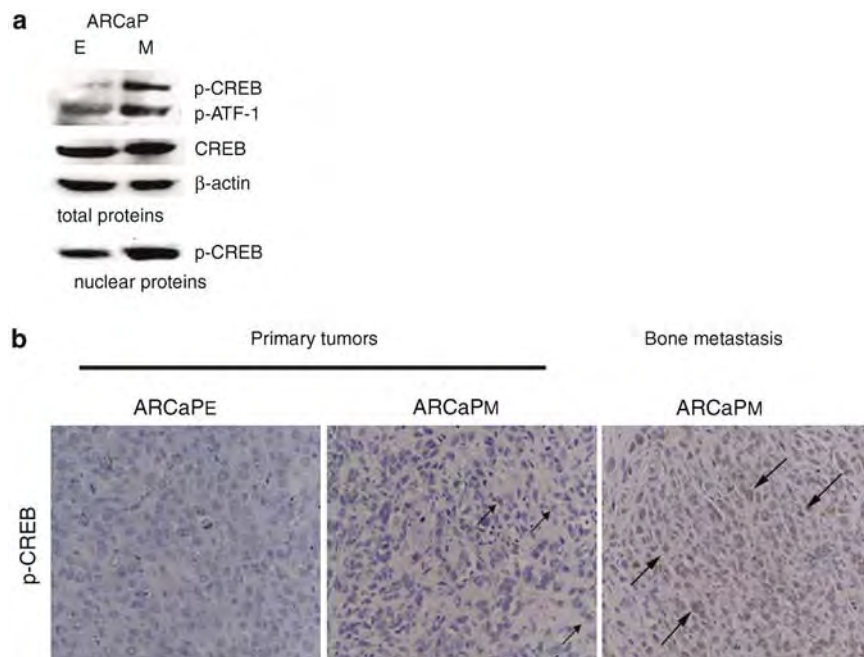
**Figure 2** CREB phosphorylation is associated with bone-metastatic potential and EMT. (**a**) Western blot analysis demonstrated increased expression of p-CREB in whole-cell lysates and nuclear portions of ARCaP$_M$ cells. (**b**) IHC staining of p-CREB increased in primary tumor specimens of ARCaP$_M$ and increased further in ARCaP$_M$ bone-metastatic tissue specimens.
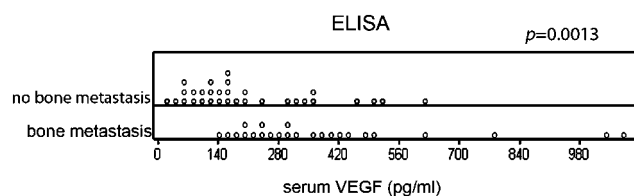


**Figure 3** Serum VEGF levels are associated with PCa bone metastasis. Dot-plot analysis showed there is a statistically significant difference between serum VEGF levels in patients with non-bone metastatic tumors ($n = 31$) and with bone-metastasis ($n = 24$).



**Figure 4** VEGF upregulation is associated with bone-metastatic potential and EMT. (**a**) Expression of VEGF isoforms VEGF$_{165}$ and VEGF$_{121}$ was increased in ARCaP$_M$ cells in normoxia. (**b**) VEGF secretion increased in ARCaP$_M$ CM ($P < 0.01$). Relative VEGF levels were normalized by dividing VEGF concentrations (pg/ml) by total protein concentrations (mg/ml) in CM.

ARCaP$_E$ cells were transiently transfected with expression vectors for wild-type CREB (WTCREB), a dominant-negative mutant of CREB (KCREB), using empty vector (pCMV) as the control. KCREB forms an inactive dimer with CREB, blocking its ability to bind cAMP-responsive element (CRE) without interfering with CREB phosphorylation (Yang *et al.*, 1996). Western blot analysis confirmed expression of WTCREB or KCREB. p-CREB expression was significantly higher in WTCREB-transfected ARCaP$_E$ cells and slightly increased in KCREB-transfected cells (Figure 5c). RT–PCR analysis showed that mRNA levels of VEGF$_{165}$ and VEGF$_{121}$ were remarkably enhanced by WTCREB but inhibited by KCREB (Figure 5d), suggesting that CREB could regulate VEGF transcription in ARCaP cells.

*HIF-1α is required for CREB regulation of VEGF in ARCaP cells*
CREB phosphorylation and binding to CRE motif are sufficient for CREB regulation of most target genes

(Mayr and Montminy, 2001). We investigated whether p-CREB directly interacts with putative CRE site(s) within VEGF promoter to regulate VEGF transcription. We performed computational analysis on the 5′-flanking sequence of the human VEGF gene using rVista 2.0 (Loots and Ovcharenko, 2004) and TRANSFAC (BIOBASE, Wolfenbüttel, German). No CRE consensus (TGA<u>C</u>GTCA) was found within 6 kb of the 5′-flanking region, though a putative CRE site was located about 5 kb upstream from the transcriptional start site, with one base variation (TGA<u>G</u>GTCA) (Figure 6a). We used a pVEGF–KpnI plasmid (Forsythe *et al.*, 1996) for a reporter assay, with a 2.65 kb fragment of VEGF promoter including a 47-bp HRE sequence (−985 to −939 bp) but not the putative CRE motif (Figure 6a). ARCaP$_E$ cells were transiently transfected with pVEGF–KpnI and then the expression vector for

WTCREB or KCREB, with pCMV as control. Luciferase activity showed that WTCREB increased and KCREB inhibited VEGF reporter activity (Figure 6b), confirming that CREB induces VEGF transcription in normoxic PCa cells and suggesting the putative CRE site may be dispensable for CREB induction of VEGF. CREB may rely on HIF-1α to regulate VEGF expression in PCa cells, as higher basal HIF-1α expression was found in ARCaP$_M$ cells compared with normoxic ARCaP$_E$ cells (Figure 6c). ARCaP$_M$ also expresses more p-CREB and VEGF (Figures 3a and 4).

HIF-1α small interfering RNA (siRNA) experiments tested whether HIF-1α-dependent gene transcription is involved in CREB regulation of VEGF transcription. HIF-1α siRNA inhibited endogenous HIF-1α expression in ARCaP$_E$ cells. FSK could stimulate VEGF transcription in control-siRNA, but not HIF-1α-siRNA-transfected ARCaP$_E$ cells (Figure 6d). These data suggest that HIF-1α and CREB activation are essential to promote VEGF expression in PCa cells.

### Activation of CREB recruits HIF-1α and facilitates its binding to VEGF promoter region

To examine whether activated CREB induced intracellular translocation of HIF-1α, ARCaP$_E$ nuclear proteins were extracted after FSK treatment (10 μM) at various time periods. Western blot analysis showed dynamic changes in expression of several CREB-interacting transcription factors in the nucleus. Thirty minutes after FSK stimulation, nuclear p-CREB and HIF-1α increased rapidly and increased further at 60 min. CBP expression in the nucleus, which directly interacts with CREB and HIF-1α (Chrivia et al., 1993; Arany et al., 1996), increased at 30 min and decreased significantly at 60 min, with only a slight increase in nuclear p300 at 30 min (Figure 7a). CREB activation seems to be accompanied by a dynamic change in nuclear accumulation of HIF-1α, CBP and p300, which may form a transcriptional complex induced by hypoxia or FSK to regulate VEGF promoter activity and HIF-1α-dependent transcription.
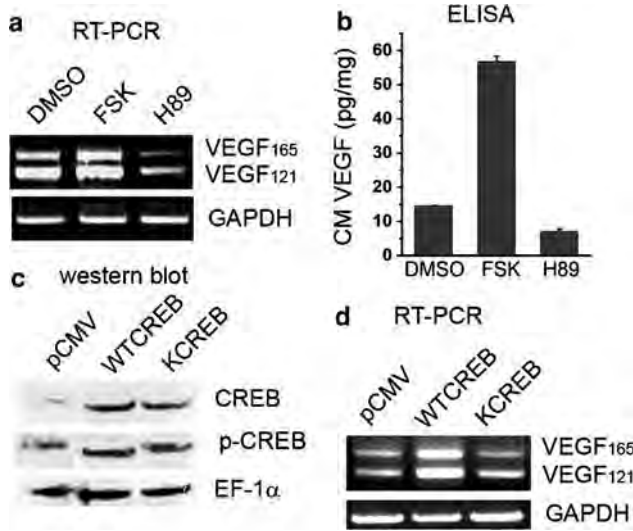


**Figure 5** CREB regulates VEGF transcription in ARCaP cells. (**a**) FSK treatment (10 μM; 4 h) induced and H89 (5 μM) inhibited VEGF transcription in ARCaP$_E$ cells. (**b**) FSK treatment (2 days) induced and H89 inhibited VEGF secretion in ARCaP$_E$ CM. (**c**) Transient expression (72 h) of pCMV (vector), WTCREB or KCREB in ARCaP$_E$ cells. (**d**) Ectopic expression (72 h) of WTCREB induced and KCREB inhibited VEGF transcription in ARCaP$_E$ cells.



**Figure 6** HIF-1α is required for CREB regulation of VEGF transcription in normoxia. (**a**) Schematic description of the human VEGF 5′-flanking region. The locations of HRE and a putative CRE site are shown relative to the transcriptional initiation site in human VEGF gene. (**b**) pVEGF–KpnI reporter activity was induced by transient expression (48 h) of WTCREB but inhibited by KCREB in ARCaP$_E$ cells. (**c**) HIF-1α expression was increased in total lysates and nucleus of ARCaP$_M$ cells. (**d**) HIF-1α siRNA transfection (48 h) reduced HIF-1α expression in ARCaP$_E$ cells. FSK (10 μM; 2 h) induced VEGF transcription in ARCaP$_E$ cells transfected with control siRNA (48 h), but not in HIF-1α siRNA-treated cells.

**Figure 7** Activation of CREB may induce a HIF-1α-dependent transcriptional complex on VEGF promoter. (**a**) FSK (10 μM) induced rapid nuclear translocation of p-CREB, HIF-1α, CBP and p300 in ARCaP$_E$ cells. (**b**) Transcription factor ELISA assay demonstrated that FSK (10 μM) induced specific-binding of ARCaP$_E$ nuclear extracts to the HRE consensus in a time-dependent manner, which was inhibited by wild-type HRE oligonucleotide, but not by mutated oligonucleotide. *COS nu. prot:* CoCl$_2$-treated COS-7 nuclear extract (5 μg); *wt. oligo*: Wild-type HRE consensus; *mut. oligo*: mutated HRE consensus; *nu. prot*: ARCaP$_E$ nuclear proteins. (**c**) ChIP assay demonstrated that FSK treatment (10 μM) induced specific binding of HIF-1α to the HRE site within the VEGF promoter in ARCaP$_E$ cells, but not in KCREB-transfected cells. (**d**) Transient expression of WTCREB induced, but KCREB inhibited, HIF-1α reporter activity in ARCaP$_E$ cells.

To determine whether CREB activation induces HIF-1α-binding to HRE, we used ELISA to quantify HIF-1α activation and binding to HRE in ARCaP$_E$ cells (Figure 7b). Five micrograms of nuclear extract from COS-7 cells treated with cobalt chloride (CoCl$_2$) was added as a positive control (Jiang et al., 1997). Wild-type HRE consensus oligonucleotide competitively inhibited binding of COS-7 nuclear extract, which contains HIF-1α to HRE; mutated consensus oligonucleotide did not. ARCaP$_E$ nuclear extracts prepared after cells were treated with FSK for various times showed a time-dependent increased binding of ARCaP$_E$ nuclear extracts to the HRE consensus that was inhibited by incubation with wild-type but not mutated HRE oligonucleotide. On the contrary, FSK did not induce binding of nuclear extracts to the HRE consensus in KCREB-transfected ARCaP$_E$ cells (Supplemental data). The data suggest that CREB activation by FSK induced specific interaction between

the ARCaP$_E$ nuclear transcription complex, which comprises CREB/HIF-1α and the HRE consensus.

We investigated whether CREB activation promoted specific binding of HIF-1α to VEGF promoter by chromatin immunoprecipitation (ChIP) assay. Fractionated chromatin from controls and FSK-treated ARCaP$_E$ cells was immunoprecipitated with HIF-1α antibody or control IgG. From the isolated DNA, a 135-bp region was amplified by PCR (Kong et al., 2005). Activation of CREB signaling by FSK showed a considerable increase in HIF-1α binding with the HRE region in ARCaP$_E$ cells, but not in KCREB-transfected ARCaP$_E$ cells (Figure 7c), demonstrating that CREB activation facilitates association of HIF-1α with VEGF promoter. Further supporting this model, HIF-1α reporter activity was significantly induced in WTCREB-transfected, but not in KCREB-transfected ARCaP$_E$ cells in the pHIF1-luc reporter assay (Figure 7d).

## Discussion

CREB regulates gene expression in a highly tissue- and cell type-specific manner (Impey et al., 2004; Zhang et al., 2005). Selective activation of CREB could promote local tumor growth and distant metastasis (Huang et al., 2006; Melnikova et al., 2006). Many modulators of CREB activity are abundant in bone tissues, such as stromal cell-derived factor-1, fibroblast growth factor, transformation growth factor (Johannessen et al., 2004) and $\beta$-2-microglobulin (Huang et al., 2006). The activation status of CREB in ARCaP$_E$ and ARCaP$_M$ cells suggests that bone microenvironments may induce CREB phosphorylation in bone-homing PCa cells. CREB activation may thereby promote osteomimicry (Huang et al., 2005) and angiogenesis (Abramovitch et al., 2004) through either a direct or indirect mechanisms. In this report, our evidence emphasized the clinicopathological link of CREB–VEGF signaling and human PCa bone metastasis.

A variety of genes targeted by CREB activation are implicated in tumorigenesis, such as cyclin D1 (Sabbah et al., 1999), cyclin A (Desdouets et al., 1995) and Bcl-2 (Arcinas et al., 2001). In a genome-wide search for the CREB 'regulon' by Impey et al., (2004), FSK treatment significantly increased VEGF transcription in PC12 cells. These results suggest that VEGF is a novel CREB target. Our analysis of 6 kb of the 5′-flanking region of human VEGF gene did not identify any CRE consensus sequence in the proximal region ($\leqslant 2$ kb) of this promoter, suggesting that CREB may regulate VEGF transcription without directly binding CRE sites. Indeed, pVEGF–KpnI, containing no CRE consensus, was still responsive to CREB modulation in ARCaP$_E$ cells (Figure 6b). CREB may directly bind CRE site(s) as a complex with other transcription factors to regulate VEGF transcription (Figure 4a). Cloning and analysis of the 6 kb 5′-flanking region of VEGF gene may elucidate the direct role of CREB in regulating VEGF expression.

VEGF expression is depressed under normoxic conditions, mainly by degradation of HIF-1$\alpha$ (Kallio et al., 1999). However, it has been demonstrated that HIF-1$\alpha$ is a positive factor regulating proliferation in certain tumors under normoxic conditions (Dang et al., 2006). As ARCaP cells express both endogenous HIF-1$\alpha$ and CREB, it is possible that CREB regulates VEGF in a HIF-1$\alpha$-dependent manner via formation of a transcription complex in normoxic PCa cells. Coordinated activation of CREB/HIF-1$\alpha$ may thereby directly contribute to the elevated serum VEGF levels in bone-metastatic PCa patients.

CREB-interacting protein (CBP) and its paralogue p300 are key regulators of RNA polymerase II-mediated transcription. By differentially associating with other transcription factors, CBP/p300 specifically regulates gene expression via intrinsic histone acetyltransferase activity (Vo and Goodman, 2001). CREB phosphorylation promotes interaction between CREB and CBP/p300 to induce CREB-dependent transcription (Chrivia et al., 1993). Most situations require additional
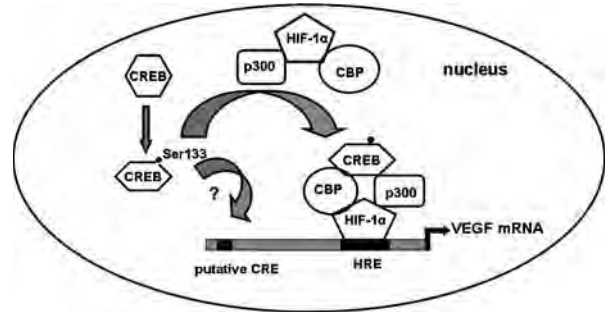


**Figure 8** Proposed model for CREB regulation of VEGF expression. CBP or p300 may be scaffold proteins for p-CREB and HIF-1$\alpha$ to form a transcriptional complex on VEGF promoter in response to CREB activation.

CREB-regulatory partners to recruiting transcriptional machinery (Zhang et al., 2005). This may explain the highly cell context-dependent regulation of various genes by CREB (Impey et al., 2004; Zhang et al., 2005). More than 40 transcription factors can interact with CBP/p300 directly. CBP/p300 may be the scaffold for various transcription complexes that regulate target gene expression. Interestingly, both CREB and HIF-1$\alpha$ interact with CBP/p300 (Chrivia et al., 1993; Arany et al., 1996) CBP/p300 may, therefore, be a physical bridge between CREB and HIF-1$\alpha$ (Figure 8).

Increased VEGF production/secretion after CREB activation also induces EMT in cancer cells. VEGF-binding and activation of VEGFR-1 in pancreatic cancer cells resulted in morphologic and molecular alterations associated with EMT (Yang et al., 2006). Our study is the first to implicate CREB–VEGF signaling in EMT and acquisition of invasive phenotypes during PCa progression.

## Materials and methods

### Collection of serum specimens
After informed consent, serum specimens (10–20 ml) for VEGF analysis were collected from patients with confirmed PCa with or without bone-scan-confirmed metastasis.

### IHC staining
Human normal/benign prostatic glands, primary PCa, and bone metastatic PCa tissue specimens were analysed for p-CREB expression by IHC as described (Xu et al., 2006). Positive p-CREB is defined as >15% positive reaction by the cell population to anti-p-CREB antibody (Cell Signaling, Beverly, MA, USA).

### Cell cultures
Human PCa cell lines ARCaP$_E$ and ARCaP$_M$ were cultured as described previously (Chung et al., 1991; Zhau et al., 1996; Xu et al., 2006). Serum-starved ARCaP cells were treated with FSK or H89 (Calbiochemicals, San Diego, CA, USA) in serum-free T-medium (Invitrogen, Carlsbad, CA, USA).

### Plasmids and transient transfection
The expression vectors for WTCREB and KCREB (Clontech, Mountain View, CA, USA) were transfected into ARCaP$_E$

cells using lipofectamine 2000 (Invitrogen) and incubated for 72 h. For siRNA treatment, ARCaP$_E$ cells were transfected with VEGF siRNA, HIF-1α siRNA or control siRNA-A (Santa Cruz Biotechnology, Santa Cruz, CA, USA) at a final concentration of 80 nM for 72 h.

*Reporter assay*
ARCaP$_E$ cells were seeded at a density of $1.5 \times 10^5$ cells per well in 12-well plates 24 h before transfection. pVEGF–KpnI (Forsythe *et al.*, 1996) (American Type Culture Collection, Manassas, VA, USA) or pHIF1-luc (Panomics, Fremont, CA, USA) was introduced using lipofectamine 2000. Data were presented as relative luciferase activity (luciferase activity normalized to internal control β-galactosidase activity).

*CM preparation*
Subconfluent cells were cultured in serum-free T-medium for 48 h before CM were collected (Huang *et al.*, 2005).

*VEGF ELISA in patients with PCa*
VEGF concentration in ARCaP CM, or serum VEGF from PCa patients was analysed using a Quantikine ELISA kit (R&D Systems, Minneapolis, MN, USA).

*Western blot analysis*
Immunoblotting analysis followed standard procedure with anti-CREB and anti-p-CREB (Cell Signaling); anti-CBP, anti-p300 (Santa Cruz Biotechnology); anti-HIF-1α (Upstate, Charlottesville, VA, USA); anti-β-actin (Sigma, St Louis, MO, USA); anti-EF1α (BD Transduction Laboratories, San Diego, CA, USA).

*Preparation of nuclear extracts*
ARCaP cells were serum-starved overnight and incubated for 2 h with FSK (10 μM) or dimethyl sulfoxide (DMSO). Nuclear proteins were prepared using a NucBuster Protein Extraction Kit (Novagen, San Diego, CA, USA).

*RT–PCR*
Total RNA (1 μg) was used as template in a reaction using the SuperScriptIII OneStep RT–PCR kit (Invitrogen). The human VEGF primers were described by Bates *et al.*, (2003). The primers for glyceraldehyde-3-phosphate dehydrogenase (GAPDH) are 5′-GTCAGTGGTGGACCTGACCT-3′ (forward) and 5′-AGGGGTCTACATGGCAACTG-3′ (reverse). The primer pair for human HIF-1α was from Santa Cruz Biotechnology. The thermal profile is 30 cycles for human VEGF or HIF-1α amplification or 20 cycles for GAPDH, with 15 s, 94°C; 30 s, 55°C; and 60 s, 68°C.

*DNA-binding assays*
An ELISA-based assay (TransAM HIF-1) to analyse HIF-1α/HRE interaction was used according to the manufacturer's protocol (ActiveMotif, Carlsbad, CA, USA). Nuclear extracts were incubated in 96-well plates precoated with the HRE consensus oligonucleotides. HIF-1α antibody was added to the reactions and an HRP-conjugated secondary antibody was used to quantify the HRE-binding activity of nuclear extracts. The ChIP assay used a ChIP-IT kit (ActiveMotif). ARCaP$_E$ cells ($1 \times 10^7$) were serum-starved overnight and replaced with fresh serum-free medium, incubated with FSK (10 μM) or DMSO for 2 h. Chromatin was sheared by enzymatic shearing for 8 min. A portion of chromatin was reversed and used as input DNA. For immunoprecipitation, 2 μg HIF-1α antibody (Santa Cruz Biotechnology) was used. PCR primers for HRE region in VEGF promoter are from published sequences (Kong *et al.*, 2005). Negative PCR primer pair included in the ChIP kit was used as negative control. PCRs were performed for 30 cycles, with primer concentration as 10 pmol/20 μl.

*Data analysis*
All data are representative of three or more experiments. Treatment effects were evaluated using a two-sided Student's *t*-test. Errors are standard error values of averaged results, and values of $P < 0.05$ were taken as a significant difference between means.

**Abbreviations**

ATF, activating transcription factor; cAMP, cyclic AMP; CBP, CREB-binding protein; ChIP, chromatin immunoprecipitation; CM, conditioned medium; CRE, cAMP-responsive element; CREB, CRE-binding protein; ELISA, enzyme-linked immunosorbent assay; EMT, epithelial-to-mesenchymal transition; FSK, forskolin; IHC, immunohistochemistry; HIF, hypoxia-inducible factor; HRE, hypoxia-response element; PCa, prostate cancer; p-CREB, phosphorylated CREB; PKA, protein kinase A; RT–PCR, reverse-transcription–PCR; siRNA, small interfering RNA; VEGF, vascular endothelial growth factor; VEGFR, VEGF receptor.

**References**

Abramovitch R, Tavor E, Jacob-Hirsch J, Zeira E, Amariglio N, Pappo O *et al.* (2004). A pivotal role of cyclic AMP-responsive element binding protein in tumor progression. *Cancer Res* **64**: 1338–1346.

Arany Z, Huang LE, Eckner R, Bhattacharya S, Jiang C, Goldberg MA *et al.* (1996). An essential role for p300/CBP in the cellular response to hypoxia. *Proc Natl Acad Sci USA* **93**: 12969–12973.

Arcinas M, Heckman CA, Mehew JW, Boxer LM. (2001). Molecular mechanisms of transcriptional control of bcl-2 and c-myc in follicular and transformed lymphoma. *Cancer Res* **61**: 5202–5206.

Bates RC, Goldsmith JD, Bachelder RE, Brown C, Shibuya M, Oettgen P *et al.* (2003). Flt-1-dependent survival characterizes the epithelial-mesenchymal transition of colonic organoids. *Curr Biol* **13**: 1721–1727.

Chen J, De S, Brainard J, Byzova TV. (2004). Metastatic properties of prostate cancer cells are controlled by VEGF. *Cell Commun Adhes* **11**: 1–11.

Chen T, Cho RW, Stork PJ, Weber MJ. (1999). Elevation of cyclic adenosine 3′,5′-monophosphate potentiates activation of mitogen-activated protein kinase by growth factors in LNCaP prostate cancer cells. *Cancer Res* **59**: 213–218.

Chrivia JC, Kwok RP, Lamb N, Hagiwara M, Montminy MR, Goodman RH. (1993). Phosphorylated CREB binds specifically to the nuclear protein CBP. *Nature* **365**: 855–859.

Chung LW, Gleave ME, Hsieh JT, Hong SJ, Zhau HE. (1991). Reciprocal mesenchymal-epithelial interaction affecting prostate tumour growth and hormonal responsiveness. *Cancer Surv* **11**: 91–121.

Dang DT, Chen F, Gardner LB, Cummins JM, Rago C, Bunz F et al. (2006). Hypoxia-inducible factor-1alpha promotes nonhypoxia-mediated proliferation in colon cancer cells and xenografts. *Cancer Res* **66**: 1684–1936.

Deeble PD, Murphy DJ, Parsons SJ, Cox ME. (2001). Interleukin-6- and cyclic AMP-mediated signaling potentiates neuroendocrine differentiation of LNCaP prostate tumor cells. *Mol Cell Biol* **21**: 8471–8482.

Desdouets C, Matesic G, Molina CA, Foulkes NS, Sassone-Corsi P, Brechot C et al. (1995). Cell cycle regulation of cyclin A gene expression by the cyclic AMP-responsive transcription factors CREB and CREM. *Mol Cell Biol* **15**: 3301–3309.

Duque JL, Loughlin KR, Adam RM, Kantoff PW, Zurakowski D, Freeman MR. (1999). Plasma levels of vascular endothelial growth factor are increased in patients with metastatic prostate cancer. *Urology* **54**: 523–527.

Ferrara N, Gerber HP, LeCouter J. (2003). The biology of VEGF and its receptors. *Nat Med* **9**: 669–676.

Ferrer FA, Miller LJ, Andrawis RI, Kurtzman SH, Albertsen PC, Laudone VP et al. (1998). Angiogenesis and prostate cancer: in vivo and in vitro expression of angiogenesis factors by prostate cancer cells. *Urology* **51**: 161–167.

Forsythe JA, Jiang BH, Iyer NV, Agani F, Leung SW, Koos RD et al. (1996). Activation of vascular endothelial growth factor gene transcription by hypoxia-inducible factor 1. *Mol Cell Biol* **16**: 4604–4613.

George DJ, Halabi S, Shepard TF, Vogelzang NJ, Hayes DF, Small EJ et al. (2001). Prognostic significance of plasma vascular endothelial growth factor levels in patients with hormone-refractory prostate cancer treated on cancer and leukemia group B 9480. *Clin Cancer Res* **7**: 1932–1936.

Huang WC, Wu D, Xie Z, Zhau HE, Nomura T, Zayzafoon M et al. (2006). beta2-microglobulin is a signaling and growth-promoting factor for human prostate cancer bone metastasis. *Cancer Res* **66**: 9108–9116.

Huang WC, Xie Z, Konaka H, Sodek J, Zhau HE, Chung LW. (2005). Human osteocalcin and bone sialoprotein mediating osteomimicry of prostate cancer cells: role of cAMP-dependent protein kinase A signaling pathway. *Cancer Res* **65**: 2303–2313.

Huber MA, Kraut N, Beug H. (2005). Molecular requirements for epithelial-mesenchymal transition during tumor progression. *Curr Opin Cell Biol* **17**: 548–558.

Impey S, McCorkle SR, Cha-Molstad H, Dwyer JM, Yochum GS, Boss JM et al. (2004). Defining the CREB regulon: a genome-wide analysis of transcription factor regulatory regions. *Cell* **119**: 1041–1054.

Jiang BH, Zheng JZ, Leung SW, Roe R, Semenza GL. (1997). Transactivation and inhibitory domains of hypoxia-inducible factor 1alpha. Modulation of transcriptional activity by oxygen tension. *J Biol Chem* **272**: 19253–19260.

Johannessen M, Delghandi MP, Moens U. (2004). What turns CREB on? *Cell Signal* **16**: 1211–1227.

Kallio PJ, Wilson WJ, O'Brien S, Makino Y, Poellinger L. (1999). Regulation of the hypoxia-inducible transcription factor 1alpha by the ubiquitin-proteasome pathway. *J Biol Chem* **274**: 6519–6525.

Kinjo K, Sandoval S, Sakamoto KM, Shankar DB. (2005). The role of CREB as a proto-oncogene in hematopoiesis. *Cell Cycle* **4**: 1134–1135.

Kitagawa Y, Dai J, Zhang J, Keller JM, Nor J, Yao Z et al. (2005). Vascular endothelial growth factor contributes to prostate cancer-mediated osteoblastic activity. *Cancer Res* **65**: 10921–10929.

Kong D, Park EJ, Stephen AG, Calvani M, Cardellina JH, Monks A et al. (2005). Echinomycin, a small-molecule inhibitor of hypoxia-inducible factor-1 DNA-binding activity. *Cancer Res* **65**: 9047–9055.

Loots GG, Ovcharenko I. (2004). rVISTA 2.0: evolutionary analysis of transcription factor binding sites. *Nucleic Acids Res* **32**: W217–W221.

Mayr B, Montminy M. (2001). Transcriptional regulation by the phosphorylation-dependent factor CREB. *Nat Rev Mol Cell Biol* **2**: 599–609.

Melnikova VO, Mourad-Zeidan AA, Lev DC, Bar-Eli M. (2006). Platelet-activating factor mediates MMP-2 expression and activation via phosphorylation of cAMP-responsive element-binding protein and contributes to melanoma metastasis. *J Biol Chem* **281**: 2911–2922.

Niu G, Wright KL, Huang M, Song L, Haura E, Turkson J et al. (2002). Constitutive Stat3 activity up-regulates VEGF expression and tumor angiogenesis. *Oncogene* **21**: 2000–2008.

Sabbah M, Courilleau D, Mester J, Redeuilh G. (1999). Estrogen induction of the cyclin D1 promoter: involvement of a cAMP response-like element. *Proc Natl Acad Sci USA* **96**: 11217–11222.

Vo N, Goodman RH. (2001). CREB-binding protein and p300 in transcriptional regulation. *J Biol Chem* **276**: 13505–13508.

Xu J, Wang R, Xie ZH, Odero-Marah V, Pathak S, Multani A et al. (2006). Prostate cancer metastasis: role of the host microenvironment in promoting epithelial to mesenchymal transition and increased bone and adrenal gland metastasis. *Prostate* **66**: 1664–1673.

Yang AD, Camp ER, Fan F, Shen L, Gray MJ, Liu W et al. (2006). Vascular endothelial growth factor receptor-1 activation mediates epithelial to mesenchymal transition in human pancreatic carcinoma cells. *Cancer Res* **66**: 46–51.

Yang YM, Dolan LR, Ronai Z. (1996). Expression of dominant negative CREB reduces resistance to radiation of human melanoma cells. *Oncogene* **12**: 2223–2233.

Zhang X, Odom DT, Koo SH, Conkright MD, Canettieri G, Best J et al. (2005). Genome-wide analysis of cAMP-responsive element binding protein occupancy, phosphorylation, and target gene activation in human tissues. *Proc Natl Acad Sci USA* **102**: 4459–4464.

Zhau HY, Chang SM, Chen BQ, Wang Y, Zhang H, Kao C et al. (1996). Androgen-repressed phenotype in human prostate cancer. *Proc Natl Acad Sci USA* **93**: 15152–15157.

Ziel KA, Campbell CC, Wilson GL, Gillespie MN. (2004). Ref-1/Ape is critical for formation of the hypoxia-inducible transcriptional complex on the hypoxic response element of the rat pulmonary artery endothelial cell VEGF gene. *FASEB J* **18**: 986–988.

Supplementary Information accompanies the paper on the Oncogene website (http://www.nature.com/onc).

## Research Article

# β2-Microglobulin Is a Signaling and Growth-Promoting Factor for Human Prostate Cancer Bone Metastasis

Wen-Chin Huang,[1] Daqing Wu,[1] Zhihui Xie,[1] Haiyen E. Zhau,[1] Takeo Nomura,[1] Majd Zayzafoon,[4] Jan Pohl,[2] Chia-Ling Hsieh,[1] M. Neale Weitzmann,[3] Mary C. Farach-Carson,[5] and Leland W.K. Chung[1]

[1]Molecular Urology and Therapeutics Program, Department of Urology and Winship Cancer Institute, [2]Microchemical and Proteomics Facility, and [3]Divison of Endocrinology and Metabolism and Lipids, Emory University School of Medicine, Atlanta, Georgia; [4]Department of Pathology, The University of Alabama at Birmingham, Birmingham, Alabama; and [5]Department of Biological Science, University of Delaware, Newark, Delaware

## Abstract

The protein factor β2-microglobulin (β2M), purified from the conditioned medium of human prostate cancer cell lines, stimulated growth and enhanced osteocalcin (OC) and bone sialoprotein (BSP) gene expression in human prostate cancer cells by activating a cyclic AMP (cAMP)–dependent protein kinase A signaling pathway. When β2M was overexpressed in prostate cancer cells, it induced explosive tumor growth in mouse bone through increased phosphorylated cAMP-responsive element binding protein (CREB) and activated CREB target gene expression, including *OC, BSP, cyclin A, cyclin D1*, and *vascular endothelial growth factor*. Interrupting the β2M downstream signaling pathway by injection of the β2M small interfering RNA liposome complex produced an effective regression of previously established prostate tumors in mouse bone through increased apoptosis as shown by immunohistochemistry and activation of caspase-9, caspase-3, and cleavage of poly(ADP-ribose) polymerase. These results suggest that β2M signaling is an attractive new therapeutic target for the treatment of lethal prostate cancer bone metastasis. (Cancer Res 2006; 66(18): 9108-16)

## Introduction

Prostate cancer bone metastasis is lethal, and currently, there is no effective therapy (1). To develop new approaches targeting prostate cancer bone metastasis, we sought to understand the reciprocal interaction between prostate cancer and bone cells at the molecular level to identify soluble factors that may be shuttled between these cells that are responsible for the maintenance of cell-specific phenotypes and behaviors. We focused specifically on the regulation of bone-restricted osteocalcin (OC) and bone sialoprotein (BSP) expression in prostate cancer cells because the expression of these proteins has been proposed to confer the ability of prostate cancer cells to grow and survive in the bone microenvironment (2, 3). OC and BSP could contribute in part to the adhesive properties of prostate cancer cells through the binding of their cell surface integrin receptors and a RGD motif of extracellular matrices (4, 5). The ability of prostate cancer cells to mimic bone by expressing OC, BSP, osteopontin, osteonectin/SPARC, and the receptor activator of nuclear factor-κB ligand

(RANKL) could further aid prostate cancer bone colonization as shown by the ability of prostate cancer cells to form mineralized bone nodules in culture (2, 3, 6). This understanding of prostate cancer and bone cell interaction has been the basis for developing novel and promising therapies for the treatment of prostate cancer bone metastasis in the clinic. Bisphosphonates, agents known to decrease bone turnover, were shown to reduce overall bone loss and improve bone pain associated with bone metastasis when applied clinically in patients with prostate or breast cancer bone metastases (7, 8). Atrasentan, an endothelin-1 (ET-1) receptor A antagonist, was found to improve quality of life and bone pain in prostate cancer patients by interfering with the interaction between ET-1, secreted by prostate cancer cells, and its receptor ET-A, located on the cell surface of osteoblasts (9). In addition, data from experimental cell lines, animal models, and clinical studies reveal that insulin-like growth factor (IGF)-I and its receptor IGFR-I, platelet-derived growth factor (PDGF) and its receptor PDGFR, and RANKL and RANK interaction are promising targets for therapeutic intervention (10–12).

β2-microglobulin (β2M) is a nonglycosylated protein composed of 119 amino acid residues with a secreted form of 99 amino acids and a molecular mass of 11,800 Da (13, 14). β2M is synthesized by all nucleated cells and forms complexes with the heavy chain of MHC class I antigen through noncovalent linkage on cell surfaces (15). MHC I is essential for the presentation of protein antigens recognized by cytotoxic T cells (16). On recognition of foreign peptide antigens on cancer cell surfaces, T cells actively bind and lyse the antigen-presenting cells. Down-regulation of MHC I occurs frequently in cancer cells, and this contributes to the immune evasiveness of cancer cells that allows them to escape from elimination by the attacking cytotoxic T cells (17). The biological functions of β2M in cancer are not clear. Increased β2M levels in bone marrow and blood specimens are correlated with a poor prognosis and the failure of multiple myeloma patients to respond to therapy (18). Urine β2M levels are elevated in advanced prostate cancer patients and correlate negatively with patient survival (19). Concentrations of serum β2M are also increased in gastrointestinal (20) and breast cancer patients (21). Hence, β2M may be useful as a prognostic and therapeutic response indicator for cancer patients. β2M is a mitogen and is capable of increasing the growth of human osteoblasts (22), human prostate cancer PC3 cells, and rat stromal cells (23) and to regulate the expression of hormone/growth factor receptors (epidermal growth factor receptor, insulin receptor, and IGF-I and IGF-II receptors) and the interaction with their ligands (24–26).

We report here that the protein factor β2M is required to maintain the bone phenotypes or osteomimicry exhibited by prostate cancer cells (2, 3). We showed that β2M activates

---

phosphorylated cyclic AMP (cAMP)–responsive element binding protein (p-CREB) with increased expression of its target genes. This activation could enhance tumor growth and angiogenesis and facilitate the recruitment of osteoblasts and osteoclasts to the site of tumor colonization in bone. This signaling axis offers an opportunity for improved clinical targeting of prostate cancer bone metastasis. Recently, we (Huang et al., 2006, AACR Annual Meeting, Abstract 4822) and others (Yang et al., 2006, AACR Annual Meeting, Abstract 2218) have shown that β2M expression is linked to the increased growth, migration, and invasion of human prostate, breast, lung, renal cancer, and myeloma cells and promoted their epithelial to mesenchymal transition (EMT). Our results established for the first time the growth and signaling roles of β2M in human prostate cancer bone metastasis and confirmed β2M/protein kinase A (PKA)/CREB signaling axis as a potential new target for therapy.

## Materials and Methods

**Cell lines and cell culture.** Human prostate cancer cell lines LNCaP, C4-2B4, DU145, PC3, and ARCaP and osteosarcoma cell line MG63 were cultured in T-medium (Life Technologies, Inc., Rockville, MD) supplemented with 5% fetal bovine serum (FBS) and 1% penicillin/streptomycin as described previously (27). The cells were maintained at 37°C in 5% CO₂. For conditioned medium collection, cells were cultured in T-medium with serum until 80% confluence. The cells were washed subsequently twice in PBS (10 mmol/L phosphate buffer and 137 mmol/L NaCl) and incubated in T-medium without serum. After 2 days of additional incubation, conditioned media were collected, centrifuged, and stored at −20°C until use.

**Purification and identification of β2M.** All purification procedures were done at 4°C. Total proteins from 100 mL of ARCaP conditioned medium were precipitated by 0% to 100% saturation of ammonium sulfate. After centrifugation, the protein precipitates were dissolved in 1 mL of PB [10 mmol/L sodium phosphate (pH 7.6) containing 0.2 mmol/L phenylmethylsulfonyl fluoride, 0.5 mmol/L DTT, protease inhibitor cocktail (Roche Molecular Biochemicals, Indianapolis, IN)] and dialyzed against 500 mL of PB twice overnight. After centrifugation of the dialyzed solution, the supernatant was passed through Centricon (YM-30, Millipore Corp., Billerica, MA) to remove the proteins with high molecular mass (>30 kDa). Protein filtrate (100 μL, ~100 μg of total proteins) was loaded into an anion exchange column (4 × 250 mm, ProPac Wax-10, Dionex, Sunnyvale, CA) preequilibrated with PB at a flow rate of 1 mL/min. The bound form proteins were eluted with a liner gradient of 0 to 1 mol/L NaCl. After analysis of human OC (hOC) promoter-luciferase activity (2) for each fraction, the purified protein fractions having promoter-luciferase activity were collected and analyzed by SDS-PAGE with silver staining (Invitrogen, Carlsbad, CA). After SDS-PAGE analysis, the NH₂-terminal amino acid sequence of this homogenous protein was determined by the Edman degradation method (28). Human β2M protein was purchased from Sigma (St. Louis, MO).

**Reverse transcription-PCR.** Total RNA was isolated from the confluent monolayer of cells using RNAzol B (TelTest, Inc., Friendswood, TX). The total RNA was used as the template for reverse transcription according to the manufacturer's instructions (Invitrogen). The oligonucleotide primer sets used for PCR analysis of cDNA were β2M [5′-ACGCGTCCGA-AGCTTACAGCATTC-3′ (forward) and 5′-CCAAATGCGGCATCTA-GAAACCTCCATG-3′ (reverse)], OC, BSP, and glyceraldehyde-3-phosphate dehydrogenase (GAPDH) as described previously (2). The thermal profile for β2M amplification is 30 cycles starting with denaturation for 1 minute at 94°C followed by 1 minute of annealing at 64°C and 30 seconds of extension at 72°C. Reverse transcription-PCR (RT-PCR) products were analyzed by agarose gel electrophoresis. Quantity One 4.1.1 Gel Doc gel documentation software (Bio-Rad, Hercules, CA) was used for quantification of β2M, OC, and BSP mRNA expression and normalized by GAPDH mRNA.

**Western blot analysis and ELISA.** Western blot was done using the Novex system (Invitrogen). Primary antibody anti-β2M and vascular endothelial growth factor (VEGF; Santa Cruz Biotechnology, Inc., Santa Cruz, CA) was used at a 1:500 dilution, and secondary antibody (Amersham Biosciences Corp., Piscataway, NJ) was used at a 1:5,000 dilution. Detection of protein bands was done with Enhanced Chemiluminescence Western Blotting Detection Reagents (Amersham Biosciences). For apoptosis analysis, rabbit polyclonal anti-caspase-9, anti-caspase-3, and anti–poly(ADP-ribose) polymerase (PARP) antibodies (1:500 dilution) were ordered from Cell Signaling Technology, Inc. (Beverly, MA). Anti-CREB, p-CREB (1:1,000), cyclin A, and cyclin D1 (1:2,000) antibodies were purchased from Cell Signaling Technology. The concentration of protein was determined by the Bradford method using Coomassie plus protein reagent (Pierce, Rockford, IL). β2M protein concentration was assayed by Quantikine IVD human β2M ELISA kit (R&D Systems, Inc., Minneapolis, MN) according to the manufacturer's instructions.

**Cell proliferation assay.** Prostate cancer cell lines were plated in 96-well plates in T-medium containing 5% FBS. After 24 hours of incubation, media were replaced by serum-free T-medium and incubated for an additional 24 hours. The cells were exposed with conditioned medium or reagents for 3 or 4 days of incubation. Cell numbers were measured every 24 hours using CellTiter 96 AQueous One Solution Cell Proliferation Assay (Promega, Madison, WI).

***In vivo* animal studies.** All of the animal experiments were approved and done in accordance with institutional guidelines. Four-week-old male athymic *nu/nu* mice (National Cancer Institute, Frederick, MD) were inoculated into the bone marrow space of the femurs with 1 × 10⁶ cells per mouse of Neo or β2M-overexpressing C4-2B cells, respectively. Blood specimens were harvested for prostate-specific antigen (PSA) assay biweekly. Serum PSA levels were determined by microparticle ELISA using the Abbott IMx machine (Abbott Laboratories, Abbott Park, IL).

**β2M small interfering RNA and antiprostate tumor study.** The specific β2M and control scramble small interfering RNA (siRNA) sequences were 5′-UUGCUAUGUGUCUGGGGUUU(dT)(dT)-3′ and 5′-UUCAUGUGUCU-GUGGGUUU(dT)(dT)-3′, respectively. For efficient RNA delivery, we used a cationic liposome formulation (29) to deliver β2M and scramble siRNA into cell lines or living mice. To test the prostate tumor growth inhibition by β2M siRNA, 4-week-old male athymic *nu/nu* mice were inoculated either with 2 × 10⁶ C4-2B cells in mouse femur or in the s.c. space of the chest regions with 2 × 10⁶ cells of PC3-Luc or C4-2B mixed with 20 mg of bone powder and 35 μL of Matrigel matrix (BD Biosciences, Bedford, MA), respectively. Three (PC3-Luc) or 4 (C4-2B) weeks later, the tumor-bearing mice were randomly divided into two groups. The mice in the treatment group received an intratumoral injection of the β2M siRNA liposome complex thrice weekly continuously for 4 weeks at a dose of 0.8 μg of siRNA mixed with 19.2 μL of liposome for each mouse. The control group was injected with the same dose of the scramble siRNA liposome complex. To assay the antitumor efficacy of β2M siRNA, real-time bioluminescence images acquired by CCD camera using a cryogenically cooled IVIS system with analysis software (Xenogen Corp., Alameda, CA; ref. 30) and serum PSA levels were used to monitor PC3-Luc and C4-2B tumor burden in nude mice, respectively.

**Immunohistochemical staining.** Detection of β2M expression and cell death of normal and tumor specimens was conducted using Dako Autostainer Plus system (Dako Corp., Carpinteria, CA). Mouse monoclonal antibody against β2M (used at 1:1,000 dilution; Santa Cruz Biotechnology) and against M30 CytoDeath (1:600; DiaPharma Group, Inc., West Chester, OH) were used. Tissues were deparaffinized, rehydrated, and subjected to pressure cooking antigen retrieval at 125°C and 20 p.s.i. for 30 seconds, 10 minutes of double endogenous enzyme block, 30 minutes of primary antibody reaction, and 30 minutes of EnVision+ Dual Link or Biotinylated Link and Streptavidin-Peroxidase System incubation. Signals were detected by adding substrate hydrogen peroxide using diaminobenzidine as the chromogen and counterstained with hematoxylin. All reagents were obtained from DAKO.

**Statistical analysis.** Statistical analyses were done as described previously (2). Student's *t* test and two-tailed distribution were applied in the analysis of statistical significance.

## Results

**Purification and identification of a soluble factor conferring enhanced hOC promoter activity in human prostate cancer cells.** We previously reported that conditioned medium of ARCaP cells can induce hOC and human BSP (hBSP) promoter activities and their respective mRNA expression through a cAMP-dependent PKA signaling pathway by human prostate cancer cells (2). To identify the responsible factor, ARCaP conditioned medium was subjected to purification by ammonia sulfate [$(NH_4)_2SO_4$] precipitation, membrane filtration (YM-30), anion exchange column chromatography, and $NH_2$-terminal amino acid sequencing of the final purified product. The respective fractions collected from the various purification steps were subjected to hOC promoter-luciferase activity analysis in C4-2B cells, an androgen-independent human prostate cancer cell line of the LNCaP lineage (31). Figure 1*A* shows that anion exchange chromatography fractions eluted between 0.20 and 0.22 mol/L NaCl seem to contain the active factor capable of stimulating hOC promoter-luciferase activity. This fraction was then analyzed by SDS-PAGE and silver stain. Figure 1*B* (*left*) shows that a homogenous protein band migrating 11 kDa was observed. In addition, we used mass spectrometry to determine the exact molecular mass of this factor, which is 11,802.6 Da. $NH_2$-terminal amino acid sequencing of this fraction revealed that this biologically active protein to be β2M (IQRTPKIQVYSRHPA). Western blot analysis subsequently using anti-β2M antibody confirmed that this protein is β2M (Fig. 1*B, right*). β2M, a known housekeeping gene, was further shown to be expressed uniformly among a series of human prostate cancer and bone cell lines as assessed by semiquantitative RT-PCR (Fig. 1*C*). As expected, β2M protein, conducted by Western blot (Fig. 1*D*),

correlated directly with the ability of the conditioned medium to stimulate hOC promoter-luciferase activity, which was higher in the conditioned medium collected from the more aggressive ARCaP than from the less aggressive LNCaP cells with the soluble factor presented as the secreted form (2).

**β2M is responsible for the activation of hOC and hBSP promoter-luciferase activities in selective prostate cancer cell lines.** To validate that β2M is the active soluble factor responsible for the stimulation of hOC and hBSP promoter-luciferase activities in prostate cancer cells, we exposed C4-2B cells to ARCaP conditioned medium either in the presence or absence of anti-β2M neutralizing antibody. Both hOC and hBSP promoter-luciferase activities were induced by ARCaP conditioned medium, and the fold of the promoter activation seemed to be dependent on the concentrations of β2M protein in the conditioned medium (Fig. 2*A*). We observed that the activated hOC and hBSP promoter-luciferase activities were blocked by a neutralizing anti-β2M antibody but not by the control IgG (Fig. 2*A*). This study was also confirmed by a similar experiment where β2M conditioned medium was collected from C4-2B cells stably transfected with a β2M expression vector (Fig. 2*B*). As shown, β2M conditioned medium stimulated hOC and hBSP promoter-luciferase activities, which were blocked by the presence of anti-β2M antibody but not IgG. Finally, we ratified our data using β2M protein and confirmed a dose-dependent up-regulation of the promoter-luciferase activity in C4-2B cells, which were also suppressed by anti-β2M but not control antibody (Fig. 2*C*).

**β2M activates OC and BSP mRNA expression and stimulates the growth of human prostate cancer cells through activation of CREB.** To further evaluate whether β2M up-regulates the
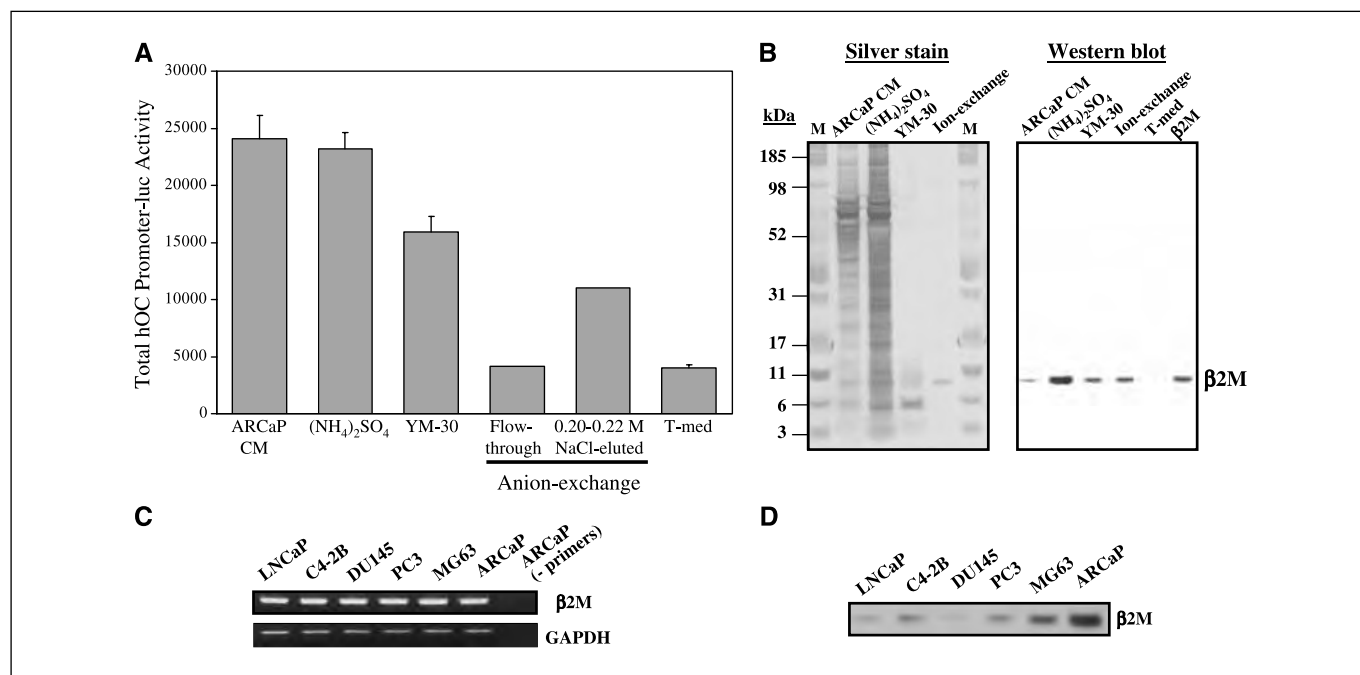


**Figure 1.** Purification and identification of β2M from human prostate cancer cell conditioned medium and the expression of β2M in various human prostate cancer cell lines. *A,* total hOC promoter-luciferase activity was analyzed on the addition of each fraction collected from the purification steps. *T-med,* fresh T-medium as a background control. *Columns,* mean of two independent experiments; *bars,* SD. *B,* SDS-PAGE analysis. Silver stain (*left*) and Western blot (*right*) analyses of β2M for the various purification steps. *M,* standard markers; *β2M,* commercial β2M protein (0.1 μg) was used as a positive control. Anti-β2M antibody was used for Western blot. *C,* endogenous β2M transcript expressed in human prostate cancer cell lines LNCaP, C4-2B, DU145, PC3, and ARCaP and in human osteosarcoma cell line MG63 detected by RT-PCR. Expression of GAPDH was used as a loading control. ARCaP without adding primers was used as a negative control. *D,* Western blot analysis of secreted β2M proteins collected from human prostate cancer cell line conditioned medium (20 μg of total proteins per lane).
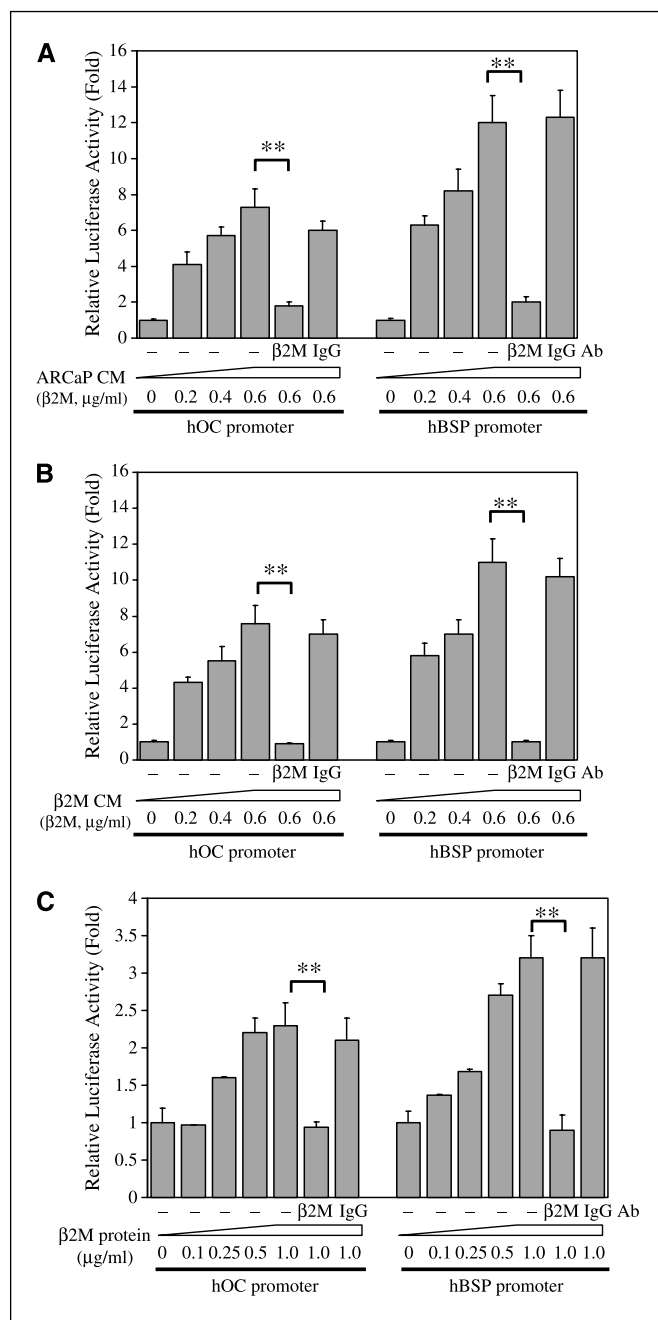
**Figure 2.** β2M regulates bone-specific gene promoter reporter activation in human prostate cancer cells. *A* and *B*, ARCaP and β2M conditioned media (*CM*) stimulated hOC and hBSP promoter-luciferase activities in C4-2B cells in a concentration-dependent pattern with β2M concentrations from 0 to 0.6 μg/mL. Anti-β2M antibody (*β2M Ab*; 10 μg/mL) can significantly inhibit the promoter reporter activation by ARCaP and β2M conditioned media. Isotype IgG (10 μg/mL) was used as a control. *Columns*, mean of three independent experiments; *bars*, SD. **, $P < 0.005$. *C*, β2M protein also induced hOC and hBSP promoter-luciferase activities in a dose-dependent manner. **, $P < 0.005$.

β2M conditioned medium (Fig. 3A, left). Consistent with the hOC and hBSP promoter-luciferase activity data, anti-β2M antibody also inhibited the mRNA expression induction by ARCaP or β2M conditioned medium. Furthermore, the ability of β2M to induce OC and BSP mRNA expression was also confirmed in an additional study, in which C4-2B cells were stably transfected with a β2M cDNA expression vector. As shown in Fig. 3A (*right*), both the endogenous OC and BSP mRNA levels were increased in cells stably transfected with β2M cDNA (B2 and C2, the two highest β2M expression clones) but not with a control neomycin-resistant empty vector (Neo).

β2M has been shown previously to enhance the growth of PC3 cells (23). To address whether β2M also stimulates the proliferation of other human prostate cancer cells, we tested β2M on the growth of a broad range of human prostate cancer cell lines, including androgen-dependent (LNCaP), androgen-independent (C4-2B, DU145, and PC3), and androgen-repressed (ARCaP) cells. All the prostate cancer cell lines responded to β2M-induced cell proliferation. In a 3-day proliferation assay, the relative cell growth increased were as follows: ARCaP, $129 \pm 8\%$; C4-2B, $121 \pm 10\%$; DU145, $120 \pm 7\%$; LNCaP, $117 \pm 7\%$; and PC3, $111 \pm 3\%$. We also compared the cell growth of B2-β2M-transfected, C2-β2M-transfected, and Neo-transfected C4-2B cell clones on plastic dishes and in soft agar. B2 and C2 clones that expressed the highest levels of β2M had the highest growth rate compared with Neo and the parental cells (−), which expressed only the endogenous levels of β2M (Fig. 3B, *top*). Anti-β2M antibody inhibited parental and Neo-transfected C4-2B cell growth in a dose-dependent manner (Fig. 3B, *bottom*). Cells expressing high levels of β2M, such as the B2 clone, required a higher amount of anti-β2M antibody (10 μg/mL) to inhibit cell growth induced by endogenous β2M than did the Neo-transfected clone (1 μg/mL). Control IgG (20 μg/mL) failed to exert a growth-inhibitory effect. We also conducted the three-dimensional anchorage-independent growth of Neo and β2M-overexpressing C4-2B cells in soft agar. The results showed a direct correlation between the size and the number of colonies formed in the soft agar and the levels of β2M expression by the C4-2B cells (Fig. 3C). These data collectively suggest that β2M is a potent stimulator for OC and BSP expression and the proliferation of prostate cancer cells *in vitro*.

To determine the possible signaling link between β2M expression and prostate cancer cell growth, we chose to evaluate the activation status of CREB, a target of β2M/PKA downstream signaling (2). We assessed the expression of CREB target genes, *cyclin A, cyclin D1*, and *VEGF* (32), which are known to control tumor cell growth and angiogenesis in nontransfected parental, Neo, and β2M-overexpressing C4-2B cells. Figure 3D shows that increased β2M expression (B2 and C2 clones) greatly promoted the protein expression of p-CREB (2.3- to 2.5-fold), cyclin D1 (3.9- to 4.1-fold), cyclin A (2.6- to 3.0-fold), and VEGF (3.3- to 3.8-fold) over that of the Neo control C4-2B cells.

**β2M supports the growth of prostate cancer cells in mouse bone *in vivo*.** Because OC and BSP accumulation by human prostate cancer cells confers increased growth and survival of cancer cells and their expression of growth regulatory CREB target genes in hosts, we further compared the growth of Neo and β2M-overexpressing C4-2B cells in mouse bone. β2M-overexpressing C4-2B cells exhibited a 16-fold increased rate of growth over that of the Neo-transfected cells, as assessed by serum PSA (33), when injected into mouse skeleton (serum PSA concentration: Neo, $103 \pm 17$ ng/mL and β2M, $1,697 \pm 500$ ng/mL) at 17 weeks after

endogenous OC and BSP mRNA, we assessed the expression of these noncollagenous bone matrix proteins using a semiquantitative RT-PCR in C4-2B cells exposed to ARCaP or β2M conditioned medium (from C4-2B cells stably transfected with a β2M expression vector). The endogenous OC and BSP mRNA expression increased by 6- to 8-fold on the exposure of C4-2B cells to ARCaP or

tumor cell inoculation (Fig. 4A and B, top). β2M does not significantly affect the PSA expression in C4-2B cells (PSA levels in Neo and β2M clones are 21.9 ± 2.1 ng/µg and 25.3 ± 2.5 ng/µg cellular protein, respectively; P = 0.15). Histomorphologic analysis of β2M tumors showed a more intense osteoblastic response in mouse femur compared with the specimens obtained from Neo tumors and normal control samples (Fig. 4B, bottom). Immuno-histochemical analysis shows that β2M tumors highly expressed β2M proteins compared with Neo and normal tissues harvested from mouse femurs using anti-β2M antibody (Fig. 4C). The observed increase in β2M expression in C4-2B tumors in mouse femurs corresponded with the increased β2M expression in primary and metastatic human prostate cancer tissues. Figure 4D shows representative immunohistochemical analysis of β2M staining in primary and bone metastatic human prostate cancer specimens. Abundant β2M staining was seen in primary prostate cancers (139 of 153 or 91% positive) and bone metastases (4 of 4 or 100% positive). Note that heterogeneity exists in the primary human prostate cancer specimens, where some of the specimen

cancer areas stained stronger than the normal, whereas in others the reverse was observed.

**β2M is an attractive new therapeutic target for the treatment of human prostate cancer bone metastasis.** Because β2M conferred increased prostate cancer cell growth in mice bone, we tested the possibility that β2M-induced intracellular signaling may be a therapeutic target. We devised a sequence-specific β2M siRNA and compared the activity of this siRNA with its control scramble β2M siRNA, delivered as a cationic liposome complex (29), to cultured cancer cells or preestablished prostate tumors in mice.

First, we assessed β2M and scramble siRNA for antagonizing β2M mRNA expression in C4-2B cells. Figure 5A shows that, in a transient transfection assay, β2M, but not scramble siRNA, effectively blocked the endogenous level of β2M mRNA. β2M protein expression, detected by Western blot and ELISA, was also inhibited by β2M siRNA but not scramble siRNA (data not shown). Corresponding with decreased β2M mRNA expression, β2M siRNA, as expected, eliminated the mRNA expression of OC and BSP
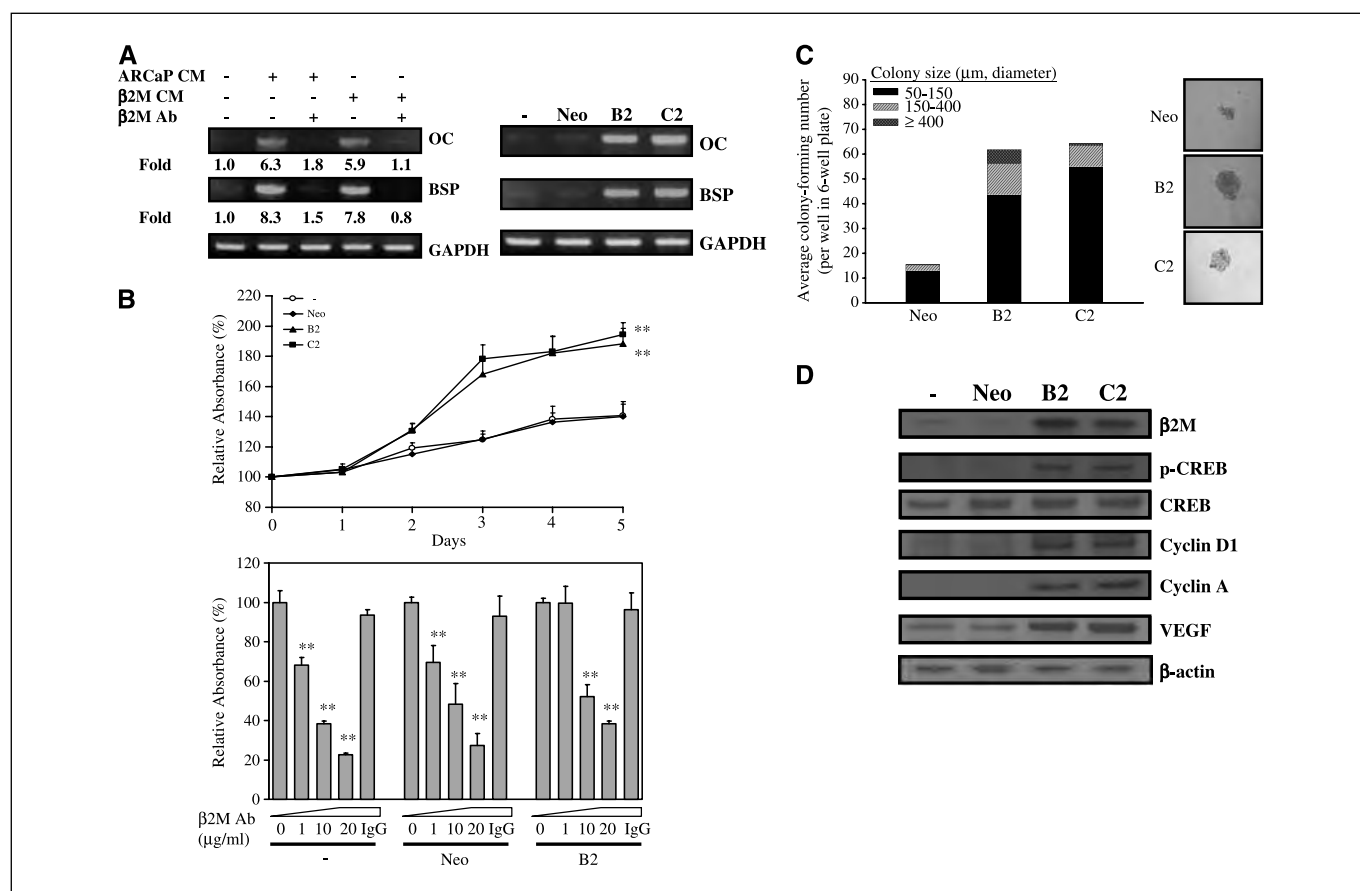


**Figure 3.** β2M enhances endogenous OC and BSP mRNA expression and stimulates the proliferation of human prostate cancer cells through activation of CREB. *A,* ARCaP and β2M conditioned media (0.6 µg/mL of β2M protein) increased OC and BSP mRNA expression in C4-2B cells, and anti-β2M antibody (10 µg/mL) inhibited the mRNA induction by conditioned medium done by RT-PCR. *Left, fold,* ratios of ARCaP or β2M conditioned medium treated in the presence or absence of anti-β2M antibody versus the vehicle-treated control; *right,* endogenous OC and BSP mRNA expression in nontransfected parental (−), Neo, and the two highest β2M-overexpressing clones (B2 and C2) in C4-2B cells was determined by RT-PCR. *B,* β2M-mediated mitogenic effect on C4-2B cells. Parental (−), Neo, B2, and C2 cells were plated in 96-well plates, and cell numbers were measured every 24 hours. **, P < 0.005, significant differences from Neo (*top*). Anti-β2M antibody inhibited C4-2B cell growth in a dose-dependent manner. Parental (−), Neo, and B2 cells were plated in 96-well plates and exposed to different concentrations of β2M antibody (0-20 µg/mL). Isotype IgG (20 µg/mL) was used as a control. Cell numbers were measured at day 3 after treatment with antibody. **, P < 0.005 (*bottom*). *C,* effect of β2M on soft agar colony-forming efficiency of C4-2B cells. Neo, B2, and C2 cells were suspended in DMEM containing 10% FBS and 0.3% agarose and then placed on top of solidified 0.6% agarose in a six-well plate. The cell colonies were measured, counted (>50 µm), and photographed (×40) after cells were cultured for 4 weeks. Average colony-forming numbers were calculated from six replicates. *D,* Western blot analysis. p-CREB, cyclin D1, cyclin A, and VEGF are highly expressed in β2M-overexpressing B2 and C2 clones compared with Neo and nontransfected (−) C4-2B cells.

**Figure 4.** β2M supports the growth of human prostate cancer cells in mouse bone. *A,* serum PSA levels were assayed every 2 weeks after inoculation of Neo (*n* = 10) and β2M (*n* = 10) C4-2B cells in mouse femur. **, *P* < 0.005. *B,* X-ray image (*top*) and histomorphologic analysis (*bottom*) of control (normal mouse bone), Neo tumors, and β2M tumors in mouse femur. X-ray images indicate that β2M regulated the explosive growth of C4-2B tumor cells in mouse bone. *C,* immunohistochemical staining (*IHC*) of control (normal mouse bone), Neo, and β2M femur tumor specimens. β2M-overexpressing C4-2B tumors stained positively with anti-β2M antibody but control and Neo tumors stained only at background levels. Magnification, ×100. *D,* immunohistochemical analysis of β2M in primary human prostate cancer and prostate cancer bone metastatic specimens. Note heterogeneity exists in the primary prostate cancer specimens (*#1* and *#2*). *N,* normal areas; *C,* cancer areas. *Inset,* background immunohistochemical analysis using control IgG. Magnification, ×100.
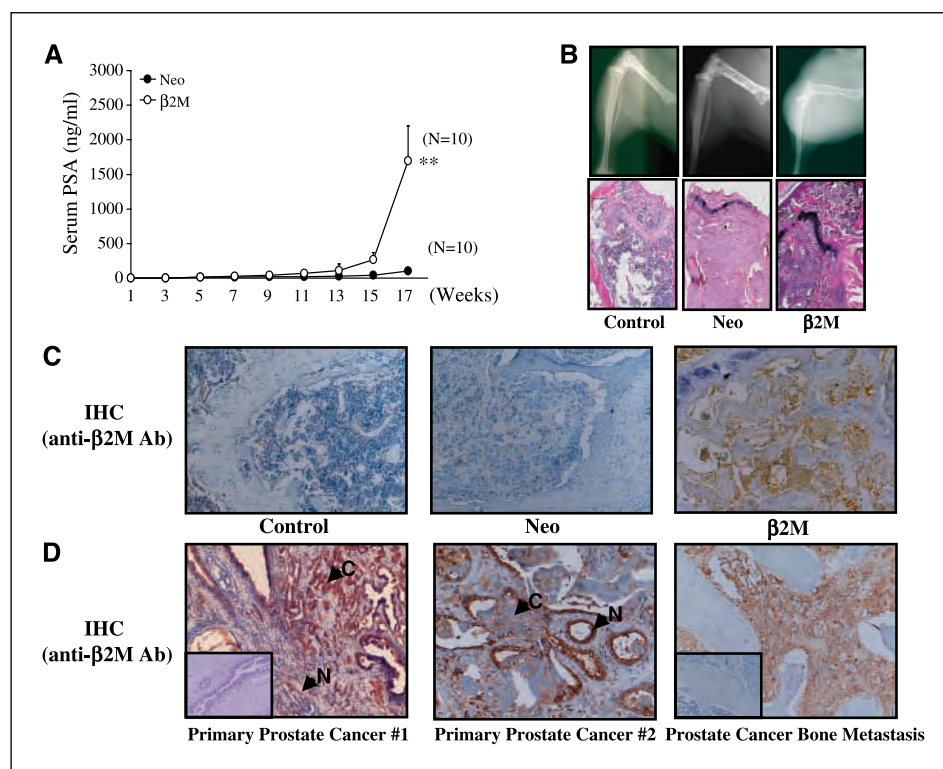
(Fig. 5*A*). β2M siRNA significantly inhibited the growth of C4-2B cells. In a 4-day proliferation assay, relative cell growth increased to 139 ± 6% and 138 ± 8% in parental nontransfected and scramble siRNA-transfected cells, respectively, whereas the growth of β2M siRNA-C4-2B cells remained at only 109 ± 3%.

Next, we validated the chronic effect of β2M siRNA on human prostate tumor growth both in bone powder xenografts (34) and in mouse skeleton (35). The bone powder was shown previously by Reddi and Huggins (34) to recapitulate bone morphogenesis and cytodifferentiation in a highly time-dependent and host microenvironment-dependent manner. Because of the known heterogeneity in human prostate cancer, we chose to test the proliferation of both C4-2B and PC3 cells and their requirement of β2M as a growth and survival signal. C4-2B and PC3 cells are documented to have different profiles of androgen receptor and response to β2M-induced hOC and hBSP promoter-luciferase activity (2). PC3 cells stably transfected with a luciferase gene (PC3-Luc) formed tumors in bone powder, with growth increase as a function of time as analyzed by a CCD Xenogen camera in mice during a 28-day siRNA treatment period (Fig. 5*B*). Although the growth of PC3-Luc tumors was not affected by injections of the scramble siRNA liposome complex, the β2M siRNA liposome complex delivered in the same manner shrank and eliminated preexisting PC3-Luc tumors grown as bone powder xenografts (Fig. 5*B* and *C, top*). Likewise, the growth of C4-2B tumors in bone powder *in vivo*, as detected by monitoring serum PSA levels, was also markedly inhibited by β2M siRNA treatment compared with scramble siRNA (Fig. 5*C, bottom*). The effect of β2M siRNA in eliminating preexisting prostate tumor growth in bone powder xenografts was also observed in mice inoculated directly with C4-2B cells in bone (data not shown). These data support the conclusion that antagonizing β2M signaling by β2M siRNA resulted in efficient targeting of the growth of human prostate tumors in mouse bone.

To investigate the molecular mechanism by which β2M siRNA induced human prostate cancer cell death, we conducted Western blot analysis to examine the activation of caspases, a hallmark of apoptosis (36). As shown in Fig. 5*D* (*left*), in C4-2B cells, β2M siRNA induced the activation of the initiator caspase, cleaved caspase-9 (37 and 35 kDa), and caspase-3 (19 and 17 kDa), which is one of the downstream effector caspases. The cleaved form of PARP (89 kDa), a factor downstream of caspase-3, was also detected in β2M siRNA-treated C4-2B cells. However, in parental (−) and scramble siRNA-treated C4-2B cells, no activated caspase-9, caspase-3, or cleaved PARP proteins were observed. Consistent with these results, marked elevation of apoptosis by β2M siRNA, as assessed by a CytoDeath M30 stain, was detected in both PC3-Luc and C4-2B bone powder xenografts (Fig. 5*D, right*). These results suggest that β2M siRNA reduced human prostate cancer cell proliferation *in vivo* and induced apoptotic death in prostate cancer cells.

## Discussion

The mortality and morbidity associated with human prostate cancer bone metastasis remains a challenge in the clinical management of human prostate cancer. Recently, new approaches have been explored to target the interphase between prostate cancer and bone, and some success has been achieved in reducing pain and improving survival and morbidity in patients with hormone refractory metastatic disease. Specifically, the use of bisphosphonate has been shown to reduce bone loss and fracture in patients treated with hormone withdrawal therapy (8). A bone-directed cotargeting strategy, killing prostate cancer cells with chemotherapy and modulating host bone cells with strontium-89, was shown to improve the overall survival of patients with hormone refractory prostate cancer (37). Atrasentan was shown to reduce bone pain and improve the quality of life of prostate cancer

patients with hormone refractory bone metastasis (9). These advances illustrate the importance of understanding the cellular interaction between prostate cancer and bone at the molecular level. In the present communication, we showed for the first time that β2M regulates the signaling pathway that confers the expression of bone matrix proteins OC and BSP and induces growth of human prostate cancer cells through the activation of the angiogenesis factor and cell cycle regulatory cyclins. By interrupting β2M-mediated downstream signaling, we observed considerable cell death and the shrinkage of preexisting prostate tumors in bone powder and mouse femur models. Cell death was confirmed by immunohistochemistry of the apoptotic M30 marker and the activation of caspases and PARP, markers known to be associated with programmed cell death.

*β2M*, a known housekeeping gene, expresses at a constant level with respect to its mRNA in many mammalian tissues and cells (38). β2M is a key protein involved in the presentation and stabilization of MHC I antigen on the cell surface. However, the role of β2M in cancer and bone metastasis is unexplored and unclear. Our present investigation revealed that β2M protein levels are variably in prostate cancer cell lines, with the levels of protein expression corresponding positively with the malignant status of the prostate cancer cells. These results suggest that the translation or stability of β2M protein must be tightly controlled to maintain cancer cell growth and survival.

Based on our published work and others, β2M-mediated signaling, but not necessarily β2M protein level in tissues or sera, contributes to enhanced prostate cancer growth and colonization in bone through four possible mechanisms (Fig. 6): First, β2M can activate cAMP-dependent PKA activity through binding to and activation of the seven-transmembrane G protein-coupled receptor or a yet-to-be-identified β2M receptor (2). This activation could induce p-CREB, which increases cell proliferation, survival, and angiogenesis (39–42) through elevated levels of cyclin A, cyclin D1, and VEGF (Fig. 3D). Second, β2M also enhances the synthesis and deposition of noncollagenous bone matrix proteins, such as OC and
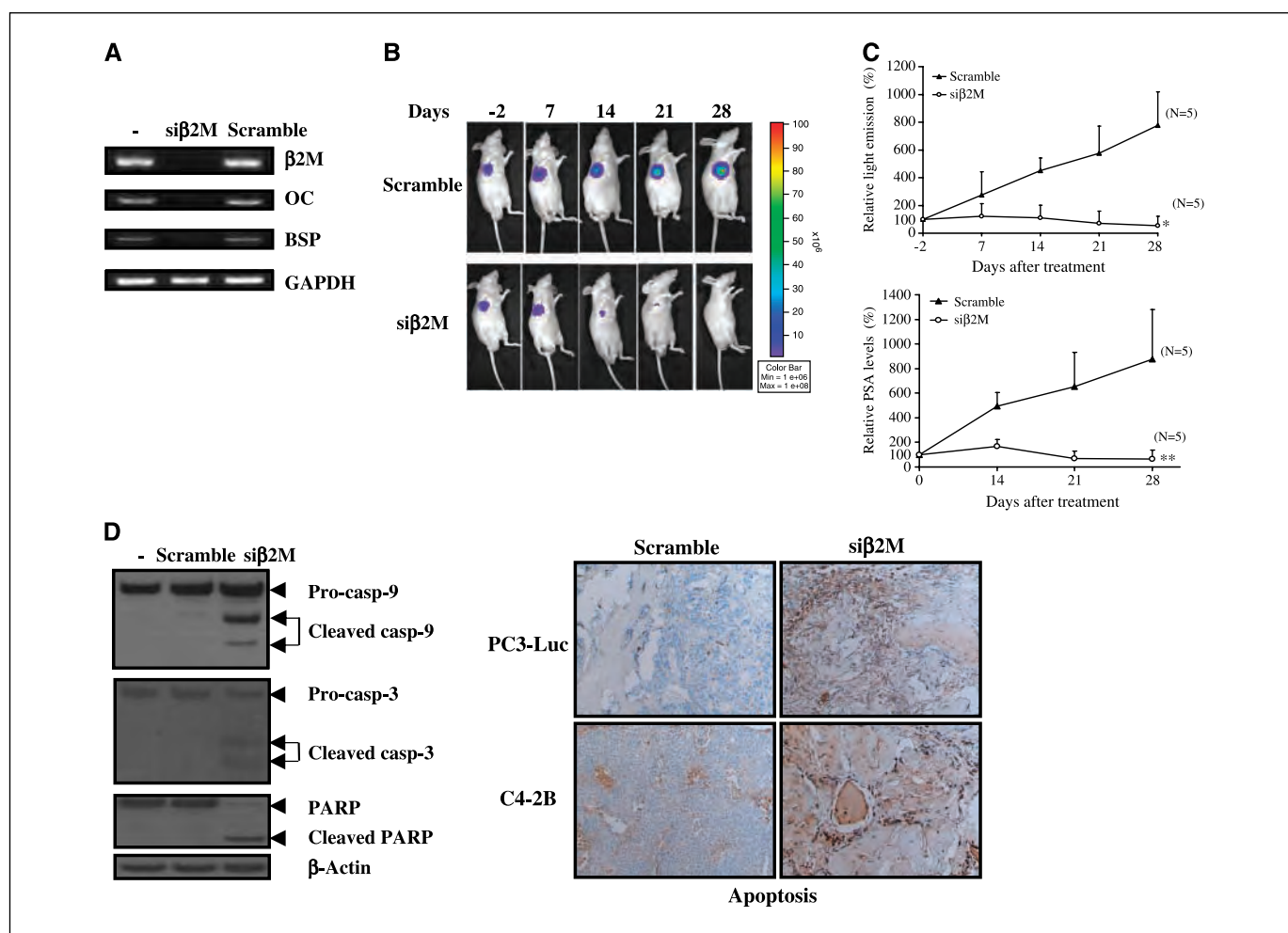


**Figure 5.** β2M siRNA down-regulates OC and BSP expression and inhibits human prostate cancer cell growth *in vivo* through an apoptotic caspase pathway. *A,* β2M siRNA (*siβ2M*) decreased β2M, OC, and BSP expression in C4-2B cells. The mRNA expression of β2M, OC, BSP, and GAPDH in nontransfected parental (−), β2M siRNA, and control scramble siRNA (*Scramble*) cells was determined by RT-PCR. *B,* real-time bioluminescence image from CCD camera monitoring of the growth of PC3-Luc cells mixed with bone powder in living mice. The light emission signals of PC3-Luc cells were dramatically decreased during the β2M siRNA treatment period in mice. *Color bar,* light emission density (the ranges from $1 \times 10^6$ to $1 \times 10^8$ photons/s/cm$^2$; $n = 5$ for each group). *C, top,* β2M siRNA significantly reduced the relative light emission of PC3-Luc cells in mice during the treatment period. *, $P < 0.05$. *Bottom,* β2M siRNA, but not scramble siRNA, greatly decreased the relative PSA levels of C4-2B cells grown as bone powder xenografts. **, $P < 0.005$. *D, left,* β2M siRNA, but not control scramble siRNA, induced the initiator cleaved caspase-9 (*casp-9*) and the downstream effector cleaved caspase-3 (*casp-3*) and cleaved PARP expression in C4-2B cells by Western blot analysis; *right,* PC3-Luc and C4-2B bone powder xenograft specimens were assessed by the CytoDeath M30 apoptotic marker staining. Magnification, ×100.

**Figure 6.** Four proposed molecular mechanisms, whereby β2M can affect osteomimicry, cancer progression, and bone metastasis in human prostate cancer. As indicated, β2M can activate cAMP/PKA signaling, its downstream p-CREB, and expression of target genes, including *OC, BSP, VEGF, cyclin A,* and *cyclin D1*. β2M also has a direct growth-promoting and antiapoptotic action that culminates in cancer cell growth and survival and through induction of EMT that facilitates further cancer cell migration, invasion, and metastasis. The numbers are corresponding with Discussion. *GPCR,* G protein-coupled receptor; *AC,* adenylate cyclase; *CRE,* cAMP-responsive element.
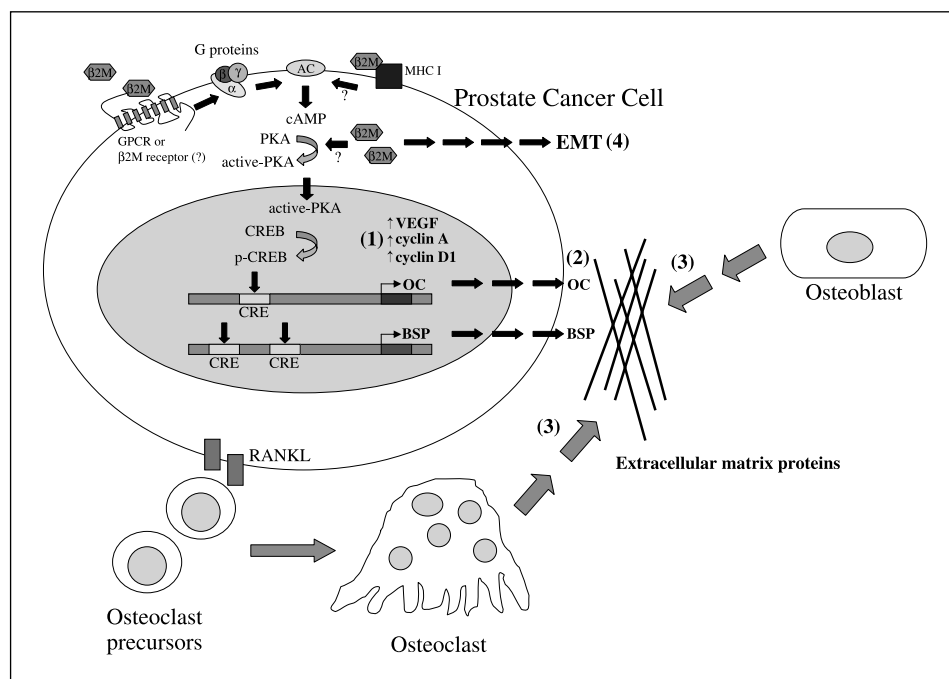
BSP, which serve as survival factors by binding to the cell surface integrin receptors (i.e., $\alpha_v\beta_3$ and $\alpha_v\beta_5$), and thus could sustain the growth and survival of prostate cancer cells in bone (43, 44). Third, OC and BSP have been shown to recruit osteoclasts and osteoblasts in the skeleton, resulting in increased bone turnover, which creates a growth factor-enriched niche that allows cancer growth and colonization in the newly "pitted" bone areas (3). Fourth, β2M (Huang et al., 2006, AACR Annual Meeting, Abstract 4822) or PKA/CREB activation (45) has been shown to promote EMT in a wide spectrum of human tumor cells, including prostate, breast, renal, and lung. Through the induction of EMT, cancer cells acquire enhanced ability to migrate, invade, and eventually gain access to the metastatic sites (46). Interrupting β2M-regulated signaling could block all of the above-mentioned pathways, which could contribute to the observed *in vivo* antitumor effects of β2M siRNA. The siRNA technique has been broadly used to investigate gene function, gene regulation, and gene-specific therapeutics (47). However, low RNA transfection efficiency and interference by serum has limited the application of this technology for gene delivery. An improved nonviral method using the cationic liposome formulation has gained popularity because of its high binding affinity with the negatively charged RNA or DNA (29) that form a complex and can efficiently carry siRNA into cancer cells or host mouse tissues with minimal immunogenicity and toxicity in immunocompromised mice (30). In the present communication, we used this cationic liposome formulation and evaluated the ability of the β2M siRNA liposome complex to inhibit the growth of preexisting human prostate tumors in bone powder and mouse femur in nude mice. We showed direct cytotoxic effects by interrupting β2M signaling in human prostate cancer cells because these tumors were grown in

immunocompromised mice. Thus, the β2M-mediated signaling pathway may contribute directly to prostate tumor growth, survival, and transdifferentiation. By blocking β2M-regulated signaling, prostate tumor death through the apoptotic cascade pathway can result. Because normal cells are insensitive to growth inhibition by β2M siRNA or anti-β2M antibody (Yang et al., 2006, AACR Annual Meeting, Abstract 2218), this suggests that cancer cells develop dependence on β2M-mediated signaling and thus are particularly vulnerable to the β2M signal blockade-induced cytotoxicity.

In summary, we have shown that β2M signaling, via a cAMP-dependent PKA pathway, CREB activation, and the expression of bone-like properties by prostate cancer cells, contributes to prostate cancer cell growth and survival in bone. By interrupting β2M signaling with sequence-specific β2M siRNA, we observed a marked decrease of expression of OC and BSP, cancer cell death, and shrinkage of preexisting prostate tumors in mice. Targeting β2M either alone or in combination with other therapeutic modalities may be a promising new approach for the treatment of lethal human prostate cancer bone metastasis.

## Acknowledgments

## References

1. Cheville JC, Tindall D, Boelter C, et al. Metastatic prostate carcinoma to bone: clinical and pathologic features associated with cancer-specific survival. Cancer 2002;95:1028–36.
2. Huang WC, Xie Z, Konaka H, et al. Human osteocalcin and bone sialoprotein mediating osteomimicry of prostate cancer cells: role of cAMP-dependent protein kinase A signaling pathway. Cancer Res 2005;65:2303–13.
3. Koeneman KS, Yeung F, Chung LW. Osteomimetic

properties of prostate cancer cells: a hypothesis supporting the predilection of prostate cancer metastasis and growth in the bone environment. Prostate 1999; 39:246–61.

4. Ganss B, Kim RH, Sodek J. Bone sialoprotein. Crit Rev Oral Biol Med 1999;10:79–98.

5. Hauschka PV. Osteocalcin: the vitamin K-dependent $Ca^{2+}$-binding protein of bone matrix. Haemostasis 1986; 16:258–72.

6. Lin DL, Tarnowski CP, Zhang J, et al. Bone metastatic LNCaP-derivative C4-2B prostate cancer cell line mineralizes *in vitro*. Prostate 2001;47:212–21.

7. Pinski J, Dorff TB. Prostate cancer metastases to bone: pathophysiology, pain management, and the promise of targeted therapy. Eur J Cancer 2005;41:932–40.

8. Smith MR. Zoledronic acid to prevent skeletal complications in cancer: corroborating the evidence. Cancer Treat Rev 2005;31 Suppl 3:19–25.

9. Nelson JB. Endothelin receptor antagonists. World J Urol 2005;23:19–27.

10. Rao K, Goodin S, Levitt MJ, et al. A phase II trial of imatinib mesylate in patients with prostate specific antigen progression after local therapy for prostate cancer. Prostate 2005;62:115–22.

11. Rubin J, Chung LW, Fan X, et al. Prostate carcinoma cells that have resided in bone have an upregulated IGF-I axis. Prostate 2004;58:41–9.

12. Wittrant Y, Theoleyre S, Chipoy C, et al. RANKL/ RANK/OPG: new therapeutic targets in bone tumours and associated osteolysis. Biochim Biophys Acta 2004; 1704:49–57.

13. Cunningham BA, Wang JL, Berggard I, Peterson PA. The complete amino acid sequence of β2-microglobulin. Biochemistry 1973;12:4811–22.

14. Gussow D, Rein R, Ginjaar I, et al. The human β2-microglobulin gene. Primary structure and definition of the transcriptional unit. J Immunol 1987;139:3132–8.

15. Pedersen LO, Hansen AS, Olsen AC, et al. The interaction between β2-microglobulin (β2m) and purified class-I major histocompatibility (MHC) antigen. Scand J Immunol 1994;39:64–72.

16. Townsend AR, Rothbard J, Gotch FM, et al. The epitopes of influenza nucleoprotein recognized by cytotoxic T lymphocytes can be defined with short synthetic peptides. Cell 1986;44:959–68.

17. Seliger B. Strategies of tumor immune evasion. BioDrugs 2005;19:347–54.

18. Bataille R, Durie BG, Grenier J. Serum β2 microglobulin and survival duration in multiple myeloma: a simple reliable marker for staging. Br J Haematol 1983; 55:439–47.

19. Abdul M, Hoosein N. Changes in β-2 microglobulin expression in prostate cancer. Urol Oncol 2000;5:168–72.

20. Auer IO, Watzel C, Greulich M. The plasma concentration of β2-microglobulin in the diagnosis of malignancy of the gastrointestinal tract. Med Klin 1979;74:1581–3.

21. Klein T, Levin I, Niska A, et al. Correlation between tumour and serum β2m expression in patients with breast cancer. Eur J Immunogenet 1996;23:417–23.

22. Evans DB, Thavarajah M, Kanis JA. Immunoreactivity and proliferative actions of β2 microglobulin on human bone-derived cells *in vitro*. Biochem Biophys Res Commun 1991;175:795–803.

23. Rowley DR, Dang TD, McBride L, et al. β-2 microglobulin is mitogenic to PC-3 prostatic carcinoma cells and antagonistic to transforming growth factor β1 action. Cancer Res 1995;55:781–6.

24. Centrella M, McCarthy TL, Canalis E. β2-microglobulin enhances insulin-like growth factor I receptor levels and synthesis in bone cell cultures. J Biol Chem 1989;264:18268–71.

25. Due C, Simonsen M, Olsson L. The major histocompatibility complex class I heavy chain as a structural subunit of the human cell membrane insulin receptor: implications for the range of biological functions of histocompatibility antigens. Proc Natl Acad Sci U S A 1986;83:6007–11.

26. Schreiber AB, Schlessinger J, Edidin M. Interaction between major histocompatibility complex antigens and epidermal growth factor receptors on human cells. J Cell Biol 1984;98:725–31.

27. Gleave M, Hsieh JT, Gao CA, von Eschenbach AC, Chung LW. Acceleration of human prostate cancer growth *in vivo* by factors produced by prostate and bone fibroblasts. Cancer Res 1991;51:3753–61.

28. Edman P. Sequence determination. Mol Biol Biochem Biophys 1970;8:211–55.

29. Zou Y, Peng H, Zhou B, et al. Systemic tumor suppression by the proapoptotic gene bik. Cancer Res 2002;62:8–12.

30. Bisanz K, Yu J, Edlund M, et al. Targeting ECM-integrin interaction with liposome-encapsulated small interfering RNAs inhibits the growth of human prostate cancer in a bone xenograft imaging model. Mol Ther 2005;12:634–43.

31. Thalmann GN, Sikes RA, Wu TT, et al. LNCaP progression model of human prostate cancer: androgen-independence and osseous metastasis. Prostate 2000;44: 91–103.

32. Beier F, LuValle P. The cyclin D1 and cyclin A genes are targets of activated PTH/PTHrP receptors in Jansen's metaphyseal chondrodysplasia. Mol Endocrinol 2002;16:2163–73.

33. Gleave ME, Hsieh JT, Wu HC, von Eschenbach AC, Chung LW. Serum prostate specific antigen levels in mice bearing human prostate LNCaP tumors are determined by tumor volume and endocrine and growth factors. Cancer Res 1992;52:1598–605.

34. Reddi AH, Huggins CB. Obligatory transformation of fibroblasts by bone matrix in rats fed sucrose ration. Proc Soc Exp Biol Med 1974;145:475–8.

35. Wu TT, Sikes RA, Cui Q, et al. Establishing human prostate cancer cell xenografts in bone: induction of osteoblastic reaction by prostate-specific antigen-producing tumors in athymic and SCID/bg mice using LNCaP and lineage-derived metastatic sublines. Int J Cancer 1998;77:887–94.

36. Thornberry NA, Lazebnik Y. Caspases: enemies within. Science 1998;281:1312–6.

37. Pandit-Taskar N, Batraki M, Divgi CR. Radiopharmaceutical therapy for palliation of bone pain from osseous metastases. J Nucl Med 2004;45:1358–65.

38. Schmittgen TD, Zakrajsek BA. Effect of experimental treatment on housekeeping gene expression: validation by real-time, quantitative RT-PCR. J Biochem Biophys Methods 2000;46:69–81.

39. Al-Wadei HA, Takahashi T, Schuller HM. Growth stimulation of human pulmonary adenocarcinoma cells and small airway epithelial cells by β-carotene via activation of cAMP, PKA, CREB, and ERK1/2. Int J Cancer 2006;118:1370–80.

40. Shankar DB, Cheng JC, Kinjo K, et al. The role of CREB as a proto-oncogene in hematopoiesis and in acute myeloid leukemia. Cancer Cell 2005;7:351–62.

41. Abramovitch R, Tavor E, Jacob-Hirsch J, et al. A pivotal role of cyclic AMP-responsive element binding protein in tumor progression. Cancer Res 2004;64:1338–46.

42. Morishita K, Johnson DE, Williams LT. A novel promoter for vascular endothelial growth factor receptor (flt-1) that confers endothelial-specific gene expression. J Biol Chem 1995;270:27948–53.

43. Karadag A, Ogbureke KU, Fedarko NS, Fisher LW. Bone sialoprotein, matrix metalloproteinase 2, and α(v)β3 integrin in osteotropic cancer cell invasion. J Natl Cancer Inst 2004;96:956–65.

44. Sung V, Stubbs JT III, Fisher L, Aaron AD, Thompson EW. Bone sialoprotein supports breast cancer cell adhesion proliferation and migration through differential usage of the α(v)β3 and α(v)β5 integrins. J Cell Physiol 1998;176:482–94.

45. Sakai D, Suzuki T, Osumi N, Wakamatsu Y. Cooperative action of Sox9, Snail2, and PKA signaling in early neural crest development. Development 2006;133:1323–33.

46. Huber MA, Kraut N, Beug H. Molecular requirements for epithelial-mesenchymal transition during tumor progression. Curr Opin Cell Biol 2005;17:548–58.

47. Elbashir SM, Harborth J, Lendeckel W, et al. Duplexes of 21-nucleotide RNAs mediate RNA interference in cultured mammalian cells. Nature 2001;411:494–8.

## Human Cancer Biology

# β₂-Microglobulin Promotes the Growth of Human Renal Cell Carcinoma through the Activation of the Protein Kinase A, Cyclic AMP – Responsive Element-Binding Protein, and Vascular Endothelial Growth Factor Axis

Takeo Nomura,[1,5] Wen-Chin Huang,[1] Haiyen E. Zhau,[1] Daqing Wu,[1] Zhihui Xie,[1] Hiromitsu Mimata,[5] Majd Zayzafoon,[6] Andrew N. Young,[2] Fray F. Marshall,[3] M. Neale Weitzmann,[4] and Leland W.K. Chung[1]

**Abstract**

**Purpose:** β₂-Microglobulin (β2M), a soluble protein secreted by cancer and host inflammatory cells, has various biological functions, including antigen presentation. Because aberrant expression of β2M has been reported in human renal cell carcinoma, we investigated the effects of β2M overexpression on cancer cell growth and analyzed its molecular signaling pathway.

**Experimental Design:** We established clonal cell lines that overexpressed β2M in human renal cell carcinoma (SN12C) cells and then examined cell growth *in vitro* and *in vivo* and studied the β2M-mediated downstream cell signaling pathway.

**Results:** Our results showed that β2M expression positively correlates with (*a*) *in vitro* growth on plastic dishes and as Matrigel colonies, (*b*) cell invasion and migration in Boyden chambers, and (*c*) vascular endothelial growth factor (VEGF) expression and secretion by cells. We found, in addition, that β2M mediates its action through increased phosphorylation of cyclic AMP – responsive element-binding protein (CREB) via the protein kinase A-CREB axis, resulting in increased VEGF expression and secretion. In convergence with this signal axis, β2M overexpression also activated both phosphatidylinositol 3-kinase/Akt and mitogen-activated protein kinase pathways. β2M overexpression induced accelerated growth of SN12C in mouse subcutis and bone. Interrupting the β2M signaling pathway using small interfering RNA led to apoptosis with increased activation of caspase-3 and caspase-9 and cleaved poly (ADP-ribose) polymerase.

**Conclusions:** Our results showed for the first time that the β2M-protein kinase A-CREB-VEGF signaling axis plays a crucial role in support of renal cell carcinoma growth and progression and reveals a novel therapeutic target.

*β₂-Microglobulin* (*β2M*), a well-known housekeeping gene, is a 12-kDa nonglycosylated polypeptide composed of 100 amino acids. β2M is synthesized by all nucleated cells and forms complexes with the heavy chain of MHC class I (1). MHC class I or HLA antigen plays an important role in tumor immunity because cancer cells present peptides that are degraded by proteasome but still recognized by cytotoxic T cells (2–4). The expression of MHC class I antigen has been observed in some cancer cells, but down-regulation or loss of HLA molecules on the surface of cancer cells is often associated with the progression of several tumor types (5–8) due in part to the ability of cancer cells to evade host immune surveillance and subsequent elimination by cytotoxic T cells. However, the biological functions of β2M in cancer and bone metastasis are still unknown.

β2M protein expression by normal and cancer cells and its clinical usefulness has been the subject of investigation for the past two decades. With few of these studies showing a direct mitogenic action of β2M (9), no study has attempted to delineate the potential signaling function of β2M in cancer cells. β2M is a soluble factor synthesized and secreted by cancer and inflammatory cells. Increased synthesis and release of β2M occur in several malignant diseases as indicated by an elevated serum or urine β2M concentration (10–18). In addition, the level of β2M is one of the most important independent prognostic factors and survival predictors in some tumors, including renal cell carcinoma (12, 14, 16). Therefore, we hypothesized that β2M is not only a surrogate marker for tumor burden but also an important signaling molecule regulating renal cell carcinoma cell growth and behavior. The

goals of this study are as follows: (*a*) to define β2M as a soluble growth factor and signaling molecule, (*b*) to characterize the downstream signaling pathways of β2M, and (*c*) to explore β2M as a novel therapeutic target in human renal cell carcinoma.

To test our hypothesis, we established stably β2M-over-expressing SN12C cells and investigated the growth and behavior of this renal cell carcinoma cell line *in vitro* and its tumor formation *in vivo*. In this report, we showed that β2M is a growth factor and a signaling molecule in renal cell carcinoma. By silencing the basal β2M expression, we observed marked induction of apoptosis as evidenced by increased caspase activities and cleaved poly(ADP-ribose) polymerase in renal cell carcinoma cells *in vitro*. We established that β2M downstream signaling is mediated by activation of the protein kinase A/cyclic AMP (cAMP)–responsive element-binding protein/vascular endothelial growth factor (PKA-CREB-VEGF) axis with potential crosstalk with phosphatidylinositol 3-kinase (PI3K)/Akt and mitogen-activated protein kinase (MAPK) signaling in human renal cell carcinoma cells.

## Materials and Methods

*Reagents.* Recombinant human β2M was purchased from Sigma (St. Louis, MO). Forskolin (Alexis Biochemicals, San Diego, CA) and *N*-[2-(*p*-bromocinnamylamino)ethyl]-5-isoquinolinesulfonamide (H-89; Alexis Biochemicals) were used for the analysis of cAMP-dependent signaling pathway.

*Cell culture.* Human renal cell carcinoma SN12C cells (19) were cultured in MEM (Life Technologies, Grand Island, NY) supplemented with 10% heat-inactivated fetal bovine serum (Bio Whittaker, Walkersville, MD), with 50 IU/mL penicillin and 50 μg/mL streptomycin (Life Technologies) in 5% $CO_2$ at 37°C.

*Plasmid construction.* For construction of the β2M expression vector, β2M cDNA was isolated by reverse transcription-PCR (RT-PCR) from cells and flanked with *Hin*dIII and *Xba*I cloning sites. After RT-PCR, the β2M cDNA (427 bp) was sequenced and subcloned into pcDNA3.1 expression vector (Invitrogen, Carlsbad, CA). The empty pcDNA3.1 expression vector was used as the control (Neo).

*Stable transfection of β2M expression vector.* Transfection was conducted using LipofectAMINE 2000 (Invitrogen) as recommended by the manufacturer. Briefly, SN12C cells were seeded in six-well plates at a density of $3 \times 10^5$ per well 24 h before transfection in medium supplemented with fetal bovine serum. Cells were transfected using 4 μg of plasmid DNA (pcDNA3.1-β2M or pcDNA3.1-Neo) and 10 μL LipofectAMINE 2000 per well. To obtain stable transfectants, the pcDNA3.1-β2M or empty vector–transfected cells were cultured in the presence of 800 μg/mL geneticin sulfate. Several isolated clones were selected, and positive clones were identified by ELISA, RT-PCR, and immunoblot analyses.

*ELISA.* β2M protein secreted by the cells was measured in culture media by a commercial ELISA kit (R&D Systems, Minneapolis, MN). Briefly, exponentially growing cells were seeded at a density of $6 \times 10^5$ per well in six-well dishes containing fetal bovine serum and cultured until 80% confluent. The medium was replaced with serum-free MEM, and conditioned medium was collected after 72 h. Expression of β2M was assessed according to the manufacturer's protocol (R&D Systems). Color develops by addition of tetramethylbenzidine, and the intensity is measured at 450 nm with dual wavelength correction at 620 nm. The concentration of total protein in conditioned medium was determined by the Bradford method using Coomassie plus protein reagent (Pierce, Rockford, IL). Secretion of vascular endothelial growth factor (VEGF) protein secreted by the cells was also measured in the conditioned medium by a commercial VEGF ELISA kit (R&D Systems).

*Cell viability assay.* Cell viability was determined with a colorimetric 3-(4,5-dimethylthiazol-2-yl)-5-(3-carboxymethoxyphenyl)-2-(4-sulfophenyl)-2*H*-tetrazolium (MTS; Promega, Madison, WI) assay. Briefly, exponentially growing cells were seeded at a density of $2 \times 10^3$ per well in 96-well plates and cultured for 4 days. Twenty microliters of MTS reagent was added to each well containing 100 μL of fresh culture medium. After a 1-h incubation period, optical absorbance at 490 nm was measured.

*Flow cytometric analysis.* For cell cycle analysis, flow cytometric analysis of propidium iodide–stained nuclei was done. Briefly, cells were plated at a density of $5 \times 10^5$ in a 60-mm dish overnight. The cells were collected by trypsinization and fixed with 70% ethanol. The fixed cells were incubated with 100 μg/mL RNase A (Sigma) for 30 min and stained with 25 μg/mL propidium iodide (Chemicon, Temecula, CA) for 30 min. Cell cycle was analyzed with a FACScan flow cytometer and CellQuest software (Becton Dickinson Labware, Lincoln Park, NJ). The data were expressed as a mean percentage from three independent experiments.

*Colony-forming assay.* Intrinsic anchorage-independent growth activity *in vitro* closely reflects the tumorigenicity of the epithelial cells (20). The cells were cultured in a two-layer Matrigel system (BD Biosciences, Bedford, MA) to prevent their attachment to the plastic surface. Cells ($1 \times 10^3$) were trypsinized to single-cell suspensions, resuspended in Matrigel (150 μL, 3.7 mg/mL), and added to a pre-set Matrigel layer in 24-well plates. The top Matrigel cell layers were covered with culture medium containing 10% fetal bovine serum. Colonies >200 μm in 10 randomly selected fields were scored 14 days after plating.

*Invasion and migration assays.* Cancer cell invasion and migration were assayed in Companion 24-well plates (Becton Dickinson Labware) with 8-μm-porosity polycarbonate filter membrane. A suspension of $5 \times 10^4$ cells in 100 μL of medium was layered in the upper compartment of a well with 15 μg/mL collagen I (BD Biosciences) as attractant in the lower compartment. After incubation at 37°C for 48 h, the cells on the upper surface of the filters were removed by swabbing with a cotton swab, and cells that had migrated to the lower surface were stained with 0.5% crystal violet. After washing, stain was eluted from migratory cells with Sorensen's solution. The absorbance of each well was measured at 590 nm. For invasion assays, the same procedures described above were used, except filters were precoated with Matrigel (BD Biosciences) at a 1:4 dilution with medium.

*RNA preparation and RT-PCR reaction.* Total RNA was isolated from confluent cell monolayers using the RNeasy Mini kit (Qiagen, Valencia, CA). Total RNA (2-5 μg) was used as template, and oligo-dT (0.5 μg) was added for reverse transcription and amplification in a reaction volume of 20 μL according to the manufacturer's instructions (Invitrogen). After reverse transcription reaction, first-strand cDNA (2 μL) was used for PCR with a PTC-100 programmable thermal controller (MJ Research, Inc., Waltham, MA). The oligonucleotide primer sets used for PCR analysis of cDNA are human β2M (427 bp) 5′-ACGCGTCCGAAGCTTACAGCATTC-3′ (forward) and 5′-CCAAATG-CGGCATCTAGAAACCTCCATG-3′ (reverse), human VEGF (404 bp) 5′-CGAAGTGGTGAAGTTCATGGATG-3′ (forward) and 5′-TTCTGT-ATCAGTCTTTCCTGGT-3′ (reverse), human neuropilin 1 (210 bp) 5′-AGGACAGAGACTGCAAGTATGAC-3′ (forward) and 5′-AACATT-CAGGACCTCTCTTGA-3′ (reverse), and glyceraldehyde-3-phosphate dehydrogenase (450 bp) 5′-ACCACAGTCCATGCCATCA-3′ (forward) and 5′-TCCACCACCCTGTTGCTGT-3′ (reverse). The thermal profile for human β2M amplification is 40 cycles, starting with denaturation of 1 min at 94°C followed by 1 min of annealing at 64°C and 30 s for extension at 72°C. For human VEGF and neuropilin 1 amplification, the thermal profile is 35 cycles, starting with denaturation for 15 s at 94°C followed by 30 s of annealing at 60°C and 1 min of extension at 68°C. The program for glyceraldehyde-3-phosphate dehydrogenase amplification is 25 cycles, starting with denaturation for 30 s at 94°C followed by 30 s of annealing at 60°C and 1 min of extension at 72°C. The RT-PCR products were analyzed by 1.0% agarose gel

electrophoresis. Quantity one-4.1.1 Gel Doc gel documentation software (Bio-Rad, Hercules, CA) or NIH Image (version 1.55) was used for quantification of each mRNA expression normalized by glyceraldehyde-3-phosphate dehydrogenase mRNA expression.

***Immunoblot analysis.*** Protein was extracted from cell pellets with a lysis buffer [50 mmol/L Tris (pH 8), 150 mmol/L NaCl, 0.02% NaN$_3$, 0.1% SDS, 1% NP40, 0.5% sodium deoxycholate, and 1 mmol/L phenylmethylsulfonyl fluoride] in the presence of protease inhibitor cocktail (Roche Applied Science, Indianapolis, IN). Samples containing equal amounts of protein (30 μg) were electrophoresed on 8% to 16% Tris-Glycine gels (Invitrogen) and transferred to nitrocellulose membranes. After blocking with T-TBS containing 5% nonfat milk powder, the membranes were incubated with mouse monoclonal antibody against β2M (1:500 dilution; Santa Cruz Biotechnology, Santa Cruz, CA) or rabbit polyclonal antibodies against PKA C (1:1,000 dilution; Cell Signaling, Danvers, MA), phospho-PKA C (Thr[197]; 1:1,000 dilution; Cell Signaling), CREB (1:1,000 dilution; Cell Signaling), phospho-CREB (Ser[133]; 1:1,000 dilution; Cell Signaling), Akt (1:1,000 dilution; Cell Signaling), phospho-Akt (1:1,000 dilution; Cell Signaling), extracellular signal-regulated kinase (ERK; 1:1,000 dilution; Santa Cruz Biotechnology), phospho-ERK (1:1,000 dilution; BioSource, Camarillo, CA), VEGF (1:200 dilution; Santa Cruz Biotechnology), VEGFR-2 (Flk-1; 1:1,000 dilution; Cell Signaling), neuropilin 1 (1:500 dilution; Santa Cruz Biotechnology), caspase-3 (1:1,000 dilution; Cell Signaling), caspase-9 (1:500 dilution; Cell Signaling), and poly(ADP-ribose) polymerase (1:1,000 dilution; Cell Signaling), respectively, at 4°C overnight. After washing with T-TBS, the membranes were incubated with corresponding secondary antibodies, which were conjugated with horseradish peroxidase (Santa Cruz Biotechnology). The blots were stripped and reprobed with anti-β-actin antibody (1:5,000 dilution; Sigma). Immunoreactive bands were visualized with enhanced chemiluminescence (Amersham Pharmacia Biotech, Little Chalfont, United Kingdom). Relevant cell signaling pathways were confirmed by the use of appropriate pathway-specific inhibitors. To analyze inhibition of the PI3K/Akt and MAPK pathways, cells were treated with LY294002 (Calbiochem, Darmstadt, Germany) and U0126 (Calbiochem) for 30 min or 6 h, respectively.

***Transient transfection of β2M small interfering RNA.*** SN12C cells were transiently transfected either with β2M small interfering RNA (siRNA) duplex (si-β2M; final concentration of 40 nmol/L) or a control siRNA (a random scrambled sequence: si-Scr; final concentration of 40 nmol/L) using LipofectAMINE 2000 according to the manufacturer's instructions. Sequences of the siRNA against β2M and control scramble synthesized by Invitrogen are 5′-UUGCUAUGUGUCUGGGUUU(dT)(dT)-3′ and 5′-UUCAUGUGUCUGUGGGUGUU(dT)(dT)-3′, respectively. Following transfection, cells were subjected to MTS assay, and invasion and migration assays or immunoblot analysis with the antibodies against β2M, caspase-3, caspase-9, and poly(ADP-ribose) polymerase.

***In vivo animal experiment.*** The effect of β2M on osteoclastogenesis and tumorigenicity *in vivo* was assessed in tumor-bearing nude mice. Four-week-old male athymic nude mice (19-21 g; BALB/c *nu/nu* mice, National Cancer Institute, Frederick, MD) were housed in accordance with the NIH guidelines using an animal protocol approved by the Institutional Animal Care and Use Committee of Emory University. Cells were trypsinized, and single-cell suspensions ($1 \times 10^6$ cells) of each subclone were then injected into both tibias ($n = 8$). The estimated volume of bone tumors was calculated by three axes ($X$, $Y$, and $Z$) measured from a radiograph using the formula of $\pi/6XYZ$ (21). Tumor size was also quantified by measuring hind limb diameter every 5 days. For s.c. injection, $2 \times 10^6$ cells were mixed 1:1 with Matrigel and then injected into the flank ($n = 8$). S.c. tumor mass was measured in two dimensions with calipers, and the tumor volume was calculated every 5 days according to the equation $(l \times w^2) / 2$, where $l$ = length and $w$ = width (22). Animals were sacrificed by $CO_2$ asphyxiation if the tumor volumes exceeded the allowable size, and tumor weights were measured. At the time of sacrificing the mice, both hind limbs and

tumor tissues were harvested for immunohistochemistry and H&E staining. Selected specimens of tibia were subjected to micro-computed tomography analysis using established procedures (23).

***Immunohistochemical protocol.*** After sacrifice, s.c. tumor tissues were fixed with 10% buffered formalin and embedded in paraffin. The tibias were removed and fixed with 10% buffered formalin and decalcified in 10% EDTA solution. Sections from the formalin-fixed, paraffin-embedded tissues were cut to 4 μm and deparaffinized in xylene followed by treatment with a graded series of ethanol and rehydration in PBS. For antigen retrieval, the slides were treated with a Target Retrieval Solution (S1699; DAKO, Carpinteria, CA) in a pressure cooker at 125°C and 20 p.s.i. for 30 s. Next, sections were immersed in 3% hydrogen peroxide and then incubated in 2% goat serum. The sections were incubated with the following antibodies overnight at 4°C: CREB (Cell Signaling), phospho-CREB (Ser[133]; Cell Signaling), MIB-1 (DAKO) for Ki-67, anti-human VEGF (PeproTech, London, England), platelet/endothelial cell adhesion molecule 1 (M-20; Santa Cruz Biotechnology) for CD31, and β$_2$-microglobulin (BBM.1; Santa Cruz Biotechnology). They were diluted 100×, 40×, 1×, 100×, 600×, and 500×, respectively, with PBS containing 1% bovine serum albumin. After washing with PBS, sections were incubated with secondary antibodies, which were conjugated with peroxidase-labeled amino acid polymer (DAKO). The immune complex was visualized using a 3,3′-diaminobenzidine peroxytrichloride substrate solution (DAKO). Slides were then counterstained with hematoxylin and mounted. For bone samples, tartrate-resistant acid phosphate staining was also done for detecting osteoclasts. Osteoclasts were determined as tartrate-resistant acid phosphate–positive staining multinuclear cells using light microscopy. The number of osteoclasts per millimeter of bone was determined by examination of tartrate-resistant acid phosphate–stained sections at ×10 magnification.

In parallel, human renal nonmalignant and carcinoma tissue specimens were also stained with antibody against β2M (Santa Cruz Biotechnology) to confirm the expression of β2M. These tissue specimens were obtained from the Kidney Satellite Tissue Bank of Emory University under institutionally approved protocols.

***Evaluation of β2M, pCREB/CREB, Ki-67, VEGF, and microvessel density.*** To assess β2M and VEGF expression, whole sections were scored semiquantitatively using a visual grading system based on the intensity of staining (−, negative; ±, equivocal; +, weak; ++, moderate; +++, strong), according to the intensity of chromogen deposition in the majority of cancer cells evaluated independently by two observers. Two groups were considered for the statistical analysis: intensity levels −, ±, and + and strong focal staining pattern or diffuse light staining were considered low-intensity staining, whereas ++, +++, and strong diffuse staining pattern were considered high-intensity staining. The evaluation of pCREB/CREB and Ki-67 expression was based on the proportion of positive-stained cells among a total of 1,000 cells that were counted. For the quantification of microvessel density, 10 random 0.739 mm$^2$ per field at ×200 magnification were captured, and microvessels were counted.

***Statistical analysis.*** Values were expressed as means ± SE. Statistical analysis was done using the Student's *t* test or one-way ANOVA. Relationships between qualitative variables were determined using the $\chi^2$ test. $P$s $< 0.05$ were considered statistically significant.

## Results

***Expression of β2M in human renal tissue specimens.*** The expression of β2M was assessed by immunohistochemistry in 12 human renal tissue specimens containing both normal and renal cell carcinoma (two, five, and five patients of G$_1$, G$_2$, and G$_3$ clear cell carcinoma, respectively) within each specimen. The expression of β2M was detected in all renal cell carcinoma tissues (Fig. 1A, *right*), but β2M staining was sparse and only found in the luminal border of normal renal tubules adjacent
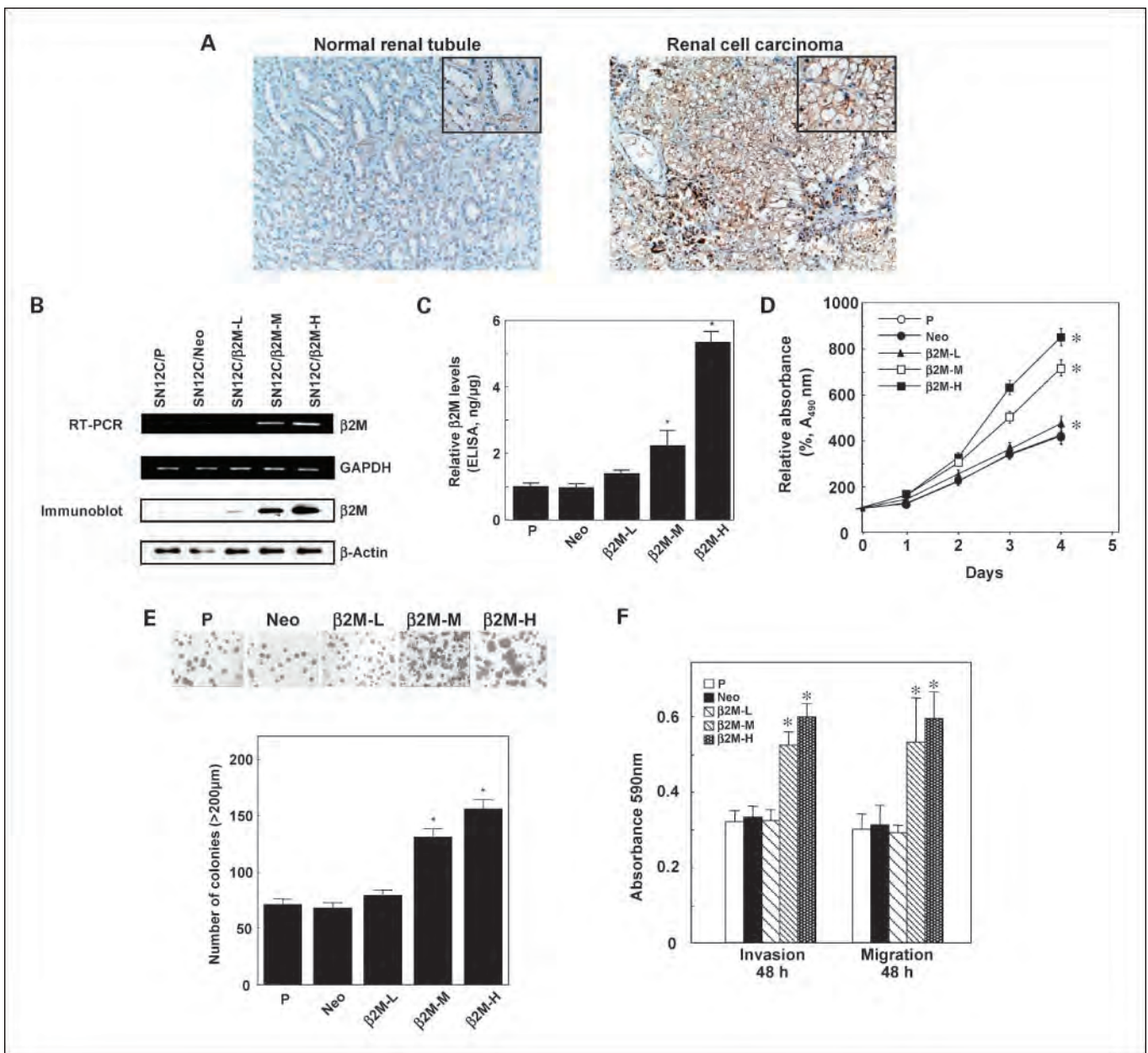
**Fig. 1.** Expression of β2M in tissue specimens of renal cell carcinoma and effects of β2M on cancer cell growth and behavior. *A,* immunohistochemical staining of β2M in human renal nonmalignant and carcinoma tissue specimens. Negative or weak β2M stains were observed in normal renal tissue (*left*), whereas renal cell carcinoma tissue (clear cell carcinoma, $G_2$) stained positively and strongly with anti-β2M antibody (*right*). Magnification, ×100. Inset, magnified image. Magnification, ×200. *B,* RT-PCR and immunoblot analyses of cell lysates derived from SN12C subclones. Relative expression values of β2M mRNA were normalized by the amounts of glyceraldehyde-3-phosphate dehydrogenase (*GAPDH*) mRNA expression. *C,* β2M concentration was measured by ELISA in conditioned medium. ng β2M protein/μg total protein. The value of the control (SN12C/P) was taken as 1, and other values were calculated from this. Columns, mean from three independent experiments; bars, SE. *, $P < 0.01$ compared with SN12C/P and SN12C/Neo cells. *D,* the effects of β2M on cell proliferation in each subclone were determined by MTS assay. Points, mean from three independent experiments; bars, SE. *, $P < 0.01$ compared with SN12C/P and SN12C/Neo cells. *E,* the effects of β2M on anchorage-independent growth of SN12C subclones. After 14 d of incubation, visible colonies (>200 μm) were photographed (*top*) and counted (*bottom*). Columns, mean from three independent experiments collected from each experimental group; bars, SE. *, $P < 0.01$ compared with SN12C/P and SN12C/Neo cells. *F,* the effects of β2M on invasion and migration of SN12C subclones. $A_{590\ nm}$ values correspond to cells that migrated to the lower side of the filter. Columns, mean from three independent experiments; bars, SE. *, $P < 0.05$ compared with SN12C/P and SN12C/Neo cells.

to renal cell carcinoma tissues (Fig. 1A, *left*). β2M was largely membrane bound in all cancer cells, and in some cases, it was also expressed focally in the cell cytoplasm.

***Expression levels of β2M in human renal cell carcinoma cell lines and in parental and β2M-transfected SN12C subclones.*** All human renal cell carcinoma cell lines examined in this study expressed β2M protein as evaluated by immunoblot analysis.

Compared with ACHN cells, SN12C and Caki-1 cells expressed higher levels of β2M by 2.0- and 1.8-fold, respectively. To understand the roles of β2M in cell proliferation and apoptosis, we chose to study SN12C cells because of its high levels of β2M expression, which can be subjected to overexpression or knockdown manipulation of β2M protein. Parental SN12C cells (SN12C/P) were stably transfected with the human β2M

cDNA expression vector pcDNA3.1-β2M or pcDNA3.1-Neo vector alone as a control. We selected three clones labeled as having low (L), medium (M), or high (H) levels of β2M expression for further characterization. These clones were subjected to semiquantitative RT-PCR and immunoblot analyses to confirm the level of β2M expression (Fig. 1B). In the following experiments, we used two clones (SN12C/β2M-H expressing high β2M levels and SN12C/β2M-M expressing medium β2M levels) for molecular analysis. SN12C/P and the derivative SN12C/P transfected with empty pcDNA3.1 vector (SN12C/Neo) served as controls.

*β2M protein secretion by parental and derivative SN12C subclones.* We first examined the β2M protein level in culture medium as determined by ELISA in each subclone. β2M protein was undetectable in cell free MEM culture medium. The concentrations of β2M in the supernatants from β2M-overexpressing transfectants were significantly higher than those of SN12C/P and SN12C/Neo ($P < 0.01$; Fig. 1C). Moreover, β2M secretion in the conditioned medium correlated with the protein expression levels of β2M observed by immunoblot (Fig. 1B) in derivative SN12C subclones. These results confirm that β2M is a soluble factor secreted by SN12C cells.

*Overexpression of β2M in SN12C promotes cell proliferation in vitro.* To determine the possible role of β2M in promoting renal cell carcinoma cell growth, we examined the growth rates of each subclone by MTS assay. The growth rates of β2M-overexpressing transfectants were significantly higher than those of SN12C/P and SN12C/Neo ($P < 0.01$; Fig. 1D). SN12C/β2M-M and SN12C/β2M-H had significantly higher growth rates than SN12C/β2M-L ($P < 0.01$). These results suggest that β2M is an effective soluble growth-promoting factor for SN12C cells *in vitro*. We found that ectopic expression of β2M increases cell number by increasing cells in the proliferative phase as assessed by flow cytometry. SN12C/β2M-H cells were observed to have a substantial decreased percentage of cells in the $G_0$-$G_1$ phase ($36.8 \pm 2.1\%$, $P < 0.01$), with a corresponding increased percentage of cells in S ($43.9 \pm 0.6\%$, $P < 0.01$) and $G_2$-M phase ($19.4 \pm 2.7\%$) when compared with SN12C/Neo cells ($G_0$-$G_1$: $54.0 \pm 3.8\%$, S: $28.8 \pm 2.8\%$, $G_2$-M: $17.3 \pm 1.0\%$). These results collectively suggest that β2M increases renal cell carcinoma cell number primarily through increased cell proliferation.

*Effect of β2M on anchorage-independent growth of SN12C cells in Matrigel.* To determine the effect of β2M expression on anchorage-independent growth of SN12C cells, we did a colony formation assay in Matrigel. The numbers of colonies formed by β2M-overexpressing transfectants (SN12C/β2M-M: $130 \pm 9$ and SN12C/β2M-H: $157 \pm 9$) were significantly higher than those of SN12C/P ($72 \pm 4$, $P < 0.01$), SN12C/Neo ($68 \pm 4$, $P < 0.01$), and SN12C/β2M-L ($77 \pm 4$, $P < 0.01$; Fig. 1E).

*Effect of β2M on the invasion and migration of SN12C cells.* We next analyzed whether the β2M expression level correlated with the *in vitro* invasiveness of cells as tested by their capacity to pass through a Matrigel barrier as assayed in a modified Boyden chamber. In comparison with SN12C/P and SN12C/Neo, SN12C/β2M-M and SN12C/β2M-H presented with a 1.6- and 1.9-fold higher invasiveness, respectively, at 48 h after seeding ($P < 0.05$; Fig. 1F). The ability of β2M-overexpressing transfectants to invade through Matrigel increased with increased β2M expression. This increased invasiveness led us to examine if β2M may also affect cell migration,

a key component of the invasive process. β2M overexpression increased cell migration in SN12C/β2M-M and SN12C/β2M-H by 1.7- and 1.9-fold, respectively, in comparison with SN12C/P and SN12C/Neo ($P < 0.05$; Fig. 1F). These results suggest that β2M increases *in vitro* SN12C cell invasion and migration.

*β2M activates the PKA-CREB-VEGF axis in SN12C cells.* To determine whether phosphorylation of CREB may be mediated through an activation of the PKA signaling pathway induced by β2M, we assessed the effects of β2M, forskolin (a PKA signaling pathway activator), and H-89 (an inhibitor of PKA signaling) on activation of phosphorylation of CREB in SN12C/P cells. We evaluated the effects of conditioned media (0.5 μg/mL) from SN12C/β2M-H cells, recombinant β2M protein (0.5 μg/mL), or forskolin (5 μmol/L) on the activation of phosphorylation of CREB in SN12C/P cells. In parallel, we also evaluated the effects of H-89 (5 μmol/L), which inhibited phosphorylation of CREB in cells treated with conditioned media containing β2M, recombinant β2M, or forskolin with VEGF expression as the signal output. The expression of VEGF roughly paralleled the levels of phosphorylation of CREB (Fig. 2A). Activation of cAMP-dependent PKA signaling pathway by β2M or forskolin resulted in increased phosphorylation of CREB and increased expression of VEGF, and these effects can be blocked by H-89 in SN12C/P cells (Fig. 2A). In response to β2M overexpression, we found elevated levels of phosphorylation of CREB/activating transcription factor-1 and VEGF165 and VEGF121 mRNAs and VEGF protein associated with SN12C subclones that expressed variable levels of β2M (Fig. 2B). Consistent with these results, we also found 2.5- and 3.1-fold increased VEGF secretion by SN12C/β2M-M and SN12C/β2M-H cells, respectively ($P < 0.05$; Fig. 2C), when compared with SN12C/P cells. Next, we investigated the expression of VEGFR-2 (Flk-1) and its co-receptor neuropilin 1 by RT-PCR and immunoblot analyses. Although there was no change in the expression level of VEGFR-2, RT-PCR and immunoblot analyses showed that neuropilin 1 mRNA and protein expression were elevated in SN12C/β2M-M and SN12C/β2M-H compared with SN12C/P and SN12C/Neo (Fig. 2D). These results suggest that activation of PKA-CREB signaling elevated VEGF and VEGFR-2 co-receptor neuropilin 1 expression in SN12C cells.

*Differential regulation of PI3K/Akt and MAPK pathways by β2M in SN12C cells.* To determine if there is a convergence of cell signaling among β2M/PKA/CREB, PI3K/Akt, and MAPK, we examined the basal and β2M-activated status of the PI3K/Akt and MAPK signaling pathways. The status of phosphorylation of both kinases was analyzed using phospho-specific antibodies. As shown in Fig. 2E, Akt was highly phosphorylated in SN12C/β2M-M and SN12C/β2M-H compared with SN12C/P and SN12C/Neo cells. We also found moderate increase in the phosphorylation of ERK in SN12C/β2M-M and SN12C/β2M-H compared with SN12C/P and SN12C/Neo cells. These results suggest that activation of PI3K/Akt and MAPK pathways can be triggered as the consequence of ectopic expression of β2M in SN12C cells. β2M has a profound effect on the PI3K/Akt pathway but a more modest effect on the phosphorylation of ERK, although protein levels of non-phosphorylated Akt and ERK were not affected by β2M transfection. Thus, the PI3K/Akt pathway seems to play a more dominant role in conferring β2M-mediated increases in cell proliferation in SN12C cells.

Consistent with these observations, we evaluated the effect of LY294002 (a PI3K inhibitor) and U0126 (a MAPK inhibitor)
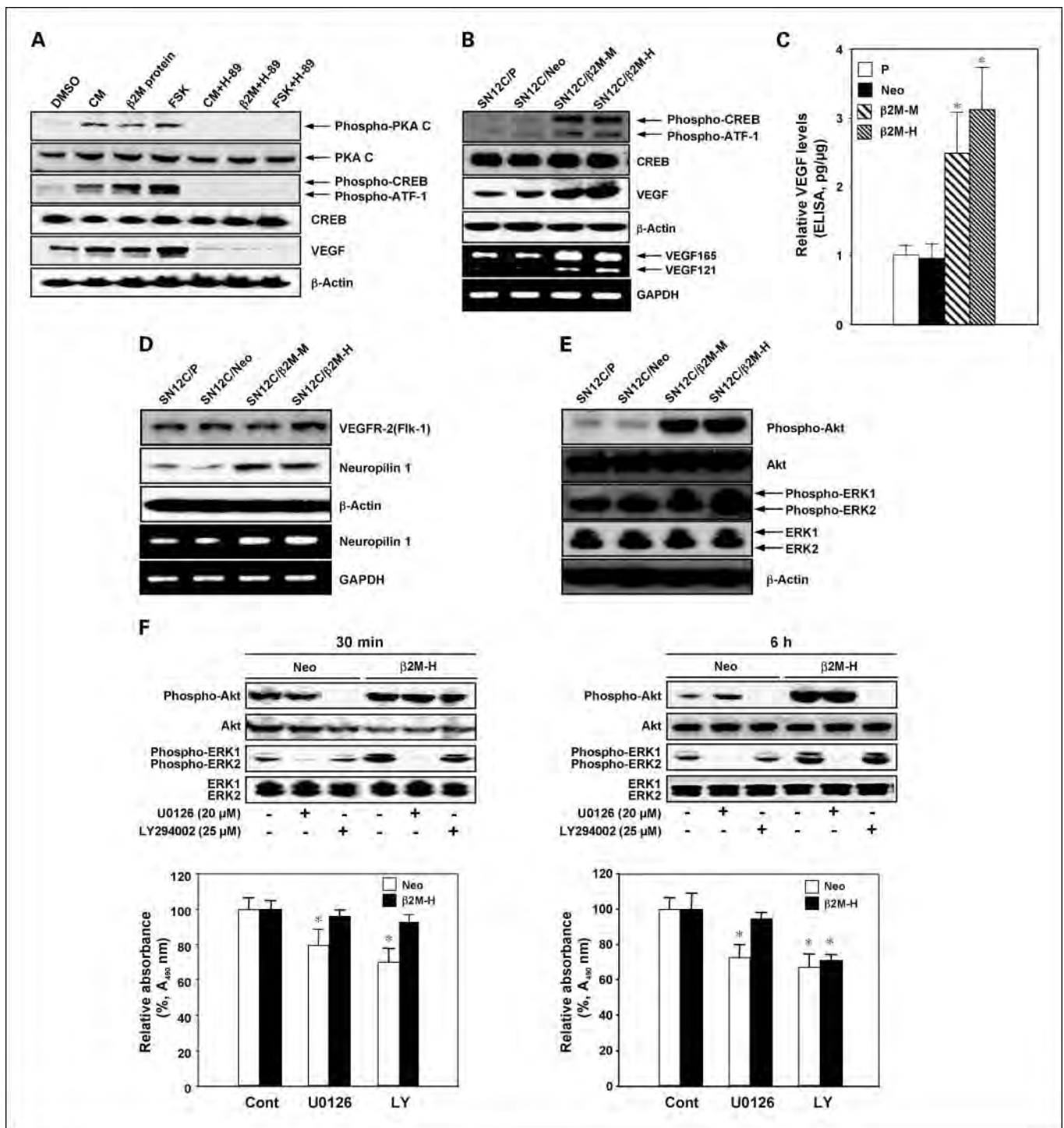
**Fig. 2.** β2M-mediated PKA-CREB signaling pathway and effects of β2M on the expression levels of CREB, VEGF, VEGFR-2, neuropilin 1, ERK1/2, and Akt and on the activation of CREB, ERK1/2, and Akt in SN12C subclones. *A,* SN12C/P cells were exposed to SN12C/β2M-H conditioned medium (*CM*; 0.5 μg/mL), recombinant human β2M protein (0.5 μg/mL) and forskolin (*FSK*; 5 μmol/L) for 24 h. H-89 (5 μmol/L) was added to SN12C/P cells for 2 h and then exposed to SN12C/β2M-H conditioned medium (0.5 μg/mL), recombinant human β2M protein (0.5 μg/mL), and forskolin (5 μmol/L) for an additional 24 h. Phosphorylation of PKA C and CREB was determined by immunoblot analysis using phospho-PKA C (Thr[197]) and phospho-CREB (Ser[133]) antibodies, and levels of expression of PKA C, CREB, and VEGF were also determined by immunoblot analyses. *B,* levels of expression of CREB and VEGF were determined by RT-PCR and immunoblot analyses in each subclone. Phosphorylation of CREB was determined by immunoblot analysis using phospho-CREB antibody in SN12C subclones. *C,* VEGF concentration was measured by ELISA in conditioned medium of each subclone. pg VEGF protein/μg total protein. The value of the control (SN12C/P) was taken as 1, and other values were calculated from this. Columns, mean from three independent experiments; bars, SE. *, *P* < 0.05 compared with SN12C/P and SN12C/Neo cells. *D,* levels of expression of VEGFR-2 (Flk-1) and its co-receptor neuropilin 1 were determined by RT-PCR and immunoblot analyses in each subclone. Immunoblot was done using VEGFR-2 (Flk-1) and neuropilin 1 antibodies. *E,* phosphorylation of Akt and ERK1/2 was determined by immunoblot analysis using phospho-Akt (Ser[473]) and phospho-ERK1/2 (Thr[185]/Tyr[187]) antibodies in each subclone. Blots were stripped and reprobed with antibodies against total Akt, total ERK, and β-actin. *F,* the transfectants were pretreated with U0126 (20 μmol/L) or LY294002 (*LY*; 25 μmol/L) for 30 min (*left*) or 6 h (*right*) and cultured for 12 h. Immunoblot analysis was done using antibodies that specifically recognize total and phospho-Akt and ERK1/2 (*top*). Cell survival was then determined by MTS assay (*bottom*). Columns, mean from three independent experiments; bars, SE. *, *P* < 0.05 compared with nontreatment SN12/Neo or SN12C/β2M-H cells.

on these respective pathways in SN12C cells overexpressing β2M. SN12C/Neo cells served as controls. Twenty micromolars of U0126 treatment for 30 min and 6 h significantly decreased SN12C/Neo cell numbers as determined by MTS assay ($P < 0.05$). In contrast, although 20 μmol/L U0126 treatment for 30 min blocked phosphorylation of ERK induced by β2M in SN12C/β2M-H, this treatment had no significant effect on cell number (Fig. 2F, *left*). The same dose of U0126 treatment for 6 h also completely blocked phosphorylation of ERK, whereas

it did not significantly decrease cell number in SN12C/β2M-H cells (Fig. 2F, *right*). When cells were treated with 25 μmol/L LY294002 for 30 min, this treatment had no significant effect on Akt phosphorylation in SN12C/β2M-H but had a significant depressant effect of the SN12C/Neo cells (Fig. 2F, *left*). When cells were treated with 25 μmol/L LY294002 for 6 h, phosphorylation of Akt was almost completely blocked in SN12C/β2M-H and SN12C/Neo cells (Fig. 2F, *right*). The suppression of Akt phosphorylation by LY294002 correlated with the
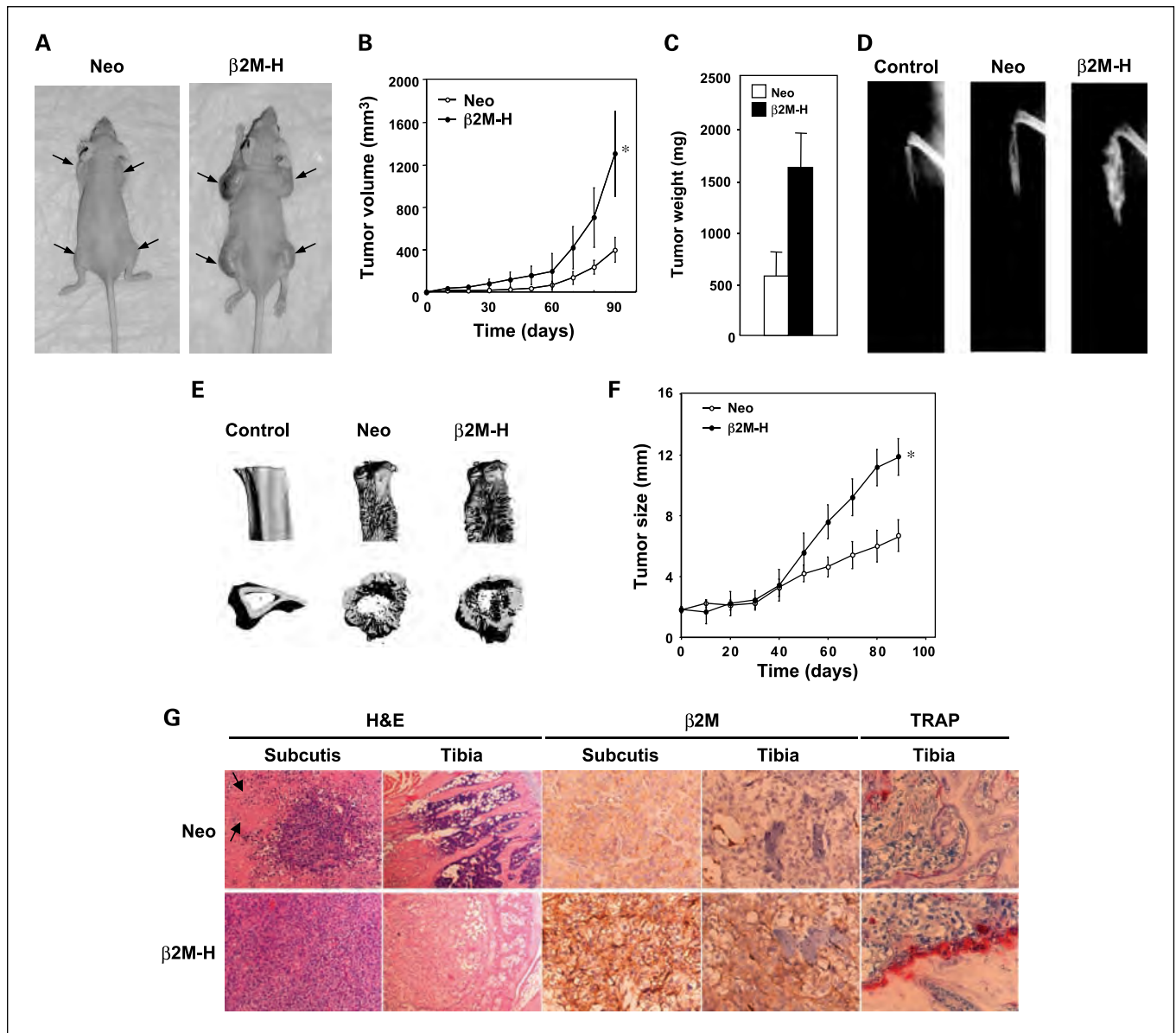


**Fig. 3.** S.c. and intratibial tumor growth in nude mice. *A*, SN12C/Neo or SN12C/β2M-H cells were injected bilaterally s.c. into nude mice, forming four tumors per mouse. Representative macroscopic appearance of nude mice injected with SN12C/Neo clone or SN12C/β2M-H s.c. Arrows indicate s.c. tumor formation. *B*, tumor volumes were measured every 5 d (only 10-d tumor volumes were plotted). Points, mean of eight tumors for each group; bars, SE. *, $P < 0.01$ compared with SN12C/Neo. *C*, animals were euthanized and tumors were excised and weighed. Columns, mean of tumor weights for each group; bars, SE. *, $P < 0.01$ compared with SN12C/Neo. *D*, SN12C/Neo or SN12C/β2M-H cells were injected intratibially into nude mice. Representative radiographs of nude mice tibia at autopsy. Radiographs revealed marked osteolytic lesions with occasional foci of strongly osteoblastic lesions in the SN12C/β2M-H–implanted tibias compared with SN12C/Neo–implanted tibias. *E*, micro-computed tomography images revealed massive osteoblastic and osteolytic reactions to tibias implanted with SN12C/β2M-H compared with SN12C/Neo–implanted tibias. *F*, tumor size was quantified every 5 d by measuring hind limb diameter (only 10-d tumor volumes were plotted). Points, mean of eight tibias for each group; bars, SE. *, $P < 0.01$ compared with SN12C/Neo. *G*, H&E, immunohistochemical staining of β2M, and tartrate-resistant acid phosphate (*TRAP*) staining in SN12C/Neo–implanted (*top*) and SN12C/β2M-H–implanted (*bottom*) tumors. H&E subcutis: magnification, ×100. Tibia: magnification, ×40. β2M staining: magnification, ×200. Multinuclear cells that stained red after tartrate-resistant acid phosphate staining determined osteoclasts. Magnification, ×200.

**Table 1.** Immunohistochemical analysis of subcutaneous and bone tumors induced by β2M-transfected SN12C cells in athymic nude mice

| Group | β2M | pCREB/CREB (%) | Ki-67 (%) | VEGF | Microvessel density (mm$^2$) |
|---|---|---|---|---|---|
| Subcutaneous tumor | | | | | |
| SN12C/Neo ($n = 8$) | + | $52 \pm 5$ | $31 \pm 8$ | ± | $36 \pm 11$ |
| SN12C/β2M-H ($n = 8$) | +++* | $83 \pm 11^{\dagger}$ | $82 \pm 8^{\dagger}$ | +++* | $132 \pm 17^*$ |
| Bone tumor | | | | | |
| SN12C/Neo ($n = 8$) | − | $38 \pm 4$ | $45 \pm 6$ | + | $31 \pm 10$ |
| SN12C/β2M-H ($n = 8$) | ++* | $85 \pm 10^{\dagger}$ | $82 \pm 5^{\dagger}$ | +++$^{\dagger}$ | $105 \pm 12^*$ |

*$P < 0.001$ compared with Neo.
$^{\dagger}P < 0.005$ compared with Neo.

enhanced cell death in SN12C/β2M-H and SN12C/Neo cells ($P < 0.05$). These results in aggregate indicate that the PI3K/Akt signaling pathway plays a crucial role in cell proliferation in β2M-transfected cells, although cell proliferation regulated by β2M, at least in part, originated from an activated MAPK signaling activity.

*β2M overexpression induces accelerated SN12C tumor growth in nude mice.* To determine whether β2M overexpression may enhance SN12C tumor growth in mice, we compared the growth of the SN12C/β2M-H and SN12C/Neo cells injected s.c. in athymic nude mice. Figure 3A shows photographs of s.c. xenografted tumors in nude mice. Mice were sacrificed on day 90 after s.c. injection. Figure 3B shows that the mice injected with SN12C/β2M-H formed significantly bigger tumors compared with SN12C/Neo at the time the mice were sacrificed (mean volume = $318 \pm 116$ mm$^3$ versus $1,306 \pm 371$ mm$^3$; SN12C/Neo versus SN12C/β2M-H, $n = 8$ for each group; $P < 0.01$). Figure 3C also shows that tumor weight in SN12C/β2M-H group was significantly elevated by 2.9-fold compared with SN12C/Neo group ($P < 0.01$). Histologic evaluation showed that SN12C/Neo tumors were composed of numerous necrotic areas compared with SN12C/β2M-H tumors grown as xenografts s.c. (Fig. 3G, *arrows*). Immunohistochemical staining using anti-β2M antibody confirmed β2M expression in SN12C/β2M-H tumors with strong and heterogeneous membrane staining of β2M in comparison with SN12C/Neo tumors (Fig. 3G; Table 1).

We also evaluated the behavior of the β2M-overexpressing clone in nude mouse bone. Radiographs showed bigger lesions for tibias implanted with SN12C/β2M-H compared with tibias implanted with SN12C/Neo (Fig. 3D). As shown in Fig. 3E, massive osteoblastic and osteolytic changes in tibias implanted with SN12C/β2M-H were also observed by micro-computed tomography. The tumor size was significantly greater in tibias implanted with SN12C/β2M-H compared with tibias implanted with SN12C/Neo ($n = 8$ for each group; $P < 0.01$; Fig. 3F). The estimated volume of bone tumors was also measured by radiograph at the end point of the animal experiment. End point tumor volume in SN12C/β2M-H tumors was significantly increased by 2.7-fold compared with SN12C/Neo tumors [median volume (range): 78.2 (14.7-257.9) mm$^3$ versus 214.8 (101.1-800.1) mm$^3$; SN12C/Neo versus SN12C/β2M-H, $n = 8$ for each group; $P < 0.001$]. Histology revealed that unlike SN12C/Neo tumor cells, SN12C/β2M-H tumor cells seem to be highly aggressive replacing bone marrow and destroying much of the cortical shafts (Fig. 3G). Immunohis-

tochemical staining using anti-β2M antibody confirmed that SN12C/β2M-H tumors showed strong cytoplasmic staining with variable degrees of membrane staining compared with SN12C/Neo tumors harvested from mice tibias (Fig. 3G; Table 1). We observed a large number of tartrate-resistant acid phosphate–positive osteoclasts at the bone/tumor interface in SN12C/β2M-H tumors, indicating that osteoclasts, directly adjacent to tumor cells, were with increased activity (Fig. 3G). Histomorphometric analysis of SN12C/β2M-H tumors showed a 3.0-fold increase of osteoclasts compared with SN12C/Neo tumor ($4.5 \pm 0.7$ osteoclasts/mm versus $13.6 \pm 2.1$ osteoclasts/mm; SN12C/Neo versus SN12C/β2M-H; $n = 8$ for each group; $P < 0.01$). These results suggest that β2M-overexpressing renal cell carcinoma cells enhanced osteolysis through accelerated osteoclastogenesis.

*Immunohistochemical analysis.* Table 1 summarizes the immunohistochemical findings. For s.c. tumors, although equivalent anti-CREB antibody staining was observed in SN12C/Neo and SN12C/β2M-H tumors, substantial higher anti-pCREB antibody stained cell nuclei were observed in SN12C/β2M-H than those of SN12C/Neo tumors (Fig. 4). The mean percentage of pCREB$^+$/CREB$^+$ tumor cells in SN12C/Neo tumors and SN12C/β2M-H tumors was $52 \pm 5\%$ and $83 \pm 11\%$, respectively ($P < 0.005$). The mean percentage of Ki-67–positive tumor cells in SN12C/β2M-H tumors was also significantly increased compared with SN12C/Neo tumors ($31 \pm 8\%$ versus $82 \pm 8\%$, SN12C/Neo versus SN12C/β2M-H, $P < 0.005$). We analyzed angiogenesis by using anti-VEGF and anti-CD31 antibodies. All the tumor cells stained positively for VEGF; however, tumor cells in SN12C/β2M-H tumors stained strongly and uniformly for VEGF compared with SN12C/Neo tumors (Fig. 4). Microvessel density correlated with expression of VEGF in both groups. Both VEGF expression and microvessel density were found to be significantly higher in SN12C/β2M-H tumors compared with SN12C/Neo tumors (Table 1). Comparison of immunohistochemistry of bone versus s.c. tumors showed parallelism of expression of all these proteins with comparable level of differences (Fig. 4; Table 1).

*Effect of β2M siRNA on cell proliferation, apoptosis, invasion, and migration.* Because β2M conferred increased SN12C cell growth *in vitro* and *in vivo*, we tested the possibility that β2M-induced intracellular signaling may be a therapeutic target. SN12C cells were transiently transfected with either si-β2M or si-Scr. After 72 h, cells were harvested and subjected to immuno-blot analysis, showing that si-β2M effectively down-regulated

the expression of β2M (Fig. 5A, *left*). This inhibition persisted in cells 7 days after transfection (Fig. 5A, *right*). Next, we examined the growth rates of each cell by MTS assay. si-β2M significantly inhibited the growth of SN12C cells compared with nontransfected parental (−), Lipo-Control, and si-Scr–transfected cells ($P < 0.01$; Fig. 5B). To investigate the molecular mechanism of this cell growth inhibition by si-β2M, activation of caspase-9 and caspase-3 and subsequent cleavage of poly(ADP-ribose) polymerase were investigated by immunoblot analysis. si-β2M but not si-Scr induced the activation and processing of caspase-9 and caspase-3 and cleavage of poly(ADP-ribose) polymerase (Fig. 5C). These results suggest that β2M siRNA reduced cell proliferation via induction of apoptosis in SN12C cells.

We then tested whether the inhibition of β2M expression in SN12C cells was sufficient to decrease cell invasion and migration. As shown in Fig. 5D, *in vitro* invasion and migration of cells transfected with si-β2M was reduced by 60.2% and 46.5% of the control, respectively ($P < 0.05$). These results suggest that β2M siRNA negatively affected the behavior of SN12C cells.

## Discussion

The association between β2M protein and cancer has received much attention in the past decades because of its participation in host immune defense mechanisms (2–4). Because β2M forms a complex and presents the MHC class I molecule to the cell surface, it is not surprising to note that malignant cancer cells lose MHC class I antigen, decreases steady-state level of β2M, and become immune evasive (5–8). However, data accumulated in the literature suggested otherwise. That is, most of the studies showed increased expression of β2M levels in renal cancer tissues, cells, and serum of cancer patients (10–18), but none of these studies defined the possible directive roles β2M in cell growth and signaling. To verify whether β2M has oncogenic activity and is a signaling molecule seems beneficial for establishing a new therapeutic target. The goals of this study are as follows: (*a*) to define the biological effects of β2M in human renal carcinoma cells in culture and in experimental animal models, (*b*) to characterize the downstream signaling pathways of β2M in a cell model of human renal cell carcinoma, and (*c*) to explore β2M as a novel target of therapy for human renal cell carcinoma. Results of this study have allowed us to expand the growth and cell signaling roles of β2M beyond stabilization and presentation of MHC class I molecule in cells. Our results also raise the question that β2M must have a far-reaching function than the common belief of a housekeeping gene in cells.

In the present study, we showed that (*a*) β2M promoted the proliferation, invasion, and migration of human renal cell carcinoma cells *in vitro*; (*b*) β2M increased renal cell carcinoma tumor growth in mouse s.c. space and in the skeleton; (*c*) β2M activated the phosphorylation of CREB through cAMP-dependent PKA signaling and up-regulated its target genes, which include the mRNAs and proteins of VEGF and neuropilin 1; (*d*) β2M activated not only β2M/PKA/CREB signaling but also activated its convergent signaling network PI3K/Akt and MAPK; and (*e*) down-regulation of β2M signaling by siRNA significantly inhibited renal cell carcinoma cell growth via induction of apoptosis and inhibition of cancer cell invasion and migration.

Although the dose-dependent growth and signaling roles of β2M was shown only in a human renal cell carcinoma cell line, these effects are likely to be applicable to human renal cell carcinoma in general because we and others have shown that β2M expression is up-regulated in human renal cancer tissues (24–26), and that the growth and signaling roles of β2M were observed in other independent studies using human prostate (27), breast, and lung cancer cells.[7] To our knowledge, this is the first report to show the possible directive growth and signaling roles of β2M in human renal cell carcinoma.

*β2M*, a well-known housekeeping gene, is a 12-kDa non-glycosylated polypeptide composed of 100 amino acids. It is one of the components of MHC class I molecules on the cell surface of all nucleated cells. Its major-characterized function is to interact with and stabilize the tertiary structure of the MHC class I α-chain (1). In addition, MHC molecules, including β2M, play an important role in regulating tumor immunity as well as cellular and humoral immunities (2, 3). The complex roles of β2M in cancer and bone metastasis, however, are descriptive and largely undefined. Increased synthesis and release of β2M, as indicated by an elevated serum or urine β2M concentration, occurs in several malignant diseases, including prostate cancer, lung cancer, renal cell carcinoma, myeloma, and lymphocytic malignancies as well as autoimmune and infectious diseases (10–17). In these malignancies, serum β2M level is a significant prognostic factor. Therefore, we hypothesized that β2M is not only a surrogate biomarker for tumor burden but may also regulate cancer cell growth and survival. To test this hypothesis, we established clonal cell lines of a human renal cell carcinoma (SN12C) that overexpresses β2M and examined whether β2M might have direct effects on cell growth, invasion, and migration *in vitro* in a dose-dependent manner and tumor growth *in vivo*. We also evaluated the possible intracellular signaling roles of β2M. In addition, we investigated whether β2M may be a new therapeutic target.

Our results clearly showed that β2M is an effective growth-promoting soluble factor for SN12C cells *in vitro*. This observation supports the conclusion that β2M plays an important role in regulating the growth and survival of cancer cells, and it seems compatible with the clinical data that high levels of serum β2M are associated with high tumor burden and poor prognosis (14, 28, 29). In addition, β2M-mediated cell growth was associated with cell cycle progression. It has been reported that β2M stimulates cell proliferation accompanied by a significant decrease of population doubling time in prostate cancer cell lines (9). There seems to be conflicting reports that either β2M (30, 31) or β2M antibody (32) suppresses the proliferation of myeloma cell lines. Take together, β2M is likely to have a direct mitogenic activity and play a role in modulating cell proliferation in solid tumors, probably in a cell context–dependent manner.

In this study, β2M expression levels were positively correlated with cancer cell growth, invasion, and migration in β2M-overexpressing transfectants. Although multiple mechanisms of β2M-mediated signaling can contribute to enhanced cancer cell growth and altered cell behaviors, little is known about the exact roles of β2M in signaling pathways at present. We showed

---

[7] T. Nomura et al. β2-Microglobulin-mediated cell signaling promotes human prostate, breast, lung and renal cancer growth in mice. 2006 AACR Annual Meeting Abstract 4822.
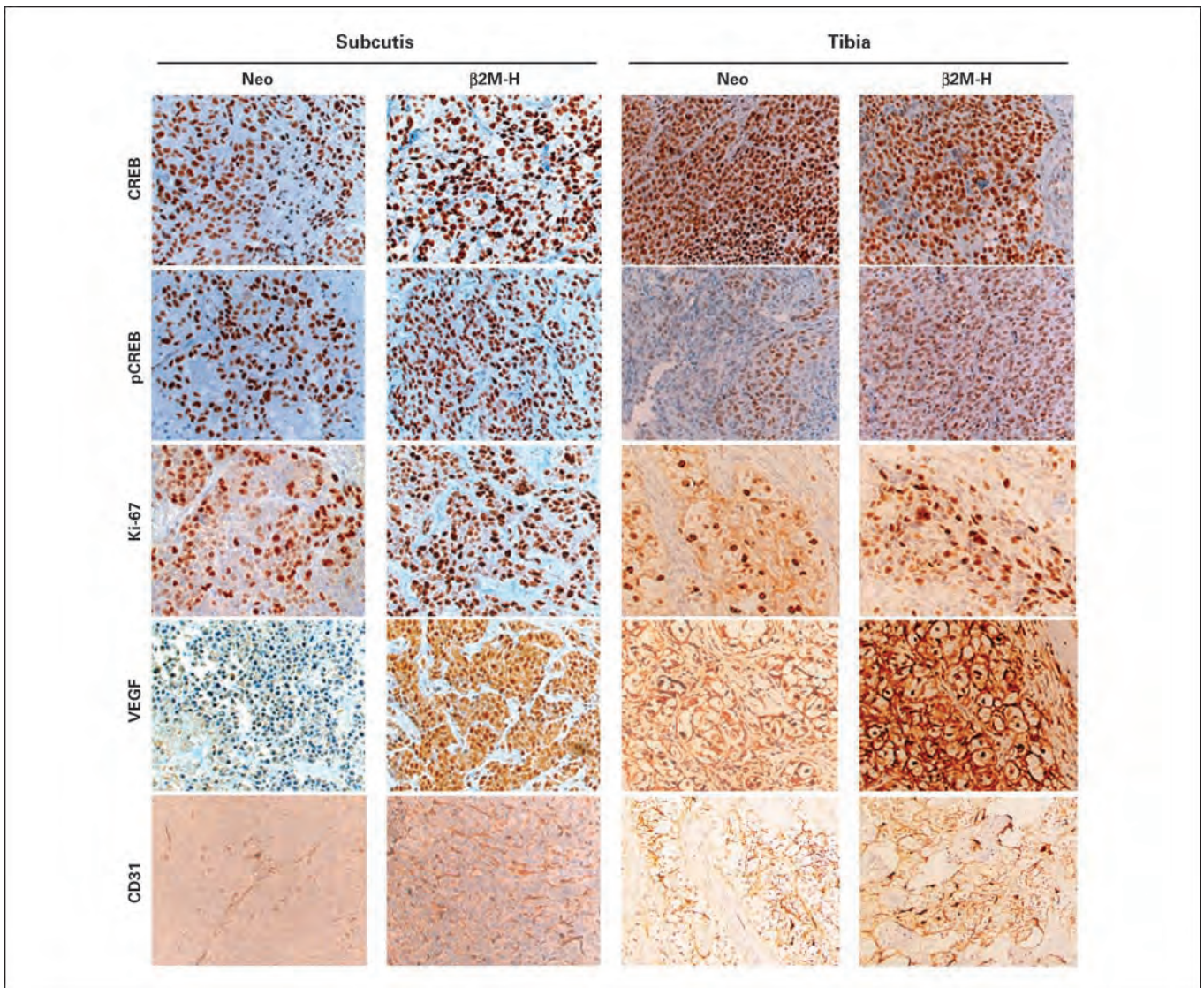
**Fig. 4.** Immunohistochemical determination of CREB, phosphorylated CREB (*pCREB*), Ki-67, VEGF, and CD31 in s.c. and intratibial tumors in nude mice. S.c. and intratibial tumors from SN12C/Neo or SN12C/β2M-H were harvested and processed for immunohistochemical analysis. The sections were stained for CREB, pCREB, Ki-67, VEGF (magnification, ×200), and CD31 (magnification, ×100).

that β2M activates CREB through cAMP-dependent PKA signaling and up-regulates the mRNA and protein levels of VEGF, resulting in increased cell proliferation. CREB is a bZIP transcription factor that transcriptionally activates a large number of downstream target genes, such as growth factors, angiogenesis factors, cell signaling–mediated genes, and genes involved in proliferation and survival, through cAMP response elements (33–36). Activation of CREB consequently could contribute to increased cancer cell growth and angiogenesis. VEGF, known as an important mediator of angiogenesis, is a highly specific mitogen for endothelial cells and cancer cells through receptors VEGFR-1 (Flt-1) and VEGFR-2 (Flk-1/KDR; ref. 37). Moreover, some reports have shown that PI3K and/or MAPK are important as a necessary signaling component of VEGF-mediated cell progression via ligand-receptor interaction (38, 39). In this study, we also found that increased secretion of VEGF and activation of both PI3K/Akt and MAPK signaling pathways occurred in β2M-overexpressing transfectants.

Together with the results, activation of phosphorylation of CREB may induce the transcriptional activation of VEGF, which plays a critical role in human renal cell carcinoma.[8] It is possible that signaling convergence may occur between VEGF-VEGFR and PI3K/Akt and MAPK signaling. Activation of CREB has also been reported to be activated by PI3K/Akt and MAPK (40–42). These results in sum suggest that β2M-mediated VEGF and VEGFR-2 co-receptor neuropilin 1 expression and signaling may be central to β2M-induced renal cell carcinoma cell growth, migration, and invasion *in vitro* and tumor growth in mouse s.c. space and skeleton.

Additionally, immunohistochemical study confirmed the relationship between β2M expression and cell proliferation

---

[8] D. Wu et al. cAMP-responsive element-binding protein regulates vascular endothelial growth factor expression and its implication in human prostate cancer bone metastasis.

and angiogenesis *in vivo*. β2M overexpression was associated with an increase in tumor cell proliferation (Ki-67) and angiogenesis (VEGF expression level and microvessel density) that correlated with a significant increase in phosphorylation of CREB in both s.c. and bone tumors. VEGF has been shown to be an important factor involved in the development of tumor blood supply in the progression of solid tumors (43). Numerous published reports describe the association of microvessel density with VEGF expression (44–46). VEGF can also substitute for pro-osteoclastogenic cytokine macrophage colony-stimulating factor and up-regulate receptor activator of nuclear factor-κB expression in osteoclast precursors, thus promoting osteoclastogenesis (47, 48). In the present study, we observed a large number of osteoclasts in β2M-overex-

pressed bone tumor. The tumors are largely osteolytic, although osteoblastic foci can be detected by both histopathology and X-ray of the skeleton. Our findings agree with previous reports that β2M promotes osteoclast formation (31), and that osteoclasts are essential for cell survival and proliferation in myeloma (49). It has been also reported that VEGF acts as an osteolytic factor in breast cancer bone metastasis (50). β2M may enhance tumor growth in bone via β2M-induced osteoclastogenesis and VEGF induction. Our results, therefore, support the current concept that β2M enhances tumor progression through enhanced angiogenesis, cell survival, and osteoclastogenesis when metastasized to bone. In this study, we showed that cancer cells may require intracellular β2M for their survival. For example, by interrupting β2M expression using its
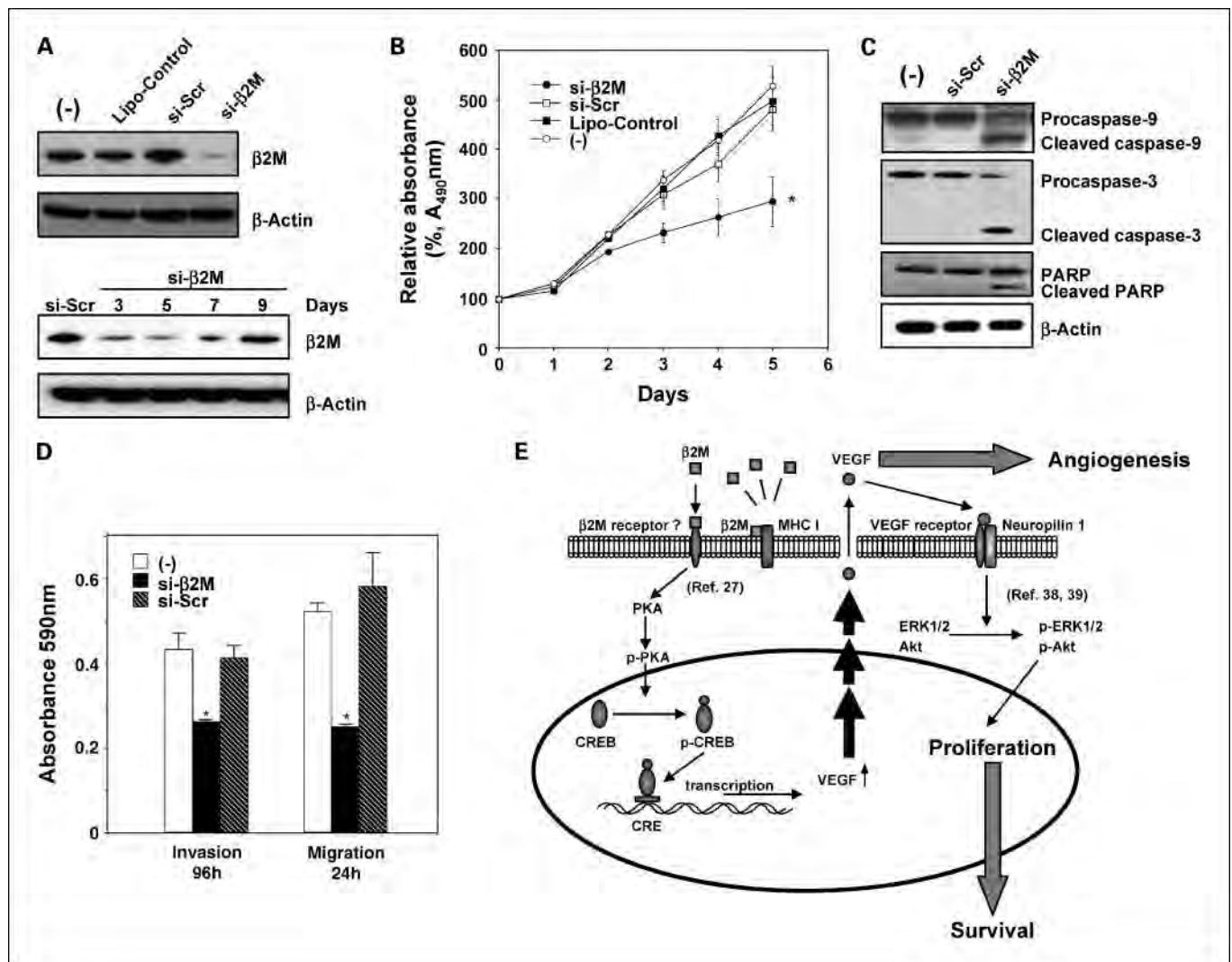


**Fig. 5.** Effects of β2M siRNA on cell proliferation, apoptosis, invasion, and migration in SN12C cells. *A,* β2M siRNA (si-β2M), LipofectAMINE 2000 control (*Lipo-Control*), and control scramble siRNA (si-Scr) were added to the media using lipophilic transfection-enhancing reagent (LipofectAMINE 2000). Cells were harvested after 72 h, and immunoblot analysis was done using anti-β2M antibody (*top*). For duration of β2M inhibition in SN12C cells, SN12C cells were transfected with si-Scr or si-β2M, and cells were lysed 3, 5, 7, and 9 d after transfection as indicated (*bottom*). *B,* effects of si-β2M on cell proliferation of SN12C cells were determined by MTS assay. Points, mean from three independent experiments; bars, SE. *, $P < 0.01$ compared with nontransfected parental (−), LipofectAMINE 2000 control, and si-Scr−transfected cells. *C,* si-β2M but not si-Scr induced activation and processing of caspase-9 and caspase-3 and cleavage of poly(ADP-ribose) polymerase (*PARP*) in SN12C cells. *D,* effects of si-β2M on invasion and migration of SN12C cells. $A_{590nm}$ values correspond to cells that migrated to the lower side of the filter. Columns, mean from three independent experiments; bars, SE. *, $P < 0.05$ compared with nontransfected parental (−) and si-Scr−transfected cells. *E,* proposed molecular mechanism, whereby β2M can affect cancer progression in human renal cell carcinoma. β2M can activate cAMP-dependent PKA activity through an unknown receptor, and then this activation can induce activation of CREB, which increases angiogenesis, cell proliferation, and survival via activation of VEGF signaling and its downstream cell survival pathways PI3K/Akt and MAPK.

sequence-specific β2M siRNA, we observed activated apoptosis in SN12C cells. Thus, β2M signaling may be an attractive new therapeutic target for the treatment of human renal cell carcinoma.

In summary, the present study provides evidence that β2M enhances the growth and survival of human renal cell carcinoma cells via PKA/CREB activation, VEGF signaling, and cell survival signaling, including the PI3K/Akt and MAPK pathways (Fig. 5E). It is tempting to speculate that aberrant β2M expression facilitates tumor progression and bone metastasis, and that β2M signaling may be an attractive new therapeutic target. Further studies are required to determine the precise molecular mechanisms by which β2M regulates cancer cell growth, invasion, and migration, and, conversely, interruption of β2M signaling induced cancer cell apoptosis.

## Acknowledgments

## References

1. Bjorkman PJ, Parham P. Structure, function, and diversity of class I major histocompatibility complex molecules. Annu Rev Biochem 1990;59:253–88.
2. Ploegh HL, Orr HT, Strominger JL. Major histocompatiblity antigens: the human (HLA-A, -B, -C) and murine (H-2K, H-2D) class I molecules. Cell 1981;24:287–99.
3. Parham P, OhtaT. Population biology of antigen presentation by MHC class I molecules. Science 1996;272:67–74.
4. Salter RD, Benjamin RJ, Wesley, et al. A binding site for theT-cell co-receptor CD8 on the alpha 3 domain of HLA-A2. Nature 1990;345:41–6.
5. Garrido F, CabreraT, Concha A, Glew S, Ruiz-Cabello F, Stern PL. Natural history of HLA expression during tumour development. Immunol Today 1993;14:491–9.
6. Chen HL, Gabrilovich D,Tampe R, Girgis KR, Nadaf S, Carbone DP. A functionally defective allele of TAP1 results in loss of MHC class I antigen presentation in a human lung cancer. Nat Genet 1996;13:210–3.
7. Amiot L, Onno M, LamyT, et al. Loss of HLA molecules in B lymphomas is associated with an aggressive clinical course. Br J Haematol 1998;100:655–63.
8. Hicklin DJ,Wang Z, Arienti F, Rivoltini L, Parmiani G, Ferrone S. β₂-Microglobulin mutations, HLA class I antigen loss, and tumor progression in melanoma. J Clin Invest 1998;101:2720–9.
9. Rowley DR, DangTD, McBride L, Gerdes MJ, Lu B, Larsen M. Beta-2 microglobulin is mitogenic to PC-3 prostatic carcinoma cells and antagonistic to transforming growth factor beta 1 action. Cancer Res 1995;55:781–6.
10. Abdul M, Hoosein N. Changes in beta-2 microglobulin expression in prostate cancer. Urol Oncol 2000;5:168–72.
11. Solheim JC. Class I MHC molecules: assembly and antigen presentation. Immunol Rev 1999;172:11–9.
12. Rajkumar SV, Greipp PR. Prognostic factors in multiple myeloma. Hematol Oncol Clin North Am 1999;13:1295–314.
13. Nissen MH, Bjerrum OJ, PlesnerT, Wilken M, Rorth M. Modification of beta-2-microglobulin in sera from patients with small cell lung cancer: evidence for involvement of a serine protease. Clin Exp Immunol 1987;67:425–32.
14. RasmusonT, Grankvist K, Ljungberg B. Serum beta 2-microglobulin and prognosis of patients with renal cell carcinoma. Acta Oncol 1996;35:479–82.
15. Mavridis AK, Tsiara S, Makis A, et al. TNF-alpha and beta-2M in patients with B cell chronic lymphocytic leukemia. J Exp Clin Cancer Res 1998;17:445–8.
16. Sadamori N, Mine M, Hakariya S, et al. Clinical significance of beta-2-microglobulin in serum of adult T cell leukemia. Leukemia 1995;9:594–7.
17. Gressner AM, Neu HH. N-terminal procollagen peptide and beta 2-microglobulin in synovial fluids from inflammatory and non-inflammatory joint diseases. Clin Chim Acta 1984;141:241–5.
18. Bunning RA, Haworth SL, Cooper EH. Serum β₂-microglobulin levels in urological cancer. J Urol 1979;121:624–5.
19. Naito S, Walker SM, Fidler IJ. *In vivo* selection of human renal cell carcinoma cells with high metastatic potential in nude mice. Clin Exp Metastasis 1989;7:381–9.
20. Passaniti A, Isaacs JT, Haney JA, et al. Stimulation of human prostatic carcinoma tumor growth in athymic nude mice and control of migration in culture by extracellular matrix. Int J Cancer 1992;51:318–24.
21. Inoue K, Karashima T, Fukata S, et al. Effect of combination therapy with a novel bisphosphonate, minodronate (YM529), and docetaxel on a model of bone metastasis by human transitional cell carcinoma. Clin Cancer Res 2005;11:6669–77.
22. Bissery MC, Guenard D, Gueritte-Voegelein F, Lavelle F. Experimental antitumor activity of taxotere (RP 56976, NSC 628503), a taxol analogue. Cancer Res 1991;51:4845–52.
23. Arrington SA, Schoonmaker JE, Damron TA, Mann KA, Allen MJ. Temporal changes in bone mass and mechanical properties in a murine model of tumor osteolysis. Bone 2006;38:359–67.
24. Buszello H, Ackermann R. Expression of HLA class-I antigens on renal cell carcinoma and non-transformed renal tissue. Eur Urol 1992;21:70–4.
25. Buszello H, Ackermann R. Immunohistochemical studies on the expression of HLA class I antigens in renal cell carcinoma: comparison of primary and metastatic tumor tissue. Eur Urol 1994;25:158–63.
26. Gastl G, Ebert T, Finstad CL, et al. Major histocompatibility complex class I and class II expression in renal cell carcinoma and modulation by interferon gamma. J Urol 1996;155:361–7.
27. HuangW-C,Wu D, Xie Z, et al. β₂-Microglobulin is a signaling and growth-promoting factor for human prostate cancer bone metastasis. Cancer Res 2006;66:9108–16.
28. Cuzick J, Cooper EH, MacLennan IC. The prognostic value of serum beta 2 microglobulin compared with other presentation features in myelomatosis. Br J Cancer 1985;52:1–6.
29. Bataille R, GrenierJ, Sany J. Beta-2-microglobulin in myeloma: optimal use for staging, prognosis, and treatment—a prospective study of 160 patients. Blood 1984;63:468–76.
30. Mori M, Terui Y, Ikeda M, et al. β₂-Microglobulin identified as an apoptosis-inducing factor and its characterization. Blood 1999;94:2744–53.
31. Min R, Li Z, Epstein J, Barlogie B,Yi Q. β₂-Microglobulin as a negative growth regulator of myeloma cells. Br J Haematol 2002;118:495–505.
32. Yang J, Qian J, Wezeman M, et al. Targeting β₂-microglobulin for induction of tumor apoptosis in human hematological malignancies. Cancer Cell 2006;10:295–307.
33. Al-Wadei HA, Takahashi T, Schuller HM. Growth stimulation of human pulmonary adenocarcinoma cells and small airway epithelial cells by beta-carotene via activation of cAMP, PKA, CREB and ERK1/2. Int J Cancer 2006;118:1370–80.
34. HuangW-C, Xie Z, Konaka H, Sodek J, Zhau HE, Chung LWK. Human osteocalcin and bone sialoprotein mediating osteomimicry of prostate cancer cells: role of cAMP-dependent protein kinase A signaling pathway. Cancer Res 2005;65:2303–13.
35. Shanker DB, Cheng JC, Sakamoto KM. Role of cyclic AMP response element binding protein in human leukemias. Cancer 2005;104:1819–24.
36. Abramovitch R, Tavor E, Jacob-Hirsch J, et al. A pivotal role of cyclic AMP-responsive element binding protein in tumor progression. Cancer Res 2004;64:1338–46.
37. Neufeld G, Cohen T, Gengrinovitch S, Poltorak Z. Vascular endothelial growth factor (VEGF) and its receptors. FASEB J 1999;13:9–22.
38. Kroll J, Waltenberger J. The vascular endothelial growth factor receptor KDR activates multiple signal transduction pathways in porcine aortic endothelial cells. J Biol Chem 1997;272:32521–7.
39. Thakker GD, Hajjars DP, Muller WA, Rosengart TK. The role of phosphatidilinositol 3-kinase in vascular endothelial growth factor signaling. J Biol Chem 1999;274:10002–7.
40. Kwon EM, Raines MA, Blenis J, Sakamoto KM. Granulocyte-macrophage colony-stimulating factor stimulation results in phosphorylation of cAMP response element-binding protein through activation of pp90RSK. Blood 2000;95:2552–8.
41. Joo EK, Broxmeyer HE, Kwon HJ, et al. Enhancement of cell survival by stromal cell-derived factor-1/CXCL12 involves activation of CREB and induction of Mcl-1 and c-Fos in factor-dependent human cell line MO7e. Stem Cells Dev 2004;13:563–70.
42. Nicholson KM, Anderson NG. The protein kinase B/Akt signaling pathway in human malignancy. Cell Signal 2002;14:381–95.
43. Jubb AM, Pham TQ, Handy AM. Expression of vascular endothelial growth factor, hypoxia inducible factor 1 alpha, and carbonic anhydrase IX in human tumours. J Clin Pathol 2004;58:335–6.
44. Frangou EM, Lawson J, Kanthan R. Angiogenesis in male breast cancer. World J Surg Oncol 2005;3:16.
45. Jubb AM, Hurwitz HI, Bai W, et al. Impact of vascular endothelial growth factor-A expression, thrombospondin-2 expression, and microvessel density on the treatment effect of bevacizumab in metastatic colorectal cancer. J Clin Oncol 2006;24:217–27.
46. Fureder W, Krauth M-T, Sperr WR, et al. Evaluation of angiogenesis and vascular endothelial growth factor expression in the bone marrow of patients with aplastic anemia. Am J Pathol 2006;168:123–30.
47. Niida S, Kaku M, Amano H, et al. Vascular endothelial growth factor can substitute for macrophage colony-stimulating factor in the support of osteoclastic bone resorption. J Exp Med 1999;190:293–8.
48. Yao S, Liu D, Pan F, Wise GE. Effect of vascular endothelial growth factor on RANK gene expression in osteoclast precursors and on osteoclastogenesis. Arch Oral Biol 2006;51:596–602.
49. Yaccoby S, Pearse RN, Johnson CL, Barlogie B, Choi Y, Epstein J. Myeloma interacts with the bone marrow microenvironment to induce osteoclastogenesis and is dependent on osteoclast activity. Br J Haematol 2002;116:278–90.
50. Aldridge SE, Lennard TWJ, Williams JR, Birch MA. Vascular endothelial growth factor acts as an osteolytic factor in breast cancer metastases to bone. Br J Cancer 2005;92:1531–7.

MOLECULAR
CANCER

**RESEARCH**

# Vascular endothelial growth factor regulates myeloid cell leukemia-1 expression through neuropilin-1-dependent activation of c-MET signaling in human prostate cancer cells

Shumin Zhang[1], Haiyen E Zhau[2], Adeboye O Osunkoya[1,3], Shareen Iqbal[1], Xiaojian Yang[2,4], Songqing Fan[5], Zhengjia Chen[6], Ruoxiang Wang[1], Fray F Marshall[1], Leland WK Chung[2], Daqing Wu[1*]

## Abstract

**Background:** Myeloid cell leukemia-1 (Mcl-1) is a member of the Bcl-2 family, which inhibits cell apoptosis by sequestering pro-apoptotic proteins Bim and Bid. Mcl-1 overexpression has been associated with progression in leukemia and some solid tumors including prostate cancer (PCa). However, the regulatory mechanism for Mcl-1 expression in PCa cells remains elusive.

**Results:** Immunohistochemical analyses revealed that Mcl-1 expression was elevated in PCa specimens with high Gleason grades and further significantly increased in bone metastasis, suggesting a pivotal role of Mcl-1 in PCa metastasis. We further found that vascular endothelial growth factor (VEGF) is a novel regulator of Mcl-1 expression in PCa cells. Inhibition of endogenous Mcl-1 induced apoptosis, indicating that Mcl-1 is an important survival factor in PCa cells. Neuropilin-1 (NRP1), the "co-receptor" for $VEGF_{165}$ isoform, was found to be highly expressed in PCa cells, and indispensible in the regulation of Mcl-1. Intriguingly, $VEGF_{165}$ promoted physical interaction between NRP1 and hepatocyte growth factor (HGF) receptor c-MET, and facilitated c-MET phosphorylation *via* a NRP1-dependent mechanism. $VEGF_{165}$ induction of Mcl-1 may involve rapid activation of Src kinases and signal transducers and activators of transcription 3 (Stat3). Importantly, NRP1 overexpression and c-MET activation were positively associated with progression and bone metastasis in human PCa specimens and xenograft tissues.

**Conclusions:** This study demonstrated that Mcl-1 overexpression is associated with PCa bone metastasis. Activation of $VEGF_{165}$-NRP1-c-MET signaling could confer PCa cells survival advantages by up-regulating Mcl-1, contributing to PCa progression.

## Background

Acquisition of apoptosis resistance is characteristic of invasive tumor cells. Elevated expression of anti-apoptotic proteins is associated with tumor progression clinically and experimentally [1]. Myeloid cell leukemia-1 (Mcl-1), a member of the Bcl-2 family, sequesters pro-apoptotic proteins Bim and Bid, thereby inhibiting mitochondrial outer membrane permeabilization, a central control point of apoptosis [2,3]. Mcl-1 overexpression is associated with progression in leukemia [4] and some

solid tumors including prostate cancer (PCa) [5-7]. Mcl-1 was elevated in primary PCa with high Gleason grades and metastatic tumors compared to that in prostatic intraepithelial neoplasia (PIN) or lower grade tumors, suggesting a pivotal role of Mcl-1 in PCa progression [5].

Angiogenesis favors tumor cell survival, thereby contributing to progression [1]. Vascular endothelial growth factor (VEGF) is a critical pro-angiogenic factor that induces proliferation and migration of endothelial cells within tumor vasculature [8]. VEGF is expressed as several alternately spliced isoforms. $VEGF_{165}$ is predominant, with optimal bioavailability, and responsible for VEGF biological potency, whereas $VEGF_{121}$ is less potent but freely diffusible. VEGF binds two highly-

\* Correspondence: dwu2@emory.edu
[1]Department of Urology and Winship Cancer Institute, Emory University School of Medicine, Atlanta, GA, USA

related receptor tyrosine kinases, VEGF-R1 and VEGF-R2 [8]. Neuropilin-1 (NRP1) was originally identified as a receptor for the semaphorin 3 subfamily mediating neuronal guidance and axonal growth [9]. It was subsequently found to specifically bind $VEGF_{165}$ but not $VEGF_{121}$ on endothelial cells and tumor cells [9,10]. NRP1 lacks a typical kinase domain, primarily functioning as a "co-receptor" to form ligand-specific receptor complexes. In response to $VEGF_{165}$, NRP1 couples with VEGF-Rs to signal in endothelial cells. Though VEGF-R1 and VEGF-R2 are usually absent or expressed at very low levels in PCa cells [11], aberrant upregulation of NRP1 has been frequently observed in high grade and metastatic PCa and other solid tumors [9,12-16]. Ectopic expression of NRP1 in PCa cells induced cell migration, increased tumor size and microvessel density, and inhibited apoptosis [17]. These observations suggested that NRP1 may be critical for PCa progression. Nonetheless, the mechanism by which NRP1 transmits VEGF signaling in PCa cells lacking VEGF-Rs remains unclear.

Previously we reported that serum VEGF levels correlate to bone metastatic status in PCa patients, and activation of VEGF signaling in PCa cells is associated with invasive phenotypes in experimental models [18]. In this study, we correlate Mcl-1 overexpression to PCa progression towards bone metastasis, and provide evidence that VEGF regulates Mcl-1 expression through NRP1-dependent activation of c-MET in PCa cells.

## Results
### Elevated Mcl-1 expression is associated with PCa progress and bone metastasis
To investigate the clinical significance of Mcl-1 in PCa progression, immunohistochemical (IHC) analyses were performed to determine the expression of Mcl-1 in a human PCa tissue microarray with matched normal adjacent tissue and bone metastatic bone specimens (Figure 1a). We defined tumors with Gleason score 2-6 as well-differentiated (n = 2), Gleason score 7 as intermediately-differentiated (n = 26) and Gleason score 8-10 as poorly-differentiated (n = 43). Mcl-1 immunointensity was increased from normal tissues to well-differentiated cancer and further elevated in high grade PCa, although the difference between Mcl-1 intensity in intermediate- and poorly-differentiated cancers was not statistically significant ($p$ = 0.93). Intriguingly, Mcl-1 staining in bone metastatic tumors (n = 6) was remarkably increased compared to that in either intermediate- or poorly-differentiated PCa ($p$ < 0.002). These data correlated elevated Mcl-1 expression to clinical PCa progression, particularly bone metastasis.
### Mcl-1 is a survival factor in human PCa cells
We have established several lines of human PCa models that closely mimic the clinical progression of PCa bone

metastasis, including the ARCaP model [19,20]. When inoculated either orthotopically or intracardially, $ARCaP_M$ cells are capable of metastasizing spontaneously to bone and soft tissues, forming mixed osteoblastic and osteolytic lesions in mouse skeleton [19,21,22]. The $ARCaP_M$-C2 subclone, derived from metastatic bone tissues after two rounds of intracardiac injection of $ARCaP_M$ cells in athymic mice, forms predictable metastases to bone, adrenal gland and other soft tissue with higher propensity and shorter latency [21,22] (Figure 1b). Reverse transcription-PCR (RT-PCR) and immunoblotting analyses found that Mcl-1 was substantially expressed by $ARCaP_M$ cells, and further increased in $ARCaP_M$-C2 cells (Figure 1c). Similarly, increased Mcl-1 expression was observed in metastatic C4-2 and C4-2B cells [23] when compared to their parental, androgen-dependent human PCa cell line LNCaP (Additional file 1, Figure S1a). These results suggested a possible association between Mcl-1 expression and invasive phenotypes of PCa cells.

To examine the function of Mcl-1 in PCa cell survival, a Mcl-1 small-interfering RNA (siRNA) was transfected into $ARCaP_M$ cells. siRNA treatme nt effectively inhibited Mcl-1 expression and significantly reduced $ARCaP_M$ cell viability by ~36% after 72 h (Figure 1d). Annexin V staining by fluorescence-activated cell sorting (FACS) analysis showed that the Mcl-1 siRNA induced apoptosis in 24.4-2.3% of $ARCaP_M$ cells (Figure 1e). These results indicated that Mcl-1 may be an important survival factor in PCa cells.
### VEGF regulates Mcl-1 expression in human PCa cells
Previously we reported that $ARCaP_M$ cells express high levels of endogenous VEGF, regulated by a cyclic AMP-response element binding protein (CREB)-hypoxia-inducible factor (HIF)-dependent mechanism in normoxic conditions [18]. In the present study, RT-PCR assay that could differentiate mRNA expression of $VEGF_{165}$ and $VEGF_{121}$ isoforms [18] was performed in $ARCaP_M$ and $ARCaP_M$-C2 cells, showing a significant increase in the expression of both VEGF isoforms in $ARCaP_M$-C2 cells, as confirmed at protein level by enzyme-linked immunosorbent assay (ELISA) (Figure 2a). Similarly, C4-2 cells express higher levels of VEGF when compared to LNCaP cells (Additional file 1, Figure S1b). These data suggested that VEGF expression is elevated in metastatic PCa cells.

VEGF potently stimulates endothelial cell proliferation and migration, an underlying mechanism for angiogenesis during tumor progression. However, neither exogenous human $VEGF_{165}$ (Figure 2b) nor $VEGF_{121}$ (Additional file 1, Figure S1c) significantly affected the proliferation of $ARCaP_M$ cells at a non-saturating range (5-100 ng/ml), suggesting that VEGF is not a potent mitogen in PCa cells. Intriguingly, $VEGF_{165}$ was found
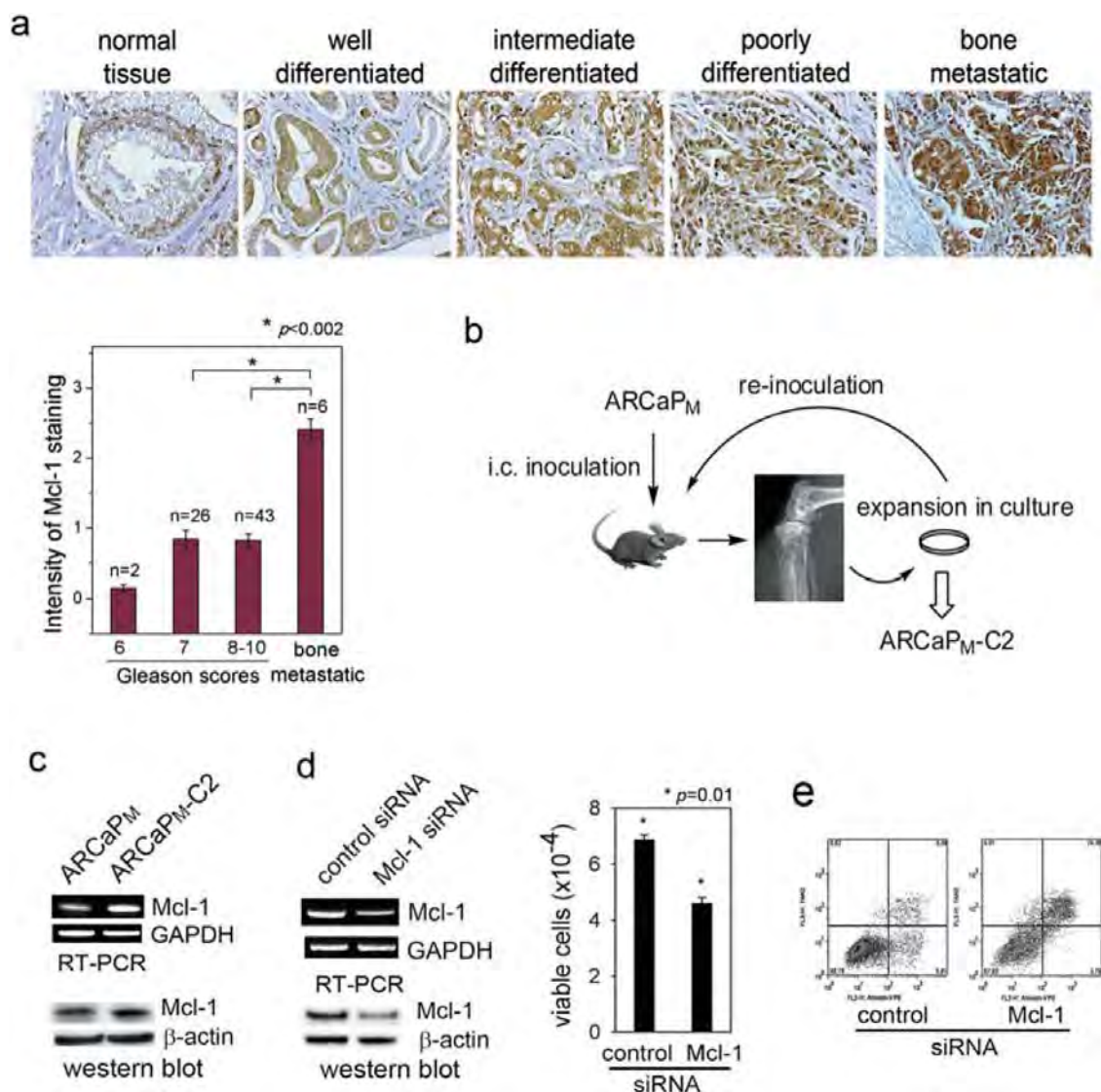
**Figure 1 Mcl-1 is a survival factor in human PCa cells**. (a) IHC staining of Mcl-1 in human PCa tissue microarray consisting of normal adjacent tissues, primary PCa and bone metastases. (b) Intracardiac (i.c) injection of ARCaP$_M$ cells in athymic mice resulted in metastases to bone and soft tissues. The ARCaP$_M$-C2 subclone was derived from metastatic bone tissues after two rounds of intracardiac inoculation of ARCaP$_M$ cells. (c) Endogenous Mcl-1 expression in the ARCaP$_M$ model was examined by RT-PCR and western blotting analyses. (d) Effect of Mcl-1 siRNA on ARCaP$_M$ cell viability. Subconfluent ARCaP$_M$ cells on a 6-well plate were transiently transfected with Mcl-1 siRNA (30 nM) for 72 h. Endogenous expression of Mcl-1 at the mRNA and protein levels, and cell viability of ARCaP$_M$ cells as counted with trypan blue staining, were significantly inhibited by Mcl-1 siRNA treatment compared to the control. (e) Effects of Mcl-1 siRNA on ARCaP$_M$ cell apoptosis. Subconfluent ARCaP$_M$ cells were transfected with Mcl-1 siRNA or control siRNA for 72 h, expression of annexin V was measured by FACS.

to rapidly induce Mcl-1 mRNA expression in a dose- and time-dependent manner, with the maximum accumulation of Mcl-1 mRNA after 2 h-incubation at the concentration of 10 ng/ml. Western blot analysis confirmed a remarkable increase of Mcl-1 protein in ARCaP$_M$ cells (Figure 2c) and LNCaP cells (Additional file 1, Figure S1d) treated with VEGF$_{165}$. Conversely, when ARCaP$_M$ cells were transfected with a VEGF siRNA nucleotide that selectively inhibited expression of VEGF$_{165}$ but not VEGF$_{121}$, expression of Mcl-1, but not

Bcl-2, was reduced after 72 h (Figure 2d). Notably, Mcl-1 expression was not affected by VEGF$_{121}$ treatment (Additional file 1, Figure S1e). These results indicated that VEGF$_{165}$ may specifically regulate Mcl-1 expression in PCa cells.

### Differential expression of VEGF-Rs in PCa cells
Expression of VEGF-Rs was examined in several PCa cell lines with human umbilical vein endothelial cells (HUVEC) as a positive control (Figure 3a, and Additional file 1, Figure S1f). VEGF-R1 was undetectable in
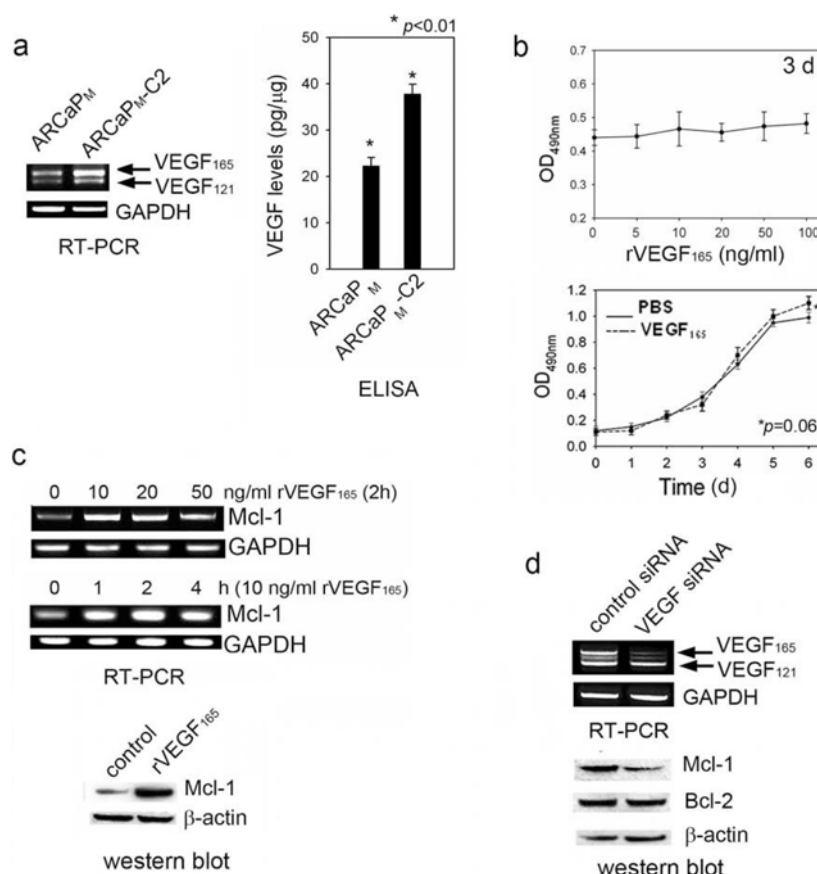
**Figure 2 VEGF$_{165}$ regulates Mcl-1 expression in PCa cells**. (a) VEGF expression in ARCaP$_M$ and ARCaP$_M$-C2 cells, as determined by RT-PCR and ELISA (conditioned medium). (b) Effects of recombinant VEGF$_{165}$ on cell proliferation as determined by MTS assay. Top, ARCaP$_M$ cells were seeded in 96-well plates ($1 \times 10^3$ cells/well) for 24 h, and serum-starved overnight. The cells were further incubated with varying concentrations of VEGF$_{165}$ in serum-free T-medium for 72 h. Bottom, ARCaP$_M$ cells were incubated with PBS or VEGF$_{165}$ (50 ng/ml) in serum-free T-medium for varying times. (c) VEGF$_{165}$ effects on Mcl-1 expression. ARCaP$_M$ cells were treated with VEGF$_{165}$ at indicated concentrations and times, and Mcl-1 mRNA expression was measured. For immunoblotting, ARCaP$_M$ cells were incubated with VEGF$_{165}$ (10 ng/ml) for 72 h. (d) Effects of VEGF siRNA on Mcl-1 expression. ARCaP$_M$ cells were transfected with VEGF siRNA or control siRNA (80 nM) for 72 h.

PCa cells. Only very low expression of VEGF-R2 could be observed in ARCaP$_M$-C2 cells. However, NRP1 was ubiquitously expressed in PCa cells at a level comparable to that in HUVEC, and higher in metastatic ARCaP$_M$-C2, PC3, C4-2 and C4-2B cells. NRP2, the "co-receptor" for VEGF-C [8], was not detected in PCa cells. These data implied that NRP1 may be the major receptor mediating VEGF effects in PCa cells.

## NRP1 regulates both basal expression and VEGF induction of Mcl-1 in PCa cells

The role of NRP1 in the regulation of Mcl-1 expression was investigated. ARCaP$_M$ cells cultured in serum-containing T-medium were transiently transfected with a NRP1 expression vector. Compared to the control, ectopic expression of NRP1 resulted in increased Mcl-1 at both the mRNA and protein levels (Figure 3b). Conversely, transfection with a NRP1 siRNA specifically inhibited NRP1 and reduced endogenous Mcl-1 expression in

ARCaP$_M$ cells (Figure 3c). These data indicated that NRP1 may be required and sufficient for basal expression of Mcl-1 in PCa cells. Further, ARCaP$_M$ cells were transfected with NRP1 siRNA or control siRNA, and incubated with VEGF$_{165}$ in serum-free T-medium for indicated time. Figure 3d showed that expression of NRP1 siRNA, but not control siRNA, abrogated VEGF$_{165}$ induction of Mcl-1 in ARCaP$_M$ cells. These data indicated an indispensible role of NRP1 in mediating VEGF$_{165}$ induction of Mcl-1 in PCa cells.

## c-MET signaling is required for VEGF regulation of Mcl-1 in PCa cells

Since NRP1 does not contain typical kinase receptor sequences [24], we hypothesized that NRP1 may interact with certain tyrosine kinase receptor(s) to transmit VEGF autocrine signal in PCa cells lacking VEGF-Rs. Two recent studies independently demonstrated that NRP1 physically binds c-MET, and potentiates c-MET activation in
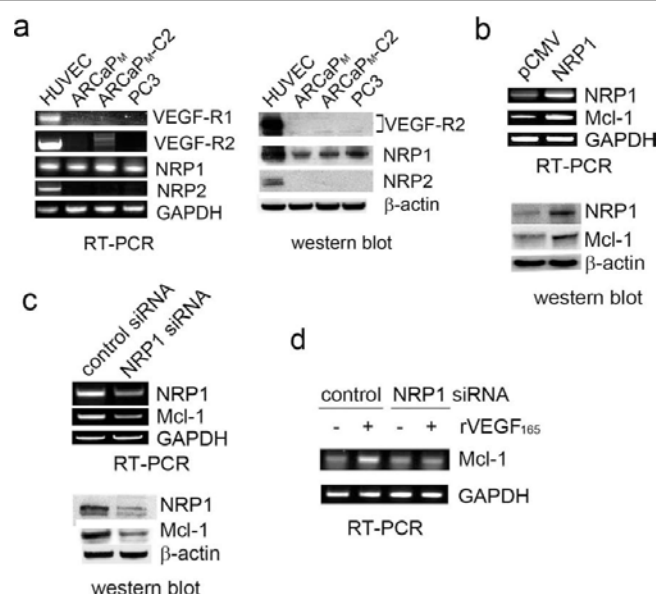
**Figure 3 NRP1 is required for basal expression and VEGF$_{165}$ induction of Mcl-1 in ARCaP$_M$ cells**. (a) Expression of VEGF-Rs in PCa cells and HUVEC. (b) Effect of ectopic expression of NRP1 on Mcl-1 basal level. Subconfluent ARCaP$_M$ cells on 6-well plates were transfected with pCMV-NRP1 or pCMV-XL4 (16 μg) for 48 h (for RT-PCR) or 72 h (for immunoblotting). (c) Effects of NRP1 siRNA on Mcl-1 basal expression. ARCaP$_M$ cells were transfected with NRP1 siRNA or control siRNA (60 nM) for 48 h (for RT-PCR) or 72 h (for immunoblotting). (d) Effects of NRP1 siRNA on VEGF$_{165}$ induction of Mcl-1. ARCaP$_M$ cells were transfected with NRP1 siRNA or control siRNA for 48 h, respectively. Cells were then serum-starved overnight, and treated with VEGF$_{165}$ (10 ng/ml) or PBS for 2 h.



**Figure 4 c-MET signaling is required for VEGF$_{165}$ induction of Mcl-1 in ARCaP$_M$ cells**. (a) Effects of c-MET inhibition on Mcl-1 expression. ARCaP$_M$ cells were transfected with c-MET siRNA or control siRNA (30 nM) for 72 h. (b) Effects of recombinant HGF treatment (10 ng/ml) on Mcl-1 expression at RNA (0, 2, 4 and 6 h) and protein levels (72 h). (c) ARCaP$_M$ cells were transfected with c-MET siRNA or control siRNA for 48 h, serum-starved overnight, and treated with VEGF$_{165}$ (10 ng/ml) for 2 h. (d) ARCaP$_M$ cells were treated with PHA-665752 (0.5 μM) or dimethyl sulfoxide (DMSO) for 2 h, before treatment with VEGF$_{165}$ (10 ng/ml) or PBS for 2 h.

response to HGF stimulation in human glioma and pancreatic cancer cells [25,26]. It is therefore plausible that c-MET may be involved in VEGF regulation of Mcl-1 in PCa cells. Indeed, HGF activation of c-MET signaling has been shown to transcriptionally increase Mcl-1 expression in primary human hepatocytes [27].

A c-MET siRNA construct was transfected into ARCaP$_M$ cells, which effectively inhibited endogenous c-MET (Figure 4a). c-MET siRNA treatment reduced Mcl-1 protein expression, suggesting that c-MET is involved in maintaining basal expression of Mcl-1 in PCa cells. Interestingly, however, recombinant HGF treatment did not significantly affect Mcl-1 expression at either RNA or protein levels (Figure 4b), indicating that HGF-dependent activation of c-MET signaling is not sufficient to induce Mcl-1 expression in these cells.

We further investigated whether c-MET signaling is required for VEGF$_{165}$ induction of Mcl-1. Indeed, VEGF$_{165}$ only induced Mcl-1 expression in ARCaP$_M$ cells transfected with control siRNA, not in those expressing c-MET siRNA (Figure 4c). PHA-665752, a c-MET selective inhibitor [28], was used to treat ARCaP$_M$ cells prior to addition of VEGF$_{165}$. PHA-665752 significantly attenuated VEGF$_{165}$ induction of Mcl-1 in ARCaP$_M$ cells (Figure 4d). These data indicated that c-MET signaling is required for VEGF regulation of Mcl-1 in PCa cells.

## VEGF induces c-MET activation by a NRP1-dependent mechanism in PCa cells

c-MET activation involves phosphorylation of several tyrosine residues including those at positions 1230, 1234, and 1235 [29]. To assess whether VEGF$_{165}$ could induce c-MET activation, and whether this process was mediated by NRP1, ARCaP$_M$ cells were transiently transfected with NRP1 siRNA or control siRNA before VEGF$_{165}$ treatment. VEGF$_{165}$ induced rapid phosphorylation of c-MET at Tyr1230/1234/1235 residues in ARCaP$_M$ cells transfected with control siRNA, but this effect was significantly attenuated by expression of NRP1 siRNA. Expression of total c-MET protein was not affected by siRNA treatment (Figure 5a). These data indicated that VEGF$_{165}$ activated c-

MET signaling independent of HGF, and NRP1 may be indispensible in this process.

## VEGF promotes interaction between NRP1 and c-MET in PCa cells

To explore whether VEGF could induce physical interaction between NRP1 and c-MET, an immunoprecipitation assay was performed in ARCaP$_M$ cells treated with VEGF$_{165}$ for varying times. First, endogenous NRP1 protein was immunoprecipitated (Figure 5b, upper). There was a constitutive association between c-MET and NRP1 in the absence of VEGF$_{165}$. Upon VEGF$_{165}$ treatment, presence of c-MET in the NRP1 immunoprecipitates increased at 30 min and returned to baseline at 60 min. Phosphorylated c-MET (p-c-MET) significantly increased at 15 min following VEGF$_{165}$ treatment, reached a peak at 30 min and slightly decreased in 60 min. Reciprocal immunoprecipitation with anti-c-MET antibody confirmed an association of NRP1 with c-MET in the absence of VEGF$_{165}$. The presence of NRP1 and p-c-MET in the protein complex exhibited a similar time course following VEGF$_{165}$ stimulation, with the peak at 30 min (Figure 5b, low).

Confocal microscopy was performed to determine whether VEGF$_{165}$ promotes NRP1 interaction with c-MET
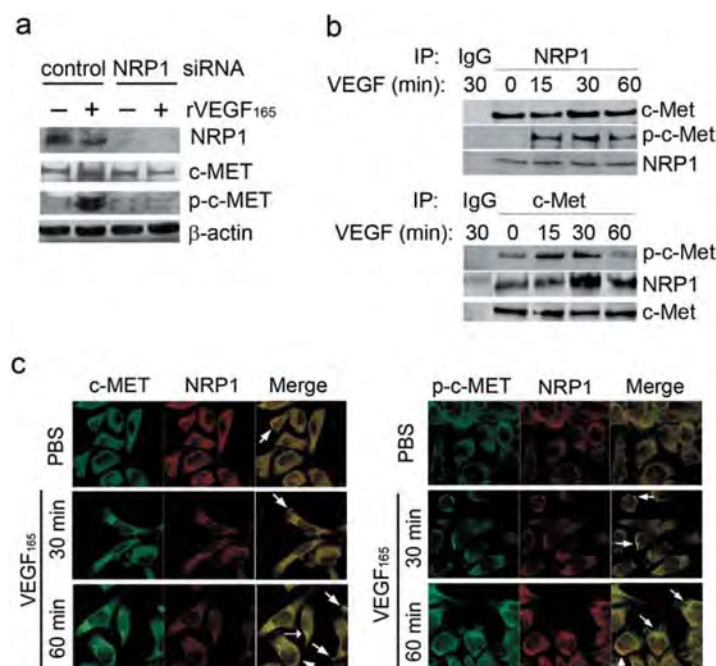


**Figure 5 VEGF$_{165}$ induces c-MET activation through a NRP1-dependent mechanism**. (a) Effects of NRP1 depletion on VEGF$_{165}$-mediated c-MET phosphorylation. ARCaP$_M$ cells were transfected with NRP1 siRNA or control siRNA for 48 h, serum-starved overnight, then treated with VEGF$_{165}$ (10 ng/ml) for 60 min. (b) Immunoprecipitation assay of NRP1-c-MET interaction. Serum-starved ARCaP$_M$ cells were treated with VEGF$_{165}$ (10 ng/ml) for the indicated times, and immunoprecipitated with anti-NRP1 (upper), or anti-c-MET (low) antibody. (c) Co-localization of NRP1 and c-MET or p-c-MET. Serum-starved ARCaP$_M$ cells were treated with VEGF$_{165}$ (10 ng/ml) or PBS for the indicated times. Immunofluorescence staining of NRP1, c-MET or p-c-MET was performed and visualized by confocal microscopy. Arrows indicate co-localization of NRP1 and c-MET or p-c-MET.

and activation of c-MET in ARCaP$_M$ cells. NRP1 and c-MET were found to be constitutively associated on plasma membrane, with the intensity of co-localization further increased at 30 min upon VEGF$_{165}$ treatment (Figure 5c, left panel). Notably, there was a more significant increase in the intensity of co-localization of NRP1 and p-c-MET following VEGF$_{165}$ stimulation (Figure 5c, right panel). The data independently supported a mechanism that NRP1 may be constitutively associated with c-MET on plasma membrane. Upon VEGF$_{165}$ binding, NRP1 may further recruit c-MET and facilitate its activation, subsequently transmitting VEGF$_{165}$ signal (Figure 6).

### Role of Src kinases and signal transducers and activators of transcription 3 (Stat3) in VEGF induction of Mcl-1 in PCa cells

Activation of the Src kinase-Stat3 pathway is an important downstream event in c-MET signaling [30,31] (refer to Figure 6). Recently, a Stat3 *cis*-element was identified in human Mcl-1 promoter [32]. We investigated whether the Src kinase-Stat3 pathway is a downstream component in NRP1 signaling in ARCaP$_M$ cells (Figure 7a). Indeed, expression of NRP1 siRNA in ARCaP$_M$ cells significantly inhibited phosphorylation of Src kinases at Tyr416 (p-Src), as well as activation of Stat3 at Tyr705 (p-Stat3), without altering expression of endogenous Src kinases and Stat3.

Next we examined whether VEGF induces activation of Src kinase-Stat3 signaling in ARCaP$_M$ cells (Figure 7b). VEGF$_{165}$ rapidly induced expression of both p-Src (Tyr416) and p-Stat3 (Tyr705) in a time-dependent manner in ARCaP$_M$ cells, with the peak at 60 min. Significantly, VEGF$_{165}$ promoted rapid intracellular translocation of p-Stat3 (Tyr705) from the cytoplasm to the



**Figure 6 A proposed model for VEGF$_{165}$ regulation of Mcl-1 in PCa cells**. NRP1 may be constitutively associated with c-MET on plasma membrane. VEGF$_{165}$ engagement recruits c-MET into the protein complex and promotes its interaction with NRP1, thereby enhancing phosphorylation of c-MET. Src kinase-Stat3 signaling is subsequently activated, resulting in nuclear translocation of p-Stat3 and activation of Mcl-1 expression. Increased intracellular Mcl-1 protects PCa cells from apoptosis.

nucleus, indicating activation of Stat3-dependent gene expression. By contrast, nuclear presence of p-Stat3 (Ser727), which has been associated with HGF-induced Mcl-1 expression in primary human hepatocytes [27], was not affected. These data indicated that Src kinase-Stat3 pathway activation may be an important event following VEGF$_{165}$ stimulation.

Finally, we assessed the role of Src kinase-Stat3 signaling in VEGF$_{165}$ regulation of Mcl-1. PP2, a selective inhibitor of Src kinases [33], was used to treat ARCaP$_M$ cells before VEGF$_{165}$ stimulation. PP2 treatment effectively abrogated VEGF$_{165}$ induction of Mcl-1 (Figure 7c). Similarly, Mcl-1 mRNA expression was rapidly induced by VEGF$_{165}$ in ARCaP$_M$ cells transfected with control siRNA, but not in the cells expressing Stat3 siRNA (Figure 7d). Collectively these data suggested that Src kinase-Stat3 signaling may be required for VEGF induction of Mcl-1 in PCa cells (Figure 6).

### NRP1 overexpression and c-MET activation are positively associated with human PCa progression and bone metastasis

To validate the clinical significance of NRP1-c-MET signaling in PCa progression, and avoid the potential bias from using human PCa cell lines, IHC analyses were performed to determine the expression of NRP1 and p-c-MET in human PCa tissue specimens. Prostatic tissue specimens of normal/benign glands, primary and bone metastatic tumors were analyzed. NRP1 expression was increased from normal/benign glands (0/5) or well-differentiated cancer (1/5) to poorly-differentiated cancers (5/5) and bone metastatic tissues (5/5) (Figure 8a). NRP1 staining was also determined in tumor specimens from the ARCaP$_M$ xenograft model in which ARCaP$_M$ cells were inoculated into athymic mice orthotopically, resulting in skeletal metastases with a short latency [21]. Consistently, NRP1 expression was significantly greater in bone metastatic tumors than in primary tumors (Figure 8b).

We and others have reported that c-MET overexpression is positively associated with PCa progression [34,35]. As shown in Figure 8c, p-c-MET was expressed at a low level in normal human prostatic tissue, but increased significantly from well-differentiated and intermediate to poorly-differentiated primary PCa. Importantly, bone metastatic PCa specimens displayed a higher expression of p-c-MET than primary PCa. p-c-MET expression was also remarkably increased in bone metastatic ARCaP$_M$ tumors (Figure 8d).

### Discussion

Aberrant overexpression of Mcl-1 has been associated with poor prognosis and resistance to chemotherapy in a variety of human cancers [36]. Sensitizing tumor cells to apoptosis induction by selectively targeting Mcl-1, in combination with conventional chemotherapy, has
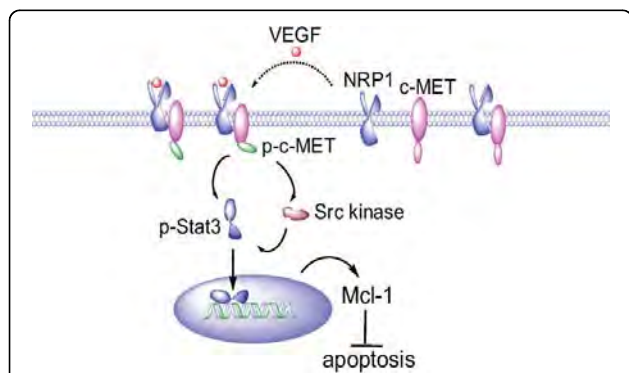
**Figure 7 Src kinase-Stat3 signaling mediates VEGF$_{165}$ induction of Mcl-1 expression in ARCaP$_M$ cells**. (a) Effects of NRP1 inhibition on phosphorylation of Src kinases and Stat3. ARCaP$_M$ cells were transfected with NRP1 siRNA or control siRNA for 72 h. (b) Effects of VEGF$_{165}$ on the phosphorylation of Src kinases and Stat3. ARCaP$_M$ cells were treated with VEGF$_{165}$ (10 ng/ml) for the indicated time, and immunoblotting was performed on total lysates (left) and nuclear extracts and cytoplasmic proteins (right). (c) Effects of Src kinases on VEGF$_{165}$ regulation of Mcl-1. ARCaP$_M$ cells were treated with PP2 (10 μM) or DMSO for 2 h before treatment with VEGF$_{165}$ or PBS. (d) Effects of Stat3 depletion on VEGF$_{165}$ induction of Mcl-1. ARCaP$_M$ cells were transfected with Stat3 siRNA or control siRNA (80 nM) for 48 h, serum-starved overnight, then treated with VEGF$_{165}$ (10 ng/ml) or PBS for 2 h.
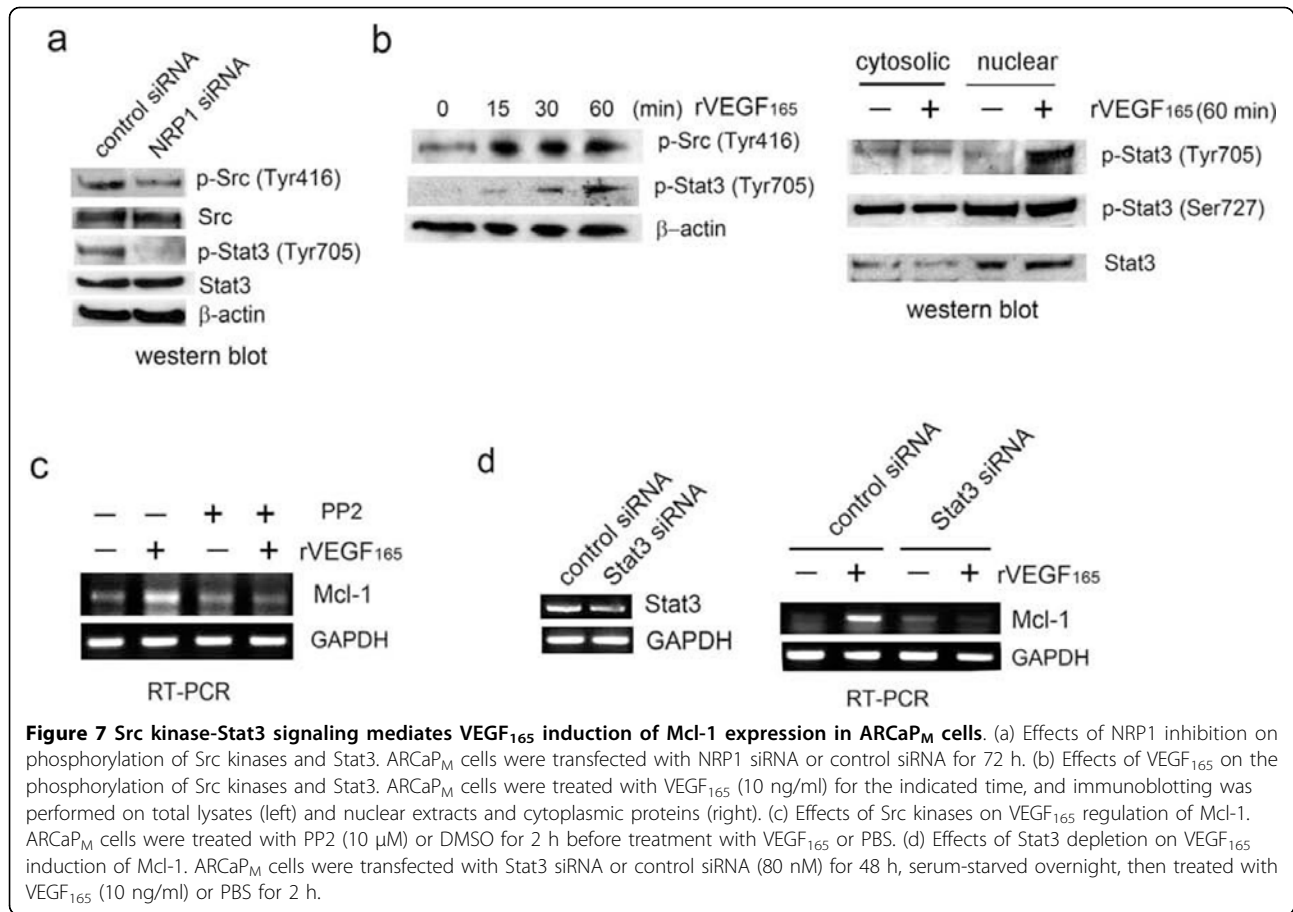
emerged as an attractive therapeutic strategy [3,37]. In this study, we presented evidence that elevated Mcl-1 expression is associated with clinical PCa progression, particularly bone metastasis. We further showed that activation of VEGF-NRP1-c-MET signaling is responsible for Mcl-1 expression, which may confer survival advantages allowing PCa cells to evade apoptosis and progress towards invasive states (Figure 6).

Only limited information are available on Mcl-1 expression profile in PCa. An early study found that Mcl-1 expression was increased at tumors (81%) compared with only 38% in PIN. The percentage of Mcl-1-positive cells was typically higher in Gleason grade 8-10 tumors and metastasis than lower grade tumors, but there was no significant difference in Mcl-1 immunointensity between high grade tumors (47%) and metastasis in lymph node (38%) and bone (50) [5]. Our present study confirmed elevated Mcl-1 expression in high grade (≥ 7) PCa, though the difference between Gleason score 7 and 8-10 tumors is not statistically significant. Intriguingly, our results revealed a remarkable increase in Mcl-1 immunointensity in bone metastasis compared to primary tumors, indicating that Mcl-1 overexpression is positively correlated to PCa progression towards metastatic status in clinical situation.

Accumulating evidence suggests that the function of VEGF in tumor progression may not be limited to angiogenesis [38]. Numerous tumor cells express significant levels of VEGF-Rs, which could engage VEGF and initiate multiple signaling responses involved in cell proliferation, survival and migration. VEGF autocrine signaling confers a degree of self-sufficiency that may be crucial to metastasis as the microenvironment becomes increasingly hostile. Nonetheless, it remains controversial whether VEGF has significant autocrine effects in PCa cells, since the "classical" VEGF-Rs, i.e., VEGF-R1 and -R2, are undetectable in most established PCa cell lines [11,39,40]. Previously we reported that serum VEGF is positively associated with bone metastatic status in PCa patients, and recapitulated this close association in the ARCaP model [18]. In this study, we investigated whether VEGF could affect PCa cell behavior in an autocrine manner. Intriguingly, VEGF$_{165}$ was found to be capable of inducing Mcl-1 expression within a non-saturating range, suggesting it may act as a survival factor in PCa cells. Moreover, NRP1 was found to be highly expressed by PCa cell lines and displayed a positive association with invasiveness, suggesting that it may be the primary receptor responsible for VEGF autocrine
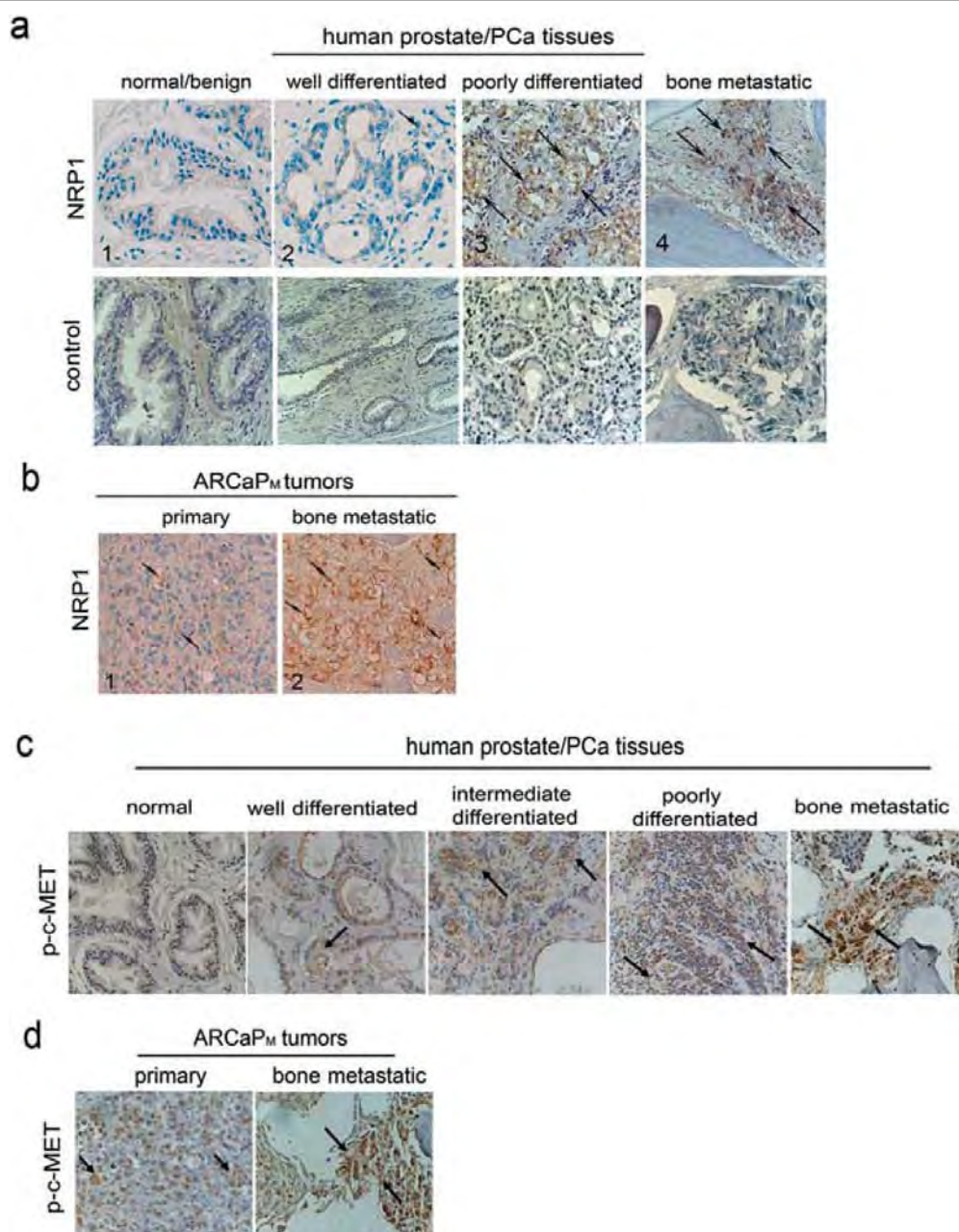
**Figure 8 Expression of NRP1 and p-c-MET is associated with bone metastatic status of human PCa specimens and the ARCaP$_M$ model**.
IHC analyses of NRP1 expression in human normal/benign, cancerous and metastatic prostatic tissue specimens (a) and primary and bone metastatic tissue specimens from ARCaP$_M$ model (b), and of p-c-MET expression in human PCa progression (c) and ARCaP$_M$ xenografts (d). Arrows indicate positively-stained cells.

effects in PCa cells. Gene transfer experiments supported an indispensible role of NRP1 in mediating VEGF$_{165}$ regulation of Mcl-1 in metastatic PCa cells. Importantly, a positive association between NRP1 expression and *in vivo* bone metastatic potential was found in ARCaP$_M$ xenografts and further confirmed in clinical PCa specimens. These data collectively support a novel role of NRP1 in PCa progression and metastasis,

presumably by transmitting the VEGF autocrine survival signal and enabling PCa cells to evade apoptosis.

NRP1 is not a typical "signaling receptor" since it lacks sequences predicted to have kinase receptor activities [24]. Direct interaction between NRP1 and VEGF-Rs or plexin A is essential to its function in prioritizing differential signals from VEGF$_{165}$ or semaphorin 3 in endothelial cells and nerve cells [24]. Recent studies found that

the NRP1 intracellular domain, especially the C-terminal three amino acids (SEA-COOH), may be required for the interaction between NRP1 and its binding partners, including NRP1-interacting protein (NIP; or RGS-GAIP-interacting protein, GIPC) and VEGF-R2 [41,42]. However, the molecular effects and mechanism for NRP1-mediated signaling in tumor cells, especially in the absence of VEGF-Rs, remain elusive. It has been proposed that NRP1 may store or sequester $VEGF_{165}$ and attract endothelial cells towards tumor, contributing to angiogenesis *via* juxtacrine or paracrine mechanisms [9,17]. In this study, we investigated whether NRP1 is required for $VEGF_{165}$ autocrine signaling in PCa cells lacking VEGF-Rs. We presented evidence that NRP1 and c-MET are physically associated on plasma membrane, and in response to $VEGF_{165}$ stimulation, their interaction may significantly facilitate further recruitment and activation of c-MET. Though the structural and molecular basis for interaction between the two receptors needs to be further investigated, this study indicates for the first time that c-MET activity can be modulated by VEGF, and the NRP1-c-MET interaction may be a critical component in transmitting the VEGF survival signal in PCa cells. It may be plausible to assign c-MET phosphorylation as an indicator for activation of NRP1 autocrine signaling in tumor cells. Using human PCa tissue specimens as the "gold standard", we observed that NRP1 and p-c-MET were both significantly increased with progression of primary PCa, and further elevated in bone metastatic PCa, suggesting that activation of NRP1-c-MET signaling may be positively associated with clinical PCa progression. It is worth noting that these results need cautious interpretation since a limited number of patient specimens was examined, and the polyclonal antibody against p-c-MET has not been fully validated for immunohistochemical analysis in tissue sections.

In human primary hepatocytes, HGF transcriptionally induced Mcl-1 expression, but not Bcl-2 or Bcl-x(L) [27]. Our studies found that, however, HGF treatment did not significantly affect Mcl-1 protein expression in $ARCaP_M$ cells, suggesting HGF activation of c-MET signaling may not be sufficient to increase Mcl-1 expression. We postulated that $VEGF_{165}$ may utilize a different mechanism to regulate Mcl-1 expression in PCa cells. An important observation supporting this hypothesis is that $VEGF_{165}$ only rapidly induced Stat3 phosphorylation at Tyr705, but not altering Ser727 phosphorylation in $ARCaP_M$ cells. In hepatocytes, however, HGF triggered Ser727, but not Tyr705, phosphorylation of Stat3 [27]. It will be intriguing to investigate the role of NRP1-c-MET interaction in differentiating extracellular ligands, i.e., $VEGF_{165}$ or HGF, and activating distinct downstream cascades leading to Mcl-1 expression in a highly cell context-dependent fashion.

Mcl-1 is a protein with very short half-life and is highly regulated at multiple levels in response to survival and differentiation signals. Rapid turnover of Mcl-1 protein can be initiated by stress (such as serum withdrawal) through caspase-mediated and proteasome-dependent degradation in tumor cells [3]. Previous study found that VEGF protects multiple myeloma cells against apoptosis by up-regulating Mcl-1 protein in a time-dependent manner, peaking at 6 h and returning to baseline after 24 h; change in Mcl-1 mRNA expression was not reported [43]. In $ARCaP_M$ cells, however, $VEGF_{165}$ treatment rapidly induced Mcl-1 mRNA expression and significantly increased Mcl-1 protein level at 72 h. Though whether $VEGF_{165}$ may also regulate Mcl-1 expression at other levels needs to be further investigated, the data presented here suggest that transcriptional activation, presumably mediated by Stat3, is an important mechanism for $VEGF_{165}$ induction of Mcl-1 in PCa cells.

Interrupting NRP1 functions with mimetic peptides and monoclonal antibodies is being developed in xenograft models of human cancers [44,45]. NRP1 monoclonal antibody has been shown to effectively inhibit tumor vascular remodeling, rendering vessels more susceptible to anti-VEGF therapy [45]. If the $VEGF_{165}$-NRP1-c-MET pathway is required for Mcl-1 expression and survival in PCa cells, it would be intriguing to evaluate whether targeting NRP1 could interrupt both NRP1-c-MET signaling in tumor cells (survival) and NRP1-VEGF-Rs signaling in endothelial cells (angiogenesis). Inhibition of NRP1 signaling may be a promising strategy alone or in combination with other therapeutic approaches for treating PCa.

## Methods
### Cell culture
Human PCa cell lines $ARCaP_M$, $ARCaP_M$-C2, PC3, LNCaP, C4-2 and C4-2B, were routinely maintained in T-medium (Invitrogen, Carlsbad, CA) with 5% fetal bovine serum (FBS). $ARCaP_M$-C2 subclone was derived from $ARCaP_M$ bone metastatic tissues as described previously [21,22]. Where specified, $ARCaP_M$ cells were serum-starved overnight, and treated with recombinant human $VEGF_{165}$, $VEGF_{121}$, HGF (R&D Systems, Minneapolis, MN), c-MET inhibitor PHA-665752 (Calbiochem, San Diego, CA), or Src kinase inhibitor (PP2) (Calbiochem) in serum-free T-medium. HUVEC (The American Type Culture Collection, Manassas, VA) were maintained in endothelial basal growth medium (EBM-2) with 2% FBS. Cell proliferation was measured using the CellTiter 96 AQ proliferation assay according to the manufacturer's instructions (Promega, Madison, WI). Viable cells were counted in triplicate using a hemacytometer and trypan blue staining.

## Immunohistochemical analysis

IHC staining of NRP1 and p-c-MET on human normal/benign prostatic glands, well- and poorly-differentiated primary PCa and bone metastatic PCa tissue specimens was performed as described previously [18] using goat anti-NRP1 antibody (C-19, Santa Cruz Biotechnology, Santa Cruz, CA; 1:100) and rabbit anti-p-c-MET (Tyr1230/1234/1235) antibody (44888G, Invitrogen; 1:100). IHC analysis of Mcl-1 expression was performed on a human PCa progression tissue microarray specimen (US BioMax, Inc., Rockville, MD) using rabbit anti-Mcl-1 antibody (S-19, Santa Cruz Biotechnology, 1:150). Matching normal serum was used as negative control. All IHC common reagents were obtained from Dako (Carpinteria, CA). Positive expression of NRP1, p-c-MET and Mcl-1 was defined as >15% positive staining in cell population.

## Transfection

The vector harboring NRP1 cDNA (pCMV-NRP1) and the control (pCMV-XL4) (Origene, Rockville, MD) were transfected into ARCaP$_M$ cells for 48-72 h using lipofectamine 2000 (Invitrogen). Small interfering RNA (siRNA) nucleotides were transfected into ARCaP$_M$ cells according to the manufacturer's instructions. VEGF siRNA, Mcl-1 siRNA, Stat3 siRNA and control siRNA-A were purchased from Santa Cruz Biotechnology. NRP1 *silencer*® select validated siRNA and *silencer*® select control siRNA[#]1 were obtained from Ambion, Inc., (Austin, TX). c-MET ON-TARGET *plus* siRNA and ON-TARGET *plus* siRNA control were purchased from Dharmacon, Inc, (Chicago, IL).

## Western blot analysis

Total cell lysates were prepared using radioimmunoprecipitation (RIPA) buffer (Santa Cruz Biotechnology). Nuclear proteins were extracted using a Novagen kit (EMD Biosciences, San Diego, CA). Immunoblotting analysis followed standard procedure [18] with anti-Stat3, anti-p-Stat3 (Ser705), anti-Src and anti-p-Src (Tyr416) (Cell Signaling, Danvers, MA); anti-p-Stat3 (Tyr705) (Upstate, Charlottesville, VA); anti-Mcl-1, anti-NRP1 (C-19), anti-NRP2, anti-VEGF-R2, and anti-c-MET (Santa Cruz Biotechnology); anti-p-c-MET (Tyr1230/1234/1235) (Invitrogen); and anti-β-actin (Sigma, St. Louis, MO).

## RT-PCR

Total RNA was prepared with Qiagen RNeasy Kit (Valencia, CA), and RT-PCR was performed using the SuperScriptIII® One-Step RT-PCR kit (Invitrogen) following the manufacturer's protocol. The specific primer pairs are: 5'-GAGGAGGAGGAGGACGAGTT-3' (forward) and 5'-GTCCGTTTTGTCCTTACGA-3' (reverse) (for Mcl-1); 5'-AGGACAGAGACTGCAAG TATGAC-3' (forward) and 5'-AACATTCAGGACCT CTCTTGA-3' (reverse) (for NRP1). The primers for VEGF, glyceraldehyde-3-phosphate dehydrogenase (GAPDH) [18] and Stat3 [46] were described previously. The primer pairs for human VEGF-R1, VEGF-R2 and NRP2 were purchased from R&D Systems.

## ELISA

Subconfluent PCa cells were cultured in serum-free T-medium for 72 h before conditioned medium was collected. VEGF concentrations were analyzed using a Quantikine ELISA kit (R&D Systems) and normalized with total protein concentrations in CM.

## Immunofluorescence and confocal imaging

Immunofluorescence was performed as described previously [47]. Goat anti-NRP1 antibody (C-19), rabbit anti-c-MET antibody (C-12, Santa Cruz Biotechnology), or rabbit anti-p-c-MET (Tyr1230/1234/1235) antibody was incubated with subconfluent ARCaP$_M$ cells at 4°C overnight. Either anti-goat Alexa Fluor® 546 or anti-rabbit Alexa Fluor® 488 secondary antibody (Invitrogen) was used at a dilution of 1:500. Cells were imaged on a Zeiss LSM 510 META [47]. In all cases, either a 63× or 100× Zeiss Plan-Apo oil objective was used (numerical aperture of 1.3 and 1.4, respectively). All images had contrast expansion performed in Adobe Photoshop.

## Immunoprecipitation

The Immunoprecipitation Starter Pack (GE healthcare Bio-Sciences Corp., Piscataway, NJ) was used according to the manufacturer's instructions. Total lysates (1 mg) were immunoprecipitated with rabbit anti-c-MET antibody (C-12), rabbit anti-NRP1 antibody (H-286, Santa Cruz Biotechnology), or normal rabbit IgG (R&D Systems). Protein A/G Sepharose 4 Fast Flow beads were added to precipitate proteins, then washed and eluted. The samples were further processed for western blot analysis.

## Apoptosis analysis

Cells were stained with an Annexin V-PE apoptosis detection kit (BD Biosciences, San Jose, CA) following the manufacturer's protocol, and measured using a fluorescence-activated cell sorting (FACS) caliber benchtop flow cytometer (Becton Dickinson, Franklin Lakes, NJ). The data were analyzed using FlowJo software (Tree Star, Inc., Ashland, OR).

## Data analysis

Significance levels for comparisons of Mcl-1 expression in different Gleason score PCa were calculated by using the 2-sample $t$ test. Treatment effects were evaluated using a two-sided Student's $t$ test. All data represent three or more experiments. Errors are S.E. values of averaged results, and values of $p < 0.05$ were taken as a significant difference between means.

**Additional file 1: Figure S1**. (a) Endogenous Mcl-1 expression in the lineage-related LNCaP, C4-2 and C4-2B cells, as determined by RT-PCR and western blotting analyses. (b) ELISA of VEGF levels in conditioned media of LNCaP and C4-2 cells, shown as relative VEGF concentrations normalized by total protein concentrations of the CM. (c) Effects of recombinant $VEGF_{121}$ on the proliferation of $ARCaP_M$ cells. $1 \times 10^3$ cells were seeded in 96-well plates for 24 h, serum-starved overnight, and cultured in the absence or presence of varying concentrations of $rVEGF_{121}$ for 72 h. MTS assay was then performed. (d) Effects of $VEGF_{165}$ on Mcl-1 expression in LNCaP cells. Subconfluent LNCaP cells were serum-starved overnight, and incubated for 72 h in the presence of $VEGF_{165}$ (10 ng/ml) or PBS. Western blotting was performed. (e) Effects of $VEGF_{121}$ on Mcl-1 expression in $ARCaP_M$ cells. Subconfluent $ARCaP_M$ cells were serum-starved overnight, and incubated for 72 h in the presence of $VEGF_{121}$ (10 ng/ml) or PBS. Western blotting was performed. (f) Expression of endogenous NRP1 in LNCaP, C4-2 and C4-2B cells, as determined by RT-PCR and western blotting analyses. (g) Nuclear expression of c-MET and p-c-MET in $ARCaP_M$ and $ARCaP_M$-C2 cells. TATA binding protein (TBP) was used as internal control of nuclear proteins. Click here for file

[ http://www.biomedcentral.com/content/supplementary/1476-4598-9-9-S1.TIFF ]

## Author details

[1]Department of Urology and Winship Cancer Institute, Emory University School of Medicine, Atlanta, GA, USA. [2]Uro-Oncology Research Program, Cedars-Sinai Medical Center, Los Angeles, CA, USA. [3]Department of Pathology Laboratory Medicine, Emory University School of Medicine, Atlanta, GA, USA. [4]Department of Urology, Xijing Hospital, Fourth Military Medical University, Xi'an, China. [5]Department of Pathology, the Second Xiangya Hospital, Central South University, Changsha, China. [6]Department of Biostatistics and Bioinformatics, Rollins School of Public Health, Emory University, Atlanta, GA, USA.

## Authors' contributions

SZ performed western blotting, immunoprecipitation, immunofluorescence confocal microscopy, and gene transfer experiments (siRNA and cDNA expression). HEZ established the ARCaP PCa progression model, provided human PCa tissue specimens, designed and performed the immunohistochemical staining of NRP1 and p-c-MET in ARCaP tumors and human PCa specimens. AOO provided human PCa tissue specimens and evaluated expression of NRP1 and p-c-MET. SF evaluated expression of Mcl-1 in PCa tissue microarray specimens. ZC performed statistical analyses. XY and SI performed cell culture and preparation of proteins and RNA samples. RW contributed to the establishment of the ARCaP animal models. FFM and LWKC participated in discussion and manuscript preparation. LWKC provided grant supports for this study. DW designed experiments and drafted manuscript. All authors read and approved the final version of this manuscript.

## Competing interests

The authors declare that they have no competing interests.

## References

1. Mehlen P, Puisieux A: **Metastasis: a question of life or death.** *Nat Rev Cancer* 2006, **6**:449-458.
2. Certo M, Del Gaizo Moore V, Nishino M, Wei G, Korsmeyer S, Armstrong SA, Letai A: **Mitochondria primed by death signals determine cellular addiction to antiapoptotic BCL-2 family members.** *Cancer Cell* 2006, **9**:351-365.
3. Akgul C: **Mcl-1 is a potential therapeutic target in multiple types of cancer.** *Cell Mol Life Sci* 2008.
4. Kitada S, Andersen J, Akar S, Zapata JM, Takayama S, Krajewski S, Wang HG, Zhang X, Bullrich F, Croce CM, Rai K, Hines J, Reed JC: **Expression of apoptosis-regulating proteins in chronic lymphocytic leukemia: correlations with In vitro and In vivo chemoresponses.** *Blood* 1998, **91**:3379-3389.
5. Krajewska M, Krajewski S, Epstein JI, Shabaik A, Sauvageot J, Song K, Kitada S, Reed JC: **Immunohistochemical analysis of bcl-2, bax, bcl-X, and mcl-1 expression in prostate cancers.** *Am J Pathol* 1996, **148**:1567-1576.
6. Zhang B, Gojo I, Fenton RG: **Myeloid cell factor-1 is a critical survival factor for multiple myeloma.** *Blood* 2002, **99**:1885-1893.
7. Maeta Y, Tsujitani S, Matsumoto S, Yamaguchi K, Tatebe S, Kondo A, Ikeguchi M, Kaibara N: **Expression of Mcl-1 and p53 proteins predicts the survival of patients with T3 gastric carcinoma.** *Gastric Cancer* 2004, **7**:78-84.
8. Ferrara N, Gerber HP, LeCouter J: **The biology of VEGF and its receptors.** *Nat Med* 2003, **9**:669-676.
9. Soker S, Takashima S, Miao HQ, Neufeld G, Klagsbrun M: **Neuropilin-1 is expressed by endothelial and tumor cells as an isoform-specific receptor for vascular endothelial growth factor.** *Cell* 1998, **92**:735-745.
10. Whitaker GB, Limberg BJ, Rosenbaum JS: **Vascular endothelial growth factor receptor-2 and neuropilin-1 form a receptor complex that is responsible for the differential signaling potency of VEGF(165) and VEGF (121).** *J Biol Chem* 2001, **276**:25520-25531.
11. Kitagawa Y, Dai J, Zhang J, Keller JM, Nor J, Yao Z, Keller ET: **Vascular endothelial growth factor contributes to prostate cancer-mediated osteoblastic activity.** *Cancer Res* 2005, **65**:10921-10929.
12. Stephenson JM, Banerjee S, Saxena NK, Cherian R, Banerjee SK: **Neuropilin-1 is differentially expressed in myoepithelial cells and vascular smooth muscle cells in preneoplastic and neoplastic human breast: a possible marker for the progression of breast cancer.** *Int J Cancer* 2002, **101**:409-414.
13. Parikh AA, Liu WB, Fan F, Stoeltzing O, Reinmuth N, Bruns CJ, Bucana CD, Evans DB, Ellis LM: **Expression and regulation of the novel vascular endothelial growth factor receptor neuropilin-1 by epidermal growth factor in human pancreatic carcinoma.** *Cancer* 2003, **98**:720-729.
14. Parikh AA, Fan F, Liu WB, Ahmad SA, Stoeltzing O, Reinmuth N, Bielenberg D, Bucana CD, Klagsbrun M, Ellis LM: **Neuropilin-1 in human colon cancer: expression, regulation, and role in induction of angiogenesis.** *Am J Pathol* 2004, **164**:2139-2151.
15. Latil A, Bieche I, Pesche S, Valeri A, Fournier G, Cussenot O, Lidereau R: **VEGF overexpression in clinically localized prostate tumors and neuropilin-1 overexpression in metastatic forms.** *Int J Cancer* 2000, **89**:167-171.
16. Kawakami T, Tokunaga T, Hatanaka H, Kijima H, Yamazaki H, Abe Y, Osamura Y, Inoue H, Ueyama Y, Nakamura M: **Neuropilin 1 and neuropilin 2 co-expression is significantly correlated with increased vascularity and poor prognosis in nonsmall cell lung carcinoma.** *Cancer* 2002, **95**:2196-2201.
17. Miao HQ, Lee P, Lin H, Soker S, Klagsbrun M: **Neuropilin-1 expression by tumor cells promotes tumor angiogenesis and progression.** *Faseb J* 2000, **14**:2532-2539.
18. Wu D, Zhau HE, Huang WC, Iqbal S, Habib FK, Sartor O, Cvitanovic L, Marshall FF, Xu Z, Chung LW: **cAMP-responsive element-binding protein regulates vascular endothelial growth factor expression: implication in human prostate cancer bone metastasis.** *Oncogene* 2007, **26**:5070-5077.
19. Zhau HY, Chang SM, Chen BQ, Wang Y, Zhang H, Kao C, Sang QA, Pathak SJ, Chung LW: **Androgen-repressed phenotype in human prostate cancer.** *Proc Natl Acad Sci USA* 1996, **93**:15152-15157.
20. Zhau HE, Li CL, Chung LW: **Establishment of human prostate carcinoma skeletal metastasis models.** *Cancer* 2000, **88**:2995-3001.
21. Xu J, Wang R, Xie ZH, Odero-Marah V, Pathak S, Multani A, Chung LW, Zhau HE: **Prostate cancer metastasis: role of the host microenvironment in promoting epithelial to mesenchymal transition and increased bone and adrenal gland metastasis.** *Prostate* 2006, **66**:1664-1673.
22. Xu J, Odero-Marah V, Wang R, Chung LW, Zhau HE: **Epithelial-mesenchymal transition and bone-specific microenvironment contribute

to the rapid skeletal metastasis in human prostate cancer. *J Urol* 2005, **173**:125.

23. Wu TT, Sikes RA, Cui Q, Thalmann GN, Kao C, Murphy CF, Yang H, Zhau HE, Balian G, Chung LW: Establishing human prostate cancer cell xenografts in bone: induction of osteoblastic reaction by prostate-specific antigen-producing tumors in athymic and SCID/bg mice using LNCaP and lineage-derived metastatic sublines. *Int J Cancer* 1998, **77**:887-894.

24. Fujisawa H, Kitsukawa T: Receptors for collapsin/semaphorins. *Curr Opin Neurobiol* 1998, **8**:587-592.

25. Matsushita A, Gotze T, Korc M: Hepatocyte growth factor-mediated cell invasion in pancreatic cancer cells is dependent on neuropilin-1. *Cancer Res* 2007, **67**:10309-10316.

26. Hu B, Guo P, Bar-Joseph I, Imanishi Y, Jarzynka MJ, Bogler O, Mikkelsen T, Hirose T, Nishikawa R, Cheng SY: Neuropilin-1 promotes human glioma progression through potentiating the activity of the HGF/SF autocrine pathway. *Oncogene* 2007, **26**:5577-5586.

27. Schulze-Bergkamen H, Brenner D, Krueger A, Suess D, Fas SC, Frey CR, Dax A, Zink D, Buchler P, Muller M, Krammer PH: Hepatocyte growth factor induces Mcl-1 in primary human hepatocytes and inhibits CD95-mediated apoptosis via Akt. *Hepatology* 2004, **39**:645-654.

28. Christensen JG, Schreck R, Burrows J, Kuruganti P, Chan E, Le P, Chen J, Wang X, Ruslim L, Blake R, Lipson KE, Ramphal J, Do S, Cui JJ, Cherrington JM, Mendel DB: A selective small molecule inhibitor of c-Met kinase inhibits c-Met-dependent phenotypes in vitro and exhibits cytoreductive antitumor activity in vivo. *Cancer Res* 2003, **63**:7345-7355.

29. Longati P, Comoglio PM, Bardelli A: Receptor tyrosine kinases as therapeutic targets: the model of the MET oncogene. *Curr Drug Targets* 2001, **2**:41-55.

30. Boccaccio C, Ando M, Tamagnone L, Bardelli A, Michieli P, Battistini C, Comoglio PM: Induction of epithelial tubules by growth factor HGF depends on the STAT pathway. *Nature* 1998, **391**:285-288.

31. Ponzetto C, Bardelli A, Zhen Z, Maina F, dalla Zonca P, Giordano S, Graziani A, Panayotou G, Comoglio PM: A multifunctional docking site mediates signaling and transformation by the hepatocyte growth factor/scatter factor receptor family. *Cell* 1994, **77**:261-271.

32. Isomoto H, Kobayashi S, Werneburg NW, Bronk SF, Guicciardi ME, Frank DA, Gores GJ: Interleukin 6 upregulates myeloid cell leukemia-1 expression through a STAT3 pathway in cholangiocarcinoma cells. *Hepatology* 2005, **42**:1329-1338.

33. Hanke JH, Gardner JP, Dow RL, Changelian PS, Brissette WH, Weringer EJ, Pollok BA, Connelly PA: Discovery of a novel, potent, and Src family-selective tyrosine kinase inhibitor. Study of Lck- and FynT-dependent T cell activation. *J Biol Chem* 1996, **271**:695-701.

34. Pisters LL, Troncoso P, Zhau HE, Li W, von Eschenbach AC, Chung LW: c-met proto-oncogene expression in benign and malignant human prostate tissues. *J Urol* 1995, **154**:293-298.

35. Knudsen BS, Gmyrek GA, Inra J, Scherr DS, Vaughan ED, Nanus DM, Kattan MW, Gerald WL, Woude Vande GF: High expression of the Met receptor in prostate cancer metastasis to bone. *Urology* 2002, **60**:1113-1117.

36. Mandelin AM, Pope RM: Myeloid cell leukemia-1 as a therapeutic target. *Expert Opin Ther Targets* 2007, **11**:363-373.

37. Chen S, Dai Y, Harada H, Dent P, Grant S: Mcl-1 down-regulation potentiates ABT-737 lethality by cooperatively inducing Bak activation and Bax translocation. *Cancer Res* 2007, **67**:782-791.

38. Mercurio AM, Lipscomb EA, Bachelder RE: Non-angiogenic functions of VEGF in breast cancer. *J Mammary Gland Biol Neoplasia* 2005, **10**:283-290.

39. Sokoloff MH, Chung LW: Targeting angiogenic pathways involving tumor-stromal interaction to treat advanced human prostate cancer. *Cancer Metastasis Rev* 1998, **17**:307-315.

40. Soker S, Kaefer M, Johnson M, Klagsbrun M, Atala A, Freeman MR: Vascular endothelial growth factor-mediated autocrine stimulation of prostate tumor cells coincides with progression to a malignant phenotype. *Am J Pathol* 2001, **159**:651-659.

41. Wang L, Mukhopadhyay D, Xu X: C terminus of RGS-GAIP-interacting protein conveys neuropilin-1-mediated signaling during angiogenesis. *FASEB J* 2006, **20**:1513-1515.

42. Prahst C, Heroult M, Lanahan AA, Uziel N, Kessler O, Shraga-Heled N, Simons M, Neufeld G, Augustin HG: Neuropilin-1-VEGFR-2 complexing requires the PDZ-binding domain of neuropilin-1. *J Biol Chem* 2008, **283**:25110-25114.

43. Le Gouill S, Podar K, Amiot M, Hideshima T, Chauhan D, Ishitsuka K, Kumar S, Raje N, Richardson PG, Harousseau JL, Anderson KC: VEGF induces Mcl-1 up-regulation and protects multiple myeloma cells against apoptosis. *Blood* 2004, **104**:2886-2892.

44. Hong TM, Chen YL, Wu YY, Yuan A, Chao YC, Chung YC, Wu MH, Yang SC, Pan SH, Shih JY, Chan WK, Yang PC: Targeting neuropilin 1 as an antitumor strategy in lung cancer. *Clin Cancer Res* 2007, **13**:4759-4768.

45. Pan Q, Chanthery Y, Liang WC, Stawicki S, Mak J, Rathore N, Tong RK, Kowalski J, Yee SF, Pacheco G, Ross S, Cheng Z, Le Couter J, Plowman G, Peale F, Koch AW, Wu Y, Bagri A, Tessier-Lavigne M, Watts RJ: Blocking neuropilin-1 function has an additive effect with anti-VEGF to inhibit tumor growth. *Cancer Cell* 2007, **11**:53-67.

46. Rivat C, Rodrigues S, Bruyneel E, Pietu G, Robert A, Redeuilh G, Bracke M, Gespach C, Attoub S: Implication of STAT3 signaling in human colonic cancer cells during intestinal trefoil factor 3 (TFF3) – and vascular endothelial growth factor-mediated cellular invasion and tumor growth. *Cancer Res* 2005, **65**:195-202.

47. Zhang S, Schafer-Hales K, Khuri FR, Zhou W, Vertino PM, Marcus AI: The tumor suppressor LKB1 regulates lung cancer cell polarity by mediating cdc42 recruitment and activity. *Cancer Res* 2008, **68**:740-748.

**PDGF Upregulates Mcl-1 Through Activation of β-catenin and HIF-1α-Dependent Signaling in Human Prostate Cancer Cells**

Shareen Iqbal[1], Shumin Zhang[1], Adel Driss[2], Zhi-Ren Liu[3], Haiyen E. Zhau[4], Omer Kucuk[5], Leland W.K. Chung[4§], Daqing Wu[1§]

[1]Department of Urology and Winship Cancer Institute, Emory University School of Medicine, Atlanta, GA, USA; [2]Department of Microbiology, Biochemistry and Immunology, Morehouse School of Medicine, Atlanta, GA, USA; [3]Department of Biology, Georgia State University, Atlanta, GA, USA; [4]Uro-Oncology Research Program, Department of Medicine, Cedars-Sinai Medical Center, Los Angeles, CA, USA; [5]Department of Hematology and Medical Oncology and Winship Cancer Institute, Emory University School of Medicine, Atlanta, GA, USA

[§]**Corresponding authors:** Dr. Daqing Wu (Email: dwu2@emory.edu), Department of Urology and Winship Cancer Institute, Emory University School of Medicine, 1365-B Clifton Road, B4108, Atlanta, GA 30322, USA; Dr. Leland W. K. Chung (Email: Leland.Chung@cshs.org), Uro-Oncology Research Program, Cedars-Sinai Medical Center, Los Angeles, CA, USA

**Running Title:** PDGF regulation of Mcl-1 in prostate cancer cells

**Abstract**

**Background:** Aberrant platelet derived growth factor (PDGF) signaling has been associated with prostate cancer (PCa) progression. However, its role in the regulation of PCa cell growth and survival has not been well characterized.

**Methodology/Principal Findings:** Using experimental models that closely mimic clinical pathophysiology of PCa progression, we demonstrated that PDGF is a survival factor in PCa cells through upregulation of myeloid cell leukemia-1 (Mcl-1). PDGF treatment induced rapid nuclear translocation of β-catenin, presumably mediated by c-Abl and p68 signaling. Intriguingly, PDGF promoted formation of the nuclear transcriptional complex of β-catenin and hypoxia-inducible factor (HIF)-1α, and the binding of HIF-1α to Mcl-1 promoter. Deletion of a putative hypoxia response element (HRE) within the Mcl-1 promoter attenuated PDGF effects on Mcl-1 expression. Blockade of PDGF receptor (PDGFR) signaling with a pharmacological inhibitor AG-17 abrogated PDGF induction of Mcl-1, and induced apoptosis in metastatic PCa cells.

**Conclusions/Significance:** Our study elucidated a crucial survival mechanism in PCa cells, indicating that interruption of the PDGF-Mcl-1 survival signal may provide a novel strategy for treating PCa metastasis.

**Introduction**

The platelet-derived growth factors (PDGF) family consists of five dimeric isoforms: PDGF-AA, -AB, -BB, -CC and -DD [1], which exert their cellular effects through two structurally similar tyrosine kinase receptors (PDGFR-α and -β) expressed by many different cell types [2]. Ligand binding to PDGFRs results in the dimerization and autophosphorylation of the receptor kinases, subsequently recruiting certain Src homology 2 (SH2) domain-containing adaptor proteins (e.g., Src, Grb2 and Shc) to specific phosphorylated tyrosine residues. Several signaling cascades, including Ras-mitogen-activated protein kinase (MAPK), phospholipase-γ and phos-phatidyl-inositol-3'-kinase (PI3K)/Akt, have been characterized as the major downstream pathways mediating PDGF functions [3]. Other adaptor molecules (e.g., the Fer and Fes tyrosine kinase family) and transcriptional factors (e.g., β-catenin) are also involved in PDGF signaling in certain cell types [4,5,6,7,8].

Aberrant PDGF expression has been frequently associated with the neoplastic component of human tumors, whereas PDGFRs are mainly found in the fibroblastic and vascular tumor stroma [9,10,11,12,13]. These observations suggested that tumor-derived PDGF may primarily act as a paracrine signaling molecule in solid tumors. Supporting this concept, recent studies have demonstrated that PDGF is a potent pro-angiogenic factor by promoting the recruitment and growth of stromal fibroblasts, perivascular cells and endothelial cells, thereby indirectly affecting tumor growth, metastatic dissemination and drug resistance [2,3,14,15,16]. Interestingly, emerging evidence indicated that PDGF autocrine signaling may also play an important role during tumor progression. Mutational activation or co-expression of PDGF ligands and receptors are capable of stimulating tumor cell growth and proliferation in several nonepithelial malignancies, including glioblastomas and osteosarcoma [17]. More recently, autocrine PDGF

3

signaling has been associated with epithelial-to-mesenchymal transition (EMT) in carcinoma cells from the breast, colon, prostate and liver, suggesting a causative role of autocrine PDGF signaling in metastasis [7,8,18,19]. Nonetheless, despite the well-established correlation between deregulated paracrine PDGF signaling and tumor progression, the functions and mechanisms of autocrine PDGF signaling in epithelial cancer cells remain elusive [3,17].

Acquisition of apoptosis resistance is characteristic of metastatic tumor cells, which may confer survival advantages during invasion, metastasis and colonization [20]. We recently correlated overexpression of myeloid cell leukemia-1 (Mcl-1), a member of the Bcl-2 family, with the progression of prostate cancer (PCa) towards bone metastasis [21]. In this study, we provide evidence that PDGF-BB is a survival factor in metastatic PCa cells by upregulating Mcl-1 expression through a signaling mechanism mediated by the transcriptional factors β-catenin and hypoxia-inducible factor (HIF)-1α.

**Materials and Methods**

*Cell Culture*

Human PCa cell lines $ARCaP_E$, $ARCaP_M$ [22], LNCaP (American Type Culture Collection, ATCC, Manassas, VA), C4-2 [23] and PC3 (ATCC) were routinely maintained in T-medium (Invitrogen, Carlsbad, CA) with 5% fetal bovine serum (FBS). For the treatments with PDGF isoforms, PCa cells seeded in 96-well plates (3,000 cell/well) were serum-starved overnight, replaced with fresh serum-free T-medium, and incubated in the presence of varying concentrations of recombinant human PDGF-AA, -AB, -BB (R&D Systems, Minneapolis, MN), or phosphate-buffered saline (PBS) for indicated times. Recombinant human interleukin-6 (IL-6) was purchased from R&D Systems. For chemotherapy drug treatment, docetaxel (Sanofi Aventis,

Bridgewater, NJ) or dimethyl sulfoxide (DMSO; Sigma-Aldrich, St. Louis, MO) was added to cells and incubated for 72 h. Cell proliferation was measured using the CellTiter 96 AQ proliferation assay according to the manufacturer's instructions (Promega, Madison, WI). Viable cells were counted in triplicate using a hemacytometer and trypan blue staining.

*Plasmids and small interfering RNAs (siRNAs)*

The full-length human Mcl-1 promoter region cloned into a firefly luciferase reporter vector pGL3-Basic (Promega, Madison, WI) was kindly provided by Dr. Steven W. Edwards (University of Liverpool, Liverpool, UK) [24]. The hypoxia-responsive element (HRE) (fragment -900 to -884)-truncated construct was obtained by digestion of the full-length promoter using KpnI (from position -3914 to -855) and then ligated using T4 DNA ligase (New England Biolabs, Ipswich, MA). Both plasmid constructs were confirmed by sequence analysis. The pHIF1-luc reporter was purchased from Panomics (Fremont, CA). TOPFlash and FOPFlash T-cell factor (TCF) reporters were obtained from Upstate (Billerica, MA). pTK-RL plasmid was purchased from Promega. Human Mcl-1 expression vector (pCMV-Mcl-1) was obtained from Origene, Inc. Human β-catenin expression plasmid was provided by Dr. Zhi-Ren Liu. ON-TARGET*plus* SMARTpool siRNAs against β-catenin, p68, PDGFR-α and PDGFR-β, and control siRNA were obtained from Dharmacon, Inc (Chicago, IL). HIF-1α and control siRNA were purchased from Santa Cruz Biotechnology, Inc. (Santa Cruz, CA). Transient transfection of DNA constructs and siRNAs was performed using Lipofectamine 2000 or Oligofectamine reagents (Invitrogen), according to the manufacturer's protocols and our published procedures [21,25].

*Western Blot Analysis*

Total cell lysates were prepared using radioimmunoprecipitation (RIPA) buffer (Santa Cruz Biotechnology, Inc.). Nuclear proteins were extracted using a Novagen kit (EMD Biosciences, San Diego, CA). Immunoblotting analysis followed standard procedures [25]. Information for the antibodies used in this study was described in Supplemental Table S1.

*Immunoprecipitation*

The Immunoprecipitation Starter Pack (GE Healthcare Bio-Sciences Corp., Piscataway, NJ) was used according to the manufacturer's instructions. Total nuclear lysates (1 mg) were immunoprecipitated with 5 µg rabbit anti-HIF-1α antibody, mouse anti-β-catenin antibody, mouse anti-c-Abl and rabbit anti-p68 antibody (Supplemental Information, Table S1), or normal IgG (R&D Systems). Protein A/G Sepharose 4 Fast Flow beads were added to precipitate proteins, then washed and eluted. The samples were further processed for Western blot analysis.

*Immunofluorescence and Confocal Imaging*

Immunofluorescence was performed as described previously [21] using mouse anti-β-catenin, rabbit anti-p68 and anti-HIF-1α antibodies (Supplemental Table S1). Cells were imaged on a Zeiss LSM 510 META. In all cases, either a 63x or 100x Zeiss Plan-Apo oil objective was used (numerical aperture of 1.3 and 1.4, respectively). All images had contrast expansion performed in Adobe Photoshop.

*Reverse Transcription-PCR (RT-PCR)*

Total RNA was prepared with Qiagen RNeasy Kit (Qiagen, Valencia, CA). The first-strand cDNA was synthesized using SuperScript ®III One-Step RT-PCR System (Invitrogen). The specific PCR primer pairs were described in Supplemental Table S2. Glyceraldehyde-3-phosphate dehydrogenase (GAPDH) mRNA was amplified to normalize RNA inputs [25].

*Chromatin Immunoprecipitation Assay (ChIP)*

6

The ChIP assay was performed using a ChIP-IT kit (ActiveMotif, Carlsbad, CA). Briefly, PCa cells were serum-starved overnight and replaced with fresh serum-free medium, incubated with PDGF-BB or PBS for indicated times. Chromatin was sheared by enzymatic shearing for 8 min. A portion of chromatin was reversed and used as input DNA. For immunoprecipitation, 2 μg HIF-1μ antibody (Millipore) was used. PCR primers for the HRE region in human Mcl-1 promoter were described in the Supplemental Table S2. PCRs were performed for 40 cycles, with primer concentration as 10 pmol/20 μl.

*Statistical Analysis*

All data represent three or more experiments. Errors are S.E. values of averaged results, and values of $p \leq 0.05$ were taken as a significant difference between means.

**Results**

*Mcl-1 is a survival factor in PCa cells*

Previously we demonstrated that Mcl-1 overexpression is associated with *in vivo* bone metastatic propensity of human PCa cells, and importantly, correlated with clinical PCa bone metastasis [21]. Consistently, using a human PCa ARCaP progression model that closely mimics the pathophysiology of bone metastasis [22], we found that Mcl-1 expression was significantly increased in highly bone metastatic ARCaP$_M$ cells when compared to that in the low-invasive counterpart ARCaP$_E$ cells (Figure 1A). We hypothesized that upregulation of Mcl-1 may confer metastatic PCa cells survival advantages, allowing them to escape apoptotic fate during invasion and dissemination and successfully establish distant metastasis [20]. Supporting this notion, ectopic expression of Mcl-1 enhanced PCa cell resistance to docetaxel (Figure 1B), a commonly used chemotherapeutic drug in hormone-refractory and metastatic PCa [26]. These results

7

indicated that upregulation of Mcl-1 may account for, at least in part, resistance to apoptosis in metastatic PCa cells.

*PDGF-BB induces Mcl-1 expression and antagonizes apoptosis in PCa cells*

Intriguingly, PDGF-BB was found to significantly induce Mcl-1 expression in PCa cells (Figure 1C, Supplemental Figure S1). Treatment with recombinant human PDGF-BB increased Mcl-1 mRNA in a dose- and time-dependent manner, though the optimal conditions for the maximum accumulation of Mcl-1 mRNA varied in different PCa cell lines. Western blot analysis confirmed the inductive effects of PDGF-BB on Mcl-1 expression at protein level. These data identified PDGF-BB as a novel regulator of Mcl-1 expression, which could provide a survival mechanism to protect PCa cells from apoptosis. Indeed, addition of PDGF-BB in PCa cell cultures effectively antagonized the cytotoxicity of docetaxel (Figure 1D).

*Expression profile of PDGF autocrine signaling components in PCa cells*

We examined the expression pattern of PDGFs and their receptors in PCa cells (Figure 2A). RT-PCR analyses showed that the PDGF isoforms were differentially expressed at mRNA level, and among them, increased PDGF-B and PDGF-D were observed in C4-2 and ARCaP$_M$ cells when compared to the parental LNCaP and ARCaP$_E$ cells, respectively. Consistent with previous studies [19], PC3 cells were found to express high levels of PDGF-D, PDGFR-α and -β. Interestingly, PDGFR-α mRNAs appeared to be substantially expressed in PCa cells, which was confirmed at protein level by Western blot analysis. In contrary, though PDGFR-β mRNAs were detected by RT-PCR in most PCa cell lines, immunoblotting analysis could only confirm protein expression in ARCaP$_E$ and ARCaP$_M$ cells (Figure 2A, right panel). Taken together, these data suggested a functional PDGF autocrine signaling in certain PCa cells.

*An autocrine PDGFR signaling mediates PDGF-BB regulation of Mcl-1 in PCa cells*

Both PDGFR-α and -β were highly expressed in bone metastatic ARCaP$_M$ cells, and rapidly phosphorylated in a time-dependent manner in response to the stimulation of exogenous PDGF-BB (Figure 2B). Interesting, depletion of either PDGFR-α or -β by isoform-specific siRNA did not block the inductive effect of PDGF-BB on Mcl-1 expression (Figure 2C, left and central panels), suggesting that activation of either receptors may be sufficient for the upregulation of Mcl-1. Supporting this hypothesis, transient transfection with a mixture of siRNAs targeting both PDGFR-α and -β inhibited the basal expression of Mcl-1, and abrogated PDGF-BB induction of Mcl-1 ARCaP$_M$ cells (Figure 2C, right panel). Alternatively, treatment with AG-17 (Tyrphostin), a selective pharmacological inhibitor of PDGFRs [27], reduced Mcl-1 expression at both mRNA and protein levels and markably increased cleavage of poly-ADP ribose polymerase (PARP), an indicator of apoptosis. These effects were attenuated by the presence of PDGF-BB in cultures (Figure 2D). Consistently, AG-17 treatment at low doses (such as 100 nM) effectively induced apoptosis in ARCaP$_E$ and ARCaP$_M$ cells (Figure 2E), indicating a pivotal role of PDGFR signaling in the survival of PCa cells.

*β-catenin mediates PDGF regulation of Mcl-1 expression in PCa cells*

Activation of the β-catenin pathway is a downstream event of PDGF signaling in certain epithelial cancer cells [7,8,28]. Western blot analysis found that β-catenin and TCF4, a major β-catenin-interacting transcription factor [29], were differentially expressed in PCa cells (Figure 3A), suggesting a functional β-catenin-TCF4 signaling in these cells. In fact, an artificial TCF promoter was activated in both the LNCaP-C4-2 and ARCaP$_E$-ARCaP$_M$ cell lineages, and the reporter activities appeared to be associated with increased *in vivo* metastatic potential in C4-2 and ARCaP$_M$ cells (Figure 3B). It is worth noting that both β-catenin and TCF4 were substantially presented in the nucleus of ARCaP$_E$ and ARCaP$_M$ cells (Figure 3A, low panel),

9

which exhibited markedly higher basal TCF activities than either LNCaP or C4-2 cells (by ~100-fold) (Figure 3B).

Upon PDGF-BB treatment, the nuclear presence of β-catenin was rapidly increased in ARCaP$_M$ cells (Figure 3C, upper panel). Consistently, TCF reporter activity was also significantly increased following PDGF-BB stimulation, which was attenuated by the pre-treatment with AG-17 (Figure 3C, bottom panel). These data indicated that PDGF-BB activated β-catenin signaling in a PDGFR-dependent manner.

To investigate the role of β-catenin in the regulation of Mcl-1 expression, ARCaP$_M$ cells were transiently transfected with a construct expressing wild-type β-catenin. RT-PCR and Western blot analyses showed that ectopic epression of β-catenin increseased Mcl-1 at both mRNA and protein levels (Figure 3D). In contrary, β-catenin depletion using a siRNA pool efficiently inhibited both the basal expression of Mcl-1 and its induction by PDGF-BB (Figure 3E). Consistently, whereas PDGF-BB significantly induced the luciferase activity of a full-length human Mcl-1 promoter in ARCaP$_M$ cells transfected with non-targeting control siRNAs, this effect was abrogated by transient depletion of endogeneous β-catenin (Figure 3F). These results suggested that activation of β-catenin signaling may be sufficient and required for Mcl-1 expression in PCa cells.

*PDGF activates p68-β-catenin signaling in PCa cells*

We investigated whether a c-Abl-p68-dependent pathway is involved in the PDGF activation of β-catenin signaling in PCa cells [7]. Western blot analyses found that c-Abl and p68 were differentially expressed in PCa cells (Figure 4A). Upon PDGF-BB treatment, tyrosine phosphorylation of c-Abl and p68 were rapidly activated, as evidenced by immunoprecipitation-immunoblotting assays (Figure 4B). Importantly, the presence of β-catenin in p68

immunoprecipitates was also increased in a time-dependent manner, suggesting an enhanced

physical association between β-catenin and p68 proteins. In fact, PDGF-BB induced rapid

nuclear translocation of p68 within 30 min (Figure 4C), which was associated with increased co-

localization of p68 and β-catenin in the nucleus (Figure 4D). These data indicated that PDGF-BB

could activate the c-Abl-p68 cascade and subsequent β-catenin signaling in PCa cells.

To examine whether p68 is required for the regulation of Mcl-1 expression, ARCaP$_M$ cells

were transfected with p68 siRNA or control siRNA, and analyzed for the expression of Mcl-1.

As shown in Figure 4E, depletion of p68 inhibited endogeneous β-catenin and effectively

attenuated PDGF-BB induction of Mcl-1 protein. Consistently, Mcl-1 promoter activity was

significantly inhibited by the treatment with p68 siRNA in ARCaP$_M$ cells, either with or without

the presence of PDGF-BB in the cultures (Figure 3F). These data indicated an indispensible

function of p68 in the regulation of Mcl-1 in PCa cells.

*PDGF-BB promotes protein interaction between β-catenin and HIF-1α in PCa cells*

Our previous studies demonstrated an important role of HIF-1α in bone metastatic PCa cells

[25]. Interestingly, transfection of a HIF-1α-specific siRNA significantly reduced Mcl-1 protein

expression in ARCaP$_M$ cells (Figure 5A), suggesting that HIF-1α may be required for Mcl-1

regulation in PCa cells. To examine whether PDGF-BB could induce physical interaction

between HIF-1α and β-catenin, nuclear proteins were prepared from ARCaP$_M$ cells treated with

PDGF-BB for varying times. Western blot analysis found that both HIF-1α and β-catenin were

rapidly increased in the nucleus (Figure 5B). A co-immunoprecipitation assay showed that in

response to PDGF-BB stimulation, nuclear presence of β-catenin rapidly increased in the HIF-1α

immunoprecipitates (Figure 5C, upper panel). Reciprocal co-immunoprecipitation with an anti-β-

catenin antibody confirmed an increased association of nuclear HIF-1α with β-catenin following

PDGF-BB treatment (Figure 5C, bottom panel). The enhanced co-localization of β-catenin and HIF-1α proteins was further demonstrated by confocal microscopy, which appeared to acheive the maximum intensity at 30 min upon PDGF-BB stimulation (Figure 5D) . These results indicated that in repsonse to PDGF-BB stimulation, β-catenin physically interacts with HIF-1α in the nucleus, which may lead to the activation of Mcl-1 transcription in PCa cells.

*A putative HRE motif is required for PDGF-BB activation of Mcl-1 promoter*

HIF-1α binds to the HRE *cis*-elements within the promoters of hypoxia-responsive genes and regulates their expression [30]. We examined whether PDGF-BB-induced nuclear accumulation of HIF-1α was associated with the activation of HRE-dependent transcription. In ARCaP$_M$ cells, PDGF-BB treatment significantly increased luciferase expression driven by an artificial HRE promoter (pHIF-luc) (Figure 6A). Interestingly, a putative HRE motif was identified within human Mcl-1 promoter region, which is located between -900 and -884 nucleotides at the 5'-upstream of transcription start site [24]. To investigate the potential role of this *cis*-element in PDGF regulation of Mcl-1 transcription, we characterized a deletion mutant of the putative HRE motif using human Mcl-1 promoter region as the template (Figure 6B). The resulting reporter construct (p-Mcl-1-Luc: ΔHRE), or the luciferase reporter driven by the full-length Mcl-1 promoter (p-Mcl-1-Luc), was transiently expressed in ARCaP$_M$ cells respectively, and treated with PDGF-BB or PBS. IL-6, which has been shown to activate Mcl-1 transcription in PCa and cholangiocarcinoma cells through a signal transducer and activator of transcription 3 (Stat3)-dependent mechanism [31,32], was included as the positive control. Luciferase activity assay showed that PDGF-BB induced the activation of p-Mcl-1-Luc promoter to a greater degree than IL-6 in ARCaP$_M$ cells. Significantly, deletion of the HRE motif not only reduced the basal activity of Mcl-1 promoter, but also abrogated the inductive effects of PDGF-BB on reporter

12

activity. In contrary, p-Mcl-1-Luc: ΔHRE, containing a Stat3-binding sequence at position between -92 and -83 [31], remained activated upon IL-6 treatment (Figure 6C). A similar effect of HRE deletion on the differential response of Mcl-1 promoter to PDGF-BB and IL-6 was also observed in C4-2 cells (Supplemental Figure S2). These data indicated that the putative HRE *cis*-element is required for PDGF-BB activation of Mcl-1 expression in PCa cells.

*PDGF-BB promotes HIF-α binding to Mcl-1 promoter region*

We investigated whether PDGF-BB promoted specific binding of HIF-1α to Mcl-1promoter by ChIP assay. Fractionated chromatin from controls and PDGF-BB-treated ARCaP$_M$ cells was immunoprecipitated with HIF-1α antibody or control IgG. From the isolated DNA, a 151-bp region was amplified by PCR. Upon PDGF-BB stimulation, a considerable increase in HIF-1α binding with the HRE region in was observed (Figure 6D), demonstrating that PDGF-BB could facilitate association of HIF-1α with Mcl-1 promoter, thereby activating its expression.

**Discussion**

In this study, we uncovered the PDGF-Mcl-1 signaling as a crucial survival mechanism in PCa cells (Figure 7). For the first time, we demonstrated that: 1) PDGF-BB is a novel regulator of Mcl-1 expression; 2) PDGF-BB activation of autocrine PDGFR signaling promotes the interaction between β-catenin and HIF-1α, presumably through a c-Abl-p68-dependent mechanism; 3) a putative HRE motif is required for the basal expression and PDGF-BB activation of Mcl-1 promoter; and 4) inhibition of the PDGFR-Mcl-1 signaling using a small-molecule inhibitor AG-17 could activate apoptotic response in metastatic PCa cells. These results support that targeting PDGF-Mcl-1 pathway may provide a novel strategy for treating PCa metastasis.

13

Activation of PDGFR signaling may be coupled with multiple downstream pathways in the regulation of cell growth, proliferation, migration and survival [3]. In tumor-associated endothelial and fibroblast stromal cells, PDGF has been shown to activate Akt- and MAPK-dependent survival mechanisms [33,34,35,36]. Yet, it remains elusive on the molecular mechanism by which PDGF exerts its functions in epithelial cancer cells. Recent data have linked autocrine PDGF signaling to the activation of β-catenin pathway. For instance, PDGF-AB was found to induce nuclear β-catenin accumulation via a PI3K-dependent mechanism, thereby protecting hepatocellular carcinoma cells from anoikis during metastatic dissemination [8]. In human colon cancer cells, PDGF-BB induces EMT [7] and upregulates cyclin D1 and c-Myc [37] by activating β-catenin-dependent gene expression. In both cases, PDGF-BB induces the phosphorylation of c-Abl kinase, which subsequently recruits p68, an RNA helicase with ATPase activity, and activates its phosphorylation. Phosphorylated p68 binds β-catenin and promotes its nuclear translocation by displacing Axin from β-catenin and blocking β-catenin degradation, eventually  promoting the interaction of β-catenin with TCF/LEF and the assembly of transcription complexes [7]. In this study, we provided molecular evidence demonstrating that in PCa cells that express high basal levels of p68 and β-catenin, PDGF could significantly promote physical interaction and rapid nuclear translocation of p68 and β-catenin. Importantly, p68 depletion in PCa cells led to the inhibition of Mcl-1 expression and induction of apoptosis, as evidenced by the appearance of cleaved PARP (Supplemental Figure S3). These results, for the first time, underscored a critical role of p68 in the regulation of PCa cell survival. Interestingly, a recent study demonstrated that p68 is actually a novel coactivator of androgen receptor (AR) [38], another transcription factor interacting with β-catenin in certain PCa cells (such as LNCaP and C4-2) [39]. It would be intriguing to further investigate the dynamic

14

interaction between p68, β-catenin and p68, and its biological consequences in these cells. In addition, other pathways may be involved in the PDGF activation of β-catenin signaling. For example, PDGF-BB treatment was found to induce rapid phosphorylation of both Akt and glycogen synthase kinase 3-β (GSK-3β) (Supplemental Figure S4), which may also contribute to the elevated intracellular levels and nuclear accumulation of β-catenin [40].

Our data confirmed a highly active β-catenin/TCF signaling in ARCaP cells and correlated the TCF reporter activity with the *in vivo* metastatic potential (Figure 3A, 3B), indicating these cells could be used as an excellent model system for investigating β-catenin signaling in PCa progression [41]. Though PDGF-BB activated the full-length human Mcl-1 promoter (Figure 3F) in a similar manner to its effect on the luciferase expression driven by an artificial TCF-binding motif (pTOPFlash), it appeared that human Mcl-1 promoter does not contain any consensus sequences of TCF/ lymphoid enhancer-binding factor (LEF). These results suggested that certain transcription factor(s), other than TCF, could be responsible for β-catenin activation of Mcl-1 transcription. One of such candidates was cAMP-response element-binding protein (CREB), which has been implicated in the regulation of Mcl-1 expression through the PI-3K/Akt signaling pathway [42] and highly expressed in ARCaP cell lineage [25]. Western blotting analyses, however, could not detect a significant increase in nuclear CREB expression upon PDGF treatment (data not shown), suggesting that CREB may not be involved in the β-catenin-dependent activation of Mcl-1 transcription. Intriguingly, the transcription factor HIF-1α was found to be rapidly increased in the nucleus and physically interact with β-catenin following PDGF-BB stimulation, which may mediate Mcl-1 transcription by binding to HRE site(s) within the promoter. These data are consistent with a previous study showing that β-catenin can switch its binding partner from TCF4 to HIF-1α and enhance HIF-1α-mediated transcription, and this

15

dynamic reassembly of β-catenin with HIF-1α may allow colorectal cancer cells to rapidly adapt

to hypoxic stress and survive [43]. It is important to note that unlike the cited work, our studies

were performed in normoxic PCa cell cultures. Since ARCaP cells substantially express HIF-1α

even under normoxia [25], PDGF may significantly affect the expression of hypoxia-responsive

or HRE-containing genes by promoting the interaction between β-catenin and HIF-1α in a Wnt-

independent mechanism. Upregulation of Mcl-1, as a consequence, could provide pivotal

protection against apoptotic signals during dissemination and colonization when the majority of

cancer cells remain under normoxia.

Earlier studies reported high expression of PDGFRs in both localized and metastatic PCa,

which could be detected in 88% of primary tumors and 80% of the metastases [10,44]. However,

it remains controversial as to which PDGFR isoforms are expressed in PCa cells and primarily

responsible for autocrine PDGF signaling [12,45,46]. These conflicting results may partially

arise from the potential non-specificity of antibodies used in the cited studies, but more

importantly, may reflect the intrinsic heterogeneity of human cancers, especially when at their

late-stages. In this study, we were able to detect the expression of both PDGFR isoforms in

several established PCa cell lines by RT-PCR and Western blot analyses. Given the fact that both

PDGFR-α and -β have been implicated in the progression of bone metastatic PCa

[10,12,13,44,47], our study focused on the function of PDGF-BB since it is the only PDGF

isoform that binds all the three receptor dimeric combinations (PDGFR-αα, -ββ and -αβ) with

high affinity [2,48]. To determine which PDGFR isoform is required for PDGF regulation of

Mcl-1, we transfected PCa cells with specific siRNAs against PDGFR-α or -β. Interestingly, the

single depletion of neither PDGFR-α nor PDGFR-β inhibited Mcl-1 expression in ARCaP$_M$ cells,

suggesting that the PDGF-BB signal could be transduced via the two independent but

16

complementary receptors to activate Mcl-1 expression in PCa cells expressing both isoforms.

Supporting this notion, dual depletion of both receptors simultaneously using a mixture of

siRNAs against PDGFR-α and -β effectively inhibited Mcl-1 expression. Alternatively, treatment

with AG-17 or imatinib, two pan-PDGFR inhibitors that could inhibit the tyrosine kinase activity

of both PDGFR-α and -β, also reduced Mcl-1 levels in ARCaP$_M$ cells (Supplemental Figure S5).

Furthermore, in PCa cells that predominantly express one PDGFR isoform (for example,

PDGFR-α is the major isoform in C4-2 cells; Figure 2A, right panel), it is plausible to expect that

inhibition of the isoform alone could affect Mcl-1 expression. Indeed, transfection of PDGFR-α

siRNA in C4-2 cells significantly inhibited Mcl-1 (Supplemental Figure S6). These findings

support a model that PDGF-BB could activate both PDGFR isoforms in the regulation of Mcl-1

in PCa cells in a context-dependent manner, which may have important implication in the

evaluation of PDGFR expression at tissue levels in clinical PCa specimens.

Interaction between PCa and bone microenvironment is crucial to the bone tropism of PCa

metastasis, which is identified at autopsy in up to 90% of patients dying from the disease [49].

Tumor-initiated bone resorption promotes the release and activation of multiple growth factors

immobilized in bone matrix, including PDGF. These locally expressed and tumor-derived PDGF

could activate PDGFR signaling in surrounding stroma (including stromal cells, endothelial cells

and pericytes) and promote angiogenesis. As a potent mitogen for osteoblasts, PDGF also

significantly contribute to the osteoblastic phenotype of PCa bone metastasis [50]. These effects,

taken together, may provide a favorable microenvironment for the survival and outgrowth of

bone metastatic PCa.  These facts provided rationale for evaluating the potential of treating PCa

bone metastasis with small-molecule PDGFR inhibitors. In earlier studies, imatinib sensitized

bone marrow stromal and endothelial cells to paclitaxel treatment and significantly suppressed

17

PCa bone metastasis in experimental models [51,52]. Disappointingly, however, recent clinical trials with imatinib only achieved limited success due to unexpected severe side effects in patients [47]. These observations highlighted the importance of a better understanding of PDGF signaling in bone metastasis PCa. Our study delineated a novel signaling axis that may allow PCa cells to escape apoptosis during dissemination and colonization by activating PDGF-Mcl-1 pathway in metastatic cancer cells. It is plausible to hypothesize that PDGF-BB may be crucial in mediating the "vicious cycle" between tumor and bone microenvironment, not only promoting angiogenesis in surrounding stroma but also sustaining survival in PCa cells (Figure 7). Supporting this model, PDGF-BB was found to be elevated in PC3-MM2 cells implanted in the mouse bone cortex, and interestingly, activated PDGFR-β was only detected in tumor lesions growing adjacent to bone and the tumor-associated endothelium [52,53]. Given the clinical significance of both PDGF and Mcl-1 in PCa bone metastasis [21,50], specific targeting of PDGF-Mcl-1 survival pathway in PCa cells (autocrine signaling) and co-targeting of microenvironment (paracrine signaling) could provide a new strategy to disrupt the vicious cycle and efficaciously treat metastatic PCa.

**Acknowledgements**

**Supporting Information**

Supporting Information includes six Supplemental Figures and two Supplemental Tables.

18

**Figure Legends**

**Fig. 1. PDGF-BB upregulates Mcl-1 and protects PCa cells from apoptosis.** (A) Mcl-1

protein expression in the lineage-related ARCaP$_E$ and ARCaP$_M$ cells. (B) Ectopic expression of

Mcl-1 in ARCaP$_M$ cells and the effects on docetaxel cytotoxicity in ARCaP$_M$ cells. pCMV:

vector control. (C) Upper and middle panels: The dose- and time-dependent effects of PDGF-BB

on Mcl-1mRNA expression in ARCaP$_M$ cells; bottom panel: The effects of PDGF-BB treatment

(20ng/ml, 72 h) on Mcl-1 protein expression in ARCaP$_M$ cells. (D) The effects of exogenous

PDGF-BB on the cytotoxicity of docetaxel in ARCaP$_M$ cells, as determined by the MTS assay.


**Fig. 2. Activation of the PDGFR signaling is required for Mcl-1 expression in PCa cells.** (A)

Expression profile of PDGFR signaling components in PCa cells, as analyzed by RT-PCR and

Western blotting. (B) The effects of PDGF-BB (20 ng/ml) on the phosphorylation of PDGFR-α

and -β in ARCaP$_M$ cells. (C) The effects of depleting PDGFR-α or/and -β on Mcl-1 protein

expression in ARCaP$_M$ cells. The cells were transfected with either isotype-specific siRNAs

targeting PDGFR-α (left panel, 30 nM) or PDGFR- β (central panel, 100 nM), or a mixture of

PDGFR-α and -β siRNAs (right panel) for 48 h, serum-starved overnight, and incubated in the

presence or absence of PDGF-BB (20 ng/ml) for 72 h. (D) Upper panel: The time-dependent

effects of AG-17 (100 nM) on Mcl-1 mRNA expression in ARCaP$_M$ cells; bottom panel: The

effects of AG-17 treatment on the expression of Mcl-1 and cleaved PARP in the presence (20

ng/ml) or absence of PDGF-BB (20 ng/ml) in ARCaP$_M$ cells. (E) The effects of AG-17 treatment

(100 nM, 72 h) on the viability of ARCaP$_E$ and ARCaP$_M$ cells.

19

**Fig. 3. β-catenin mediates PDGF regulation of Mcl-1 expression in PCa cells.** (A) Expression

profile of β-catenin-TCF signaling components in PCa cells. (B) TCF reporter activity in the

LNCaP-C4-2 and ARCaP$_E$-ARCaP$_M$ cells. (C) Upper panel: The effects of PDGF-BB (20 ng/ml)

on the nuclear translocation of β-catenin in ARCaP$_M$ cells; Bottom panel: The effects of PDGF-

BB (20 ng/ml) on TCF reporter activity in the presence (100 nM) or absence of AG-17. (D) The

effects of ectopic expression of β-catenin (72 h) on Mcl-1 expression at both mRNA and protein

levels. (E) The effects of β-catenin depletion on PDGF-BB regulation of Mcl-1 expression in

ARCaP$_M$ cells. The cells were transfected with β-catenin siRNA or control siRNA (30 nM) for

48 h, serum-starved overnight, and incubated in the presence or absence of PDGF-BB (20 ng/ml)

for 72 h. (F) The effects of β-catenin depletion on Mcl-1 reporter activity in ARCaP$_M$ cells. The

cells were transfected with β-catenin or control siRNA (30 nM) for 48 h, and further transfected

with a human Mcl-1 reporter for 24 h. Following serum starvation overnight, the cells were

incubated in the presence or absence of PDGF-BB (20 ng/ml) for 48 h.


**Fig. 4. PDGF-BB activates the c-Abl-p68-β-catenin signaling cascade in PCa cells.** (A)

Expression of c-Abl and p68 in PCa cells. (B) The effects of PDGF-BB (20 ng/ml) on the

phosphorylation of c-Abl and p68, and the expression of β-catenin in the p68 immunoprecipitates

in ARCaP$_M$ cells. (C) The effects of PDGF-BB (20 ng/ml) on the nuclear translocation of p68 in

ARCaP$_M$ cells. (D) Confocal microscopy analysis of the effects of PDGF-BB on the co-

localization of β-catenin and p68 in the nucleus in a time course experiment in ARCaP$_M$ cells. (E)

The effects of p68 depletion on PDGF regulation of Mcl-1 in ARCaP$_M$ cells. The cells were

transfected with p68 or control siRNA (30 nM) for 48 h, serum-starved overnight, and incubated

in the presence or absence of PDGF-BB (20 ng/ml) for 72 h. (F) The effects of p68 depletion on

20

Mcl-1 reporter activity in ARCaP$_M$ cells. The cells were transfected with p68 or control siRNA (30 nM) for 48 h, and further transfected with human Mcl-1 reporter for 24 h. Following serum starvation overnight, the cells were incubated in the presence or absence of PDGF-BB (20 ng/ml) for 48 h.

**Fig. 5. PDGF-BB promotes protein interaction between β-catenin and HIF-1α in PCa cells.** (A) The effects of HIF-1α depletion on Mcl-1 expression in ARCaP$_M$ cells. The cells were transfected with HIF-1α or control siRNA (30 nM) for 72 h, and analyzed for Mcl-1 expression by immunoblotting. (B) Western blot analysis of the effects of PDGF-BB (20 ng/ml) on the nuclear translocation of β-catenin and HIF-1α in ARCaP$_M$ cells. (C) Co-immunoprecipitation assays of the effects of PDGF-BB (20 ng/ml) on the interaction between β-catenin and HIF-1α in the nucleus in ARCaP$_M$ cells. (D) Confocal microscopy of the effects of PDGF-BB (20 ng/ml) on the co-localization of β-catenin and HIF-1α in the nucleus in ARCaP$_M$ cells.

**Fig. 6. A putative HRE site is required for PDGF-BB activation of Mcl-1 promoter.** (A) The effects of PDGF-BB on the HIF-1 reporter activity in ARCaP$_M$ cells. The cells were transiently transfected with HIF-1 reporter or pGL3 for 24 h, serum-starved and incubated in the presence or absence of PDGF-BB (20 ng/ml) for 48 h. (B) Schematic diagram of human Mcl-1 promoter and its deletion mutation at the putative HRE site. (C) The effects of deleting the putative HRE site on PDGF regulation of Mcl-1 promoter activity in ARCaP$_M$ cells. IL-6 (200 ng/ml) was included as the positive control. (D) ChIP assay of the effects of PDGF-BB treatment (20 ng/ml) on HIF-1α binding to human Mcl-1 promoter region in ARCaP$_M$ cells.

**Fig. 7. A proposed model for PDGF-BB regulation of Mcl-1 expression in PCa cells.** The engagement of PDGF-BB to PDGFR dimers activates the c-Abl-p68 cascade, which subsequently stablizes β-catenin and promotes its nuclear translocation. In the nucleus, interaction between β-catenin and HIF-1α increases the binding of HIF-1α to the HRE site within Mcl-1 promoter, thereby activating the transcription of Mcl-1 gene. Upregulation of Mcl-1 antagonizes apoptotic signals and confers survival advantages to metastatic PCa cells. Furthermore, tumor-derived and locally expressed PDGF may mediate the interactions between PCa and bone microenvironment. Co-targeting the PDGF signaling in PCa cells (autocrine) and microenvironment (paracrine) could provide a new strategy to disrupt the "vicious cycle" and efficaciously treat metastatic PCa.

## References

1. Heldin CH, Eriksson U, Ostman A (2002) New members of the platelet-derived growth factor family of mitogens. Arch Biochem Biophys 398: 284-290.

2. Pietras K, Sjoblom T, Rubin K, Heldin CH, Ostman A (2003) PDGF receptors as cancer drug targets. Cancer Cell 3: 439-443.

3. Andrae J, Gallini R, Betsholtz C (2008) Role of platelet-derived growth factors in physiology and medicine. Genes Dev 22: 1276-1312.

4. Kim L, Wong TW (1995) The cytoplasmic tyrosine kinase FER is associated with the catenin-like substrate pp120 and is activated by growth factors. Mol Cell Biol 15: 4553-4561.

5. Yokote K, Margolis B, Heldin CH, Claesson-Welsh L (1996) Grb7 is a downstream signaling component of platelet-derived growth factor alpha- and beta-receptors. J Biol Chem 271: 30942-30949.

6. Darnell JE, Jr. (1997) STATs and gene regulation. Science 277: 1630-1635.

7. Yang L, Lin C, Liu ZR (2006) P68 RNA helicase mediates PDGF-induced epithelial mesenchymal transition by displacing Axin from beta-catenin. Cell 127: 139-155.

8. Fischer AN, Fuchs E, Mikula M, Huber H, Beug H, et al. (2007) PDGF essentially links TGF-beta signaling to nuclear beta-catenin accumulation in hepatocellular carcinoma progression. Oncogene 26: 3395-3405.

9. Mathew P, Thall PF, Jones D, Perez C, Bucana C, et al. (2004) Platelet-derived growth factor receptor inhibitor imatinib mesylate and docetaxel: a modular phase I trial in androgen-independent prostate cancer. J Clin Oncol 22: 3323-3329.

10. Ko YJ, Small EJ, Kabbinavar F, Chachoua A, Taneja S, et al. (2001) A multi-institutional phase ii study of SU101, a platelet-derived growth factor receptor inhibitor, for patients with hormone-refractory prostate cancer. Clin Cancer Res 7: 800-805.

11. Hofer MD, Fecko A, Shen R, Setlur SR, Pienta KG, et al. (2004) Expression of the platelet-derived growth factor receptor in prostate cancer and treatment implications with tyrosine kinase inhibitors. Neoplasia 6: 503-512.

12. Fudge K, Wang CY, Stearns ME (1994) Immunohistochemistry analysis of platelet-derived growth factor A and B chains and platelet-derived growth factor alpha and beta receptor expression in benign prostatic hyperplasias and Gleason-graded human prostate adenocarcinomas. Mod Pathol 7: 549-554.

13. Singh D, Febbo PG, Ross K, Jackson DG, Manola J, et al. (2002) Gene expression correlates of clinical prostate cancer behavior. Cancer Cell 1: 203-209.

14. Pietras K, Pahler J, Bergers G, Hanahan D (2008) Functions of paracrine PDGF signaling in the proangiogenic tumor stroma revealed by pharmacological targeting. PLoS Med 5: e19.

15. Ostman A, Heldin CH (2007) PDGF receptors as targets in tumor treatment. Adv Cancer Res 97: 247-274.

16. Pietras K, Rubin K, Sjoblom T, Buchdunger E, Sjoquist M, et al. (2002) Inhibition of PDGF receptor signaling in tumor stroma enhances antitumor effect of chemotherapy. Cancer Res 62: 5476-5484.

17. Ostman A (2004) PDGF receptors-mediators of autocrine tumor growth and regulators of tumor vasculature and stroma. Cytokine Growth Factor Rev 15: 275-286.

18. Jechlinger M, Sommer A, Moriggl R, Seither P, Kraut N, et al. (2006) Autocrine PDGFR signaling promotes mammary cancer metastasis. J Clin Invest 116: 1561-1570.

19. Kong D, Wang Z, Sarkar SH, Li Y, Banerjee S, et al. (2008) Platelet-derived growth factor-D overexpression contributes to epithelial-mesenchymal transition of PC3 prostate cancer cells. Stem Cells 26: 1425-1435.

20. Mehlen P, Puisieux A (2006) Metastasis: a question of life or death. Nat Rev Cancer 6: 449-458.

21. Zhang S, Zhau HE, Osunkoya AO, Iqbal S, Yang X, et al. (2010) Vascular endothelial growth factor regulates myeloid cell leukemia-1 expression through neuropilin-1-dependent activation of c-MET signaling in human prostate cancer cells. Mol Cancer 9: 9.

22. Zhau HE, Odero-Marah V, Lue HW, Nomura T, Wang R, et al. (2008) Epithelial to mesenchymal transition (EMT) in human prostate cancer: lessons learned from ARCaP model. Clin Exp Metastasis 25: 601-610.

23. Wu TT, Sikes RA, Cui Q, Thalmann GN, Kao C, et al. (1998) Establishing human prostate cancer cell xenografts in bone: induction of osteoblastic reaction by prostate-specific

antigen-producing tumors in athymic and SCID/bg mice using LNCaP and lineage-derived metastatic sublines. Int J Cancer 77: 887-894.

24. Akgul C, Turner PC, White MR, Edwards SW (2000) Functional analysis of the human MCL-1 gene. Cell Mol Life Sci 57: 684-691.

25. Wu D, Zhau HE, Huang WC, Iqbal S, Habib FK, et al. (2007) cAMP-responsive element-binding protein regulates vascular endothelial growth factor expression: implication in human prostate cancer bone metastasis. Oncogene 26: 5070-5077.

26. Pienta KJ, Smith DC (2005) Advances in prostate cancer chemotherapy: a new era begins. CA Cancer J Clin 55: 300-318; quiz 323-305.

27. Gazit A, Yaish P, Gilon C, Levitzki A (1989) Tyrphostins I: synthesis and biological activity of protein tyrosine kinase inhibitors. J Med Chem 32: 2344-2352.

28. Singh PK, Wen Y, Swanson BJ, Shanmugam K, Kazlauskas A, et al. (2007) Platelet-derived growth factor receptor beta-mediated phosphorylation of MUC1 enhances invasiveness in pancreatic adenocarcinoma cells. Cancer Res 67: 5201-5210.

29. Clevers H (2004) Wnt breakers in colon cancer. Cancer Cell 5: 5-6.

30. Wenger RH, Stiehl DP, Camenisch G (2005) Integration of oxygen signaling at the consensus HRE. Sci STKE 2005: re12.

31. Isomoto H, Kobayashi S, Werneburg NW, Bronk SF, Guicciardi ME, et al. (2005) Interleukin 6 upregulates myeloid cell leukemia-1 expression through a STAT3 pathway in cholangiocarcinoma cells. Hepatology 42: 1329-1338.

32. Cavarretta IT, Neuwirt H, Untergasser G, Moser PL, Zaki MH, et al. (2007) The antiapoptotic effect of IL-6 autocrine loop in a cellular model of advanced prostate cancer is mediated by Mcl-1. Oncogene 26: 2822-2832.

33. Langley RR, Fan D, Tsan RZ, Rebhun R, He J, et al. (2004) Activation of the platelet-derived growth factor-receptor enhances survival of murine bone endothelial cells. Cancer Res 64: 3727-3730.

34. Kitadai Y, Sasaki T, Kuwai T, Nakamura T, Bucana CD, et al. (2006) Expression of activated platelet-derived growth factor receptor in stromal cells of human colon carcinomas is associated with metastatic potential. Int J Cancer 119: 2567-2574.

35. Kodama M, Kitadai Y, Sumida T, Ohnishi M, Ohara E, et al. (2010) Expression of platelet-derived growth factor (PDGF)-B and PDGF-receptor beta is associated with lymphatic metastasis in human gastric carcinoma. Cancer Sci 101: 1984-1989.

36. Song N, Huang Y, Shi H, Yuan S, Ding Y, et al. (2009) Overexpression of platelet-derived growth factor-BB increases tumor pericyte content via stromal-derived factor-1alpha/CXCR4 axis. Cancer Res 69: 6057-6064.

37. Yang L, Lin C, Zhao S, Wang H, Liu ZR (2007) Phosphorylation of p68 RNA helicase plays a role in platelet-derived growth factor-induced cell proliferation by up-regulating cyclin D1 and c-Myc expression. J Biol Chem 282: 16811-16819.

38. Clark EL, Coulson A, Dalgliesh C, Rajan P, Nicol SM, et al. (2008) The RNA helicase p68 is a novel androgen receptor coactivator involved in splicing and is overexpressed in prostate cancer. Cancer Res 68: 7938-7946.

39. Truica CI, Byers S, Gelmann EP (2000) Beta-catenin affects androgen receptor transcriptional activity and ligand specificity. Cancer Res 60: 4709-4713.

40. Doble BW, Woodgett JR (2003) GSK-3: tricks of the trade for a multi-tasking kinase. J Cell Sci 116: 1175-1186.

41. Chesire DR, Ewing CM, Gage WR, Isaacs WB (2002) In vitro evidence for complex modes of nuclear beta-catenin signaling during prostate growth and tumorigenesis. Oncogene 21: 2679-2694.

42. Wang JM, Chao JR, Chen W, Kuo ML, Yen JJ, et al. (1999) The antiapoptotic gene mcl-1 is up-regulated by the phosphatidylinositol 3-kinase/Akt signaling pathway through a transcription factor complex containing CREB. Mol Cell Biol 19: 6195-6206.

43. Kaidi A, Williams AC, Paraskeva C (2007) Interaction between beta-catenin and HIF-1 promotes cellular adaptation to hypoxia. Nat Cell Biol 9: 210-217.

44. Chott A, Sun Z, Morganstern D, Pan J, Li T, et al. (1999) Tyrosine kinases expressed in vivo by human prostate cancer bone marrow metastases and loss of the type 1 insulin-like growth factor receptor. Am J Pathol 155: 1271-1279.

45. George DJ (2002) Receptor tyrosine kinases as rational targets for prostate cancer treatment: platelet-derived growth factor receptor and imatinib mesylate. Urology 60: 115-121; discussion 122.

46. Paulsson J, Sjoblom T, Micke P, Ponten F, Landberg G, et al. (2009) Prognostic significance of stromal platelet-derived growth factor beta-receptor expression in human breast cancer. Am J Pathol 175: 334-341.

47. Mathew P, Thall PF, Bucana CD, Oh WK, Morris MJ, et al. (2007) Platelet-derived growth factor receptor inhibition and chemotherapy for castration-resistant prostate cancer with bone metastases. Clin Cancer Res 13: 5816-5824.

48. Williams LT (1989) Signal transduction by the platelet-derived growth factor receptor. Science 243: 1564-1570.

49. Rana A, Chisholm GD, Khan M, Sekharjit SS, Merrick MV, et al. (1993) Patterns of bone metastasis and their prognostic significance in patients with carcinoma of the prostate. Br J Urol 72: 933-936.

50. Roodman GD (2004) Mechanisms of bone metastasis. N Engl J Med 350: 1655-1664.

51. Kim SJ, Uehara H, Yazici S, Langley RR, He J, et al. (2004) Simultaneous blockade of platelet-derived growth factor-receptor and epidermal growth factor-receptor signaling and systemic administration of paclitaxel as therapy for human prostate cancer metastasis in bone of nude mice. Cancer Res 64: 4201-4208.

52. Uehara H, Kim SJ, Karashima T, Shepherd DL, Fan D, et al. (2003) Effects of blocking platelet-derived growth factor-receptor signaling in a mouse model of experimental prostate cancer bone metastases. J Natl Cancer Inst 95: 458-470.

53. Langley RR, Fidler IJ (2007) Tumor cell-organ microenvironment interactions in the pathogenesis of cancer metastasis. Endocr Rev 28: 297-321.

**Figure 1**
Click here to download high resolution image
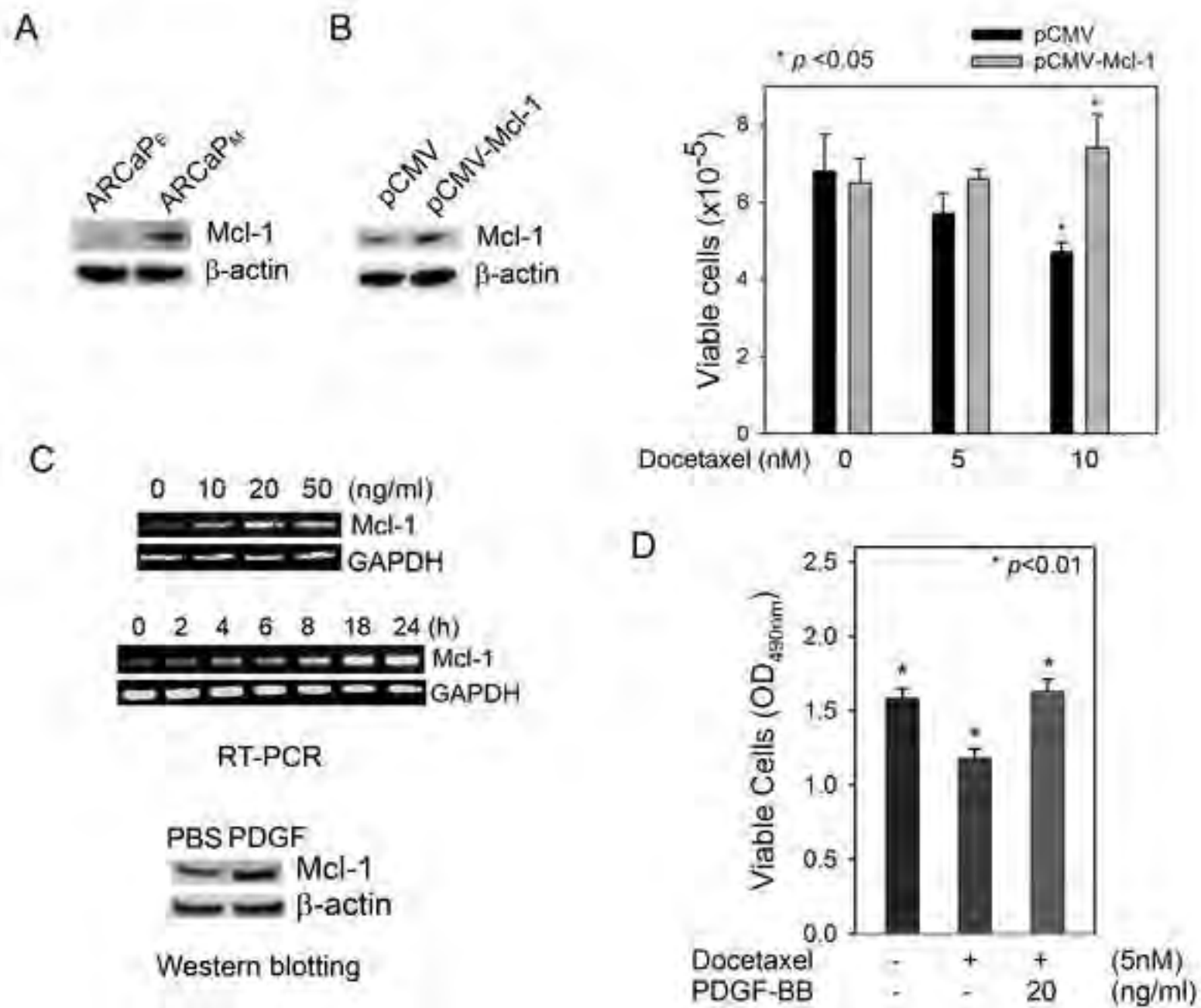
**Figure 2**
Click here to download high resolution image



A RT-PCR; Western blotting

B PDGF time course

C siRNA experiments

D RT-PCR; Western blotting

E Cell viability (%)
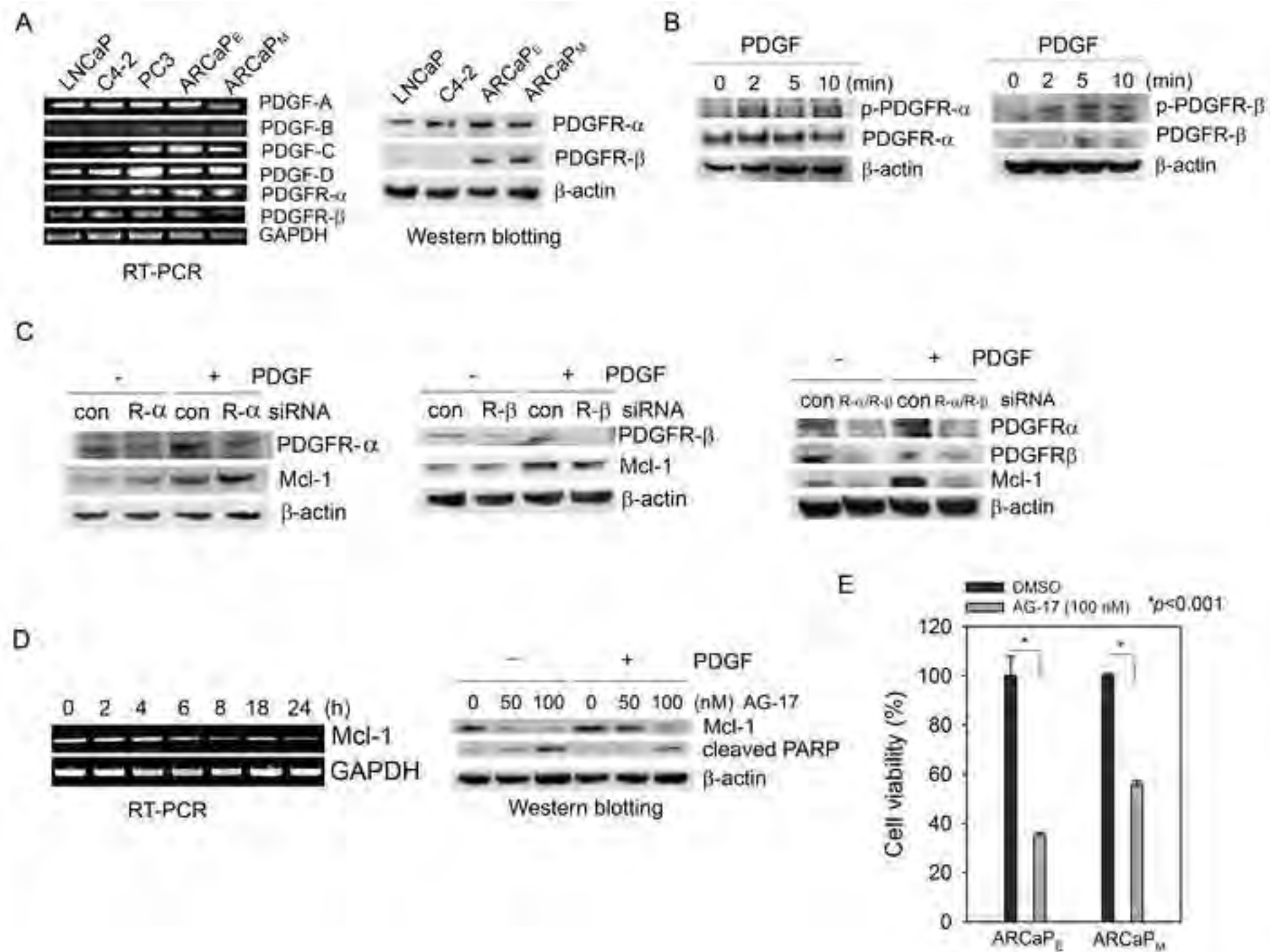
**Figure 3**
Click here to download high resolution image

**A**

LNCaP  C4-2  ARCaP$_E$  ARCaP$_M$

c-Abl
p68
β-actin

total proteins

p68
TBP

nuclear proteins

**B**

IP: c-Abl

0  15  30  (min)

p-c-Abl
c-Abl

IP: p68

0  15  30  (min)

β-catenin
p-p68 (Tyr)
p68

**C**

0  15  30  (min)

p68
TBP

nuclear proteins

**D**

merge    p68    β-catenin    DAPI

time (min)

0
15
30

**E**

PBS    PDGF

con  p68  con  p68  siRNA

p68
β-catenin
Mcl-1
β-actin

**F**

PBS
PDGF-BB

*,**$p<0.01$

Mcl-1 promoter activity (RLU)

60000
50000
40000
30000
20000
10000
0

siRNA    control    p68

**Figure 7**
Click here to download high resolution image

PDGF-BB

PDGFRs

p-c-Abl

p-p68

β-catenin

apoptosis

Mcl-1

HIF-1α    mcl-1

HRE

cancer cells

osteoblasts

stromal cells

endothelial cells
pericytes
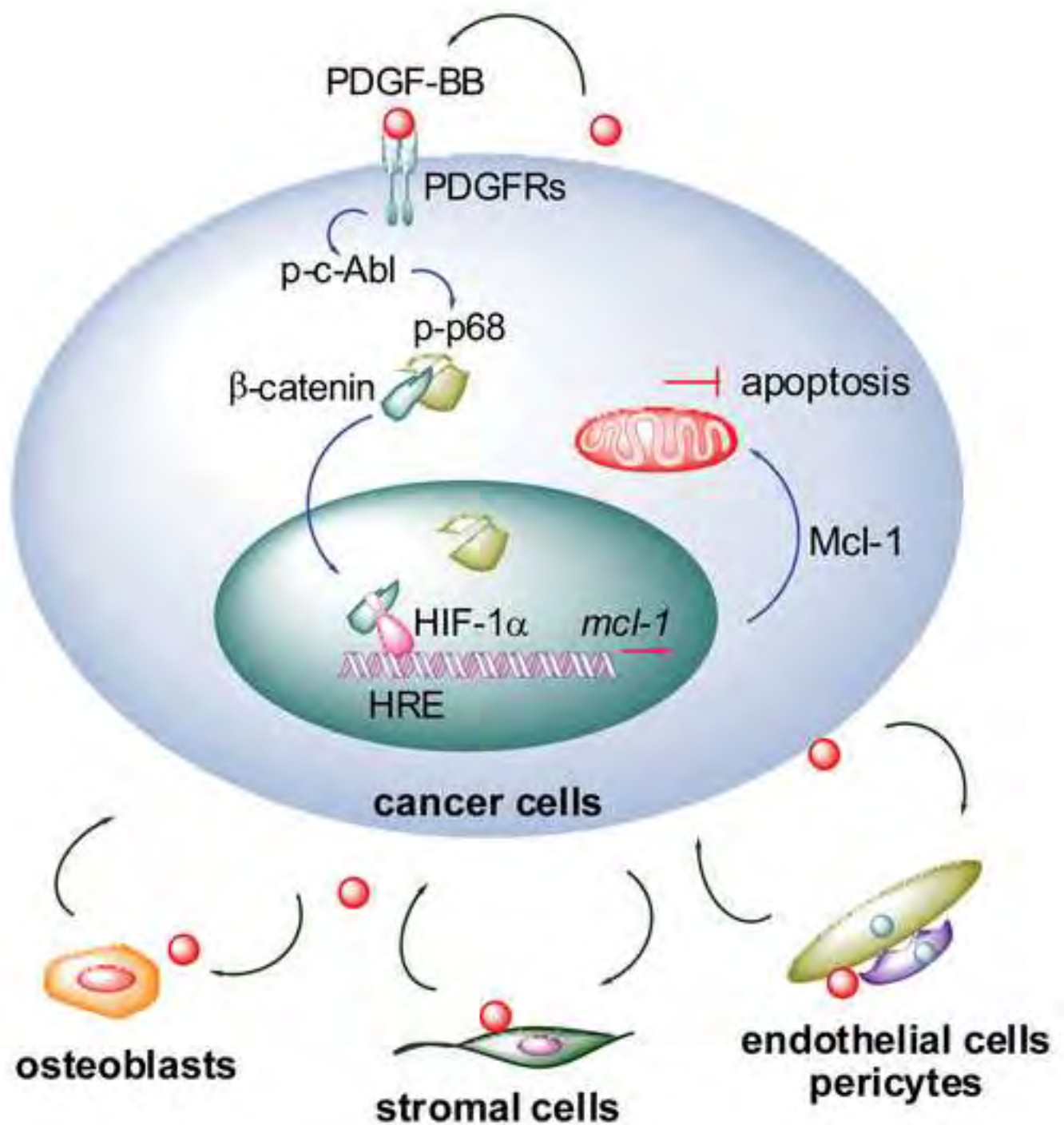
**Supporting Information**

Click here to download Supporting Information: Supporting Information.pdf

*Cancer Therapy: Preclinical*

# BKM1740, an Acyl-Tyrosine Bisphosphonate Amide Derivative, Inhibits the Bone Metastatic Growth of Human Prostate Cancer Cells by Inducing Apoptosis

Seong Il Seo,[2] Lajos Gera,[3] Haiyen E. Zhau,[1] Wei Ping Qian,[1] Shareen Iqbal,[1] Nicole A. Johnson,[1] Shumin Zhang,[1] Majd Zayzafoon,[4] John Stewart,[3] Ruoxiang Wang,[1] Leland W.K. Chung,[1] and Daqing Wu[1]

**Abstract**

**Purpose:** Survivin overexpression has been associated with an unfavorable outcome in human PCa; however, its role in metastasis remains elusive. We aim to (*a*) evaluate the clinical implications of survivin expression in PCa bone metastasis; (*b*) determine *in vivo* efficacy of BKM1740, a small-molecule compound, against PCa skeletal growth and survival; and (*c*) investigate molecular mechanism by which BKM1740 augments apoptosis in bone metastatic PCa cells.

**Experimental Design:** Survivin expression was analyzed in PCa specimens and experimental models. Bone metastatic C4-2 and ARCaP$_M$ cell lines were used to evaluate the *in vitro* effects of BKM1740 and molecular mechanism for the induction of apoptosis. C4-2 cells were grown intratibially in athymic nude mice to evaluate the *in vivo* efficacy of BKM1740. Tumor growth in mouse bone was assessed by serum prostate-specific antigen and radiography and confirmed by immunohistochemical analyses.

**Results:** Survivin expression is positively associated with clinical PCa bone metastasis. BKM1740 induced apoptosis in PCa cells by repressing survivin. Mice with established C4-2 tumors in tibia showed a marked decrease in serum prostate-specific antigen and much improved bone architecture radiographically after treatment with BKM1740. Immunohistochemical assays of mouse tumor samples confirmed that the *in vivo* effects were mediated by inhibition of survivin and induction of apoptosis.

**Conclusions:** Survivin expression is associated with PCa bone metastasis. BKM1740 treatment specifically inhibited survivin and induced apoptosis *in vitro* and was efficacious in retarding PCa skeletal growth in a mouse model. BKM1740 is a promising small-molecule compound that could be used to treat PCa bone metastasis.

Bone metastasis and skeletal complications are the major contributing factors to human prostate cancer (PCa) morbidity and mortality (1). The gain of function of antiapoptotic factors and/or loss of function of proapoptotic proteins may allow PCa cells to evade apoptosis during dissemination and growth in bone tissue (2). As a member of the inhibitor of apoptosis family, survivin intersects multiple survival signals and is highly differentially expressed in cancer (3). In PCa, survivin overexpression has frequently been associated with an unfavorable outcome. Survivin expression is significantly elevated in tumors with a high Gleason score and lymph node metastasis (4, 5). Survivin also mediates resistance to antiandrogen therapy, chemotherapy, and irradiation (6–8). However, despite the well-defined function of survivin in antagonizing death signals during tumorigenesis, little is known about its role in tumor invasion and metastasis (9).

Currently, several strategies are being pursued to target survivin expression or interrupt its antiapoptotic function. Some have been in clinical trials for a variety of human cancers (see ref. 10 for review). Some small-molecule antagonists exert their antitumor function by indirectly targeting pathways implicated in survivin regulation (such as STA-21 inhibition

### Translational Relevance

Bone metastasis is the leading cause of prostate cancer (PCa) death. Current therapy does not improve patient survival. It is critical to identify novel targets for developing efficacious treatments. This study showed that overexpression of survivin, a critical antiapoptotic protein, is associated with clinical PCa progression and bone metastasis. We developed BKM1740, a small-molecule acyl-tyrosine bisphosphonate amide derivative, and found that BKM1740 efficaciously retards PCa skeletal growth in athymic nude mice. Mechanistic study confirmed that the *in vivo* effects were mediated by specific inhibition of survivin and induction of apoptosis. This study validated the clinical implications of survivin expression in PCa bone metastasis and may have a significant effect on the development of efficacious and safe therapeutic regimens for metastatic PCa and other types of cancers.

of the signal transducer and activator of transcription 3 pathway or flavopiridol inhibition of cyclin-dependent kinase 1 activity) or by perturbing protein-protein interaction between survivin and its partners (such as shepherdin, a peptidyl antagonist that may disrupt the interaction between heat shock protein 90 and survivin). Some agents have been developed to directly suppress survivin expression, including an antisense molecule (LY218130B) and transcriptional repressors (YM155 and EM-1421). In established human PCa PC-3 xenografts, YM155, a small imidazolium-based compound, was shown to specifically suppress survivin transcription (11). Two phase I trials for YM155 have been completed in 41 patients with PCa, non–Hodgkin lymphoma, or colorectal cancer. The treatment was well tolerated and exhibited encouraging antitumor efficacy (12). Nonetheless, the portfolio of truly survivin-directed antagonists or suppressors available for clinical testing, particularly in metastatic cancer, is small (10).

Bradykinin-related compounds are emerging as promising antitumor agents (13–15). In experimental models for human PCa and lung cancer, a bradykinin antagonist peptide dimer, B-9870 (CU201), and its nonpeptide mimetic, BKM-570, suppress tumor growth and act synergistically with standard chemotherapy drugs such as cisplatin and Taxotere (16–18). Mechanistic study indicated that the bradykinin-related compounds induce caspase-dependent apoptosis in cancer cells while inhibiting angiogenesis and reducing tissue permeability mediated by matrix metalloproteinases (MMP) in tumors (15). Therefore, these compounds may be pluripotent anticancer agents. To explore novel drugs that may specifically target bone metastatic PCa cells, we developed a BKM-570 analogue conjugated with an aminobisphosphonate group. This compound, termed BKM1740, was found to be efficacious in retarding skeletal growth of human PCa cells through direct inhibition of survivin in a xenograft model.

## Materials and Methods

***Cell lines and culture conditions.*** Human PCa cell lines LNCaP, C4-2 (19), ARCaP$_E$, and ARCaP$_M$ (20) were regularly maintained in T-medium (Invitrogen) supplemented with 5% fetal bovine serum (Sigma), 100 IU/L penicillin G, and 100 μg/L streptomycin at 37°C under 5% $CO_2$.

***Chemicals.*** BKM1740 was developed and synthesized by Gera in the Stewart laboratory according to previously described methods (18, 21, 22). For the *in vitro* and *in vivo* studies, the BKM1740 was dissolved in DMSO (Sigma) at 10 mg/mL stock solution and its purity was determined to be a minimum of 99% by high-performance liquid chromatography.

***Cell proliferation assay.*** Cell proliferation was measured using the CellTiter 96 AQueous Non-Radioactive Cell Proliferation Assay [3-(4,5-dimethylthiazol-2-yl)-5-(3-carboxymethoxyphenyl)-2-(4-sulfophenyl)-2*H*-tetrazolium salt (MTS) assay; Promega]. Briefly, cells suspended in T-medium plus 5% fetal bovine serum were added to 96-well plates at 5,000 per well in sextuplicate. After 24 h of culture, BKM1740 or DMSO was added in various concentrations, and cells were cultured for the indicated time. Combined MTS/phenazine methosulfate solution (20 μL/well) was added to the cells and the absorbance at 490 nm was recorded after 1 h of incubation at 37°C using a microplate reader (Bio-Rad Laboratories). Cell viability was expressed as relative survival with controls recorded as 100%.

***Reporter assay.*** Cells were seeded at a density of $1.5 \times 10^5$ per well in 12-well plates 24 h before transfection. pSurvivin-luc1430 (23) and pRL-TK (as internal control; Promega) were introduced using Lipofectamine 2000 (Invitrogen). A Dual-Luciferase Reporter Assay kit (Promega) was used to determine the firefly luciferase activity and *Renilla* luciferase activity. Data were presented as relative luciferase activity (firefly luciferase activity normalized to *Renilla* luciferase activity).

***Western blot analysis.*** Total cell lysates were prepared using radio-immunoprecipitation assay buffer (Santa Cruz Biotechnology). Protein concentrations in the supernatants were measured with the bicinchoninic acid protein assay kit (Pierce Biotechnology). Total protein (50 μg) was loaded to each lane, resolved on a 4% to 12% NuPAGE Bis-Tris–buffered (pH 7.0) polyacrylamide gel (Invitrogen), and transferred onto a nitrocellulose membrane (Bio-Rad Laboratories). The membrane was incubated with anti-survivin (Novus Biologicals), anti-caspase-3, anti-cleaved caspase-3, anti-caspase-8, anti-cleaved caspase-8, anti-caspase-9, anti-poly(ADP-ribose) polymerase (Cell Signaling), and anti-myeloid cell leukemia-1 (Mcl-1) and MMP-9 (Santa Cruz Biotechnology), with anti-β-actin (Sigma) or anti-EF1α (BD Transduction Laboratories) as loading controls. The reactive bands were visualized by an enhanced chemiluminescence assay kit (Amersham Pharmacia Biotech). Quantification of band intensity was measured by densitometry and analyzed with ImageJ (NIH). Relative protein expression was expressed as fold change compared with control (β-actin or EF1α).

***Reverse transcription-PCR.*** Total RNA was prepared using a Qiagen RNeasy kit. One microgram was used as a template in a reaction using the SuperScript III One-Step reverse transcription-PCR (RT-PCR) kit (Invitrogen). The primer pairs specific for human survivin are 5′-ccaccgcatctctacattca-3′ (forward) and 5′-gcactttcttcgcagtttc-3′ (reverse); for human Mcl-1, 5′-gaggaggaggaggacgagtt-3′ (forward) and 5′-gtcccggttttgtccttacga-3′ (reverse). The primers for vascular endothelial growth factor (VEGF) and glyceraldehyde-3-phosphate dehydrogenase were described previously (24). The thermal profile is 23 cycles for human survivin, Mcl-1, and VEGF amplification or 20 cycles for glyceraldehyde-3-phosphate dehydrogenase, with 94°C, 15 s; 55°C, 30 s; and 68°C, 60 s. Quantification of band intensity was measured by densitometry and analyzed with ImageJ. Relative mRNA abundance was expressed as fold change compared with control (glyceraldehyde-3-phosphate dehydrogenase).

***Condition medium preparation.*** Subconfluent C4-2 cells were serum starved overnight and further treated with BKM1740 or DMSO in fresh serum-free T-medium for 48 h before condition media were collected (24).

***ELISA.*** Vascular endothelial cell growth factor (VEGF) concentration was analyzed using a Quantikine ELISA kit (R&D Systems).

*Apoptosis analysis.* Cells treated with DMSO or BKM1740 were trypsinized and washed with PBS and resuspended in Annexin-binding buffer (BD PharMingen). Cells were then stained with both Annexin V-phycoerythrin and 7-amino-actinomycin for 15 min at room temperature. The stained samples for apoptosis assay were measured using a fluorescence-activated cell sorting (FACS) caliber bench-top flow cytometer (Becton Dickinson). The data were analyzed using FlowJo software (Tree Star, Inc.). The experiments were repeated at least thrice independently.

*Assessment of* **in vivo** *effects of BKM1740 on human prostate tumor xenografts in mouse bone.* All animal procedures were done in compliance with Emory University Institutional Animal Care and Use Committee and NIH guidelines. A total of $1.0 \times 10^6$ C4-2 cells were inoculated in mouse bilateral tibia using a previously established procedure (25, 26). Blood specimens (70 μL) were obtained from the retro-orbital sinus vein every 2 wk for serum prostate-specific antigen (PSA) determination. Serum PSA was determined by microparticle ELISA using an Abbott IMx instrument (Abbott Laboratories). A total of 20 athymic male nude mice (BALB/c *nu/nu*; National Cancer Institute, Bethesda, MD) were divided into two groups: a vehicle control group ($n = 11$) and a BKM1740 treatment group ($n = 9$). The treatments were initiated at 4 wk after tumor cell inoculation with confirmed tumors in bone by X-ray and positive serum PSA (25, 27). BKM1740 was dissolved in 100% DMSO as a stock solution of 10 mg/mL. Mice were given BKM1740 every 2 d at 5 mg/kg via the i.p. route for an 8-wk period. Control mice received vehicle injections for the same duration. Mice were weighed every week and tumor growth in bilateral tibia was followed by serum PSA and X-ray every 2 wk. Mice were sacrificed 8 wk after the initiation of treatment. The bilateral tibia were removed, fixed in 10% neutralized formalin for 48 h, and decalcified in EDTA (pH 7.2) for 15 d. Tibia specimens were dehydrated and paraffin embedded for immunohistochemical analyses. To assess the systemic toxicity of BKM1740, athymic nude mice ($n = 4$) were administered at a high dose of 20 mg/kg via the i.p. route, twice per week, for 4 wk.

*Immunohistochemical analysis.* Survivin expression was analyzed in five human normal/benign prostatic glands, five each of well-differentiated and poorly differentiated primary PCa, and four bone metastatic PCa tissue specimens. Cell proliferation (Ki67), cell death (M30), and survivin in bone tumor specimens obtained from control and BKM1740-treated mice (two in each group) were conducted. Antibodies used were goat polyclonal antibody against Ki67 (1:500; Santa Cruz Biotechnology), mouse monoclonal antibody against M30 CytoDeath (1:500; DiaPharma Group, Inc.), and rabbit polyclonal antibody against survivin (1:200; Novus Biologicals). Tissues were deparaffinized, rehydrated, and subjected to 5-mn pressure-cooking antigen retrieval, 10-min double endogenous enzyme block, and 30-min primary antibody incubation, and subjected to 30-min DakoCytomation EnVision+ horseradish peroxidase reagent (for M30 and survivin) or 15 min each of biotinylated link and streptavidin-peroxidase label reagents (for Ki67) incubation. Signals were detected by adding substrate hydrogen peroxide using diaminobenzidine as chromogen and counterstained by hematoxylin. All reagents were obtained from Dako Corp. Matching sera and IgG were used as negative controls. Relative expression of Ki67, M30, and survivin was shown as the number of positively stained cells in 200 cells ± SE at three randomly selected areas at ×100 magnification.

*Data analysis.* All data represent three or more experiments. Treatment effects were evaluated using a two-sided Student's *t* test. Errors are SE values of averaged results, and values of $P < 0.05$ were taken as a significant difference between means.

## Results

*Elevation of survivin is correlated to bone metastasis status in human PCa tumors.* To investigate the clinicopathologic significance of survivin expression in human PCa progression, we analyzed the immunohistochemical protein expression of
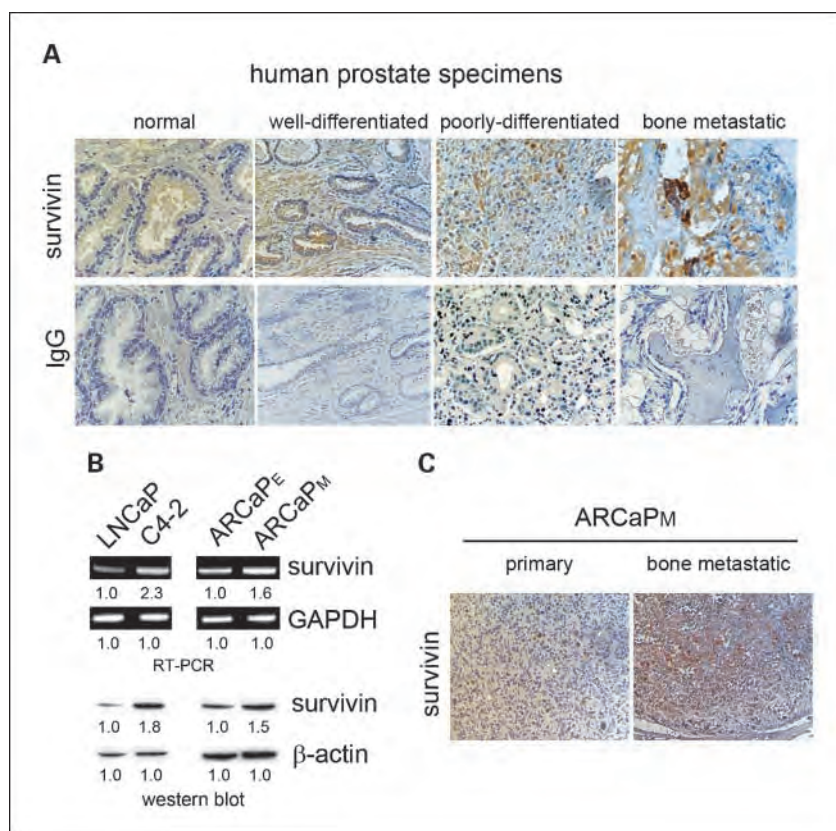


**Fig. 1.** Survivin expression is associated with bone metastasis in human PCa specimens and the ARCaP experimental model. *A,* survivin expression increased during PCa progression from normal to primary cancer to bone metastasis. *B,* RT-PCR and Western blot analyses of survivin expression in human PCa cell models. Survivin increased in bone metastatic C4-2 and ARCaP_M cells compared with their parental LNCaP and ARCaP_E cells. Relative expression was expressed as fold change compared with controls. GAPDH, glyceraldehyde-3-phosphate dehydrogenase. *C,* survivin expression in bone metastatic ARCaP_M tumor was higher than in primary tumor.

survivin in primary and bone metastatic PCa tissue. We defined well-differentiated PCa as Gleason score ≤6 and poorly differentiated PCa as Gleason score ≥8. Survivin expression was undetectable to marginal in all normal/benign glands ($n = 5$) and increased from well-differentiated cancer ($n = 5$) to poorly differentiated cancers ($n = 5$). Importantly, survivin was highly expressed in all bone metastatic PCa tumor specimens ($n = 4$; Fig. 1A). These data suggest that survivin expression is positively associated with PCa progression, particularly bone metastasis.

We have established several lines of human PCa cells that represent a continuum of PCa progression closely mimicking the clinical pathophysiology of bone metastasis (see ref. 28 for review). Two lineage-related sets of PCa cells were used in this study: the LNCaP-C4-2 model (19, 29) and the ARCaP$_E$-ARCaP$_M$ model (20, 24, 30). RT-PCR and Western blotting analyses indicated that survivin expression was elevated in highly bone metastatic C4-2 and ARCaP$_M$ PCa cell lines compared with the less invasive parental cell lines LNCaP and ARCaP$_E$ (Fig. 1B). ARCaP$_M$ cells were inoculated into athymic mice s.c., which resulted in metastases to bone tissues within a short latency period (20, 31). Survivin expression was examined by immunohistochemical staining of the ARCaP$_M$ tumor specimens from either the primary site (s.c. injection) or metastatic bone. Consistently, survivin protein level was significantly increased in bone metastatic tumor compared with the primary tumor (Fig. 1C). These data obtained from *in vivo* PCa models validate a positive correlation between survivin expression and the bone metastatic propensity observed in clinical specimens.

*BKM1740 induces apoptosis in metastatic PCa cells.* BKM1740 is an acyl-tyrosine bisphosphonate amide derivative, which was developed from the key chemical structure of BKM-570, F5c-OC2Y [$N$-(2,3,4,5,6-pentaflurocinnamoyl)-$O$-(2,6-dichlorobenzyl)-tyrosine; refs. 18, 22]. BKM1740 is expected to have potent antitumor activity exhibited by the F5c-OC2Y moiety and can be selectively taken up and adsorbed to mineral surfaces in bone because of the introduction of the aminobisphosphonate moiety (32).

We first evaluated the cytotoxic effects of BKM1740 on bone metastatic PCa cells. C4-2 and ARCaP$_M$ cells were exposed to the indicated concentrations of BKM1740 for various durations and cell proliferation was determined by MTS assay. BKM1740 was found to inhibit the *in vitro* growth of C4-2 (Fig. 2B) and ARCaP$_M$ cells (Fig. 2C) in a dose- and time-dependent manner, with 50% inhibition (IC$_{50}$) observed at 2 and 9 μmol/L, respectively. Interestingly, compared with C4-2 cells, ARCaP$_M$ only responded to BKM1740 treatment significantly within a narrow dose range (between 8 and 10 μmol/L), suggesting that this cell line is more resistant to the cytotoxicity of BKM1740 (Fig. 2C).

To further elucidate the mechanism for the effects of BKM1740 on PCa cell viability, we determined Annexin V expression, an indicator of apoptosis, in C4-2 cells treated with BKM1740 at the indicated concentrations for 24 h (Fig. 3A). Fluorescence-activated cell sorting analysis indicated that BKM1740 treatment significantly induced apoptosis in C4-2 cells in a dose-dependent manner. Greater than 40% cell death can be achieved in 24 h with 5 μmol/L BKM1740 (Fig. 3B). Expression of caspases was determined by Western blot analysis of C4-2 cells treated with 5 μmol/L BKM1740. Activation of

caspase-3, caspase-8, and caspase-9, as exhibited by increased cleaved protein bands at 17, 40, and 35 kDa, respectively, was observed after incubation with BKM1740 for 12 h. Cleavage of poly(ADP-ribose) polymerase, an indicator of apoptosis shown as a band at 89 kDa, also increased significantly (Fig. 3C). These data suggest that BKM1740 induces apoptosis in metastatic PCa cells through a caspase-dependent pathway.

*BKM1740 specifically inhibits expression of survivin in metastatic PCa cells.* Multiple factors are involved in the regulation of cell death by apoptosis (33). To elucidate the specific signaling pathway(s) mediating the cytotoxicity of BKM1740 in PCa cells, we analyzed the expression of several antiapoptotic proteins in C4-2 cells treated with BKM1740 (Fig. 4A and B). RT-PCR assay indicated that BKM1740 significantly inhibited survivin expression at the mRNA level. BKM1740 treatment did not significantly affect the expression of antiapoptotic protein Mcl-1 (34). Expression of VEGF, inhibited by treatment with BKM-570 in a previous study (22), was not affected by BKM1740 at either the mRNA (Fig. 4A) or protein level (Fig. 4B). Western blot analysis confirmed the inhibition of survivin protein expression following BKM1740 treatment in C4-2 and ARCaP$_M$ cells (Fig. 4A and C). Basal expression of MMP-9, an important MMP implicated in PCa metastasis (22, 35), was not detected in C4-2 cells by Western blot analysis (data not shown) and not affected by BKM1740 treatment in ARCaP$_M$ cells (Fig. 2C).

C4-2 cells were transiently transfected with a survivin-luciferase reporter (pSurvivin-luc1430) composed of a 1,430-bp region of human survivin promoter (23). The cells were further treated with BKM1740 at the indicated concentrations for 24 h before the luciferase activity assay was done. The data indicated that BKM1740 inhibited the survivin reporter activity in a dose-dependent manner (Fig. 4D), suggesting that survivin transcription was suppressed by BKM1740 treatment in C4-2 cells, which was consistent to the RT-PCR results (Fig. 4A). Taken together, these data showed that BKM1740 specifically inhibits survivin expression in bone metastatic PCa cells, which may mediate the activation of caspase-dependent apoptotic death caused by this compound.

*BKM1740 treatment inhibits* in vivo *C4-2 tumor growth in mouse skeleton.* To evaluate the *in vivo* effect of BKM1740 against the growth of bone metastatic PCa tumors, we treated athymic nude mice bearing intratibial C4-2 xenografts with BKM1740 at a dose of 5 mg/kg by the i.p. route, once every 2 days. The treatment started on day 28 (4 weeks) after tumor inoculation and continued for 8 weeks. Tumor growth and responsiveness to BKM1740 treatment were determined by serum PSA and skeletal X-ray. As shown in Fig. 5A, there was a significant reduction in serum PSA levels in the BKM1740-treated groups compared with vehicle control at 8 weeks ($P < 0.05$). Representative radiographs are shown in Fig. 5B. Compared with the vehicle control, C4-2 tumor-bearing bone treated with BKM1740 displayed improved architecture with reduced osteolytic destruction and osteoblastic lesions (Fig. 5B, *left*). These X-ray results were consistent with the inhibitory effects of BKM1740 treatment on serum PSA levels in C4-2 tumor-bearing mice. Mice treated with BKM1740 gained weight comparably with the controls (data not shown). To assess the potential *in vivo* toxicity of BKM1740 treatment, athymic nude mice without C4-2 tumor inoculation were treated with a high dose of BKM1740 (20 mg/kg) for 4 weeks. No systemic toxicity
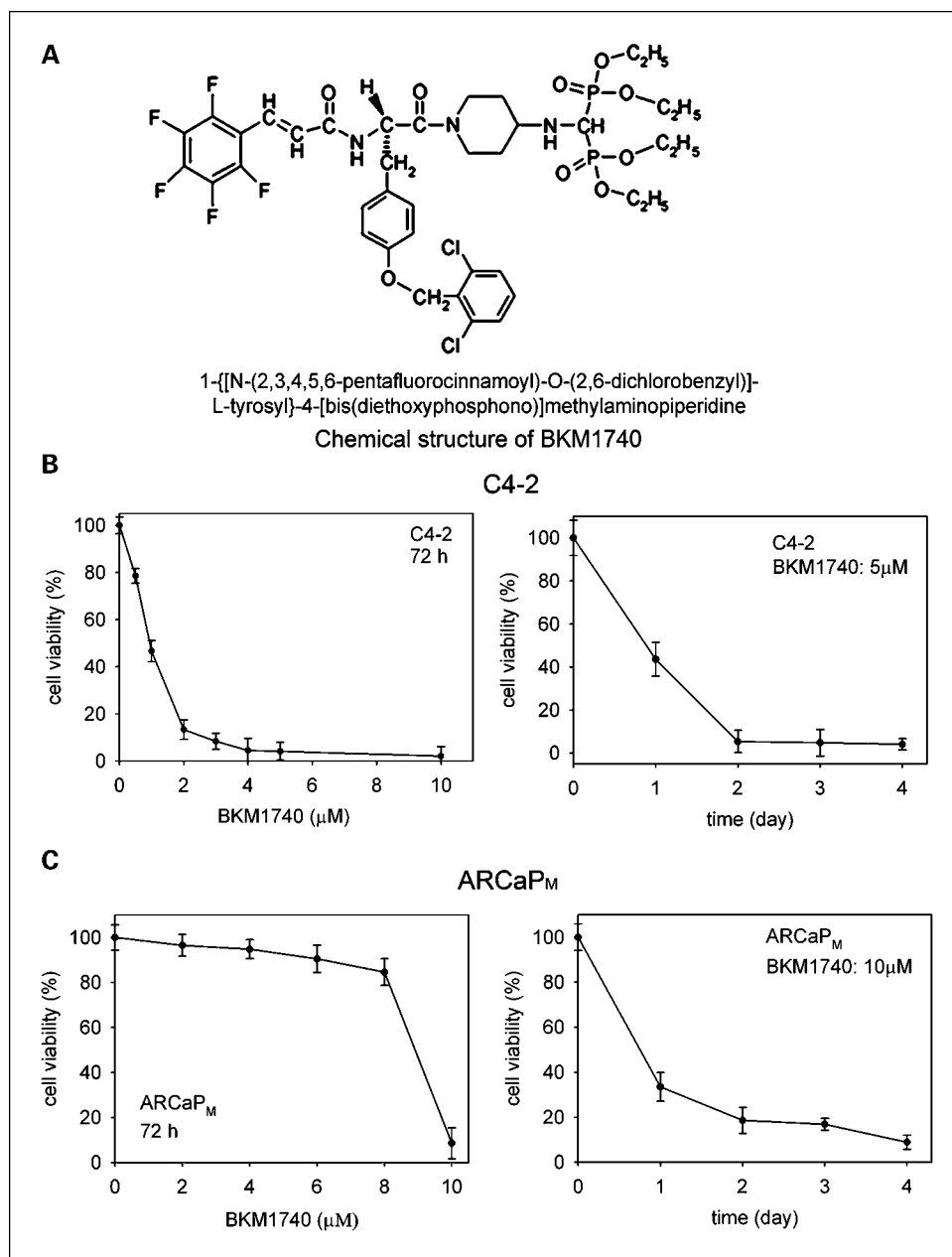
**Fig. 2.** BKM1740, an acyl-tyrosine bisphosphonate amide derivative, inhibits *in vitro* proliferation of C4-2 and ARCaP$_M$ cells. *A*, chemical structure of BKM1740. *B* and *C*, BKM1740 effects on proliferation of C4-2 (*B*) and ARCaP$_M$ cells (*C*). PCa cells were cultured in the presence of BKM1740 at indicated concentrations for various durations. The effects of BKM1740 treatment on cell numbers were evaluated using MTS assay.

was observed, and the mice gained body weight during the treatment (Supplementary Data). X-ray radiography showed intact bone architecture like that in normal mouse (Fig. 5B, *right*). These results suggested negligible *in vivo* acute toxicity of BKM1740 treatment.

*Immunohistochemical analysis of human PCa xenografts subjected to BKM1740 treatment.* The effects of BKM1740 treatment on C4-2 tumor growth in tibia were confirmed by immunohistochemical analyses of the harvested tumor specimens at the termination of the experiments. Immunohistochemical staining of mouse tibia indicated that compared with vehicle control, BKM1740 treatment resulted in (*a*) markedly decreased cell proliferation (Ki67) and massive apoptosis (M30) in tumor tissues and (*b*) significant inhibition of survivin expression (Fig. 6A). These differences are statistically significant (Fig. 6B). The data confirmed that the *in vivo* effects

of BKM1740 on C4-2 tumor growth were mediated by suppression of survivin expression and induction of apoptosis in PCa tumors.

## Discussion

Current regimens treating metastatic PCa by conventional hormone therapy, chemotherapy, or radiation therapy have not resulted in improved patient survival (36). New approaches targeting bone with bisphosphonates to slow down skeletal events, and bone-directed chemotherapy and radiation therapy using strontium-89 or samarium-153, have been approved by the Food and Drug Administration for the clinical treatment of bone metastasis in PCa and breast cancer (37). In addition, "cotargeting" both the tumor and its stromal microenvironment using gene therapy approaches, and drug therapy

targeting osteoblasts, osteoclasts, marrow stromal cells, bone-derived endothelium, cell adhesion to extracellular matrices, or selected growth factor pathways (see refs. 2, 38 for reviews), has shown promise in a large number of bone metastasis models. In this study, we present evidence indicating that BKM1740, a novel bradykinin-related compound conjugated with aminobisphosphonate, induced massive apoptosis and retarded tumor growth in a human PCa bone metastasis model. These data suggest that BKM1740 is an attractive compound for evaluation as a PCa skeletal metastasis drug.

Aberrant signal transduction in both tumors and the bone microenvironment is critical in defining the invasiveness of PCa cells. "Targeted therapy" to interrupt specific signaling pathways implicated in PCa progression is a promising approach supported by recent experimental and clinical studies (39). Multiple signaling molecules have been identified as possible "targets" for rational drug design. Among them, survivin is considered uniquely promising for two reasons: (*a*) survivin intersects multiple signaling networks implicated in the inhibition of apoptosis and therefore blockade of the survivin signal will interrupt tumor progression regardless of the genetic background of the tumor and (*b*) survivin is overexpressed by virtually all solid tumors but undetectable or at very low levels in most terminally differentiated normal tissues; therefore,

survivin-based therapy may specifically target tumors with a favorable toxicity profile (3).

Although survivin expression has been correlated to advanced stages of PCa with higher Gleason scores and lymph node metastasis (4, 5), its role in PCa bone metastasis remains elusive. To validate survivin as a rational target for PCa bone metastasis, we first investigated the clinical significance of survivin in human PCa progression. The data showed that survivin expression is positively associated with higher Gleason scores in primary prostatic tumors, indicating that survivin is important in tumorigenesis. Intriguingly, survivin expression is further increased in bone metastatic PCa specimens, which we confirmed in PCa bone metastatic models of LNCaP-C4-2 and ARCaP. Despite the limited numbers of tumor specimens (which were extremely difficult to obtain), these results for the first time suggest a crucial role for survivin in the progression of advanced PCa toward bone metastasis. We hypothesize that overexpression of survivin may confer survival advantages to metastatic PCa cells that allow them to successfully disseminate and colonize. Inhibition of survivin expression may reverse this and induce regression of tumor growth in bone.

Bradykinin-related compounds are being explored as promising anticancer drugs. Several bradykinin antagonists and their mimetic have been found to effectively inhibit tumor growth in



**Fig. 3.** BKM1740 induces apoptosis in metastatic PCa cells. *A,* C4-2 cells were treated with BKM1740 at the indicated concentrations for 24 h, and Annexin V fluorescence-activated cell sorting (*FACS*) analysis was done. *B,* percentage of apoptotic cells induced by BKM1740 treatment. *C,* Western blot analysis of activation of caspase pathways. C4-2 cells were exposed to 5 μmol/L BKM1740 for 12 h. Activated caspase-3, caspase-8, and caspase-9 and cleavage of poly(ADP-ribose) polymerase (*PARP*) were detected by the increased banding of proteins at 17, 40, 35, and 89 kDa, respectively. Relative expression was expressed as fold change compared with the EF1α controls.
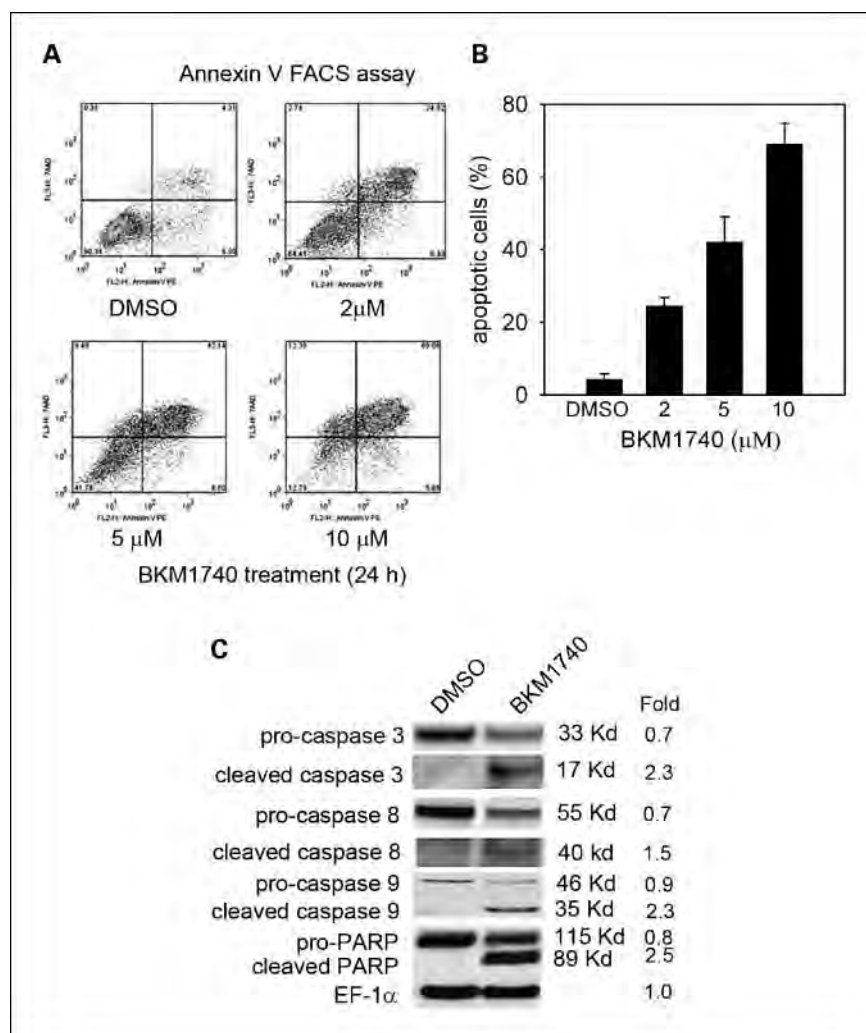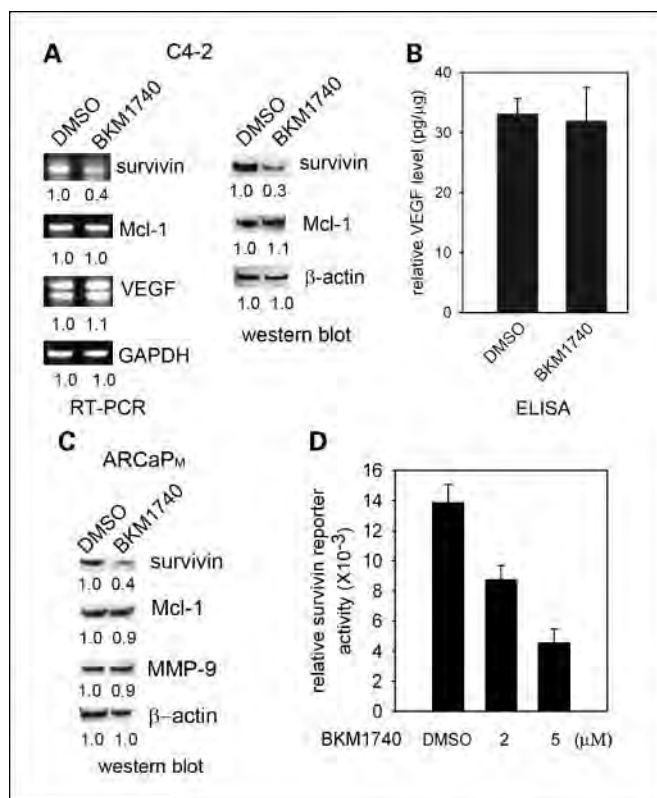
**Fig. 4.** BKM1740 inhibits survivin expression in metastatic PCa cells. *A,* BKM1740 specifically suppresses survivin expression at both RNA and protein levels in C4-2 cells. Left, C4-2 cells were exposed to 5 μmol/L BKM1740 for 12 h. Total RNA was collected and analyzed by RT-PCR for survivin, Mcl-1, and VEGF, with glyceraldehyde-3-phosphate dehydrogenase as loading control. Right, C4-2 cells were treated with 5 μmol/L BKM1740 for 24 h, and total lysates were analyzed for the expression of survivin and Mcl-1. Relative expression was expressed as fold change compared with the β-actin controls. *B,* ELISA of VEGF levels in conditioned medium of C4-2 cells treated with BKM1740 or vehicle for 48 h. Relative VEGF levels were normalized by dividing VEGF concentrations (pg/mL) by total protein concentrations (mg/mL) in condition medium. *C,* BKM1740 specifically suppresses survivin expression in ARCaP$_M$ cells. ARCaP$_M$ cells were treated with 10 μmol/L BKM1740 for 24 h, and total lysates were analyzed for the expression of survivin, Mcl-1, and MMP-9. Relative expression was expressed as fold change compared with the β-actin controls. *D,* C4-2 cells were cotransfected with pSurvivin-luc1430 and pRL-TK (internal control) for 48 h before exposure to BKM1740 at the indicated concentrations for a further 24-h incubation. Total lysates were analyzed for luciferase activity induced by the survivin promoter and normalized to the *Renilla* luciferase activity.

animal models of PCa and lung cancer (13–16, 18, 40). One of the peptide-based antagonists, CU201, is entering a phase I clinical trial for lung cancer. Mechanistic study showed that CU201 induced cancer cell apoptosis as a "biased" agonist by inhibiting Gα$_q$ activation and downstream events and by stimulating Gα$_{12,13}$ and downstream cascades (17). Intriguingly, these compounds may act as pluripotent molecules that could simultaneously inhibit cancer cell proliferation by inducing apoptosis, and interrupt angiogenesis by reducing VEGF expression (18). To develop novel anticancer reagents that specifically target PCa bone metastasis, we designed BKM1740 as an analogue that incorporates the key "anticancer" structure (F5c-OC2Y) of BKM-570 and an aminobisphosphonate group to improve specific delivery of the compound into bone, thereby increasing its bioavailability in tumor tissues residing in bone. The mechanism-based evidence presented here shows that (*a*) BKM1740 specifically inhibited survivin

expression at both the mRNA and protein levels and induced tumor regression in a mouse model of PCa bone metastasis, suggesting that BKM1740 and its derivatives could be novel small-molecule chemicals that effectively treat PCa bone metastasis, and (*b*) the design scheme for BKM1740 as a "pluripotent" compound could serve as a valuable principle in rational drug development.

Bisphosphonates are nonhydrolyzable pyrophosphate analogues, which have been shown to have inhibitory effects on metastasis-induced osteoclastic bone resorption (32, 41). Introduction of an aminobisphosphonate moiety in BKM1740 was expected to increase its bioavailability in bone metastatic tumor lesions and retain the inhibitory effects on bone resorption initiated by metastatic PCa. However, whether this compound retains the inhibitory activity of the bisphosphonate moiety on the osteolysis process is not clear. Future studies will examine the *in vitro* effects of BKM1740 on osteoclast activity and formation and assess the *in vivo* effects on osteolytic process and bone turnover using the model established in the current study. The results will validate the design strategy for BKM1740 and provide valuable information for developing alternative candidates.

Interestingly, recent studies suggest that bisphosphonates may have direct anticancer activity (42, 43). For example, zoledronic acid was found to be capable of inhibiting *in vitro* proliferation of LNCaP and PC-3 PCa cells (44). Because BKM1740 is conjugated with bisphosphonate, we do not
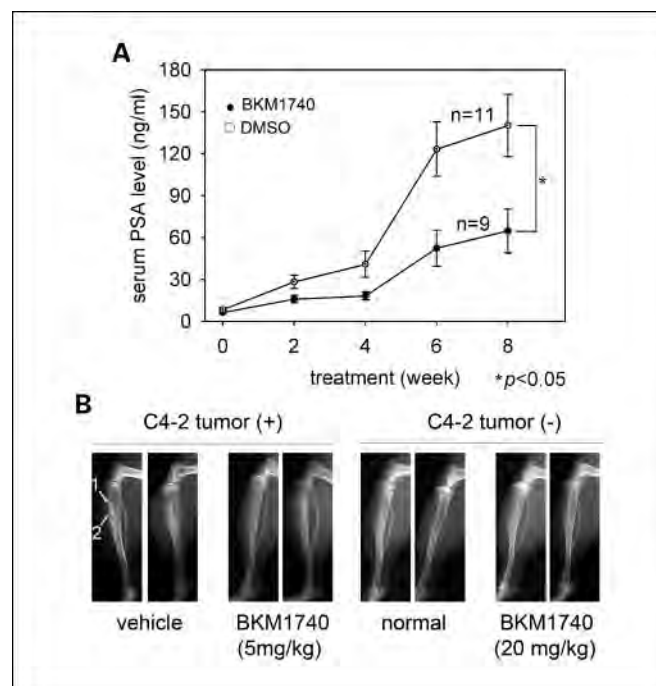


**Fig. 5.** BKM1740 induces regression of PCa skeletal tumor in C4-2 mouse xenografts. *A,* i.p. injection of BKM1740 reduced serum PSA in mice bearing C4-2 skeletal tumors compared with control group after 8 wk of treatments (*P* < 0.05). ○, vehicle control group; ●, BKM1740-treated group. *B,* representative chromatograms of the bones in each group as detected by X-ray, showing that BKM1740 treatment improves bone X-ray appearances in comparison with control group. Left, tumor-bearing athymic nude mice treated with either vehicle or BKM1740 at a dose of 5 mg/kg, every 2 d, for 8 wk. The osteolytic lesion and osteoblastic lesion in the tumor-bearing bone were indicated by arrows 1 and 2, respectively. Right, normal athymic nude mice or only treated with BKM1740 at a dose of 20 mg/kg, twice per week, for 4 wk.

**Fig. 6.** BKM1740 treatment exhibits growth-inhibitory and proapoptotic activity against C4-2 tumor xenografts in mice. *A,* BKM1740 treatment inhibited cell proliferation (Ki67), induced apoptosis (M30), and suppressed survivin expression *in vivo* by immunohistochemical analysis. *B,* comparative quantification of BKM1740 treatment as opposed to controls on the expression of markers of cell proliferation, apoptosis, and survivin expression ($P < 0.05$).
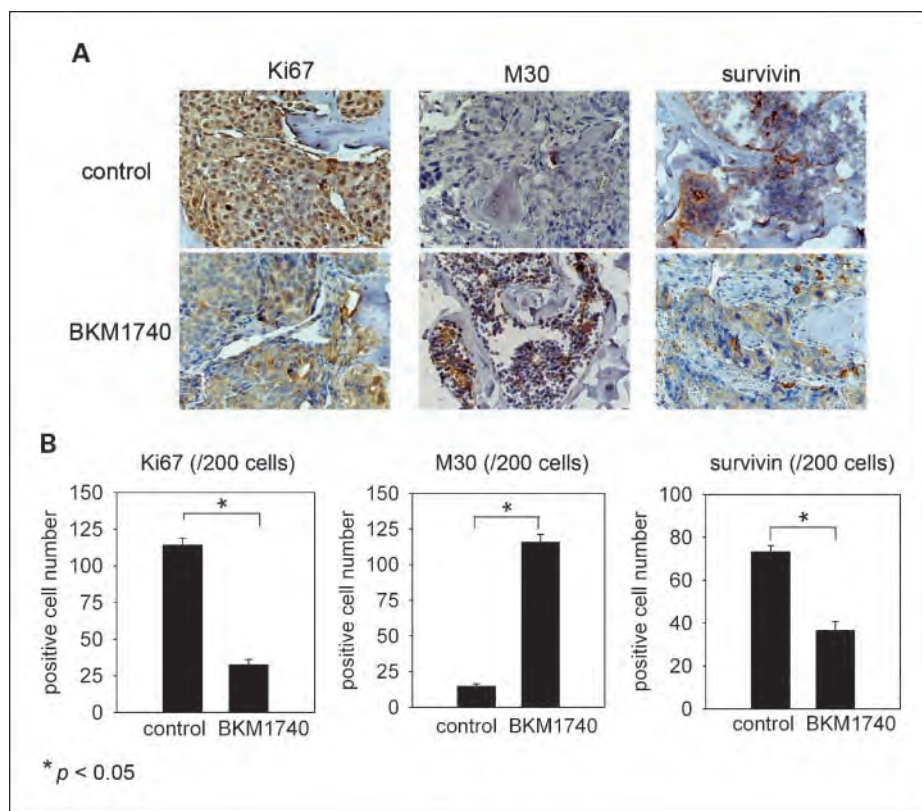
exclude the possibility that its inhibitory effects on PCa cell survival were partially due to the bisphosphonate moiety. However, the zoledronic acid concentration used in the cited study was much higher (68 μmol/L zoledronic acid in apoptosis analysis; ref. 44) than the BKM1740 concentration used in this report. Further, zoledronic acid only exhibited significant efficacy inhibiting PCa tumor growth in mouse bone, not in s.c. models (44), indicating that zoledronic acid activity on PCa skeletal growth is mainly attributable to indirect effects related to decreased osteolysis. These observations support our notion that the proapoptotic activity of BKM1740 may be primarily mediated by the effects of its F5c-OC2Y moiety on survivin expression.

Multiple growth factors and proteases are involved in PCa growth, survival, and invasion (2, 45, 46). A previous study by Stewart et al. (15) found that CU201 and BKM-570 significantly inhibited angiogenesis by reducing VEGF expression and decreased tissue permeability mediated by MMPs in a PC-3 model. Because BKM1740 is derived from BKM-570, we examined whether it has similar effects on the expression of VEGF and MMPs in C4-2 cells. The data indicated that BKM1740 treatment did not affect VEGF mRNA expression or protein secretion. Unlike in PC-3 cells, basal expression of MMP-9 was undetectable in C4-2 cells and not affected significantly by BKM1740 treatment in ARCaP$_M$ cells. Taken together, these results suggested that BKM1740-induced C4-2 tumor regression in bone may be primarily mediated by specific inhibition of survivin and induction of apoptosis.

Survivin overexpression in human cancers has been associated with resistance to conventional chemotherapy and irradiation therapy (6–8). Furthermore, treatment with certain mitotic inhibitor-based drugs such as Taxol may result in

arresting the mitotic process and subsequent accumulation of survivin in the G$_2$-M phase of cell cycle, which eventually counteracts Taxol-induced apoptosis (47). Inhibition of survivin, particularly by small-molecule suppressants, could sensitize the resistant cells to apoptosis induction, thereby augmenting therapeutic responses (10). Several strategies are being pursued to down-regulate survivin expression and increase the efficacy of chemotherapy in PCa and breast cancer (7, 11). With the shown efficacy of BKM1740 in suppressing survivin and inducing apoptosis in invasive PCa cells, it can be expected that a combination treatment with BKM1740 and chemotherapeutic agents such Taxotere may have therapeutic advantages over a single regimen for the treatment of PCa bone metastasis.

In conclusion, our study shows that BKM1740 is a novel small acyl-tyrosine bisphosphonate amide analogue that specifically suppresses survivin expression and induces massive apoptosis in bone metastatic PCa cells. *In vivo* experiments validated its efficacy in inducing regression of pre-established bone metastatic PCa tumors without acute toxicity. Extensive studies of BKM1740 function and further development of its analogues could provide a novel therapeutic strategy for treating bone metastasis in PCa and other human cancers.

## Disclosure of Potential Conflicts of Interest

## Acknowledgments

# References

1. Jemal A, Siegel R, Ward E, Murray T, Xu J, Thun MJ. Cancer statistics, 2007. CA Cancer J Clin 2007;57: 43–66.
2. Chung LW, Baseman A, Assikis V, Zhau HE. Molecular insights into prostate cancer progression: the missing link of tumor microenvironment. J Urol 2005; 173:10–20.
3. Altieri DC. Molecular circuits of apoptosis regulation and cell division control: the survivin paradigm. J Cell Biochem 2004;92:656–63.
4. Kishi H, Igawa M, Kikuno N, Yoshino T, Urakami S, Shiina H. Expression of the survivin gene in prostate cancer: correlation with clinicopathological characteristics, proliferative activity and apoptosis. J Urol 2004; 171:1855–60.
5. Shariat SF, Lotan Y, Saboorian H, et al. Survivin expression is associated with features of biologically aggressive prostate carcinoma. Cancer 2004;100: 751–7.
6. Nomura T, Yamasaki M, Nomura Y, Mimata H. Expression of the inhibitors of apoptosis proteins in cisplatin-resistant prostate cancer cells. Oncol Rep 2005;14: 993–7.
7. Zhang M, Mukherjee N, Bermudez RS, et al. Adenovirus-mediated inhibition of survivin expression sensitizes human prostate cancer cells to paclitaxel *in vitro* and *in vivo*. Prostate 2005;64:293–302.
8. Zhang M, Latham DE, Delaney MA, Chakravarti A. Survivin mediates resistance to antiandrogen therapy in prostate cancer. Oncogene 2005;24:2474–82.
9. Ouhtit A, Matrougui K, Bengrine A, Koochekpour S, Zerfaoui M, Yousief Z. Survivin is not only a death encounter but also a survival protein for invading tumor cells. Front Biosci 2007;12:1260–70.
10. Altieri DC. Survivin, cancer networks and pathway-directed drug discovery. Nat Rev Cancer 2008;8: 61–70.
11. Nakahara T, Takeuchi M, Kinoyama I, et al. YM155, a novel small-molecule survivin suppressant, induces regression of established human hormone-refractory prostate tumor xenografts. Cancer Res 2007;67: 8014–21.
12. Tolcher AW, Antonia S, Lewis LD, et al. A phase I study of YM155, a novel survivin suppressant, administered by 168 hour continuous infusion to patients with advanced solid tumors [abstract 3014]. Proc Am Soc Clin Oncol Annu Meet 2006; 24:3014.
13. Stewart JM. Bradykinin antagonists as anti-cancer agents. Curr Pharm Des 2003;9:2036–42.
14. Stewart JM. Bradykinin antagonists: discovery and development. Peptides 2004;25:527–32.
15. Stewart JM, Chan DC, Simkeviciene V, et al. Bradykinin antagonists as new drugs for prostate cancer. Int Immunopharmacol 2002;2:1781–6.
16. Chan DC, Gera L, Stewart JM, et al. Bradykinin antagonist dimer, CU201, inhibits the growth of human lung cancer cell lines *in vitro* and *in vivo* and produces synergistic growth inhibition in combination with other antitumor agents. Clin Cancer Res 2002; 8:1280–7.

17. Chan D, Gera L, Stewart J, et al. Bradykinin antagonist dimer, CU201, inhibits the growth of human lung cancer cell lines by a "biased agonist" mechanism. Proc Natl Acad Sci U S A 2002;99:4608–13.
18. Stewart JM, Gera L, Chan DC, et al. Combination cancer chemotherapy with one compound: pluripotent bradykinin antagonists. Peptides 2005;26: 1288–91.
19. Wu HC, Hsieh JT, Gleave ME, Brown NM, Pathak S, Chung LW. Derivation of androgen-independent human LNCaP prostatic cancer cell sublines: role of bone stromal cells. Int J Cancer 1994;57:406–12.
20. Xu J, Wang R, Xie ZH, et al. Prostate cancer metastasis: role of the host microenvironment in promoting epithelial to mesenchymal transition and increased bone and adrenal gland metastasis. Prostate 2006; 66:1664–73.
21. Gera L, Stewart JM, Fortin JP, Morissette G, Marceau F. Structural modification of the highly potent peptide bradykinin B1 receptor antagonist B9958. Int Immunopharmacol 2008;8:289–92.
22. Gera L, Chan DC, York EJ, et al. Combination cancer chemotherapy with a single agent: bradykinin peptide antagonists and their mimetics. Proceedings of the 28th European Peptide Symposium (Flegl M, Fridkin M, Gilon C, Slaninova J, editors), Kenes, Geneva, 2005. p. 846–7.
23. Li F, Altieri DC. Transcriptional analysis of human survivin gene expression. Biochem J 1999;344 Pt 2: 305–11.
24. Wu D, Zhau HE, Huang WC, et al. cAMP-responsive element-binding protein regulates vascular endothelial growth factor expression: implication in human prostate cancer bone metastasis. Oncogene 2007;26: 5070–7.
25. Wu TT, Sikes RA, Cui Q, et al. Establishing human prostate cancer cell xenografts in bone: induction of osteoblastic reaction by prostate-specific antigen-producing tumors in athymic and SCID/bg mice using LNCaP and lineage-derived metastatic sublines. Int J Cancer 1998;77:887–94.
26. Matsubara S, Wada Y, Gardner TA, et al. A conditional replication-competent adenoviral vector, Ad-OC-E1a, to cotarget prostate cancer and bone stroma in an experimental model of androgen-independent prostate cancer bone metastasis. Cancer Res 2001; 61:6012–9.
27. Shigemura K, Arbiser JL, Sun SY, et al. Honokiol, a natural plant product, inhibits the bone metastatic growth of human prostate cancer cells. Cancer 2007; 109:1279–89.
28. Zhau HE, Li CL, Chung LW. Establishment of human prostate carcinoma skeletal metastasis models. Cancer 2000;88:2995–3001.
29. Thalmann GN, Anezinis PE, Chang SM, et al. Androgen-independent cancer progression and bone metastasis in the LNCaP model of human prostate cancer. Cancer Res 1994;54:2577–81.
30. Zhau HY, Chang SM, Chen BQ, et al. Androgen-repressed phenotype in human prostate cancer. Proc Natl Acad Sci U S A 1996;93:15152–7.

31. Xu J, Odero-Marah V, Wang R, Chung LWK, Zhau HE. Epithelial-mesenchymal transition and bone-specific microenvironment contribute to the rapid skeletal metastasis in human prostate cancer. J Urol 2005;173:125.
32. Saad F, Gleason DM, Murray R, et al. A randomized, placebo-controlled trial of zoledronic acid in patients with hormone-refractory metastatic prostate carcinoma. J Natl Cancer Inst 2002;94: 1458–68.
33. Hengartner MO. The biochemistry of apoptosis. Nature 2000;407:770–6.
34. Krajewska M, Krajewski S, Epstein JI, et al. Immunohistochemical analysis of bcl-2, bax, bcl-X, and mcl-1 expression in prostate cancers. Am J Pathol 1996;148: 1567–76.
35. Lokeshwar BL. MMP inhibition in prostate cancer. Ann N Y Acad Sci 1999;878:271–89.
36. Oh WK, Kantoff PW. Management of hormone refractory prostate cancer: current standards and future prospects. J Urol 1998;160:1220–9.
37. Bagi CM. Targeting of therapeutic agents to bone to treat metastatic cancer. Adv Drug Deliv Rev 2005;57: 995–1010.
38. Pienta KJ, Smith DC. Advances in prostate cancer chemotherapy: a new era begins. CA Cancer J Clin 2005;55:300–18; quiz 23–5.
39. Clines GA, Guise TA. Molecular mechanisms and treatment of bone metastasis. Expert Rev Mol Med 2008;10:e7.
40. Stewart JM, Gera L, Chan DC, et al. Bradykinin-related compounds as new drugs for cancer and inflammation. Can J Physiol Pharmacol 2002;80: 275–80.
41. Berenson JR, Rajdev L, Broder M. Managing bone complications of solid tumors. Cancer Biol Ther 2006; 5:1086–9.
42. Hirbe AC, Rubin J, Uluckan O, et al. Disruption of CXCR4 enhances osteoclastogenesis and tumor growth in bone. Proc Natl Acad Sci U S A 2007;104: 14062–7.
43. Miwa S, Mizokami A, Keller ET, Taichman R, Zhang J, Namiki M. The bisphosphonate YM529 inhibits osteolytic and osteoblastic changes and CXCR-4-induced invasion in prostate cancer. Cancer Res 2005;65:8818–25.
44. Corey E, Brown LG, Quinn JE, et al. Zoledronic acid exhibits inhibitory effects on osteoblastic and osteolytic metastases of prostate cancer. Clin Cancer Res 2003;9:295–306.
45. Chung LW, Huang WC, Sung SY, et al. Stromal-epithelial interaction in prostate cancer progression. Clin Genitourin Cancer 2006;5:162–70.
46. Chung LW, Kao C, Sikes RA, Zhau HE. Human prostate cancer progression models and therapeutic intervention. Hinyokika Kiyo 1997;43:815–20.
47. Ling X, Bernacki RJ, Brattain MG, Li F. Induction of survivin expression by taxol (paclitaxel) is an early event, which is independent of taxol-mediated $G_2$/M arrest. J Biol Chem 2004;279:15196–203.

npg

ORIGINAL ARTICLE

# EPLIN downregulation promotes epithelial–mesenchymal transition in prostate cancer cells and correlates with clinical lymph node metastasis

S Zhang[1], X Wang[2], AO Osunkoya[1,3], S Iqbal[1], Y Wang[1], Z Chen[2], S Müller[3], Z Chen[4], S Josson[5], IM Coleman[6], PS Nelson[6], YA Wang[7], R Wang[5], DM Shin[2], FF Marshall[1], O Kucuk[1,2], LWK Chung[5], HE Zhau[5] and D Wu[1]

[1]Department of Urology and Winship Cancer Institute, Emory University School of Medicine, Atlanta, GA, USA; [2]Department of Hematology and Medical Oncology, Winship Cancer Institute, Emory University School of Medicine, Atlanta, GA, USA; [3]Department of Pathology & Laboratory Medicine, Emory University School of Medicine, Atlanta, GA, USA; [4]Department of Biostatistics and Bioinformatics, Rollins School of Public Health, Emory University, Atlanta, GA, USA; [5]Uro-Oncology Research Program, Department of Medicine, Cedars-Sinai Medical Center, Los Angeles, CA, USA; [6]Division of Human Biology, Fred Hutchinson Cancer Research Center, University of Washington, Seattle, WA, USA and [7]Ocean NanoTech, LLC, Springdale, AR, USA

Epithelial–mesenchymal transition (EMT) is a crucial mechanism for the acquisition of migratory and invasive capabilities by epithelial cancer cells. By conducting quantitative proteomics in experimental models of human prostate cancer (PCa) metastasis, we observed strikingly decreased expression of EPLIN (epithelial protein lost in neoplasm; or LIM domain and actin binding 1, LIMA-1) upon EMT. Biochemical and functional analyses demonstrated that EPLIN is a negative regulator of EMT and invasiveness in PCa cells. EPLIN depletion resulted in the disassembly of adherens junctions, structurally distinct actin remodeling and activation of β-catenin signaling. Microarray expression analysis identified a subset of putative EPLIN target genes associated with EMT, invasion and metastasis. By immunohistochemistry, EPLIN downregulation was also demonstrated in lymph node metastases of human solid tumors including PCa, breast cancer, colorectal cancer and squamous cell carcinoma of the head and neck. This study reveals a novel molecular mechanism for converting cancer cells into a highly invasive and malignant form, and has important implications in prognosis and treating metastasis at early stages.
*Oncogene* advance online publication, 30 May 2011; doi:10.1038/onc.2011.199

## Introduction

Acquisition of migratory and invasive capabilities by cancer cells at the primary site is the first step in tumor

Correspondence: Dr D Wu, Department of Urology and Winship Cancer Institute, Emory University School of Medicine, 1365 Clifton Road, NE, Building B, B4108, Atlanta, GA 30322, USA.
E-mail: dwu2@emory.edu or Dr HE Zhau, Uro-Oncology Research Program, Department of Medicine, Cedars-Sinai Medical Center, Los Angeles, CA, USA.
E-mail: Haiyen.Zhau@cshs.org

metastasis (Fidler, 2003). This process resembles epithelial–mesenchymal transition (EMT), a highly conserved cellular program in embryonic development. During EMT, epithelial cells lose polarity and gain motility through downregulation of epithelial markers, disruption of the cadherin/catenin adhesion complex and re-expression of mesenchymal molecules, which are necessary for invasion and metastasis. Although demonstrating this potentially rapid and transient process *in vivo* has been difficult, and data linking this process to tumor progression are limited and controversial, mounting experimental and clinical evidence, however, supports a crucial role for EMT in cancer metastasis. A number of EMT-related factors and pathways, such as Snail, wnt/β-catenin and hedgehog signaling have been shown to be shared by embryonic development and tumor progression. The EMT concept, therefore, provides valuable insight into molecular and cellular mechanisms controlling metastasis (Thiery *et al.*, 2009).

Metastatic cancer cells are characterized by high motility and invasiveness (Yamazaki *et al.*, 2005). Efficient migration and invasion require cancer cells to establish and maintain defined morphological features, often with lost cell polarity. Although stabilization of the actin cytoskeleton is important to the maintenance of an epithelial phenotype, dynamic remodeling of the actin network is crucial for invasive cancer cells to leave the primary tumor, invade through the basement membrane and extravasate to establish metastases at distant organs. However, cell signaling pathways involved in the regulation of cell-cell adhesion and the actin cytoskeleton network in metastatic cancer cells have not been fully elucidated (Machesky and Tang, 2009).

EPLIN (epithelial protein lost in neoplasm; or LIM domain and actin binding 1, LIMA-1) was initially identified as an actin-binding protein that was preferentially expressed in human epithelia but frequently lost in cancerous cells (Maul and Chang, 1999; Song *et al.*, 2002). Two EPLIN isoforms, the 600-residue EPLIN-α and 759-residue EPLIN-β, differ only at the 5′-end, where an alternative RNA-processing event extends the

2

reading frame of EPLIN-β by an additional 160 amino acids (Maul and Chang, 1999; Chen *et al*., 2000). EPLIN contains a centrally located LIM domain that may allow EPLIN to dimerize with itself or associate with other proteins. Both the N- and C-termini of EPLIN bind actin to promote the parallel formation of filamentous actin polymer (F-actin) structures by crosslinking and bundling actin filaments. EPLIN also inhibits the Arp2/3-mediated nucleation of actin filaments and suppresses F-actin depolymerization (Maul *et al*., 2003). A recent study demonstrated EPLIN as a key molecule linking the cadherin–catenin complex to F-actin (Abe and Takeichi, 2008), which may simultaneously stabilize the adhesion belt formed by the adherens junctions and a bundle of cortical actin filaments near the apical surface of epithelial cells (Pokutta and Weis, 2007). The direct interaction between EPLIN and α-catenin via both the N- and C-terminal regions is indispensable for the formation of apical actin belt. These observations indicate that EPLIN may be critical to the maintenance of epithelial phenotypes. Nevertheless, investigation into the role of EPLIN in tumor progression remains rudimentary. A recent report inversely correlated EPLIN expression with the aggressiveness and clinical outcome of breast cancer (Jiang *et al*., 2008).

By conducting quantitative proteomics using an experimental model of human prostate cancer (PCa) metastasis, we observed strikingly decreased EPLIN expression upon EMT. Biochemical and functional analyses indicated that EPLIN is a negative regulator of EMT and invasiveness in PCa cells. Importantly, EPLIN downregulation correlated with lymph node metastases in PCa and other solid tumors. These studies reveal a novel role of EPLIN in the regulation of EMT and tumor metastasis.

## Results

### *Quantitative proteomic analysis of protein expression profile in a prostate cancer EMT model*
Previously we reported the androgen refractory cancer of the prostate (ARCaP) cell lineage as an experimental model that resembles the classical descriptions of EMT and closely mimics the clinical pathophysiology of PCa metastasis (Xu *et al*., 2006; Zhau *et al*., 2008). The more epithelial ARCaP$_E$ and more mesenchymal ARCaP$_M$ cells are lineage-related, defined as genetically identical, but behaviorally and phenotypically different. ARCaP$_E$ cells display typical cobblestone morphology and have a relatively low bone metastatic propensity (12.5%) after intracardiac injection in immunocompromised mice, whereas ARCaP$_M$ cells have spindle-shaped fibroblastic morphology associated with increased expression of vimentin and reduced expression of epithelial markers. Importantly, the switch in morphology and gene expression in ARCaP$_M$ cells is associated with high metastatic propensity to skeleton (100%) and soft tissues (33% to adrenal gland). We and others reported that EMT in ARCaP$_E$ cells can be induced by soluble growth factors *in vitro* or by direct interaction with mouse skeleton *in situ* (Graham *et al*., 2008; Zhau *et al*., 2008).

To gain an unbiased insight into the molecular mechanisms underlying PCa EMT, we used an internally standardized gel-free quantitative proteomic technique, cleavable isotope-coded affinity tag (cICAT) analysis using stable isotope tags ($^{12}$C and $^{13}$C), in combination with two-dimensional liquid chromatography-tandem mass spectrometry (Khwaja *et al*., 2006, 2007), to compare protein expression patterns in the total lysates of ARCaP$_E$ and ARCaP$_M$ cells. We identified 343 unique proteins as expressed in both ARCaP$_E$ and ARCaP$_M$ cells when a ProtScore threshold of 1.3 was used (corresponding to >95% protein confidence) (Table 1a). Among them, 76 proteins showed differential expression between the cell lines that was considered statistically significant with a *P*-value <0.05: a total of 31 proteins were found to be increased (≥1.20-fold) and 45 proteins were found to be downregulated (≤0.85-fold) in ARCaP$_M$ cells (Table 1b). These proteins had diverse molecular functions, including cell structure and motility, cell communication, DNA binding and gene expression, metabolism and signal transduction (Supplementary Figure S1). In agreement with our previous reports (Xu *et al*., 2006; Zhau *et al*., 2008), proteomics validated increased expression of mesenchymal marker (vimentin) and decreased expression of epithelial markers (cytokeratin-8 and -18) in ARCaP$_M$ cells.

### *EPLIN downregulation is associated with EMT in the experimental models of prostate cancer*
Intriguingly, a striking downregulation of EPLIN-β (by 4.5-fold, Table 1b) was observed in ARCaP$_M$ cells. Western blotting (Figure 1a, left panel) and immunocytochemical (Figure 1a, right panel, top) analyses confirmed that both EPLIN-β and -α isoforms were abundantly expressed in ARCaP$_E$ cells and reduced significantly in ARCaP$_M$ cells. Consistently, immunohistochemical (IHC) analysis showed that EPLIN was substantially expressed in ARCaP$_E$ tumor subcutaneously inoculated in athymic nude mice, but significantly reduced in ARCaP$_M$ tumor (Figure 1a, right panel, bottom). These data indicated that EPLIN downregulation correlated with increased *in vivo* metastatic potential in the ARCaP EMT model. Supporting this notion, a similar association between EPLIN expression and invasive phenotypes was observed in other experimental models of PCa and squamous cell carcinoma of the head and neck (SCCHN) (Supplementary Figure S2). It was interesting to note that the two EPLIN isoforms were differentially expressed in a cell context-dependent manner: EPLIN-α is prevalently presented in SCCHN cells (Supplementary Figure S2B), whereas EPLIN-β is the major isoform in LNCaP, C4-2 and MCF-7 cells (Supplementary Figures S3A and B). In comparison, EPLIN-α and -β appeared to be equally expressed by ARCaP and PC3 cells (Figure 1a, Supplementary Figure S3A).

### *EPLIN depletion promotes EMT and induces the remodeling of the actin cytoskeleton*
To investigate the role of EPLIN in the regulation of EMT, ARCaP$_E$ cells were transiently transfected with

**Table 1** Quantitative proteomic analysis of protein expression in PCa cells

| Confidence (ProtScore) cutoff | Proteins identified | Proteins before grouping | Distinct peptides | Spectra identified | % of total spectra |
|---|---|---|---|---|---|
| *a. Report statistics of cICAT proteomics in ARCaP$_E$ and ARCaP$_M$ cells (2338 total spectra):* | | | | | |
| >99 (2.0) | 160 | 804 | 798 | 1823 | 78.0 |
| >95 (1.3) | 343 | 1607 | 998 | 2178 | 93.2 |
| >66 (0.47) | 458 | 2064 | 1121 | 2319 | 99.2 |

| Accession | Protein | Fold change[†,a] |
|---|---|---|
| *b. Proteins significantly altered in ARCaP$_E$ and ARCaP$_M$ cells* | | |
| *Increased expression* | | |
| IPI00103355.1 | Cytochrome P450 2F1 | 2.0225 |
| IPI00418471.5 | Vimentin | 1.8046 |
| IPI00418169.3 | Annexin A2 isoform 1 | 1.6253 |
| IPI00220327.2 | Keratin, type II cytoskeletal 1 | 1.5625 |
| IPI00556038.2 | cDNA FLJ20203 fis, clone COLF1334 | 1.4706 |
| IPI00014537.3 | Isoform 1 of calumenin precursor | 1.4183 |
| IPI00013991.1 | Isoform 1 of tropomyosin beta chain | 1.3734 |
| IPI00550766.1 | NNP-1 protein | 1.3666 |
| IPI00376215.2 | Isoform 2 of DNA-dependent protein kinase catalytic subunit | 1.3567 |
| IPI00414264.2 | Sorcin isoform b | 1.3444 |
| IPI00171152.1 | Abhydrolase domain-containing 11 isoform 2 | 1.3379 |
| IPI00217468.2 | Histone H1.5 | 1.315 |
| IPI00018349.5 | DNA replication licensing factor MCM4 | 1.3106 |
| IPI00183695.8 | Protein S100-A10 | 1.3048 |
| IPI00398585.5 | Isoform 2 of Hook homolog 2 | 1.3004 |
| IPI00025491.1 | Eukaryotic initiation factor 4A-I | 1.2984 |
| IPI00741886.2 | PREDICTED: similar to HLA class II histocompatibility antigen, DRB1-1 beta chain precursor | 1.2858 |
| IPI00157351.3 | OTTHUMP00000045700 | 1.2857 |
| IPI00009901.1 | Nuclear transport factor 2 | 1.2782 |
| IPI00003362.2 | Hypothetical protein | 1.2753 |
| IPI00797917.1 | 26-kDa protein | 1.263 |
| IPI00220766.3 | Lactoylglutathione lyase | 1.2527 |
| IPI00025512.2 | Heat-shock protein beta-1 | 1.2498 |
| IPI00023006.1 | Actin, alpha cardiac muscle 1 | 1.2437 |
| IPI00478970.1 | Hypothetical protein MGC16372 | 1.2418 |
| IPI00029048.2 | Tubulin-tyrosine ligase-like protein 12 | 1.2403 |
| IPI00029744.1 | Single-stranded DNA-binding protein, mitochondrial precursor | 1.2339 |
| IPI00009904.1 | Protein disulfide-isomerase A4 precursor | 1.23 |
| IPI00220301.4 | Peroxiredoxin-6 | 1.2163 |
| IPI00791157.1 | 16-kDa protein | 1.2157 |
| IPI00216691.4 | Profilin-1 | 1.2029 |
| *Decreased expression* | | |
| IPI00019205.1 | Protein C14orf4 | 0.1028 |
| IPI00218130.2 | Glycogen phosphorylase, muscle form | 0.2191 |
| IPI00008918.1 | Isoform beta of LIM domain and actin-binding protein 1; EPLIN-beta | 0.2218 |
| IPI00384897.3 | PREDICTED: similar to Mucin-5B precursor | 0.2543 |
| IPI00032313.1 | Protein S100-A4 | 0.5059 |
| IPI00003110.2 | Growth factor independence-1B | 0.5779 |
| IPI00744835.1 | Isoform Sap-mu-9 of proactivator polypeptide precursor | 0.5838 |
| IPI00291809.4 | PREDICTED: similar to ankyrin repeat domain 24 | 0.6056 |
| IPI00219757.12 | Glutathione *S*-transferase P | 0.6144 |
| IPI00218914.4 | Retinal dehydrogenase 1 | 0.6313 |
| IPI00030154.1 | Proteasome activator complex subunit 1 | 0.6323 |
| IPI00789310.1 | 37-kDa protein | 0.6374 |
| IPI00797038.1 | Mitochondrial phosphoenolpyruvate carboxykinase 2 isoform 1 precursor | 0.6586 |

**Table 1** Continued

| Accession | Protein | Fold change[†,a] |
|---|---|---|
| IPI00746205.1 | Proteasome activator subunit 2 | 0.6848 |
| IPI00747047.1 | Treacle major isoform | 0.6892 |
| IPI00418790.2 | Echinoderm microtubule-associated protein-like 5 | 0.694 |
| IPI00514204.3 | Lamin A/C | 0.7052 |
| IPI00215911.2 | DNA-(apurinic or apyrimidinic site) lyase | 0.7139 |
| IPI00017297.1 | Matrin-3 | 0.7177 |
| IPI00784347.1 | Keratin, type I cytoskeletal 18 | 0.7218 |
| IPI00472448.1 | Isoform 1 of HLA class I histocompatibility antigen, A-11 alpha chain precursor | 0.7227 |
| IPI00554648.2 | Keratin, type II cytoskeletal 8 | 0.7258 |
| IPI00018755.1 | High-mobility group protein 1-like 10 | 0.726 |
| IPI00017510.3 | Cytochrome *c* oxidase subunit-2 | 0.7319 |
| IPI00007752.1 | Tubulin beta-2C chain | 0.7489 |
| IPI00794319.1 | 9-kDa protein | 0.7515 |
| IPI00337544.7 | Phosphodiesterase 4D-interacting protein isoform-5 | 0.7561 |
| IPI00303476.1 | ATP synthase subunit beta, mitochondrial precursor | 0.7733 |
| IPI00292387.5 | Isoform Alpha of nucleolar phosphoprotein p130 | 0.7842 |
| IPI00024920.1 | ATP synthase delta chain, mitochondrial precursor | 0.7913 |
| IPI00550020.2 | Parathymosin | 0.7927 |
| IPI00647118.1 | 14-kDa protein | 0.8043 |
| IPI00007765.5 | Stress-70 protein, mitochondrial precursor | 0.8068 |
| IPI00549248.4 | Isoform 1 of nucleophosmin | 0.8094 |
| IPI00020984.1 | Calnexin precursor | 0.8123 |
| IPI00000874.1 | Peroxiredoxin-1 | 0.8196 |
| IPI00025086.3 | Cytochrome *c* oxidase subunit 5A, mitochondrial precursor | 0.8253 |
| IPI00008527.3 | 60S-Acidic ribosomal protein P1 | 0.8263 |
| IPI00301311.1 | Isoform 2 of protein SET | 0.8291 |
| IPI00791301.1 | 46-kDa protein | 0.8342 |
| IPI00218200.7 | B-cell receptor-associated protein 31 | 0.8344 |
| IPI00075248.10 | Calmodulin | 0.8388 |
| IPI00479694.1 | PREDICTED: similar to 40S ribosomal protein S26 | 0.8427 |
| IPI00002459.4 | Annexin VI isoform 2 | 0.8438 |
| IPI00000816.1 | 14-3-3 Protein epsilon | 0.8477 |

Abbreviations: ARCaP$_E$, epithelial androgen refractory cancer of the prostate; ARCaP$_M$, mesenchymal ARCap; cICAT, cleavable isotope-coded affinity tag; PCa, prostate cancer.
Report parameters: ProtScore threshold: 1.20; show competitor proteins within ProtScore: 1.20; Software version: 1.0.2.
[a]Ratio: relative protein expression in ARCaP$_M$ vs ARCaP$_E$ cells.
[†]$P < 0.05$.

an EPLIN small-interfering RNA (siRNA) that effectively inhibited expression of both EPLIN-β and -α isoforms (Figure 1b, left panel). ARCaP$_E$ cells expressing control siRNA showed a cobblestone-like morphology similar to parent ARCaP$_E$ cells, with tight cell-cell contacts in monolayer cultures. EPLIN depletion in ARCaP$_E$ cells led to loss of cell-cell contacts and the emergence of spindle-shaped and mesenchymal-like morphology (Figure 1b, right panel), indicating the occurrence of EMT in these cells.

Previous studies have demonstrated an important function of EPLIN in stabilizing the actin cytoskeleton (Song *et al.*, 2002; Maul *et al.*, 2003). To investigate whether EPLIN depletion in PCa cells was associated with the reorganization of the actin cytoskeleton, immunofluorescent confocal microscopy was performed (Figure 1c,
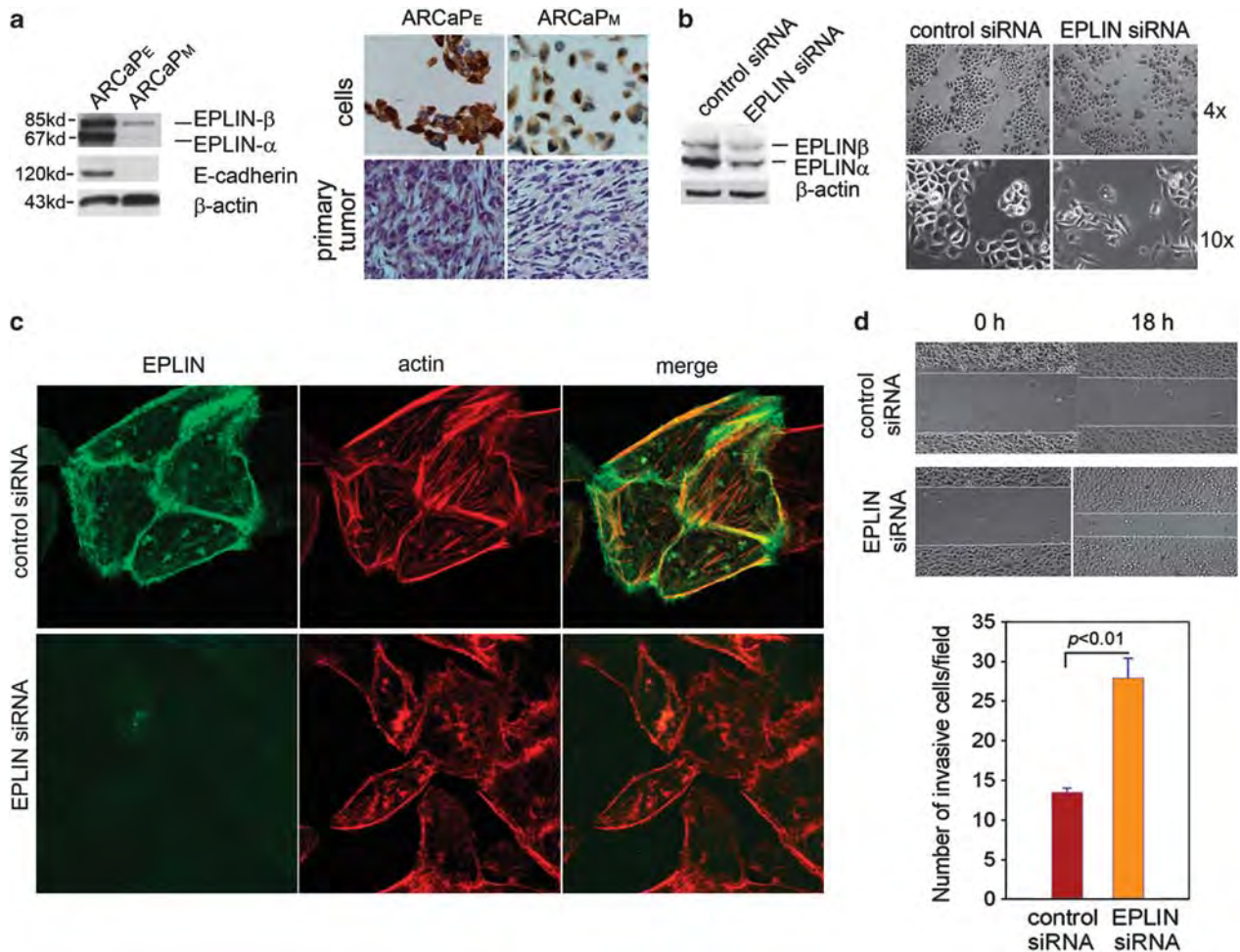
**Figure 1** EPLIN depletion promotes EMT and enhances *in vitro* migration and invasion. (**a**) Expression of EPLIN in ARCaP cells and xenograft tumors. Left panel: western blot analysis of EPLIN and E-cadherin in ARCaP$_E$ and ARCaP$_M$ cells. Right panel: immunocytochemical and immunohistochemical staining of EPLIN expression in ARCaP cells (top) and subcutaneous tumor tissues (bottom). (**b**) Left panel: effects of EPLIN siRNA transfection (72 h) on EPLIN protein expression in ARCaP$_E$ cells. Right panel: effects of EPLIN siRNA transfection on the morphology of ARCaP$_E$ cells. (**c**) Immunofluorescence staining of EPLIN and phalloidin staining of F-actin in ARCaP$_E$ cells transfected with EPLIN or control siRNA for 72 h. (**d**) Effects of EPLIN siRNA transfection on the *in vitro* migration (left panel) and invasion (right panel) in ARCaP$_E$ cells. The assays were performed at 18 h following cell seeding. Bars denote the standard error ($n = 3$).

Supplementary Figure S4). In ARCaP$_E$ cells expressing control siRNA, EPLIN largely colocalized with actin stress fibers as revealed by phalloidin staining. EPLIN was also associated with circumferential fibers that were characterized by a circular arrangement along the adhesion belt and bundles of actin filaments linked to the plasma membrane. EPLIN siRNA transfection reduced EPLIN that colocalized with the circumferential fibers and induced actin remodeling, which was manifested as the disassembly of cellular stress fibers, a concomitant gain of actin foci and formation of prominent membrane ruffles. These data indicated that upon EPLIN depletion, PCa cells may undergo active reorganization of the actin cytoskeleton, which could contribute to increased migratory and invasive capabilities (Yilmaz and Christofori, 2010).

*EPLIN depletion enhances* in vitro *migration and invasion*
We further investigated whether the morphological change of ARCaP$_E$ cells was associated with invasive

behavior *in vitro*. Indeed, EPLIN depletion significantly increased the migratory capability of ARCaP$_E$ cells in a wound-healing assay (Figure 1d, upper panel). The infiltration of ARCaP$_E$ cells through Matrigel in a modified Boyden chamber was also remarkably increased (by ∼twofold) following EPLIN siRNA transfection (Figure 1d, bottom panel). Such effects of EPLIN siRNA transfection were also observed in other PCa (LNCaP, PC3) and human breast cancer (MCF-7) cells (Supplementary Figures S3B–E). These data suggest that EPLIN downregulation could significantly enhance the *in vitro* invasive capabilities in epithelial cancer cells.

*EPLIN depletion suppresses E-cadherin, activates β-catenin signaling and enhances chemoresistance*
We established eight ARCaP$_E$ sublines that, respectively, expressed four different 29-mer EPLIN short-hairpin RNAs (shRNAs) (Supplementary Table S5). These sublines showed similar morphological, biochem-
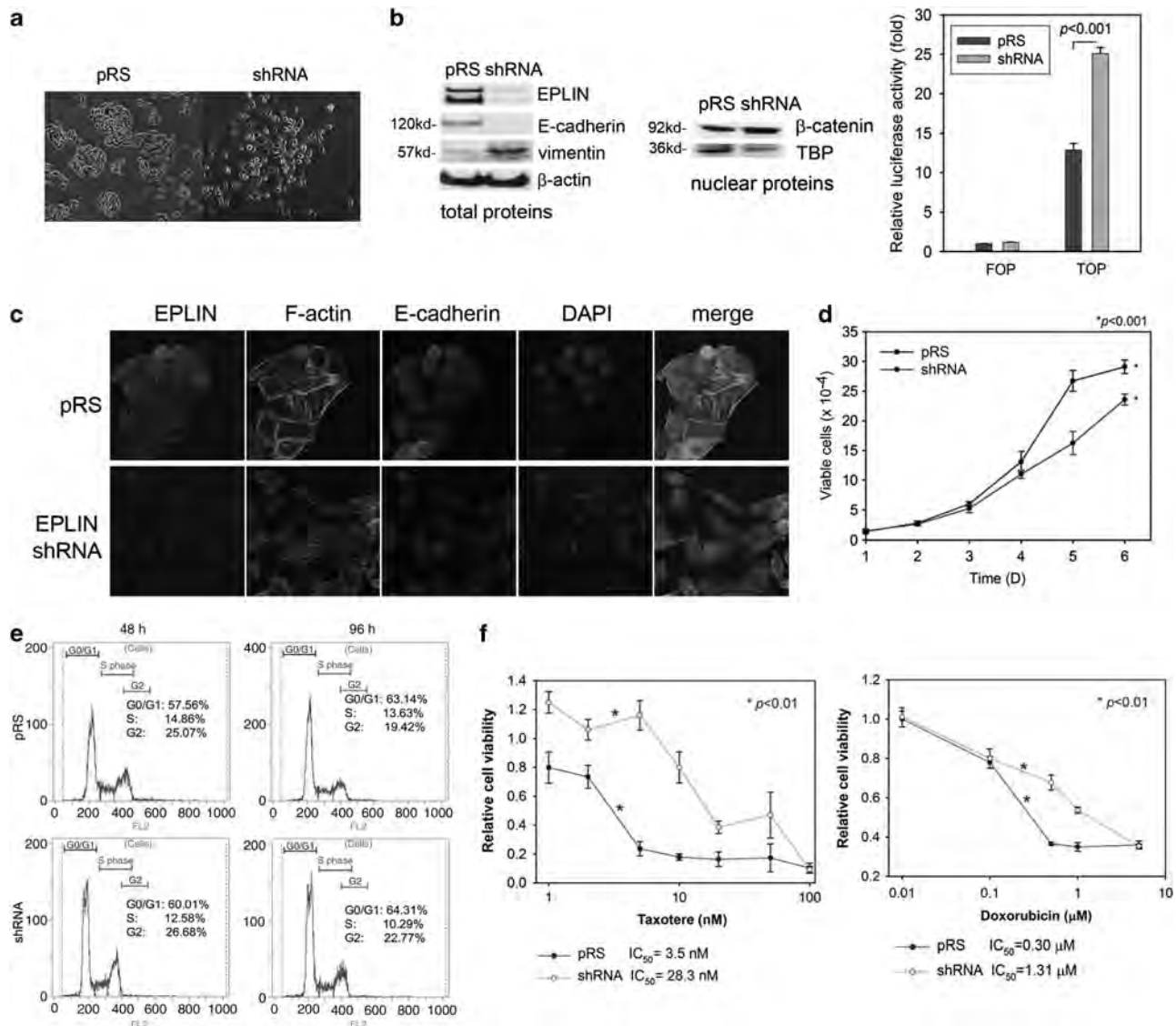
**Figure 2** EPLIN depletion inhibits E-cadherin expression, activates β-catenin signaling, suppresses proliferation and enhances chemoresistance. (**a**) Comparison of the morphology of ARCaP$_E$ cells stably expressing EPLIN shRNA (ARCaP$_E$-shRNA, clone #102) or control pRS (ARCaP$_E$-pRS) constructs. (**b**) Effects of EPLIN depletion on the expression of EMT markers (E-cadherin and vimentin, left panel), nuclear translocation of β-catenin (central panel), and T-cell factor promoter activity (right panel) in ARCaP$_E$ cells. Bars denote the standard error ($n=3$). (**c**) Effects of EPLIN depletion on the actin cytoskeleton and membrane E-cadherin expression in ARCaP$_E$ cells. (**d**) Proliferation of ARCaP$_E$-shRNA cells and control cells. Bars denote the standard error ($n=6$). (**e**) Cell cycle profiles of ARCaP$_E$-shRNA and control cells at 48 and 96 h following cell seeding. $y$ axis: cell numbers. (**f**) Effects of EPLIN depletion on the chemoresistance to docetaxel and doxorubicin in ARCaP$_E$ cells, as analyzed by MTT assays.

ical and behavior characteristics. One of such ARCaP$_E$ sublines (ARCaP$_E$-shRNA clone #102) expressing a shRNA sequence of 5′-TAATAGACGGCAATGGAC CTCACTATCAT-3′ was used as the representative. Consistently, ARCaP$_E$-shRNA cells showed a typical mesenchymal morphology compared with epithelial-like control cells (ARCaP$_E$-pRS), indicating the occurrence of EMT upon EPLIN depletion (Figure 2a). Biochemical analyses found that EPLIN inhibition led to decreased E-cadherin, increased vimentin, nuclear translocation of β-catenin and activation of T-cell factor reporter (Figure 2b). Confocal microscopy further demonstrated that shRNA expression resulted in down-

regulation of E-cadherin on plasma membrane, disassembly of adherens junctions and structurally distinct actin remodeling in PCa cells (Figure 2c). Interestingly, it appeared that EPLIN depletion slightly inhibited proliferation of ARCaP$_E$ cells (Figure 2d), which was associated with an arrested cell cycle progression at the G0/G1 and G2 phases (Figure 2e). On the other hand, however, EPLIN depletion significantly enhanced cell resistance to the treatment of docetaxel and doxorubicin (by ∼eightfold and ∼4.4-fold, respectively) (Figure 2f). These results indicated an important role of EPLIN in the regulation of EMT, actin dynamics, proliferation and survival in PCa cells.
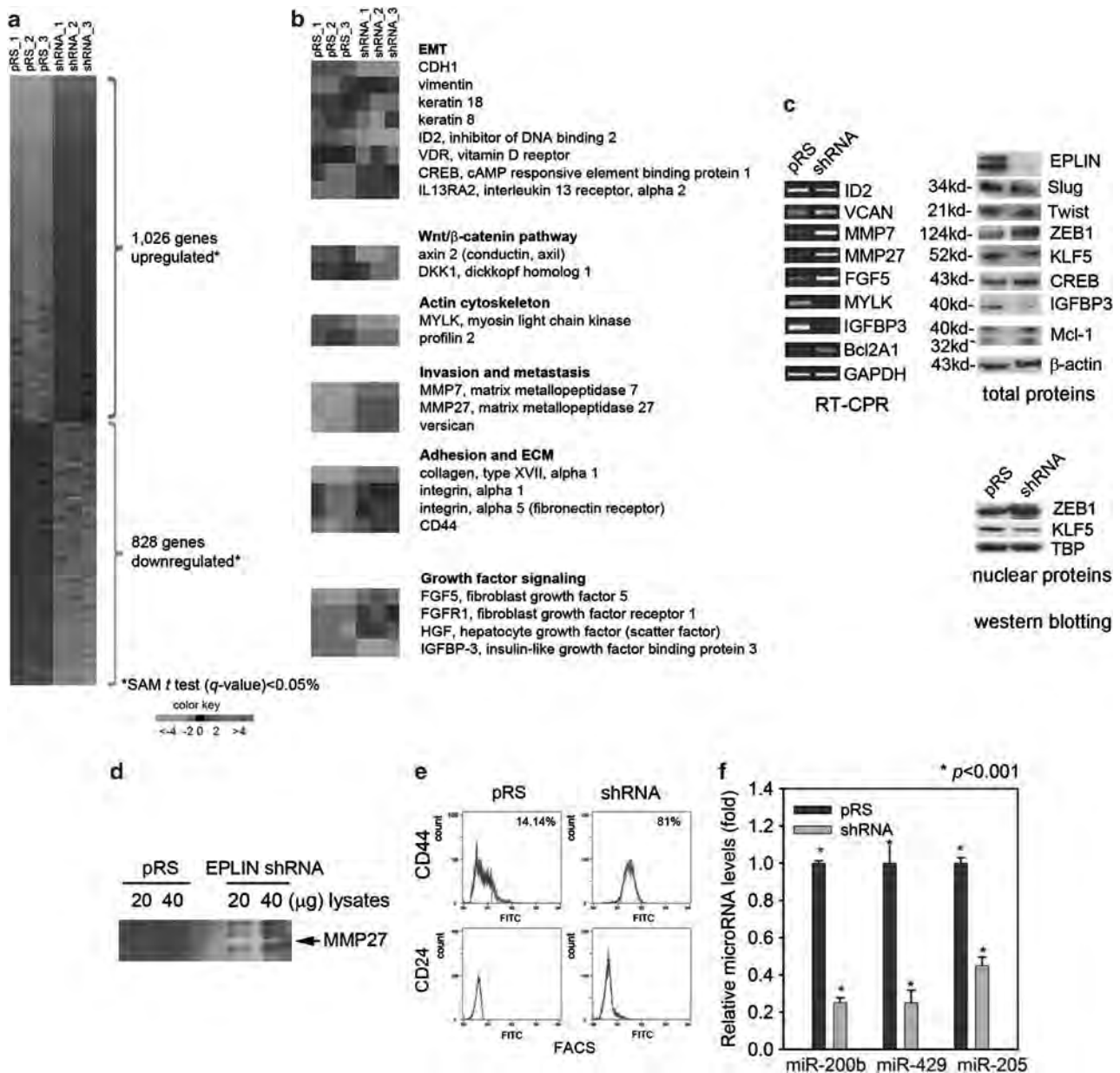
**Figure 3** EPLIN downregulation activates multiple pro-EMT genes. (**a**) Microarray analysis of gene expression profile in ARCaP$_E$-pRS and ARCaP$_E$-shRNA cells. (**b**) Selected genes affected by EPLIN depletion in ARCaP$_E$ cells. (**c**) Validation of several putative EPLIN target genes. Left panel: RT–PCR analysis of the effects of EPLIN depletion on the expression of several selected genes in ARCaP$_E$ cells. Right panel: western blot analysis of the effects of EPLIN depletion on protein expression in the total lysates (top) and nuclear extracts (bottom) in ARCaP$_E$ cells. (**d**) Effects of EPLIN depletion on the expression of active MMP-27 in ARCaP$_E$ cells, as analyzed by gelatin zymogram. (**e**) Effects of EPLIN depletion on the membrane expression of CD44 in ARCaP$_E$ cells, as analyzed by fluorescence-activated cell sorting. $y$ axis: cell numbers. (**f**) Real-time qPCR analysis of the effects of EPLIN depletion on the expression of miR-200b, miR-429 and miR-205 in ARCaP$_E$ cells.

*EPLIN affects a subset of genes involved in EMT and invasion*

To identify genes that are potentially affected by EPLIN, we analyzed the transcriptome of ARCaP$_E$-shRNA cells and control cells. Microarray analysis found that there were 1,026 genes significantly upregulated and 828 genes significantly downregulated in ARCaP$_E$-shRNA cells (Figure 3a), which could be categorized into different function clusters (Supplementary Tables S1 and S2), including those involved in the

regulation of EMT, Wnt/β-catenin signaling, actin cytoskeleton, invasion and metastasis, adhesion and extracellular matrix remodeling and growth factor signaling (Figure 3b; Supplementary Tables S3 and S4). Several approaches were used to validate the differential expression of selected putative EPLIN target genes. Reverse transcription-PCR assays (Figure 3c, left panel) demonstrated increased expression of versican, matrix metalloproteinase-7, Bcl-2A, fibroblast growth factor 5, and downregulation of inhibitor of differentiation 2,
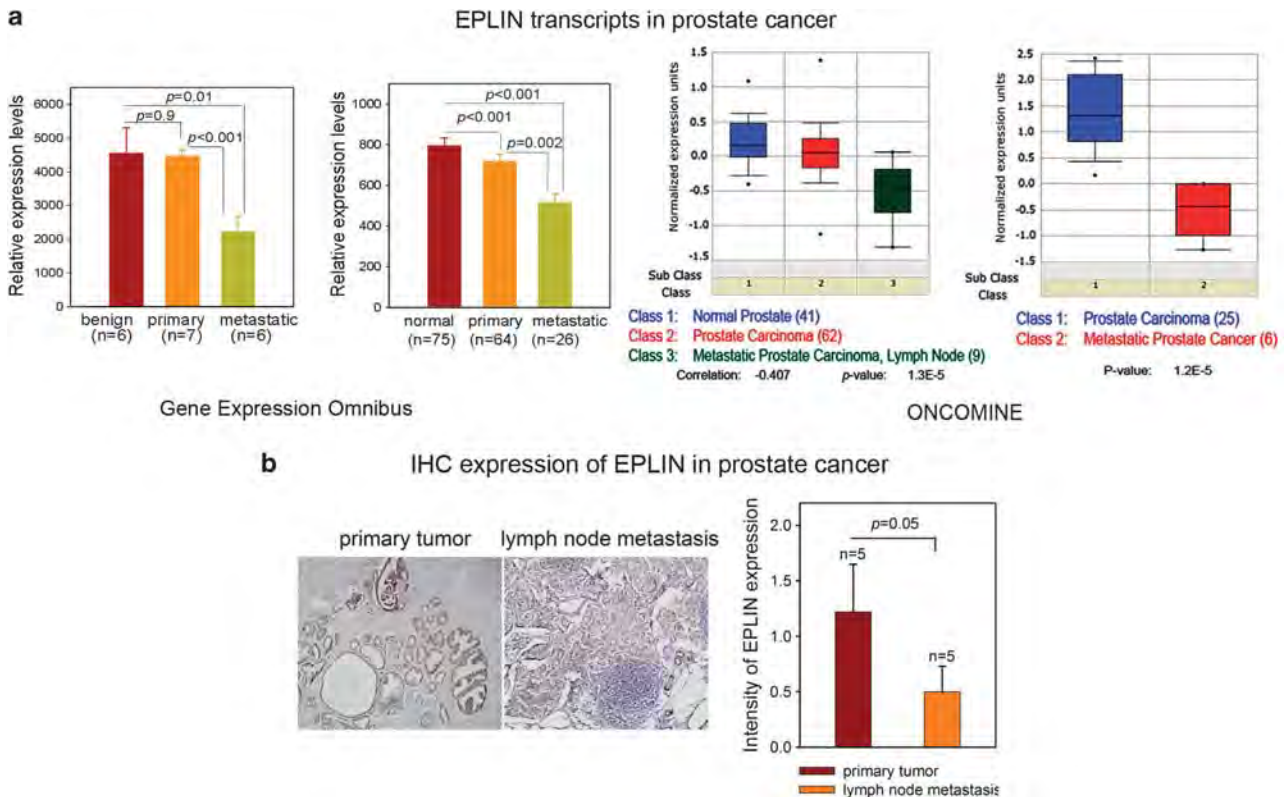
**Figure 4** EPLIN downregulation correlates with PCa lymph node metastasis. (**a**) Microarray data mining of EPLIN transcript expression in primary and metastatic PCa. (**b**) IHC expression of EPLIN were examined in matched pairs of specimens from primary and lymph node metastatic PCa and compared for the statistical significance. Bars denote the standard error.

myosin light chain kinase and insulin-like growth factor-binding protein-3 in ARCaP$_E$-shRNA cells. Western blot analyses (Figure 3c, right panel) confirmed downregulation of insulin-like growth factor-binding protein-3 at protein level, and showed that EPLIN depletion increased expression of cAMP-responsive element-binding protein and myeloid cell leukemia-1 whose upregulation has been associated with clinical PCa metastasis (Wu et al., 2007; Zhang et al., 2010). EPLIN depletion significantly increased expression of zinc-finger E-box-binding homeobox 1, a potent EMT activator that transcriptionally suppresses E-cadherin expression (Wellner et al., 2009), whereas it inhibited Krueppel-like factor 5, a zinc-finger transcription factor implicated in PCa progression (Dong and Chen, 2009). Consistently, increased presence of zinc-finger E-box-binding homeobox 1 and reduced expression of Krueppel-like factor 5 in the nucleus of ARCaP$_E$-shRNA cells were observed. Expression of Slug and Twist, two master regulators of EMT, was not affected by EPLIN depletion in PCa cells. Zymogram assay (Figure 3d) showed that expression of activated MMP-27 was significantly increased upon EPLIN silencing. EPLIN depletion also resulted in a remarkable increase ($\sim$5.6-fold) in the proportion of ARCaP$_E$ cells carrying the CD44$^{high}$/CD24$^{negative}$ marker profile associated with cancer stem cell sub-population (Klarmann et al., 2009) (Figure 3e). Interestingly, EPLIN shRNA suppressed expression of several microRNAs, including

miR-205 and two miR-200 family members (miR-200b and miR-429) (Figure 3f), whose downregulation is thought to be the essential feature of EMT and acquisition of cancer stem cell properties (Lang et al., 2009). These data indicate that EPLIN downregulation may coordinately activate multiple pro-EMT programs in PCa cells.

*EPLIN downregulation is associated with lymph node metastasis in prostate cancer, breast cancer, colon cancer and SCCHN*
We searched two global cancer transcriptome databases, that is, the Gene Expression Omnibus and ONCO-MINE, for the expression pattern of EPLIN in a number of epithelial cancers. Analyses on four independent sets of microarray data on clinical PCa (Lapointe et al., 2004; Yu et al., 2004; Varambally et al., 2005; Chandran et al., 2007) revealed that EPLIN transcripts were expressed at a similar level in primary tumors and normal prostatic tissues, but were remarkably reduced in metastatic tumors (Figure 4a). We examined the IHC staining of EPLIN in matched pairs of PCa tissue specimens from primary PCa and lymph node metastases. As shown in Figure 4b, EPLIN expression was significantly reduced in lymph node metastases.

Analyses of the ONCOMINE database found that metastatic colon cancer expresses significantly lower levels of EPLIN transcripts compared with primary tumors
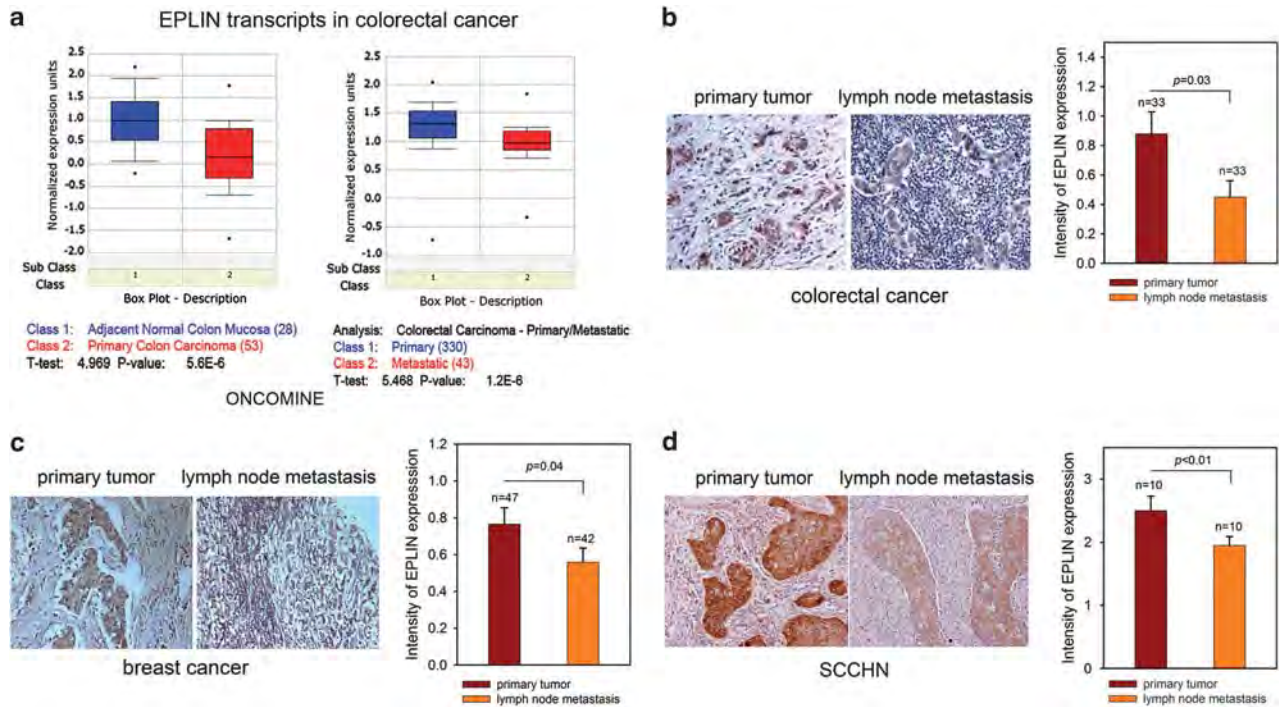
**Figure 5** EPLIN downregulation correlates with clinical lymph node metastasis in breast cancer, colorectal cancer and SCCHN. (**a**) Microarray data mining of EPLIN transcript expression in primary and metastatic colorectal cancer. IHC expression of EPLIN were examined in matched pairs of tumor tissues specimens or TMAs and compared for the statistical significance in human colorectal cancer (**b**), breast cancer (**c**) and SCCHN (**d**). Bars denote the standard error.

(Figure 5a). We examined IHC expression of EPLIN in a human colorectal cancer tissue microarray consisting of matched pairs of primary tumors and lymph node metastases. Figure 5b shows that EPLIN expression was significantly decreased in lymph node metastatic tumors. Similarly, EPLIN immunointensity was markedly reduced in breast cancer lymph node metastases compared with their matched primary tumors (Figure 5c). We finally evaluated IHC expression of EPLIN in 10 pairs of tissue specimens from primary and lymph node metastatic SCCHN. EPLIN expression was also decreased in lymph node metastases (Figure 5d). Collectively, these observations suggested that EPLIN downregulation might be an indicator of clinical metastasis in PCa and several other epithelial cancers.

**Discussion**

In this study, a quantitative proteomics characterized a remarkable downregulation of EPLIN upon EMT in an experimental model of PCa metastasis. Biochemical and functional evidence revealed that EPLIN is a negative regulator of EMT and invasiveness in PCa cells. EPLIN downregulation was found to significantly disrupt epithelial structures, induce actin cytoskeleton remodeling, affect specific gene expression profiles and activate a pro-EMT program. Importantly, using human tumor specimens as the 'gold standard', an inverse correlation between EPLIN expression and clinical lymph node metastasis was observed in a variety of solid tumors.

These studies elucidate a causal role of EPLIN in EMT and support its new function as a tumor metastasis suppressor (Figure 6).

Emerging proteomic techniques offer robust and unbiased approaches for molecular profiling of the complex metastatic process, including EMT, at the protein level (Varambally et al., 2005). However, to date only a limited number of proteomic studies were reported in EMT models of human cancer (Mathias and Simpson, 2009). In this report, we utilized a quantitative proteomic approach, that is, cICAT in combination with two-dimensional liquid chromatography-tandem mass spectrometry, to characterize protein profile in a novel model for PCa EMT and metastasis. A panel of 76 proteins were found to be significantly altered in the epithelial-like and low-invasive ARCaP$_E$ cells and the mesenchymal-like and highly metastatic ARCaP$_M$ cells. Of those, several have been identified to be associated with EMT and metastasis in previous proteomic studies, including increased expression of vimentin, tropomyosin and heat-shock protein β-1, and reduced expression of cytokeratin-8, -18 and 14-3-3ε (Willipinski-Stapelfeldt et al., 2005; Keshamouni et al., 2006, 2009; Wei et al., 2008; Larriba et al., 2010). We also observed a concurrent upregulation of S100A10 and its annexin A2 ligand in ARCaP$_M$ cells, which is interesting as activation of the S100A10/Annexin A2 signaling has been associated with plasminogen activation and increased tumor invasion and metastasis (Kwon et al., 2005; O'Connell et al., 2010). These results validated the application of quantitative proteo-

Epithelial-like, low-invasive cancer cells   Mesenchymal-like, highly-invasive cancer cells
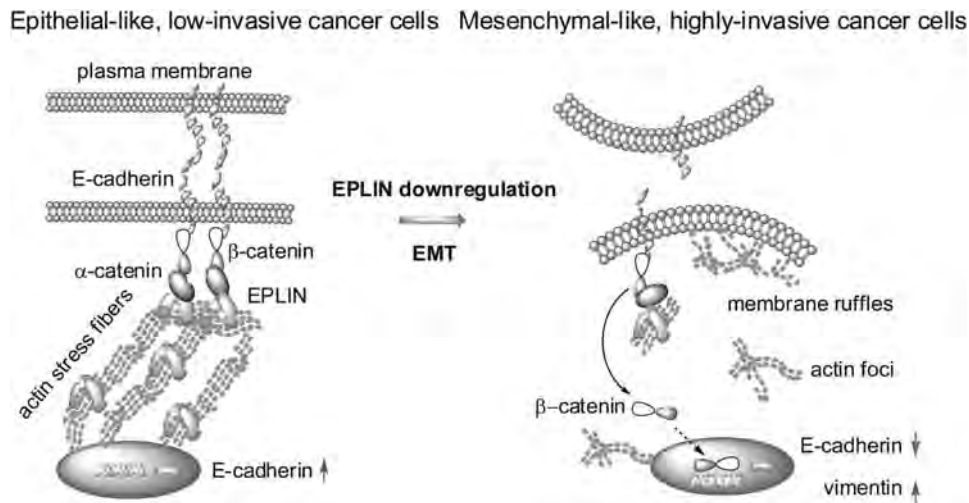


**Figure 6** A proposed model for the role of EPLIN in PCa EMT and metastasis. Epithelial-like, low-invasive cancer cells (such as ARCaP$_E$) are joined by adherens junctions mediated by E-cadherin. The cytoplasmic tails of cadherin dimers bind to intracellular β-catenin. α-catenin binds to β-catenin, and is linked with actin filaments via EPLIN. EPLIN downregulation results in the disintegration of adherens junctions, remodeling of the actin cytoskeleton and activation of β-catenin signaling, which may further lead to the activation of multiple pro-EMT and -metastasis genes. These morphological, molecular and cellular alterations may significantly contribute to EMT and increase the invasiveness of PCa cells.

mics in identifying key factors implicated in EMT and the acquisition of invasiveness in PCa cells.

At the cellular levels, EMT is characterized by the disappearance of the apical-basal polarity in epithelial cells. Remodeling of the actin cytoskeleton is a prerequisite for the acquisition of migratory and invasive capabilities during this process (Yamazaki et al., 2005; Machesky and Tang, 2009; Yilmaz and Christofori, 2009). Our proteomic analysis identified a functional group of proteins that have been implicated in the regulation of actin dynamics and cellular structure (Supplementary Figure S1), which includes six proteins upregulated (vimentin, keratin II, tropomysin, profilin 1, heat-shock protein β-1 and actin-α) and eight proteins downregulated (LIMA1 or EPLIN, S100A4, echinoderm microtubule associated protein like 5, lamin A/C, matrin-3, tubulin-β2C, cytokeratin-18 and -8) in AR-CaP$_M$ cells. Among them, EPLIN has been demonstrated as an indispensable component of the core cell polarity complexes, linking the cadherin–catenin complex to the actin cytoskeleton and actively stabilizing the actin bundles (Song et al., 2002; Maul et al., 2003; Abe and Takeichi, 2008). Mechanistic studies in noncancerous (such as NIH3T3) and cancerous (such as MCF-7) cells indicated that both EPLIN isoforms are capable of suppressing F-actin depolymerization and enhancing the bundling of actin filaments through an Arp2/3-mediated mechanism. Downregulation of EPLIN, therefore, may result in cytoskeletal reorganization due to a loss of stability of mature actin filament structure and facilitated turnover of filaments in epithelial cancer cells. Indeed, as revealed by confocal microscopy, EPLIN depletion in ARCaP$_E$ cells significantly reduced cellular actin stress fibers and promoted the formation of more dynamic actin filament structures such as membrane ruffling, which may contribute to

increased motility of PCa cells. Furthermore, we showed that EPLIN depletion in PCa cells could directly facilitate disassembly of the apical adherens junctions-actin machinery and redistribution of the components of the cadherin–catenin complex, thereby substantially perturbing actin dynamics. These structural alterations may promote transition to mesenchymal morphology and enhance the plasticity and migratory capabilities of epithelial cancer cells (Yamazaki et al., 2005) (Figure 6).

Accumulating evidence support that actin and actin-associated proteins are indispensable components of the regulatory machinery of eukaryotic gene transcription, for example, involving in the modulation of RNA polymerase II-dependent transcription and facilitating RNA polymerase I transcription and possibly downstream events during ribosomal RNA biogenesis (Schneider and Grosschedl, 2007; Percipalle et al., 2009). EPLIN dysregulation may have a remarkable influence on the dynamics of cytoskeleton and its interplay with nuclear architecture, thereby regulating global gene expression. In fact, it has been shown that EPLIN is required for the local accumulation of key cytokinesis proteins at the cleavage furrow during ingression, which is critical to cytokinesis and genomic stability. EPLIN depletion in Hela cells results in cytokinesis failure and formation of multinucleation and aneuploidy (Chircop et al., 2009). In this study, we identified approximately 1800 genes that were significantly affected by EPLIN depletion in PCa cells. Among them, some have been implicated in the regulation of EMT and tumor metastasis, for instance, zinc-finger E-box-binding homeobox 1 (Schmalhofer et al., 2009; Wellner et al., 2009), insulin-like growth factor-binding protein-3 (Renehan et al., 2004), versican (Sakko et al., 2003; Sung et al., 2008) and MMPs (Katiyar, 2006). Notably, EPLIN depletion in several

PCa and breast cancer cells resulted in downregulation of E-cadherin (Figure 2b, Supplementary Figure S3B), a hallmark of EMT and acquired invasiveness in most solid tumors. These interesting findings suggest that EPLIN dysregulation could profoundly affect gene expression at transcriptional levels, which may be an underlying mechanism for EPLIN regulation of EMT.

Loss of expression or function of tumor metastasis suppressors is requisite for the development of local invasion and distant metastases (Smith and Theodorescu, 2009). Previous studies have described several potential metastasis suppressor genes in PCa (Wong et al., 2007; Thiolloy and Rinker-Schaeffer, 2010). EPLIN was initially identified as an epithelial protein that is abundantly expressed in normal epithelia but significantly downregulated at mRNA level in a limited number of cancerous cells (Maul and Chang, 1999). This expression profile suggested that EPLIN might function as a suppressor of tumorigenesis in epithelial cancers. Nevertheless, the role and clinical significance of EPLIN during tumor progression remains largely unknown. Our data presented here demonstrated that EPLIN protein is substantially expressed by most low-invasive epithelial cancer cells examined, but significantly decreased in those with high invasive capabilities (Figure 1a and Supplementary Figure S2), implying the involvement of EPLIN in tumor invasion and metastasis. Biochemical and functional analyses further uncovered the function of EPLIN in the maintenance of epithelial phenotypes in low-invasive PCa cells, and a causal role of EPLIN downregulation in promoting EMT and conferring invasiveness, including enhanced migratory and invasive behaviors and resistance to chemotherapy agents. Interestingly, EPLIN depletion resulted in delayed cell cycles and suppressed in vitro proliferation, an effect that has been observed when overexpressing certain pro-metastasis genes (such as Snail, Slug) in PCa cells (Emadi Baygi et al., 2010; Liu et al., 2010; McKeithen et al., 2010), suggesting a complicated role of EPLIN in the regulation of PCa cell proliferation and differentiation.

To explore the clinical significance of EPLIN in human cancers, we analyzed the expression profile of EPLIN, based on published microarray data. In both PCa and colorectal cancer specimens, EPLIN transcripts were found to be reduced in primary tumors and further decreased in metastatic disease. These observations argue against a simple role of EPLIN as a tumor suppressor, and suggest a new function of EPLIN in late stages of tumor progression in addition to tumorigenesis (Maul and Chang, 1999; Jiang et al., 2008). Indeed, EPLIN protein could be detected at relatively high levels in primary PCa, breast cancer, colorectal cancer and SCCHN, but was significantly reduced in their matched lymph node metastases. Although the numbers of tissue specimens included in this study are limited because of the extreme difficulty of obtaining paired tumor samples from primary and metastatic human cancers, our data clearly demonstrate that EPLIN downregulation could be an indicator of tumor metastasis in a variety of epithelial cancers.

## Materials and methods

### Proteomic analysis
Quantitative proteomic analysis was performed at the Emory University Microchemical and Proteomics Facility. Total proteins from $ARCaP_E$ and $ARCaP_M$ cells were prepared in the absence of proteinase inhibitors by trichloroacetic acid precipitation and resuspended in denaturing buffer. cICAT analysis, in combination with liquid two-dimensional liquid chromatography-tandem mass spectrometry, was performed as described previously (Khwaja et al., 2006, 2007). Briefly, the $ARCaP_E$ and $ARCaP_M$ samples were separately labeled with light and heavy reagent, mixed in equal total protein ratio and digested overnight with trypsin. The peptides were then desalted using a strong cation-exchange cartridge, and the cICAT-modified, cysteine-containing peptides were enriched/purified using a monomeric avidin column (Applied Biosystems, Carlsbad, CA, USA). The biotin tag was cleaved-off by treatment with trifluoroacetic acid, and the sample was dried and reconstituted in 10% formic acid. A portion of the sample was analyzed using an Ultimate 3000 nanoHPLC system (Dionex, Sunnyvale, CA, USA) using a Vydac C18 silica column interfaced to a QSTAR XL mass spectrometer (Applied Biosystems). The MS/MS data from each salt cut were combined and processed by ProteinPilot software (Applied Biosystems) for protein identification and quantification. Only proteins with a ProtScore $>1.0$ (confidence interval $>85\%$) were considered. Proteins were considered differentially expressed if multiple peptides generated concordant cICAT ratios in both analyses. Proteins were grouped into functional categories using the UniProt Knowledgebase.

### Microarray analysis
A reference standard RNA for use in two-color oligo arrays was prepared as described previously (Arnold et al., 2009). Total RNA from triplicate preparations of control and knockdown samples, as well as reference total RNA samples were amplified and hybridized to Agilent 44K whole human genome expression oligonucleotide microarray slides (Agilent Technologies, Inc, Santa Clara, CA, USA) as previously described (Koreckij et al., 2009). Spots of poor quality or average intensity levels $<300$ were removed from further analysis. The Statistical Analysis of Microarray program (Tusher et al., 2001) was used to analyze expression differences between control and knockdown groups using unpaired, two-sample t-tests.

### Immunohistochemical analysis
Human PCa tissue specimens were obtained from the Emory University Hospital Department of Pathology. Human SCCHN tissue specimens were obtained from the Pathology Core of the Emory University Head and Neck Cancer Specialized Programs of Research Excellence. Human colorectal cancer and breast cancer tissue microarrays were purchased from the US BioMax, Inc., (Rockville, MD, USA). IHC staining of EPLIN was performed as described previously (Wu et al., 2007), using a rabbit anti-EPLIN antibody (NB100-2305, Novus Biologicals, LLC, Littleton, CO, USA) at a dilution of 1:50.

### Statistical analysis
Significance levels for comparisons of protein expression in tumor tissue specimens were calculated by using the two-sample t-test. Treatment effects were evaluated using a two-sided Student's t-test. All data represent three or more experiments. Errors are shown as s.e. values of averaged results, and values of $P \leqslant 0.05$ were taken as a significant difference between means.

## Conflict of interest

The authors declare no conflict of interest.

## Acknowledgements

## References

Abe K, Takeichi M. (2008). EPLIN mediates linkage of the cadherin catenin complex to F-actin and stabilizes the circumferential actin belt. *Proc Natl Acad Sci USA* **105**: 13–19.

Arnold RS, Sun CQ, Richards JC, Grigoriev G, Coleman IM, Nelson PS et al. (2009). Mitochondrial DNA mutation stimulates prostate cancer growth in bone stromal environment. *Prostate* **69**: 1–11.

Chandran UR, Ma C, Dhir R, Bisceglia M, Lyons-Weiler M, Liang W et al. (2007). Gene expression profiles of prostate cancer reveal involvement of multiple molecular pathways in the metastatic process. *BMC Cancer* **7**: 64.

Chen S, Maul RS, Kim HR, Chang DD. (2000). Characterization of the human EPLIN (epithelial protein lost in neoplasm) gene reveals distinct promoters for the two EPLIN isoforms. *Gene* **248**: 69–76.

Chircop M, Oakes V, Graham ME, Ma MP, Smith CM, Robinson PJ et al. (2009). The actin-binding and bundling protein, EPLIN, is required for cytokinesis. *Cell Cycle* **8**: 757–764.

Dong JT, Chen C. (2009). Essential role of KLF5 transcription factor in cell proliferation and differentiation and its implications for human diseases. *Cell Mol Life Sci* **66**: 2691–2706.

Emadi Baygi M, Soheili ZS, Schmitz I, Sameie S, Schulz WA. (2010). Snail regulates cell survival and inhibits cellular senescence in human metastatic prostate cancer cell lines. *Cell Biol Toxicol* **26**: 553–567.

Fidler IJ. (2003). The pathogenesis of cancer metastasis: the 'seed and soil' hypothesis revisited. *Nat Rev Cancer* **3**: 453–458.

Graham TR, Zhau HE, Odero-Marah VA, Osunkoya AO, Kimbro KS, Tighiouart M et al. (2008). Insulin-like growth factor-I-dependent up-regulation of ZEB1 drives epithelial-to-mesenchymal transition in human prostate cancer cells. *Cancer Res* **68**: 2479–2488.

Jiang WG, Martin TA, Lewis-Russell JM, Douglas-Jones A, Ye L, Mansel RE. (2008). Eplin-alpha expression in human breast cancer, the impact on cellular migration and clinical outcome. *Mol Cancer* **7**: 71.

Katiyar SK. (2006). Matrix metalloproteinases in cancer metastasis: molecular targets for prostate cancer prevention by green tea polyphenols and grape seed proanthocyanidins. *Endocr Metab Immune Disord Drug Targets* **6**: 17–24.

Keshamouni VG, Jagtap P, Michailidis G, Strahler JR, Kuick R, Reka AK et al. (2009). Temporal quantitative proteomics by iTRAQ 2D-LC-MS/MS and corresponding mRNA expression analysis identify post-transcriptional modulation of actin-cytoskeleton regulators during TGF-beta-Induced epithelial-mesenchymal transition. *J Proteome Res* **8**: 35–47.

Keshamouni VG, Michailidis G, Grasso CS, Anthwal S, Strahler JR, Walker A et al. (2006). Differential protein expression profiling by iTRAQ-2DLC-MS/MS of lung cancer cells undergoing epithelial-mesenchymal transition reveals a migratory/invasive phenotype. *J Proteome Res* **5**: 1143–1154.

Khwaja FW, Reed MS, Olson JJ, Schmotzer BJ, Gillespie GY, Guha A et al. (2007). Proteomic identification of biomarkers in the cerebrospinal fluid (CSF) of astrocytoma patients. *J Proteome Res* **6**: 559–570.

Khwaja FW, Svoboda P, Reed M, Pohl J, Pyrzynska B, Van Meir EG. (2006). Proteomic identification of the wt-p53-regulated tumor cell secretome. *Oncogene* **25**: 7650–7661.

Klarmann GJ, Hurt EM, Mathews LA, Zhang X, Duhagon MA, Mistree T et al. (2009). Invasive prostate cancer cells are tumor initiating cells that have a stem cell-like genomic signature. *Clin Exp Metastasis* **26**: 433–446.

Koreckij TD, Trauger RJ, Montgomery RB, Pitts TE, Coleman I, Nguyen H et al. (2009). HE3235 inhibits growth of castration-resistant prostate cancer. *Neoplasia* **11**: 1216–1225.

Kwon M, MacLeod TJ, Zhang Y, Waisman DM. (2005). S100A10, annexin A2, and annexin a2 heterotetramer as candidate plasminogen receptors. *Front Biosci* **10**: 300–325.

Lang SH, Frame FM, Collins AT. (2009). Prostate cancer stem cells. *J Pathol* **217**: 299–306.

Lapointe J, Li C, Higgins JP, van de Rijn M, Bair E, Montgomery K et al. (2004). Gene expression profiling identifies clinically relevant subtypes of prostate cancer. *Proc Natl Acad Sci USA* **101**: 811–816.

Larriba MJ, Casado-Vela J, Pendas-Franco N, Pena R, Garcia de Herreros A, Berciano MT et al. (2010). Novel snail1 target proteins in human colon cancer identified by proteomic analysis. *PLoS One* **5**: e10221.

Liu J, Uygur B, Zhang Z, Shao L, Romero D, Vary C et al. (2010). Slug inhibits proliferation of human prostate cancer cells via downregulation of cyclin D1 expression. *Prostate* **70**: 1768–1777.

Machesky LM, Tang HR. (2009). Actin-based protrusions: promoters or inhibitors of cancer invasion? *Cancer Cell* **16**: 5–7.

Mathias RA, Simpson RJ. (2009). Towards understanding epithelial-mesenchymal transition: a proteomics perspective. *Biochim Biophys Acta* **1794**: 1325–1331.

Maul RS, Chang DD. (1999). EPLIN, epithelial protein lost in neoplasm. *Oncogene* **18**: 7838–7841.

Maul RS, Song Y, Amann KJ, Gerbin SC, Pollard TD, Chang DD. (2003). EPLIN regulates actin dynamics by cross-linking and stabilizing filaments. *J Cell Biol* **160**: 399–407.

McKeithen D, Graham T, Chung LW, Odero-Marah V. (2010). Snail transcription factor regulates neuroendocrine differentiation in LNCaP prostate cancer cells. *Prostate* **70**: 982–992.

O'Connell PA, Surette AP, Liwski RS, Svenningsson P, Waisman DM. (2010). S100A10 regulates plasminogen-dependent macrophage invasion. *Blood* **116**: 1136–1146.

Percipalle P, Raju CS, Fukuda N. (2009). Actin-associated hnRNP proteins as transacting factors in the control of mRNA transport and localization. *RNA Biol* **6**: 171–174.

Pokutta S, Weis WI. (2007). Structure and mechanism of cadherins and catenins in cell-cell contacts. *Annu Rev Cell Dev Biol* **23**: 237–261.

Renehan AG, Zwahlen M, Minder C, O'Dwyer ST, Shalet SM, Egger M. (2004). Insulin-like growth factor (IGF)-I, IGF binding protein-3, and cancer risk: systematic review and meta-regression analysis. *Lancet* **363**: 1346–1353.

Sakko AJ, Ricciardelli C, Mayne K, Suwiwat S, LeBaron RG, Marshall VR et al. (2003). Modulation of prostate cancer cell attachment to matrix by versican. *Cancer Res* **63**: 4786–4791.

Schmalhofer O, Brabletz S, Brabletz T. (2009). E-cadherin, beta-catenin, and ZEB1 in malignant progression of cancer. *Cancer Metastasis Rev* **28**: 151–166.

Schneider R, Grosschedl R. (2007). Dynamics and interplay of nuclear architecture, genome organization, and gene expression. *Genes Dev* **21**: 3027–3043.

Smith SC, Theodorescu D. (2009). Learning therapeutic lessons from metastasis suppressor proteins. *Nat Rev Cancer* **9**: 253–264.

Song Y, Maul RS, Gerbin CS, Chang DD. (2002). Inhibition of anchorage-independent growth of transformed NIH3T3 cells by epithelial protein lost in neoplasm (EPLIN) requires localization of EPLIN to actin cytoskeleton. *Mol Biol Cell* **13**: 1408–1416.

Sung SY, Hsieh CL, Law A, Zhau HE, Pathak S, Multani AS et al. (2008). Coevolution of prostate cancer and bone stroma in three-dimensional coculture: implications for cancer growth and metastasis. *Cancer Res* **68**: 9996–10003.

Thiery JP, Acloque H, Huang RY, Nieto MA. (2009). Epithelial-mesenchymal transitions in development and disease. *Cell* **139**: 871–890.

Thiolloy S, Rinker-Schaeffer CW. (2010). Thinking outside the box: using metastasis suppressors as molecular tools. *Semin Cancer Biol* **21**: 89–98.

Tusher VG, Tibshirani R, Chu G. (2001). Significance analysis of microarrays applied to the ionizing radiation response. *Proc Natl Acad Sci USA* **98**: 5116–5121.

Varambally S, Yu J, Laxman B, Rhodes DR, Mehra R, Tomlins SA et al. (2005). Integrative genomic and proteomic analysis of prostate cancer reveals signatures of metastatic progression. *Cancer Cell* **8**: 393–406.

Wei J, Xu G, Wu M, Zhang Y, Li Q, Liu P et al. (2008). Overexpression of vimentin contributes to prostate cancer invasion and metastasis via src regulation. *Anticancer Res* **28**: 327–334.

Wellner U, Schubert J, Burk UC, Schmalhofer O, Zhu F, Sonntag A et al. (2009). The EMT-activator ZEB1 promotes tumorigenicity by repressing stemness-inhibiting microRNAs. *Nat Cell Biol* **11**: 1487–1495.

Willipinski-Stapelfeldt B, Riethdorf S, Assmann V, Woelfle U, Rau T, Sauter G et al. (2005). Changes in cytoskeletal protein composition indicative of an epithelial-mesenchymal transition in human micrometastatic and primary breast carcinoma cells. *Clin Cancer Res* **11**: 8006–8014.

Wong SY, Haack H, Kissil JL, Barry M, Bronson RT, Shen SS et al. (2007). Protein 4.1B suppresses prostate cancer progression and metastasis. *Proc Natl Acad Sci USA* **104**: 12784–12789.

Wu D, Zhau HE, Huang WC, Iqbal S, Habib FK, Sartor O et al. (2007). cAMP-responsive element-binding protein regulates vascular endothelial growth factor expression: implication in human prostate cancer bone metastasis. *Oncogene* **26**: 5070–5077.

Xu J, Wang R, Xie ZH, Odero-Marah V, Pathak S, Multani A et al. (2006). Prostate cancer metastasis: role of the host microenvironment in promoting epithelial to mesenchymal transition and increased bone and adrenal gland metastasis. *Prostate* **66**: 1664–1673.

Yamazaki D, Kurisu S, Takenawa T. (2005). Regulation of cancer cell motility through actin reorganization. *Cancer Sci* **96**: 379–386.

Yilmaz M, Christofori G. (2009). EMT, the cytoskeleton, and cancer cell invasion. *Cancer Metastasis Rev* **28**: 15–33.

Yilmaz M, Christofori G. (2010). Mechanisms of motility in metastasizing cells. *Mol Cancer Res* **8**: 629–642.

Yu YP, Landsittel D, Jing L, Nelson J, Ren B, Liu L et al. (2004). Gene expression alterations in prostate cancer predicting tumor aggression and preceding development of malignancy. *J Clin Oncol* **22**: 2790–2799.

Zhang S, Zhau HE, Osunkoya AO, Iqbal S, Yang X, Fan S et al. (2010). Vascular endothelial growth factor regulates myeloid cell leukemia-1 expression through neuropilin-1-dependent activation of c-MET signaling in human prostate cancer cells. *Mol Cancer* **9**: 9.

Zhau HE, Odero-Marah V, Lue HW, Nomura T, Wang R, Chu G et al. (2008). Epithelial to mesenchymal transition (EMT) in human prostate cancer: lessons learned from ARCaP model. *Clin Exp Metastasis* **25**: 601–610.

Supplementary Information accompanies the paper on the Oncogene website (http://www.nature.com/onc)

# Tumor Microenvironment Promotes Cancer Progression, Metastasis, and Therapeutic Resistance

Cell and tissue homeostasis results from the dynamic balance of cell–cell and cell–extracellular component cross-talk that regulates such cell activities as proliferation, differentiation, and apoptosis as well as secretion and activation of soluble factors and/or deposition of extracellular matrix (ECM) components.[1] This dynamic balance includes the interaction of epithelial and mesenchymal basal cells, endothelium, fibroblasts, neuroendocrine cells, smooth muscle cells, inflammatory cells and ECM, activation of laten proteins, infiltration of cytokines, and chemokine and hormone production.[1] These interactions provide the microenvironment for epithelial cells.

Organ-specific human epithelial cells maintain their polarity, grow, survive, and express tissue-specific proteins under microenvironmental regulation. These properties are unique organ-specific phenotypes conferred and maintained by interaction between epithelium and adjacent ECM secreted primarily by the stroma through intimate intercellular signaling pathways. Epithelial cells, the predominant cells of origin of adult cancer, exist in contiguous sheets composed of organized, polarized cells circumscribed by a basement membrane that separates the epithelium from the stroma. Basal cells (mesenchymal epithelial cells) underneath mature prostate epithelial cells continue to renew dying prostate epithelial cells with polarity regulation. Intercellular interaction between these cells, mediated by direct contact, soluble factors, and insoluble ECMs, will determine the growth and differentiation potentials of the entire organ. Disruption of the homeostatic interaction between epithelium and stroma could initiate and promote carcinogenesis. In these instances, carcinogenic insults may trigger additional genetic changes in the epithelial cell compartment over and beyond the inherited traits, through increased genomic instability and decreased DNA repair and apoptotic signaling. Altered

epithelial cells may trigger stromal reactions that in turn confer reciprocal signal cascades in tumor epithelium to promote further carcinogenic processes. These changes can combine or modify to produce a variety of growth factors, chemokines, cytokines, and matrix-degrading enzymes that enhance the proliferation and invasion of the tumor and confer the ability to metastasize to different organs. Ultimately, reciprocal tumor–stroma interaction culminates in increased migratory, invasive, and metastatic behavior of cancer cells.

## Prostate Tumor–Stroma Interaction

Recent evidence suggests that prostate epithelium and stroma interact in a highly organ-specific, androgen-dependent, and temporally related manner. The intimate interaction between prostate cancer and its microenvironment drives reciprocal stromal reactions to prostate tumor epithelium, creating a "vicious cycle" involving the microenvironment and cancer epithelium, which further drives tumor epithelium to develop malignant properties. Figure 1 depicted the models of vicious cycle. Our recent studies demonstrated that this model can be mimicked using a Rotary Cell Culture System (RCCS), which showed that genetic and epigenetic changes of stromal cells can drive cancer cells to become highly tumorigenic *in vivo* in animal studies (Fig 2).

Currently the "seed and soil" hypothesis of prostate cancer bone metastasis consists of three principles. First, neoplasms are biologically heterogeneous and contain subpopulations of cells with different angiogenic, invasive, and metastatic properties.[2,3] Second, the process of metastasis is selective for cells that succeed in invasion and embolization, can survive in the circulation, anchor in a distant capillary bed, and extravasate into and multiply within the organ parenchyma.[4-7] Although some of the steps in this process contain stochastic elements, as a whole, metastasis favors the survival and growth of a few subpopulations of cells that preexist within the parent neoplasm.[5,8] Thus, metastases can have a clonal origin, and different metastases can originate from the proliferation of different single cells.[9] Third, the outcome of metastasis depends on the "cross talk" of metastatic cells with homeostatic mechanisms, which the tumor cells can usurp.[10,11] Therapy for metastasis, therefore, can target not only tumor cells but also the homeostatic factors that promote tumor cell growth, survival, angiogenesis, invasion, and metastasis.

## *Laboratory Observations*

Androgen-independent and metastatic progression of human prostate epithelial cells can be promoted by coinoculating a marginally tumori-
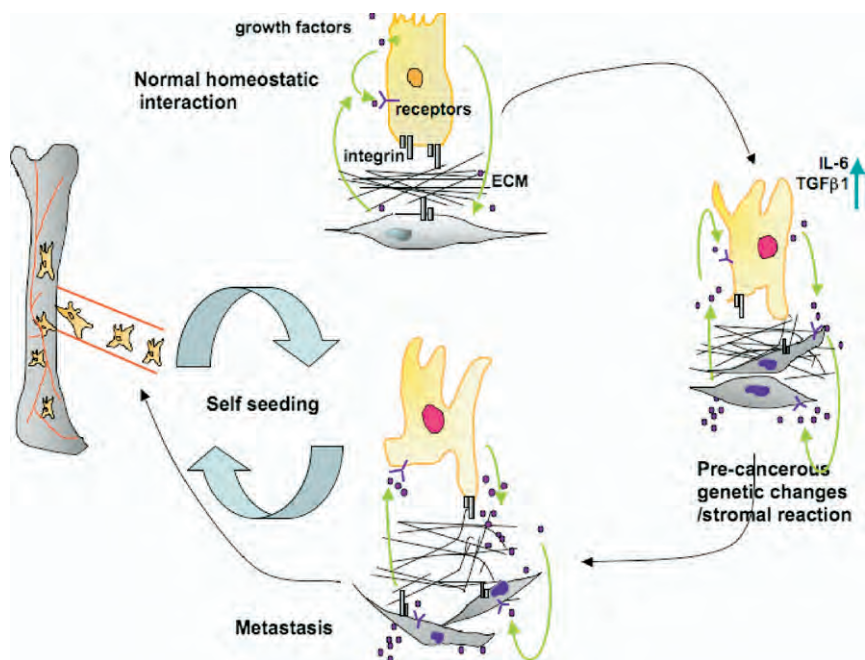
FIG 1. Vicious cycle between prostate cancer and prostate or bone stromal cells results in genetic changes in prostate or bone stromal cells through a reciprocal interaction. This reciprocal cellular interaction could contribute to the invasiveness and metastasis of humane prostate cancer cells to bone and visceral organs. The normal prostate epithelial cell homeostatic interaction with its adjacent stroma through growth factors and extracellular matrices via growth factor receptors or integrins is deranged because of genetic modifications occurring in the epithelium. The genetically altered prostate epithelial cell provokes a stromal desmoplastic reaction, which sets off a chain reaction in reciprocally modulating the cancer epithelium, which become prostate stroma independent and ivades and migrates to bone. The early migrated prostate cancer cells chipping the bone microenvironment and interaction with cells in micorenvironment which provide the education to these cells for "adopt" the cancer cells either from cell proliferated or migratory later through extravasation of prostate cancer cells. (Color version of figure is available online.)

genic human prostate cell line, LNCaP, with a human bone stromal cell line derived from an osteosarcoma *in vivo*.[12,13] By manipulating chimeric LNCaP tumor growth *in vivo* under the influence of bone stromal cells, either in the presence or absence of androgen, the derivative LNCaP sublines C4-2 and C4-2B acquired the ability to become androgen-independent and metastatic, as exhibited by their behaviors in immune-compromised mice. To ascertain that cell–cell contact rather than unknown factors from the host were responsible for conferring tumorigenic and metastatic potential to the parental LNCaP cells, we cocultured
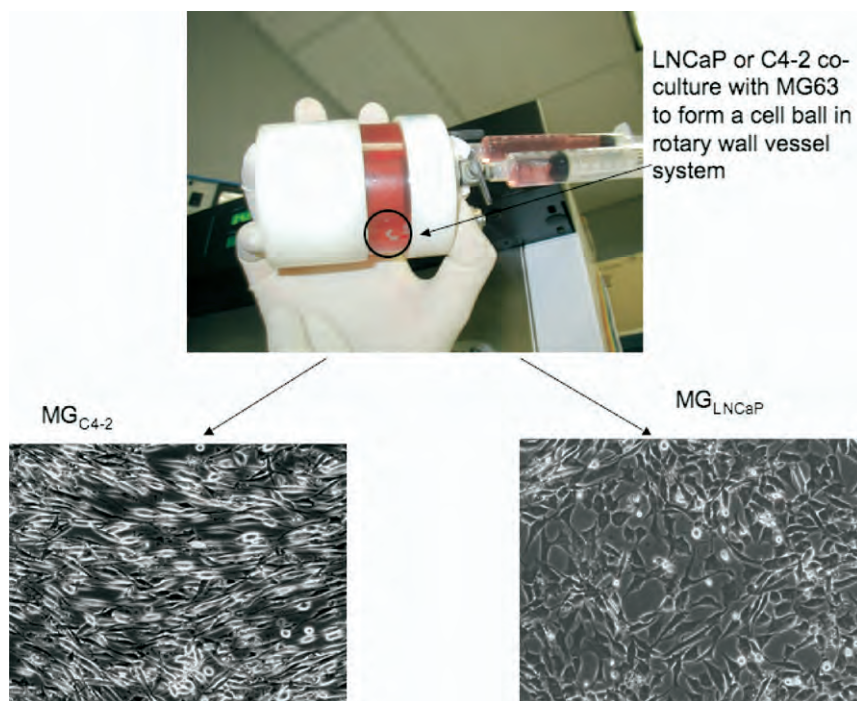
**FIG 2.** 3D-coculture of prostate cancer cells with bone stromal cell (MG63) induced permanently morphological change of MG63. Whereas $MG_{LN}$ exhibited typical spindle cell morphology with randomly dispersed patterns, $MG_{C4-2}$ cells, in contrast, exhibited directional spindle-shaped morphology with cells that are tightly packed and organized to achieve higher cell density on *in vitro* growth. (Color version of figure is available online.)

LNCaP cells with either prostate or bone stromal cells under 3-dimensional (3-D) conditions and observed similar permanent phenotypic, genotypic, and behavioral changes of the parental LNCaP cells as well as stromal cells (unpublished data), including the ability to form tumors in castrated mice and metastasize to distant organs including bone.[14,15] We further tested if the significance of stromal cells *in vitro* as observed in our laboratory by 3-D coculture can be seen *in vivo* by coinoculating tumor and stromal cells. Paired prostate fibroblast cells isolated either from benign (Pt-N) or tumor regions (Pt-C) were carefully separated and cultured. Coinoculation of the androgen-independent prostate cancer cell line, C4-2, with either Pt-N or Pt-Cs showed that chimeric tumors comprised of Pt-C/C4 to 2-Luc grew faster and formed larger tumors in the subcutaneous space than Pt-N/C4 to 2-Luc chimeric tumors (unpublished data). These results were confirmed by the measurement of serum

PSA in tumor-bearing hosts and luciferase activity associated with tumor specimens. Confirmation by other laboratories showed that prostate tumor growth *in vivo* could be accelerated by cancer-associated, but not by benign tissue-associated stromal fibroblasts.[16,17]

## Role of Prostate Fibromuscular Stromal Cells in Prostate Tumor Growth and Progression

These results taken together suggest that tumor stroma can confer "inductive" or "adaptive" cues to the responding tumor epithelium and is directly responsible for the altered behavior of tumor epithelium. However, tumor–stroma interaction is reciprocal. Not only can stroma "induce" or "select" the phenotypic and genotypic changes in tumor epithelial cells, tumor epithelium can also induce genetic and phenotypic changes in stroma after tight association *in vivo*. It appears that **both** tumor and stroma are involved in controlling tumor growth and the subsequent progression of tumor epithelium to androgen-independence and acquisition of local invasive and distant metastatic potential in experimental models of human prostate cancer (Fig 1). Genetically and phenotypically altered epithelial cells induce a stromal reaction that in turn induces a reciprocal epithelial reaction. The serial interactions form a vicious cycle that not only drives epithelial cancer progressive to androgen-independent local invasion and metastasis but also causes epithelial cells lose their apical–basal polarity and thus assume a less well differentiated state.[18,19] This dramatic alteration of the epithelial cell phenotype can lead to increased cell proliferation and tumorigenesis.[20] Recent studies indicate that several factors are involved in the reciprocal interaction between tumor and stroma cells, such as TGF-$\beta$, HGF/SF, ROS, and RNS.[1,21-25] Hill and coworkers reported the mutation of stromal cells, induced by prostate cancer epithelial cells, induced the loss of p53 and helped prostate cancer cells escape regulation.[22] In contrast to tumor-associated stroma, stromal cells associated with normal tissues have a low proliferative index, probably secrete only the factors necessary to maintain normal tissue function,[26] and appear to be less responsive to inductive cues from normal epithelium.

## Stroma Reaction to Tumor Epithelium

Since stromal cells from normal tissues are less inductive, or often noninductive, the experimental data imply that stromal cells exposed to tumor epithelium could be "activated" and acquire an inductive potential driving the subsequent neoplastic process. Two lines of evidence suggest that stromal cells regulate cancer cells. First, morphologic "desmoplastic"

stromal response to tumor epithelium often occurs around either primary or metastatic tumor epithelium.[27-29] A desmoplastic stroma response is characterized by increased proliferation of fibromuscular stromal cells and enhanced deposition of ECMs, such as tenascin or biglycan,[28,30,31] surrounding the tumor epithelium. This active process could be viewed as a part of the host defense mechanism to curtail or restrict tumor expansion.[31] Conversely, this reaction and accompanying increase in stromal cell number could provide a fertile soil supporting the growth and invasion of tumor epithelium through the increased production by stromal cells of growth factors and stroma-associated ECMs.[32,33] Thus, global changes in the microenvironment adjacent to the tumor could provide selective growth and survival advantages for certain tumor cell clones, particularly in androgen-deprived conditions. Second, stroma reaction to tumor epithelium may be *irreversible*, if the reacting stromal cells receive an "inductive cue" from tumor epithelium to undergo transdifferentiation, whereby stromal fibroblasts adjacent to the tumor epithelium convert both morphologically and phenotypically to myofibroblasts.[21,22,25]

Increased extracellular deposition, such as the increased expression of vimentin, pro-collagen I, desmin, calponin, and tenascin, has been shown in cancer-associated myofibroblasts.[25,34-38] Using the laser capture microdissection (LCM) technique, genetic aberrations were detected in the fibromuscular stromal compartment surrounding tumor epithelium, further supporting the reciprocal nature of the tumor–stroma interaction.[39] However, the mechanisms of the genetic and phenotypic response of stroma to adjacent tumor epithelium are still unclear. Several possible mechanisms may involved, including: (a) transition or interconversion of epithelium to stroma, or epithelial-mesenchymal transition (EMT)[40]; (b) irreversible induction of stroma changes, both at the morphologic and the biochemical levels, by soluble and insoluble factors secreted by tumor epithelium[15] (unpublished data); (c) selection of previously existing clones of stromal cell populations and preferential expansion of these clones based on their proliferative and survival advantages, or clonal selection[41]; and (d) the combination of (b) and (c) above; that is, after prolonged adaptation to a tumor-associated stromal microenvironment, permanent genetic changes may occur in the stroma cell population through a poorly understood adaptive mutation mechanism.[42]

## Stromal Response to Early Prostate Inflammatory Atrophy

There is emerging evidence that prostate inflammation may contribute to prostatic carcinogenesis. Chronic inflammation has been asso-

ciated with the development of malignancy in several other organs, such as esophagus, stomach, colon, liver, and urinary bladder.[43,44] Chronic inflammation is thought to incite carcinogenesis by causing cell and genome damage, promoting cellular turnover, and creating a tissue microenvironment that can enhance cell replication, angiogenesis, and tissue repair. Epidemiological data have correlated prostatitis and sexually transmitted diseases with an increased risk of prostate cancer and intake of antiinflammatory drugs and antioxidants with a decreased risk.[45] Evidence from genetic and molecular studies also supports the hypothesis that prostate inflammation and/or infection may be a cause of prostate cancer. In 1999, De Marzo and coworkers proposed that proliferative inflammatory atrophy (PIA) is a precursor to PIN and cancer.[46] Inflammatory reactions often result in the activation and recruitment of phagocytic cells (eg, neutrophils and/or tissue macrophages) whose products, such as cytokines, oxidants, and free radicals (reactive oxygen and nitrogen species), result in injury to the tissue. Repeated bouts of the immune-mediated inflammatory response phagocytic cells over many years are thought to play a major role in the pathogenesis of cancer in a number of organ systems.[44] Recent studies indicated the association of inflammation with prostate cancer and elevated expression of BCL-2, glutathione S-transferase (GSTP1), and COX-2 and reduced level of p27$^{Kip1}$ in these patients.[46-48] Another report indicated that prostate cancer stroma frequently exhibits infiltration of CD45RO(+) memory T-lymphocytes.[49] CD8(+)/CD45RO(+) T-cells mainly associate with lumen epithelium as the first line defense system for infection/inflammation responses, but CD4(+)/CD45RO(+) T-cells primary associated with stromal cells in the region of infiltration. This inflammatory infiltration could induce increased growth of myofibroblast cells in prostate cancer patients. An *in vivo* study of $H_2O_2$ and GSTs indicated that hydrogen peroxide ($H_2O_2$) enhances the expression of GSTP1,[50] suggesting that the increased expression of GSTs in PIA may be due to increased concentrations of $H_2O_2$ in the stroma microenvironment, released by phagocytic cells during the PIA stage. The hypothetical mechanism involves repeated tissue damage and regeneration in the presence of highly reactive oxygen. These reactive molecules, ie, $H_2O_2$, released from the inflammatory cells, interact with DNA in the proliferating epithelium to produce permanent genomic alterations, such as frameshift mutation, deletions, and rearrangements, as well as increasing the epithelium proliferative rate.[51,52]

## A Vicious Cycle Between Prostate Stroma and Tumor May Be Responsible for Cancer Progression in Primary Prostate Cancer

The phenotypic switch of stromal cells, extracellular matrix remodeling, increased growth factor availability, elevated protease activity, angiogenesis, and recruitment of inflammatory cells is observed in cancer progression. This stromal response to cancer shows similarity to the wound repair response,[53] and it is possible that these conditions could promote further cancer progression and malignancy. The phenotypic switch between fibroblast and myofibroblast indicates increased extracellular matrix remodeling during prostate cancer progression. In normal prostate, it has been reported that the "stromal network of collagen fibers is loosely woven, fine and smooth in texture," whereas in Gleason-score seven adenocarcinoma the collagen fibers "appeared swollen in diameter" and there is "no regularity in the spatial relationship of the fibers."[54,55] This suggests that remodeling of the extracellular matrix is one of the key features of stromal reaction in prostate cancer.

Studies using tissue and cell recombination models demonstrate that growth and differentiation of the prostate gland depend on reciprocal cellular interaction between prostate epithelium and its adjacent stroma.[17,56] Evidence also suggests that androgen receptor in the stroma rather than in the epithelium may be critical for the growth and differentiation functions of the prostate gland.[57] When normal prostate epithelium[58] or urothelium[59] was used in these studies, the inductive fetal urogenital mesenchyme determined the ultimate size of the tissue-tissue recombinant. However, when prostate tumor tissues,[60] tumor cells derived from the prostate,[61,62] or urinary bladder[63] were used in the experiments, the growth of the tissue–tissue or tissue–cell recombinants was uncontrolled and never reached a state of homeostasis. One interpretation of these results is that signaling between tumor and stroma is aberrant and resembles a vicious cycle, with dysfunctional cytokine trafficking between tumor and host cells.[1,64-66] There are several possible mechanisms for the activation of a vicious cycle between tumor and stroma: (1) tumor cells secrete putative cytokines, growth factors and/or extracellular matrices that alter the morphology and gene expression of the surrounding stroma, such that the altered stroma becomes highly inductive and reciprocally induces the growth and gene expression of tumor epithelium and thus initiates the vicious cycle. Rowley and collaborators provided evidence that stromal fibroblasts surrounding tumor epithelium underwent transdifferentiation to become a morpholog-

ically and biochemically distinct population of myofibroblasts.[25,67] Interestingly, they showed that this type of stroma response to tumor epithelium can predict PSA-free survival in patients with prostate cancer[38] and is regulated by TGF-$\beta$ and androgen secreted by cancer cells.[25] They also demonstrated that the increase of CTGF released in myofibroblasts in the prostate cancer area is the downstream reaction that can promote angiogenesis and prostate cancer tumorigenesis,[68] demonstrating a vicious cycle between prostate cancer and stroma via TGF-$\beta$/CTGF mediation. (2) Tumor cells secrete soluble factors that act in an autocrine manner to promote the vicious cycle regardless of the surrounding stroma. Under certain stress and androgen conditions, increases in growth factors, such as vascular endothelial growth factor (VEGF) production by tumor cells, have been observed.[69-71] Increased VEGF was shown to induce more oxygen stress and initiate the vicious cycle by promoting more VEGF production by tumor cells, eventually causing an accumulation of neovasculature surrounding the tumor epithelium.[72,73] (3) The intrinsic genetic instability of tumor cells can be promoted by tumor-microenvironment interaction.[22,74] A recent study by Hill and coworkers showed that inhibition of pRb in prostate cancer epithelium induced a paracrine p53 response that suppressds fibroblast proliferation in associated stroma.[22] This outstanding study showed that cancer evolution can indeed involve the selection of genetic changes in the microenvironment as a result of nonautonomous pressures imposed by oncogenic stress within the epithelium.

## Potential Factors Responsible for Activating Prostate Carcinogenesis and Driving the "Vicious Cycle" of Prostate Stroma and Tumor

*Integrins.* Integrins are a large family of glycoproteins that form cell adhesion and signaling receptors which mediate cell death, proliferation, migration, and tissue remodeling in response to stimuli from the ECM.[75] In addition to controlling cell adhesion and shape, integrins also transmit signals, either by physical association with several growth factor receptors, or directly through recruitment of nonreceptor tyrosine kinases from the focal adhesion kinase (FAK) and Src families.[76] The consequent downstream signals, especially via the mitogen-activated protein kinase (MAPK) and phosphoinositide 3-kinase (PI3K) transduction cascades, are critical for regulation of cyclin-dependent kinases (CDKs) and cell-cycle progression in a process known as "outside-in" signaling.[1] Thus, maintaining normal cellular functions is one of the modes by which integrins prevent apoptotic cell death. In addition, integrin receptors are involved in

cell resistance to apoptotic stimuli that activate the intrinsic cell death pathway (also called the stress pathway).[77,78] In this regard, integrins preserve cell viability in response to stress at several levels, including integrin-mediated activation of major cell signaling pathways such as the Ras-activated Raf-MEK-extracellular signal-regulated kinase (ERK) and the PI3K/AKT transduction cascades. These integrin-emanating signals regulate, in turn, the expression and activity of anti- and pro-apoptotic members of the Bcl-2 protein family, as well as the overall expression, function, and localization of these proteins.

The "outside-in" signal of integrin also has been demonstrated in prostate cancer cells, such as $\alpha v\beta 3$ regulation in prostate cancer local and bone metastasis. The $\alpha v\beta 3$ integrin heterodimer has been detected on many different cell types, such as macrophage, endothelial cells, osteoclasts, and prostate cancer epithelial cells.[79] The activation of $\alpha v\beta 3$ in prostate cancer cells is mediated by the FAK pathway that activates the downstream PI3K/Akt pathway.[80] This triggers alterations in cell adhesion and migration of a variety of extracellular matrix proteins, including vitronectin, fibronectin, fibrinogen, laminin, collagen, and osteopontin. $\alpha v\beta 3$ has been shown to be important for prostate cancer bone metastasis by adhesion of cancer cells to bone matrix components, such as vitronectin, osteopontin, and bone sialoprotein (BSP). Using DU145 adhesion to ECM as a model, Zheng and colleagues showed that the adhesive property of DU145 cells can be decreased by LM609, an $\alpha v\beta 3$ blocking antibody.[80,81]

Recent studies of the effects of pharmacological inhibition of the MAPK and the PI3K/AKT pathways and stress response of cancer cells demonstrated "inside-out" regulation of antistress regulation of cancer cells by integrins.[82,83] Vellon and coworkers[82] assessed the role of "inside-out" integrin-driven signaling in the Heregulin (HRG)-induced malignant phenotype of breast cancer cells. They demonstrated that MEK inhibitor U0126 and PI3K inhibitor LY294002 drastically increase $\alpha v\beta 3$ levels in breast cancer cells. These effects were associated with a decrease in cell viability and of the fraction of cells in the S- and G2/M compartment of the cell cycle. Moreover, functional blockade of $\alpha v\beta 3$ with small peptidomimetic integrin antagonists strongly antagonized the effects of U0126, indicating that the $\alpha v\beta 3$ integrin triggered Ras-Raf-MEK-ERK pathway is a major regulator of growth of HRG-overexpressing breast cancer cells. Since treatment with $\alpha v\beta 3$ antagonists specifically decreased MAPK-activation status in breast cancer cells,[84] the "outside-in" and the "inside-out" $\alpha v\beta 3$ mediated signaling seems to be transduced primarily through the ERK1/2-MAPK pathway in breast cancer cells.

Thamilselvan and coworkers[83] demonstrated the stress response of cancer cells through the "inside-out" integrin pathway regulates FAK and Src expression in response to the stress, which indicates the "inside-out" antiapoptosis pathway of integrins in cancer cells.

## Growth Factors

**Fibroblast Growth Factor (FGF).** The expression of *basic fibroblast growth factor (bFGF, FGF-2)* has been shown to be significantly increased in stromal fibroblasts in human prostate cancer and in endothelial cells compared with normal tissue. Prostate carcinoma cells have been shown to up-regulate fibroblast growth factor receptor isoforms with a high affinity for bFGF during cancer progression.[85] Accordingly, elevated sensitivity to bFGF may stimulate cancer cell proliferation and protease expression, thereby supporting tumor growth and invasion. In addition, overexpression of both FGFR-1 and FGFR-2 in prostate cancer epithelial cells has been correlated with poor differentiation in a subset of prostate cancers. Thus, there is both an increase in bFGF releasing in stromal cells and receptor expression in tumor epithelial cells, establishing a potential paracrine loop between prostate cancer cells and their surrounding stromal cells, which may be important for prostate cancer progression.[26,86,87]

bFGF also stimulates fibroblast proliferation and extracellular matrix turnover through increased deposition and protease degradation,[87] and functions as an angiogenic factor that induces endothelial cell migration, proliferation and differentiation into new blood vessels.[88] Thus bFGF may promote prostate cancer progression by inducing angiogenesis and stromal remodeling through a vicious cycle. This vicious cycle of FGF–FGFR interaction in prostate cancer cells promotes downstream signaling pathways that induce cancer cells to release factors such as VEGF and encourage angiogenesis.[89-91] A study also indicates the increase of bFGF in tumor epithelial cells due to induction of stromal bFGF,[86] thus potentially establishing a positive feedback loop. Human prostate cancer cell lines DU-145 and PC-3 have been shown to express FGF-2 and metastasize to bone.[85] Furthermore, studies of the Dunning rat model and tumor-stromal interactions show that activation of bFGF expression accompanied progression of epithelial cells to malignancy.[87,88,92] These data suggest a possible contributing role for bFGF in the vicious cycle of tumor formation and progression.

**Platelet-Derived Growth Factor (PDGF).** PDGF is a 30-kDa protein consisting of disulfide-bonded homodimers or heterodimers of $\alpha$ and $\beta$ subunits.[93] Its isoforms have been indicated as important during embry-

onic development, particularly in the formation of connective tissue in various organs.[94-97] In adult tissues, the primary function of PDGF is to stimulate wound healing via chemotaxis and mitogenesis of fibroblasts, and secretion of extracellular matrix components.[53] The normal physiologic targets for PDGF are stromal cells such as fibroblasts, endothelial cells, smooth muscle cells, and glial cells. Thus, paracrine release of PDGF stimulates stromal reaction in normal and pathologic states. Receptor binding by PDGF is known to activate intracellular tyrosine kinase, leading to autophosphorylation of the cytoplasmic domain of the receptor as well as other intracellular substrates. Specific substrates identified with the $\beta$-receptor include Src, GTPase Activating Protein (GAP), phospholyphase C (PLC-$\gamma$), and phosphotidylinositol 3-phosphate. Both PLC-$\gamma$ and GAP seem to bind with different affinities to the $\alpha$ and $\beta$ receptors, suggesting that the particular response of a cell depends on the type of receptor it expresses and the type of PDGF dimer to which it is exposed. In addition to the above, a nontyrosine phosphorylation-associated signal transduction pathway can also be activated that involves the zinc finger protein Erg-1.[98] Immunohistochemical analysis of PDGF and PDGFR indicated expression in both prostate epithelial and stromal cells. In contrast, normal epithelial cells do not express PDGF or PDGFR.[99] *In vitro* study of PDGF indicates that release of PDGF from tumor cell lines stimulates prostate stromal cell proliferation,[100] and suggests *de novo* expression of PDGF in prostate tumor progression. The production and activation of PDGF could further enhance the stromal reaction and contribute to the vicious cycle of tumor progression and stress response.[101]

*Vascular Endothelial Growth Factor (VEGF).* Recruitment of new blood vessel growth clearly illustrates the importance of carcinoma-stroma interactions during cancer progression. In normal human prostate tissue, VEGF is reportedly expressed at low levels and restricted to stromal cells. In high-grade PIN and prostate cancer, elevated expression of VEGF was observed in cancer, stroma, and vascular endothelium.[102] Endothelial cells from microvessels in the surrounding stroma must be induced to migrate into the tumor, whereby they proliferate and form new blood vessels to support tumor growth. This complex process is regulated by a delicate balance of angiogenesis inducers and angiogenesis inhibitors in the extracellular milieu. Increased activator(s) and/or decreased inhibitor(s) alter the balance and lead to the growth of new blood vessels.[103] Recent studies indicate that VEGF directly stimulates prostate tumor cells via autocrine and/or paracrine mechanisms.[104,105] Studies demonstrated

the possible role of VEGF as a mediator in the vicious cycle of tumor and stroma, in which reactive oxygen species (ROS) could participate in early prostate cancer epithelium growth and development. Increased ROS could enhance the production of VEGF, further promoting ROS concentration in stromal fibroblasts. The resulting overexpression of VEGF from stromal fibroblasts could induce Nox1, MMP-9, VEGF, and VEGFR production and increase the overall tumor growth rate.[73,106] Please see the next section for further detailed discussion of angiogenesis and stromal interaction.

*Plasminogen-Related Growth Factors (PRGFs).* Two huge molecules called *plasminogen-related growth factors (PRGFs)*, evolutionarily related to plasminogen, play an important role in inducing invasive growth in cancer progression. PRGF-1 is also called *hepatocyte growth factor/ scatter factor (HGF/SF)*. PRGF-2 is also known as *macrophage-stimulating protein (MSP)*, scatter factor-2.[107] HGF/SF has been demonstrated to be important in prostate cancer progression and metastasis, whereas MSP may be an important neurotrophic factor for embryonic development and induce superoxide anion production.[108,109] It has been shown that both HGF/SF and MSP were up-regulated in the wound repair process in a rat model.[110] HGF/SF predominantly participates in a paracrine network. Several mesenchymal-derived cells (fibroblasts) secrete HGF/SF. It has been implicated as a mediator communicating between epithelial cells and the microenvironment.[107,111] HGF/SF is secreted predominantly by stromal fibroblasts to stimulate proliferation and migration of epithelial and endothelial cells during organ development and tissue remodeling.[112] The secretion of HGF/SF as an inactive pro-HGF is converted into its bioactive form by a proteolytic cleavage by four proteases: urokinase (uPA), serine protease in the serum, coagulation factor XII, and its homologs.[107] It has also been shown that some epithelial cells secrete two potent inhibitors of pro-HGF activation (HAI-1 and -2) that tightly control HGF/SF activation.[113]

c-Met is the receptor for HGF/SF and has been reported to have increased expression in prostate cancer epithelial cells.[114] DU145 and PC3 human prostate cancer cells showed higher levels of c-Met than LNCaP, suggesting that HGF/SF and cMet interaction may increase the invasive and metastatic potential of prostate cancer cells. The secretion of HGF/SF from prostate stromal myofibroblasts significantly increased the expression of IL-1$\beta$, PDGF, bFGF, and VEGF,[115] which suggests the early induction of myofibroblast transition, secretion of HGF/SF, and its regulation of downstream microenvironment events such as angiogenesis.

Zhu and coworkers showed that DU145-conditioned media but not prostate cancer-associated myofibroblastic conditioned media displayed HGF/SF-inducing activity and also contained IL1b, bFGF and PDGF. The results of this study suggest that cytokines and growth factors produced by stromal cells can mediate the expression of HGF/SF in prostate cancer cells and hence their growth and progression.[115] HGF/SF significantly increases the migration of both normal prostate epithelial cells and prostate cancer cells; however, whereas HGF/SF stimulates the proliferation of prostate cancer cells, it inhibits the proliferation of normal prostate epithelial cells.[116] This suggests that normal and malignant prostate epithelial cells have both common and differing response pathways to HGF/SF. The modulation of the interaction between the c-Met and E-cadherin/catenin complex by HGF/SF has been reported, suggesting that HGF/SF may alter the intercellular adhesion properties of prostate cancer cells and contribute to metastasis.[117]

Studies of the role of HGF/SF in the role of cancer migration and invasion demonstrated that HGF/SF modulates the invasiveness of prostate cancer cells. Matrilysin promotes the extracellular cleavage of E-cadherin from prostate cancer cells and has been suggested as a mechanism whereby HGF/SF induces cell–cell dissociation and *in vitro* invasion.[118] This study also cultured DU145 under HGF/SF, in which HGF/SF induces scattering of DU145 prostate cancer cells *in vitro* by decreasing expression of E-cadherin and promoting translocation of the cytokine to the cytoplasm.[119] The migration of primary prostate epithelial cells is also regulated by the PI3K and Src kinase signaling pathways. Activation of the PI3K pathway requires stimulation by adhesion and motility factors secreted by prostate stromal cells. In conditioned medium of primary prostate stromal cells, HGF/SF is the major stimulator of the PI3K pathway and has been demonstrated to mediate prostate epithelial cell migration.[120]

# Regulation of Angiogenesis by the Tumor Microenvironment

The survival and growth of cells is dependent on an adequate supply of oxygen and nutrients, and on the removal of toxic molecules. Oxygen can diffuse from capillaries for only 150 to 200 $\mu$m. When distance of cells from a blood supply exceeds this range, oxygen and nutrient supplies for cells can be a problem.[121] Thus, the expansion of tumor masses beyond 1 to 2 mm in diameter depends on neovascularization, ie, angiogenesis.[122] The formation of new vasculature consists of multiple, interdependent steps. It begins with local degradation of the basement membrane

surrounding capillaries, followed by invasion of the surrounding stroma and migration of endothelial cells in the direction of the angiogenic stimulus. Proliferation of endothelial cells occurs at the leading edge of the migrating column, and the endothelial cells begin to organize into three-dimensional structures to form new capillary tubes.[123] Differences in cellular composition, vascular permeability, blood vessel stability, and growth regulation distinguish vessels in neoplasms from those in normal tissue.[124] A variety of positive and negative regulators govern vasculo-genesis, angiogenesis, and subsequent vessel maturation.[125-127] More than 20 angiogenic stimulators and inhibitors have been discovered in the past 2 decades, including vascular endothelial growth factor (VEGF), platelet-derived growth factor (PDGF), and angiopoietin (Ang).[125-128] These factors not only mediate tumor vessel formation but also affect the function of these vessels. Some of the common pro-angiogenic factors include bFGF, which induces the proliferation of a variety of cells and has also been shown to stimulate endothelial cells to migrate, increase production of proteases, and undergo morphogenesis.[129,130] VEGF has been shown to induce the proliferation of endothelial cells, increase vascular permeability, and induce production of urokinase plasminogen activator by endothelial cells.[131,132] PDGF has been shown to stimulate endothelial cell DNA synthesis and to induce production of FGF,[133] HGF/SF, that increases endothelial cell migration, invasion, and produc-tion of proteases,[134] and PDGF.[135] These factors together govern the fate of endothelial cells and new blood vessel formation in tumor progression.

## Angiogenesis Regulation by the Tumor Microenvironment

A recent study by McAlhany and coworkers showed stroma-induced angiogenesis in prostate cancer development.[136] The protein, ps20, secreted by prostate smooth muscle cells and vascular smooth muscle cells within the prostate enhances endothelial cell motility. They demon-strated 67% increased vessel density in the prostate cancer tumor region with the expression of ps20, when compared with control tumors. Correspondingly, ps20 tumors showed an average 29% greater wet weight and 58% greater volume than controls. Interestingly, this study also showed that ps20 mRNA synthesis is directly stimulated by TGF-b, which is known to influence angiogenesis in experimental models, including prostate tumor models. Tumor generated in the presence of ps20 showed 67% greater vessel density compared with control tumors. A wound healing study showed that TGF-b is released by macrophages and platelets, and serves to stimulate angiogenesis and activate fibro-blasts.[25] Thus, mechanistic evidence exists to validate comparisons

between angiogenesis in wound repair and neovascularization in prostate tumors. This evidence further emphasizes the significance of the stromal microenvironment in prostate cancer progression.

VEGF also has been showed to be a factor influencing both wound repair and tumor angiogenesis. VEGF can act as mitogen of endothelial cells. VEGF is secreted by both epithelial cells and smooth muscle cells in prostate organ development.[137] West and coworkers demonstrated that the level of VEGF in prostate cancer progression correlated to PSA levels and Gleason score, indicating the angiogenesis response in prostate cancer development.[90] The significance of these findings for understanding prostate carcinogenesis was framed by the recent work of Richard and coworkers. It is clear that prostate carcinomas originate in an androgen-sensitive manner, but eventually progress to an androgen-insensitive phenotype. From a clinical standpoint, this loss of androgen responsiveness is one of the most challenging aspects of prostate malignancies. Certainly, a more complete understanding of the evolution of a tumor to the androgen-refractory phenotype would be valuable. Richard and coworkers deciphered an androgen-mediated mechanism of VEGF modulation in a mouse prostate model. Their findings show that the secretion of VEGF is controlled by androgens. As the luminal cells secrete VEGF apically, it is probable that the androgen/VEGF-mediated angiogenesis observed in prostate development as well as in prostate tumorigenesis is primarily due to the stromal smooth muscle.[137] This hypothesis is also supported by the fact that when the prostate cancer cell line C4-2 is injected intrafemorally in mice, it showed high levels of blood support in the subcutaneous site, indicating high rates of angiogenesis (laboratory observation). This organ-specific tumorigenicity and angiogenesis also was found in human colon adenocarcinoma, which showed higher VEGF expression when subcutaneously implanted than when grown in liver.[138,139]

As mentioned before, increasing CTGF release by myofibroblasts in prostate cancer progression promotes angiogenesis and prostate cancer tumorigenesis.[68] CTGF is a member of the CCN gene family (CTGF, Cyr61, and Nov).[140-142] This family includes six structurally and functionally related proteins: CTGF[143,144]; cysteine-rich 61 (Cyr61)[145]; nephroblastoma overexpressed (NovH)[146]; and Wnt-1-induced signaling protein (WISP) 1, WISP2, and WISP3.[147] The CCN family members (excluding WISP2) share four conserved structural modules with sequence homologies similar to insulin-like growth factor-binding proteins, von Willebrand factor, thrombospondin, and cysteine knot.[142] CTGF message is potently stimulated by TGF-$\beta$1[34,148-151] and likely mediates TGF-$\beta$1-induced collagen expression in wound repair fibroblasts.[152]

CTGF is expressed by several stromal cell types, including endothelial cells, fibroblasts, smooth muscle cells, and myofibroblasts, and some epithelial cell types in diverse tissues. Consistent with its role in connective tissue biology, CTGF enhances stromal extracellular matrix synthesis[149] and stimulates proliferation, cell adhesion, cell spreading, and chemotaxis of fibroblasts.[143,149,153] CTGF was also shown to stimulate smooth muscle cell proliferation and migration.[154] In addition, CTGF is a potent stimulator of endothelial cell adhesion, proliferation, migration, and angiogenesis *in vivo*.[155-157] As might be predicted, CTGF is expressed in the reactive stromal compartment of several epithelial cancers, including mammary carcinoma, pancreatic cancer, and esophageal cancer.[158-160] Expression of CTGF is also observed in several stromal cell disorders, including angiofibromas, infantile myofibromatosis, malignant hemangiopericytomas, fibrous histiocytomas, and chondrosarcomas.[161,162] Accordingly, CTGF is considered to be a profibrosis marker.[163] Together, these findings suggest that the TGF-$\beta$ released by tumor epithelial cells, VEGF from both cancer epithelial and stromal cells, and the secretion of CTGF from tumor stromal cells create a network of cross talk between tumor, stromal, and neovascular cells to support tumor progression.

## Adhesion Molecule-Mediated Tumor Progression

Epithelium cell–cell interaction and adhesion is mediated by cadherins to establish $Ca^{2+}$-dependent adhesion.[164,165] E-cadherin is the major epithelial cadherin family member for the formation and maintenance of epithelial structures. Mesenchymal cadherins, such as N-cadherin, are preferentially expressed in migratory cells and in cells of connective tissue. Cadherins are single-span transmembrane-domain glycoproteins which, via their extracellular cadherin domains, mediate homophilic protein-protein interactions in a zipper-like fashion. The intracellular domains of cadherins interact with $\beta$-catenin, $\gamma$-catenin and p120$^{ctn}$ to assemble the cytoplasmic cell adhesion complex (CCC) that is critical for the formation of extracellular cell-cell adhesion. $\beta$-catenin and $\gamma$-catenin bind directly to $\alpha$-catenin, which links the CCC to the actin cytoskeleton.

### Switching of Cadherin in Cancer Progression

However, most cancer epithelia lose E-cadherin-mediated cell–cell adhesion during cancer progression toward malignancy, and it has been proposed that the loss of E-cadherin-mediated cell–cell adhesion is a prerequisite for tumor cell invasion and metastasis.[166] Re-establishing the functional cadherin complex, eg, by forced expression of E-cadherin,

results in reversion from an invasive mesenchymal to a benign epithelial phenotype of cultured tumor cells.[166,167] Using a transgenic mouse model of pancreatic b-cell carcinogenesis, Perl and coworkers demonstrated that the loss of E-cadherin-mediated cell–cell adhesion is one rate-limiting step in the progression from adenoma to carcinoma *in vivo*,[168] indicating the role of E-cadherin as a suppressor of tumor invasion. In a number of human cancer types that have lost E-cadherin expression, *de novo* expression of mesenchymal cadherins such as N-cadherin and cadherin-11 has been observed.[169,170] N-cadherin has been shown to promote cell motility and migration, thus showing an opposite effect as compared with E-cadherin.[171-173] N-cadherin-induced tumor cell invasion can even overcome E-cadherin mediated cell–cell adhesion.[171,174] This cadherin conversion recapitulates a well characterized phenomenon occurring during embryonic development, when epiblast cells switch from E- to N-cadherin to ingress the primitive streak or when primordial germ cells migrate to populate the genital ridge.[170,175,176] Based on these observations, a novel concept has been formulated that a "cadherin switch" is involved not only in delamination and migration of epithelial cells during embryonic development but also during the transition from a benign to an invasive, malignant tumor phenotype.[169,170]

Loss of E-cadherin function during tumor progression can be caused by a variety of genetic or epigenetic mechanisms, including mutational inactivation, chromosomal aberrations, transcriptional repression of the E-cadherin gene by the repressors Snail and Sip-1, and subsequent promoter hypermethylation and chromatin rearrangements.[177] Tyrosine phosphorylation has also previously been implicated in the regulation of cadherin function. RTKs, such as EGFR, c-Met, and FGFR, and the nonreceptor tyrosine kinase, c-Src, phosphorylate E-cadherin, N-cadherin, b-cadherin, g-cadherin, and p120$^{ctn}$, resulting in the disassembly of the cytoplasmic adhesion complex, disruption of cadherin-mediated cell adhesion, and cell scattering.[164,165] On autophosphorylation, RTKs are often ubiquitinylated by E3 ligases, such as c-Cbl, which associate with phosphorylated RTKs, resulting in the degradation of the RTK by the proteasome.[178] A novel E3 ligase, Hakai, binds tyrosine-phosphorylated E-cadherin, and by ubiquitinylation earmarks it for endocytosis and proteasome-mediated degradation.[179,180] Notably, Hakai is structurally and functionally related to c-Cbl. Consistent with the function of RTKs in the degradation of E-cadherin protein, treatment of cells with phosphatase inhibitors causes the dissociation of $\alpha$- and $\beta$-catenin from the adhesion in E-cadherin-mediated cell adhesion.[179] Interestingly, the cadherin switch in cancer cells can be recapitulated *in vitro* by treating the cells

with HGF, further underscoring the critical role of RTK-mediated changes in cell adhesion during physiological processes.[165]

E-cadherin and N-cadherin are both classical cadherins and on first sight seem to have similar mechanisms of cell–cell adhesion. Hence, the functional implication of the "cadherin switch" for tumor progression is not obvious. One possibility is that the change from E- to N-cadherin expression may provide a tumor cell with a new "homing address" to find new "neighbors." Unlike E-cadherin, N-cadherin (and, presumably, other mesenchymal cadherins) promotes a dynamic adhesion state in tumor cells, not only allowing the dissociation of single cells from the tumor mass but also their interactions with endothelial and stromal components.[169-171] On the other hand, N-cadherin may provide a pro-migratory signal to the cells expressing it. In fact, N-cadherin mediated induction of FGFR signaling has been demonstrated to occur in neurons, where it supports neurite outgrowth, an event strictly related to cell migration and invasion.[181] Hazan and coworkers in breast cancer cells demonstrated the functional cooperation between N-cadherin and FGFR signaling pathways.[174,182] Cavallaro and coworkers further showed the direct binding of N-cadherin with two different FGFRs.[183] This FGFR-N-cadherin interaction enhances the binding of FGFs to the receptor, MEK/MAPK signaling pathway, and later increases cell migration and invasion.

Association of another member of the cadherin family with an RTK has been reported for the endothelial cell-specific VE-cadherin and the major signaling receptor for VEGF, VEGFR-2.[184] Similarly to N-cadherin and FGFR, VE-cadherin is able to enhance VEGF-induced VEGFR signaling; and in the absence of VE-cadherin, endothelial cells are unable to respond to VEGF and undergo apoptosis.[185] Conversely, VE-cadherin, $\beta$-catenin, $\gamma$-catenin, and p120$^{ctn}$, but not $\alpha$-catenin, are phosphorylated on tyrosine by activated VEGFR-2.[186] However, it is not clear whether tyrosine phosphorylation of these proteins is an earmark for their degradation, as is the case for E-cadherin (see below). Because VEGF is a potent angiogenic factor and VE-cadherin (and N-cadherin) is expressed by endothelial cells during ongoing angiogenesis, these cadherins may play an important role in the fine-tuning of physiological and pathological angiogenesis, not only by modulating endothelial cell adhesion but also by influencing the activity of angiogenic growth factor signaling via RTKs.

## HGF and CD-44 Regulate Cadherin Signaling

Hepatocyte growth factor (HGF) and its cognate receptor c-Met are known inducers of cell scattering, migration, invasion, and proliferation

as well as epithelial to mesenchymal transition, tubular organization, and morphogenesis. Their involvement in cancer progression, mainly by affecting the invasive behavior of tumor cells, has been amply demonstrated in various experimental systems. In human cancers, the c-Met gene has frequently been found to be amplified, mutated, or overexpressed.[187] Together with c-Met, expression of the hyaluronan receptor CD44 is frequently upregulated in cancers.[188,189] Based on extensive alternative splicing of exon v1-v10, various isoforms exist which are further diversified by additional posttranslational modifications. Notably, the v6 isoform of CD44 seems to play a critical role in tumor metastasis: ectopic expression of v6-containing CD44 isoforms or treatment with antiv6 monoclonal antibodies modulates metastasis formation of cancer cells in animal models *in vivo* and tumor cell invasiveness *in vitro*.[189,190] Moreover, the v6 isoform of CD44 seems to be required for HGF-induced c-Met activation, and CD44v6 and c-Met are found to interact physically. Whereas the extracellular domain of CD44v6 is required and sufficient to allow HGF-induced autophosphorylation of c-Met, transfer of the signal to downstream effectors, such as MEK and MAPK, depends on the presence of the cytoplasmic tail of CD44v6.[191] Another splice variant of CD44, CD44v3, contains Ser-Gly repeats that support covalent attachment of heparan sulfate proteoglycans. CD44v3 binds a number of heparin-binding growth factors, including members of the FGF family and heparin-binding epidermal growth factor (HB-EGF). Here also, a physical association between a cell adhesion molecule and an RTK has been demonstrated; in the presence of CD44v3, binding of HB-EGF to its cognate receptor, the EGFR family member ErbB4, is facilitated.[192] Moreover, CD44v3 recruits active matrix metalloprotease 7 (MMP7; matrilysin), which then proteolytically converts HB-EGF from the precursor to its active receptor binding form. Subsequent stimulation of the receptor results in increased cell proliferation, migration, and survival. This cell surface complex between CD44v3, HB-EGF, ErbB4, and MMP7 is found on tumor cells *in vitro*, and in uterine epithelium and lactating mammary gland epithelium *in vivo*.[192] Notably, CD44, via the interaction of its cytoplasmic domain with ERM (ezrin-radixin-moesin) proteins, is also connected to the actin cytoskeleton, thereby modulating cell migration and cell shape.[188]

## Wnt Signaling Pathway Regulated by Cadherin

Cadherin-mediated cell–cell adhesion can also affect the Wnt-signaling pathway.[193] β-catenin (and γ-catenin) is usually sequestered by cadherins in the CCC. On loss of E-cadherin function, nonsequestered free

$\beta$-catenin is usually phosphorylated by glycogen synthase kinase $3\beta$ (GSK-$3\beta$) in the adenomatous polyposis coli (APC)-axin-GSK-$3\beta$ complex and subsequently degraded by the ubiquitin-proteasome pathway. In many cancer cells, loss of function of the tumor suppressor APC, mutations in $\beta$-catenin or inhibition of GSK-$3\beta$ by the activated Wnt-signaling pathway leads to the stabilization of $\beta$-catenin in the cytoplasm. Subsequently, it translocates to the nucleus, where it binds to members of the Tcf/Lef-1 family of transcription factors and modulates expression of Tcf/Lef-1-target genes, including the proto-oncogene c-Myc and cyclin D1.

Cadherins also appear to directly affect each other's function. Suppression of N-cadherin function in invasive squamous carcinoma cells results in the induction of E- and P-cadherin expression and reversion to an epithelial phenotype. In contrast, forced expression of N-cadherin in epithelial-like squamous cells causes downregulation of E- and P-cadherin and the acquisition of an invasive phenotype.[172] This implies that the expression of N-cadherin during tumor progression might be equally necessary and sufficient to overcome E-cadherin-mediated cell–cell adhesion and promote malignant tumor progression.

## Epithelial to Mesenchymal Transition (EMT) of Prostate Cancer Cells

The epithelial–mesenchymal transition (EMT) was originally defined by developmental biologists as a morphological conversion occurring at specific sites in embryonic epithelia to give rise to individual migratory cells.[194] EMT is a fundamental process in the development of most metazoans and is primarily involved in the shaping of embryos. In mammals, EMT has been associated with the formation of the parietal endoderm.[195] It is also directly involved in the formation of the mesoderm and definitive endoderm at the primitive streak during gastrulation.[196] Neural crest cells emerge from the dorsal neural epithelium through EMT before undergoing extensive migration and differentiation into many derivatives.[197] EMT has also been implicated in the ontogeny of other structures including somites and heart endocardium.[198]

Most current studies of EMT in cancer progression are performed *in vitro* with epithelial cell lines, which can be converted into fibroblast-like cells under specific culture conditions. However, not all normal or malignant cell lines share all characteristics with embryonic epithelia. In many instances, epithelial cell lines can be refractory to EMT, perhaps owing to the inaccessibility of scatter factors or to intrinsic inhibitory mechanisms. Conversely, culture conditions do not always allow epithe-

lial cells to achieve full polarity and can facilitate dispersion. The definition of an EMT, and the requirements to execute one *in vitro* are at variance with those *in vivo* and therefore cannot exactly recapitulate these events. It is therefore not surprising to find studies differing in their stringency for the various criteria for defining an EMT.

The current criteria for defining an EMT *in vitro*[194] involve the loss of epithelial cell polarity, the separation into individual cells and subsequent dispersion after the acquisition of cell motility. EMT presumably involves the disassembly of tight junctions, adherens junctions, and desmosomes as well as the reorganization of cell substrate adhesion complexes. After the loss of cell polarity, the cytoskeleton is significantly remodeled. A shift from cytokeratin intermediate filaments to vimentin is considered to be an important criterion for EMT, although vimentin is not necessarily a reliable marker of mesenchymal cells. The epithelial and mesenchymal phenotypes also show particular transcription profiles including cytoskeletal components and extracellular matrix components. It is likely that several other types of protein will be found to be associated with EMT in only one of the two states.[199]

The most outstanding study of EMT of prostate cancer cells was currently done by Zhau and coworkers, who established an ARCaP human prostate cancer cell model to study the possible relationship between the host microenvironment, EMT, the critical transition of prostate cancer cells from epithelial to mesenchymal phenotype,[40] and the tendency of prostate cancer to metastasize to bone and soft tissue. In the ARCaP human prostate cancer progression model, EMT can be promoted by cellular interaction between an ARCaP human prostate cancer cell subclone, $ARCaP_E$, and host bone or adrenal gland *in vivo*. The derivative $ARCaP_M$ and $ARCaP_{Ad}$ cells have the proclivity to metastasize to bone and adrenal gland, respectively. Through cellular interaction with host adrenal gland, they derived a secondary generation of $ARCaP_{Ad}$ cells; the second generation of $ARCaP_{Ad}$ cells had restricted ability to metastasize only to the host adrenal gland. Similar behavior also can be seen in the bone metastasis variant, $ARCaP_M$, and the loss of epithelial-like behavior as $ARCaP_E$ suggests that $ARCaP_M$ derived from $ARCaP_E$ through EMT transdifferentiation and the interaction of $ARCaP_E$ with the host bone.

Following cellular interaction between human prostate cancer $ARCaP_E$ cells and the mouse host, we observed changes in morphology, gene expression, and behavior in this cell clone to resemble a mesenchymal cell type, express mesenchymal genes, and show increased invasion and migration *in vitro* and metastasis to bone and adrenal gland in live mice.[40] The changes in gene expression profile, such as increased expression of

vimentin and N-cadherin and decreased expression of E-cadherin and cytokeratin18 and 19, are consistent with the morphologic switch by EMT, with increased metastatic potential, as reported in several other tumor types.[200-205] This observation indicated that the host microenvironment plays an important role in EMT and metastasis.[40,206] The fact that host interaction enhances EMT and promotes ARCaP cells to migrate, invade, and metastasize in this model suggests that clinical bone and adrenal gland metastases of prostate cancer cells may be acquired and facilitated by cellular interaction with the host microenvironment. Based on the results of this and our previous studies, it is likely that resident fibroblasts in the prostate, bone, or adrenal gland, or cells recruited from hosts, such as inflammatory and marrow stem cells, can instigate prostate cancer cells to gain increased malignant potential through the local production of soluble factors, reactive oxygen species and/or extracellular matrices that prompt the tumor cells for enhanced growth and metastasis. Using marginally tumorigenic LNCaP cells as a model, we showed previously that coinoculating LNCaP cells with either nontumorigenic human prostate stromal fibroblast or a human osteosarcoma cell line[12,207] formed large chimeric tumors. By cloning LNCaP cells from the chimeric tumors, we established lineage-derived LNCaP sublines C4-2 and C4-2B cells which, like other variants,[14] exhibited increased lymph node and bone metastasis.

The demonstration that ARCaP cells undergo EMT in bone or adrenal gland and gain metastatic potential for various sites has several important clinical implications for controlling cancer growth and metastasis. First, the host microenvironment includes soluble and insoluble factors associated with or secreted by osteoblasts, osteoclasts, marrow stromal, or stem cells that could play key roles promoting EMT, an important molecular transition by which cancer cells gain increased metastatic potential in response to the changing tumor microenvironment. These interactions could result in the promotion of cancer cell metastasis to soft tissues such as the adrenal gland, a documented site for human prostate cancer metastasis.[208] Second, if EMT acquired by prostate cancer cells following cellular interaction with host bone or adrenal gland occurs in patients, this could be a potential target for prevention and treatment strategies. Third, since the host microenvironment was shown to promote EMT and prostate cancer progression, host stroma-directed targeting of prostate cancer by the use of atrasentan,[209] bisphosphonates,[210] growth factor receptor antagonists,[211] antiangiogenics,[212] and radiopharmaceuticals[213] should be further explored to improve the treatment of cancer metastases.

## Tumor Microenvironment Immune Surveillance in Response to Cancer Development

The concept of immune surveillance against cancer is supported by several animal studies and various observations in humans.[214,215] These include increased prevalence of tumor development following immune suppression and the observation that the extent of intratumoral T cells is correlated with improved clinical outcome in various solid tumors.[215,216] Followed by the identification of tumor-associated antigens (TAA),[217,218] immunologic study of tumor response has become a rapidly growing field of research and clinical investigation. In the past decade, more than 60 major histocompatibility (MHC) class I-associated TAAs have been identified[219] and new TAAs are continuously being described. The appearance of tumor-specific reactions against tumor cells is dependent on a complex system. As for all antigens recognized by T cells, TAA are cleaved within the tumor cells by proteasomes into short peptides of 8 to 12 amino acids. These peptides are transported through the transporter associated with antigen presentation (TAP) into the endoplasmatic reticulum. Here, peptides with good binding affinity for the MHC class I molecules (in humans called Human Leukocyte Antigens or HLA) are naturally associated with them. The peptide/HLA complexes, stabilized by a further protein ($\beta$2-microglobulin), then migrate to the cell surface where they are exposed to potential interaction with HLA class I-restricted T cells. In an HLA-dependent fashion, TAA-derived epitopes are detected by T cells through HLA/epitope-T cell receptor (TCR) engagement. Effective T cells have been primed by presentation of TAA by professional antigen-presentation cells (APC), such as dendritic cells. Therefore, APC within tumor (resident APC) may play a major role for the development of specific T cell responses.

It is likely that immune cells influence the tumor cell phenotype and changes in tumor cells in return shape the immune response. Though a selective process, tumor cells likely adapt to immune pressure by changing their phenotype and escaping immune surveillance. Due to genetic instability, tumors continuously re-program their genotype and thus their phenotype. Several mechanisms may be involved. Tumor cells often are defective in TAA[220] or HLA molecule expression,[221,222] and/or have malfunctioning antigen-processing.[223] A loss of expression of the HLA-epitope complex on the surface of tumor cells renders their recognition by TAA-specific T cells impossible. Furthermore, HLA-epitope complex downregulation on tumor cell membranes correlates with decreased T-cell-triggering capability.[224]

Dysfunction of antigen-processing machinery might have a strong role in the coexistence of TAA-specific T-cells with cancer cells expressing the target components necessary for their recognition.[225-227] Complete TAA loss obviously eliminates one of the most important preconditions for a targeted T cell function. All given escape mechanisms happen under an assumed pressure by the immune system. Tumor/immune cell interactions are bidirectional. Tumor cells can modulate T cell function. For example, systemic and intratumor T cell dysfunction including anergic T cells and T cells with down-regulated CD3-zeta chain have been described in tumor patients.[228,229] This anergic status of T cells has been proposed as the cause of their ineffectiveness in containing tumor growth.[230] The cause of malfunction of TAA-specific T cells is not known but it is known that tumor cells can secrete immune suppressive factors, such as TGF-$\beta$.[231] Several additional variables might influence T cell function and, consequently, their clinical effectiveness.[232] These include the activation of regulatory T cells, the development of death resistance by tumor cells, involvement of natural killer cells and their receptors, and the potential contribution of Fas expression. Additionally, new data shed light on the role of transcription factors in tumor defenses against the immune system. STAT3 expression in tumor cells leads to inhibition of production of pro-inflammatory cytokines and chemokines.[233] These variables might have an important role in modulating the immune response at both the systemic level and the tumor site, and their significance for immune-system/tumor-interaction warrants further study.

Several studies have demonstrated the presence of TAA-specific T cells in peripheral blood of immunized patients, proving that the primary goal of vaccination–inducing a systemic TAA-specific immune response–can reproducibly be achieved.[234] Additionally, systemic tumor-directed T cell responses can evolve spontaneously in various malignant diseases without prior immunotherapy.[235] Although these spontaneously occurring TAA-specific T cells have been characterized as CD3$^+$CD8$^+$INF$\gamma^+$CD45RA$^+$,[236] a phenotype supposedly representative of cytotoxic effector T cells,[237] their actual function in clinical settings remains unknown. Clinically, although rare tumor responses can be achieved using peptide vaccination,[238] no conclusive correlation between systemic T cell response and clinical cancer repression has been convincingly demonstrated so far. Thus, investigations of the systemic immune response do not provide sufficient information about the interaction between host and cancer cells at the actual site of conflict in the tumor microenvironment.

# The Tumor Microenvironment Induces Cancer Migration from Primary to Distant Locations

## Steps of Metastasis

*Invasion.* Invasion, which initiates the metastatic process, consists of changes in tumor cell adherence to cells and to the extracellular matrix (ECM), proteolytic degradation of surrounding tissue, and motility to physically propel tumor cells through tissue. Tumor cell adherence to the ECM is mediated by integrins. The engagement of integrins and other attachment molecules is accompanied by the recruitment of proteases to degrade the ECM, providing a pathway for invasion.[239] Matrix metalloproteinases, plasmin, urokinase plasminogen activator, cathepsins, and heparinase, when transfected into a tumor cell line, augment invasion. Besides the destruction of ECM, proteases liberate embedded growth factors and chemokines activate latent proteins on the cell surface, and may have protective roles in tumorigenesis.[240,241] Most tumor cell movement in invasion is dynamic, involving the formation of adhesions to the ECM at the leading edge of the cell, detachment from the ECM at the trailing edge, and a ratcheting of the cell forward. Virtually every growth factor stimulates tumor cell motility *in vitro*. Pathways may be tumor-cell autonomous or may involve paracrine loops with cells in the environment.[242] Chemokines, chemotactic cytokines that bind G-protein-coupled receptors, represent another important class of motility-inducing proteins.[243] Chemokines also contribute to tumor cell invasion by inducing infiltration of tumors by macrophages and lymphocytes, which release proteases and other inflammatory stimuli.

*Regulation of Normal Bone Remodeling.* Before studying prostate cancer bone metastasis, one should appreciate the complexity of normal bone remodeling, which helps to understand the interaction of the bone microenvironment with cancer. Bone is a dynamic organ undergoing constant remodeling involving active destruction and re-synthesis of the bone matrix. Within normal adult bone, homeostatic mechanisms maintain the balance between bone-forming osteoblasts and bone-resorbing osteoclasts.[5]

Osteoblasts arise from mesenchymal osteoprogenitor cells.[244] During development, these cells secrete a complex mixture of growth factors and ECM proteins into the surrounding bone microenvironment before apoptosis or terminal differentiation into osteocytes (the cellular component of hardened bone). The majority of bone matrix proteins consist of type I collagen fibers (80-90%), which provide structural support for the mineralization of bone.[245,246] The remaining 10% to 15% consists of

proteoglycans, γ-carboxylated (gla) proteins,[247] cell adhesive proteins, and growth factors. A large number of adhesive proteins found in bone contain RGD (Arg-Gly-Asp) motifs[248-253]; examples of these are type I collagen, bone sialoprotein, fibronectin, laminin-10, osteopontin, thrombospondin, and vitronectin. The RGD motif is a well-characterized binding site for several adhesion receptors of the integrin family and, depending on substrate-receptor context, can regulate cellular motility, invasion, and growth.[254] Osteoblasts also secrete growth factors into the bone matrix, including TGF-$\beta$, IGFs, PDGF, interleukins, FGFs, and bone morphogenic proteins (BMPs).[255] These growth factors remain latent in the bone matrix but can be released and activated on proteolytic degradation of the bone. FGF, PDGF, TGF-$\beta$, and several BMPs have been reported to enhance the differentiation and growth of osteoblasts.[256-258] Thus, release of these factors from the bone matrix provides a feedback mechanism to promote bone formation and attenuate bone resorption.

Osteoclasts are differentiated cells arising from the monocyte–macrophage lineage. The primary role of the osteoclast is to resorb bone. Activated osteoclasts are recruited to the bone surface and attach through interactions with the $\alpha v\beta 3$ integrin receptor.[259-261] This interaction is crucial in the bone remodeling process; $\beta 3$ integrin knockout mice develop osteosclerosis due to the lack of functional osteoclasts.[261-263] Osteoclasts acidify the local microenvironment at the bone–osteoclast interface (resorption zone) and secrete several proteases such as MMPs and cathepsin B, L, K, and S, which are used to degrade components of the ECM. The most abundant protease expressed by osteoclasts is cathepsin K which targets type I collagen.[264,265] Whereas cathepsin K seems to be the prevalent protease in solubilization of the bone matrix, several MMPs have also been implicated in the proteolysis of bone.[266-271] Interestingly, osteoclast-secreted MMPs, MMP-9, -10, -12, and -14, do not contribute significantly to bone degradation, whereas MMP-13, an osteoblast-secreted MMP with collagenase activity, can be recruited into the resorption zone and degrade bone.[272] In addition to bone proteolysis, several MMPs have been implicated in the regulation of osteoclast signaling, migration, and invasion.[269,271,273,274] The osteoclastogenesis regulation through cathepsin and MMPs is tightly controlled through a complex network of cytokines and receptors in interaction within bone stroma. In particular, stromal expression of macrophage colony-stimulating factor (M-CSF) and the receptor activator of NF$\kappa$B ligand (RANKL) are necessary and sufficient to induce osteoclastogenesis *in vivo* and *in vitro*.[275,276] M-CSF, through binding to its receptor c-Fms, acts as a survival factor for osteoclast precursor cells, allowing them to respond to

inducers of osteoclastogenesis.[277] Expression of membrane-bound RANKL is induced in stromal cells and osteoblasts by various stimuli, including parathyroid hormone (PTH), PTH related protein (PTHrP), calcitriol, tumor necrosis factor-$\alpha$ (TNF-$\alpha$), glucocorticoids, prostaglandin E2 (PGE2), IL-1, IL-11, bFGF, and IGF-1.[278-280] Binding of RANKL to its membrane receptor RANK on osteoclast precursors activates inhibitor of NF$\kappa$B kinase (IKK), c-Jun N-terminal kinase (JNK), p38, extracellular signal-regulated kinase (ERK), and Src signaling pathways that cooperate to induce the differentiation of hematopoietic progenitors into mature osteoclasts.[281,282] Mice with homozygous deletions in either RANKL or RANK have no functional osteoclasts and develop severe osteopetrosis,[272,282,283] demonstrating the critical importance of the RANKL/RANK interaction in osteoclastogenesis. Another osteoclast regulator is osteoprotegerin (OPG), a member of the Tumor Necrosis Factor receptor (TNF) superfamily that is secreted by osteoblasts and other bone stromal cells and suppresses osteoclastogenesis by competing with RNAK for RNAKL binding.[284,285] Consistent with this, OPG-deficient mice exhibit decreased bone density due to increased osteoclast activity.[286,287]

## Participation of Bone Microenvironment in Cancer Bone Metastasis

Bone is one of the most favored sites of solid tumor metastasis, indicating that the bone microenvironment provides a fertile soil for the growth of many human tumors. In fact, patients with the most common solid tumors, such as breast, lung, and prostate carcinomas, may have the major portion of the tumor burden present in bone at death. Typical clinical presentations include pain, spinal cord compression, and pathologic fractures.[288] Pain is usually the first symptom and results from mechanical or chemical stimulation of pain receptors in the periosteum/endosteum by the growing tumor mass. Spinal cord compression results from expanding extradural tumor growth, spinal angulation secondary to vertebral collapse, or dislocation of the vertebra after pathologic fracture. Back pain, motor weakness, sensory loss, and autonomic dysfunction all are common symptoms of spinal cord compression. Pathologic fractures occur as a result of the tumor mass weakening the bone and are associated with both osteolytic and osteoblastic bone lesions.[288,289]

Bone metastases can be categorized into three distinct phenotypes: osteolytic, osteoblastic, and mixed lesions containing elements of both.[290] Patients with advanced bone metastases from primary breast cancer or prostate cancer eventually develop a mixture of both osteoblastic and

osteoclastic lesions to provide cancer cells a better environment for survival. For example, in breast cancer bone metastasis, the majority of bone lesions in patients are osteolytic, whereas approximately 15% to 30% are osteoblastic reactions. Similarly, prostate cancer shows higher osteoblastic reaction with some degrees of osteolytic reaction in bone metastasis patients.[290,291] These phenotypes reflect the perturbation of normal bone remodeling processes by the presence of tumor cells. This suggests that the pathology of each type of lesion is not static; rather, the observed phenotype in each metastatic lesion results from a shift in the dynamic equilibrium of normal bone remodeling.

The progression of prostate cancer from the androgen-dependent to androgen-independent and bone metastatic state is considered a poor and generally a more rapidly lethal prognosis. To understand the molecular basis of disease progression and develop rational new therapeutic approaches for targeting prostate cancer bone metastasis, we must first understand the multi-step processes that lead to prostate cancer metastasis to bone. As depicted in Fig 3, at the site of primary cell growth we expect prostate cancer cells to interact with prostate stromal cells and gain the ability to extravasate into the bloodstream. In the blood, prostate cancer cells are expected to survive and move as an embolus before adhering to bone marrow-associated endothelial cells. The attachment and interaction of prostate cancer cells to marrow endothelial ECMs could activate the invasive properties of prostate cancer cells and allow their extravasation into the marrow space. At the final step of this progression, prostate cancer cells interact directly with bone stromal fibroblasts, osteoblasts and osteoclasts through a series of soluble factors (eg, RANKL) via cell surface receptor (eg, RANK) to survive, proliferate, migrate, and invade and eventually replace the bone marrow components. Recent studies of cancer metastasis demonstrated that chemokines released by bone stromal cells induce cancer cells migrate to the bone area, such as the CXCL12-CCR4 interaction in breast cancer bone metastasis models.[292] It also merges the idea that self-seeding of cancer cells in bone induces the colonization of cancer cells in the distant region.[293] To sum up the seed and soil and self-seeding hypotheses, the first group of cancer cells migrates to many distant organs and later either die out or leave due to immune surveillance or environmental restrictions; however, those cells that do manage to interact with the target organ, such as bone, could introduce permanent changes in those microenvironments to serve as "fertilized" soil and also release chemokines leading cancer cells to such good environments at later stages of cancer development. Those cancer cells that do survive the process would find themselves in a more
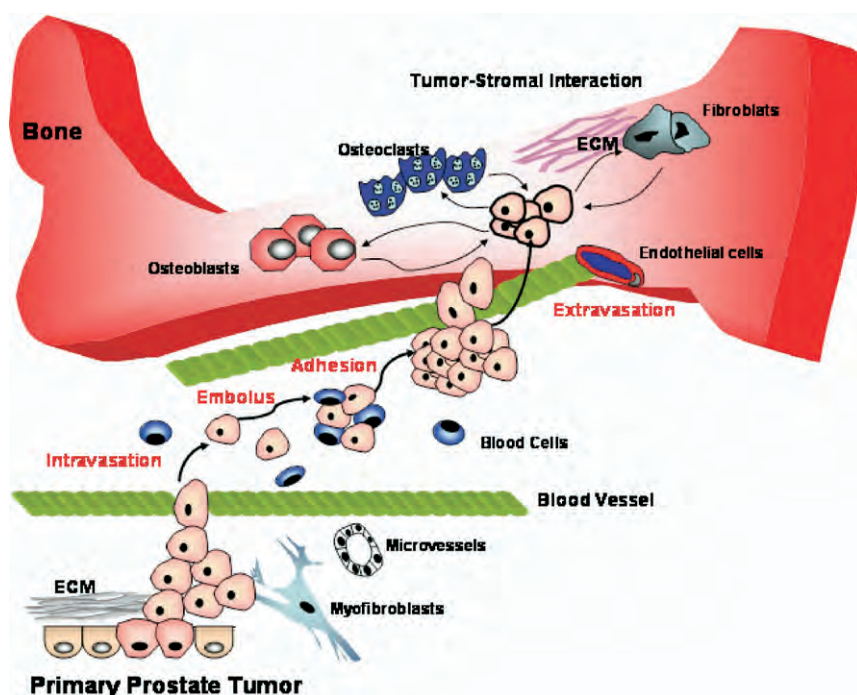
**FIG 3.** Prostate cancer bone metastasis initiated from EMT under the influence of signals from prostate cancer microenvironments. These factors can be released from many different cells in cancer associated microenvironment and together of these factors induce cancer cells epithelial to mesenchymal transition (MET). Cancer cells EMT induce cancer independently to its microenvironment and intravasation, migrate through blood vessel, anchored to specific endothelial markers and extravasation to the favor organs. Mesenchymal to epithelial transition of cancer epithelial cells induce cancer cells permanently reside to the new microenvironment and interact to the new neighbor cells in order for them to survive. These interaction induce new factors released from the stromal cells for cancer cells proliferation, survival, and invasion in these microenvironment. (Color version of figure is available online.)

welcoming microenvironment which the pioneer cancer cells contributed to. This coevolution of cancer cells and stroma that creates such microenvironments may be reflected by the presence of tumor and stroma-specific gene expression patterns.[25,38,68,294,295] To understand the cellular and molecular basis of the prostate cancer bone–stroma interaction, it is essential to delineate how the soluble growth factors and extracellular matrices participate reciprocally in the progression of prostate cancer toward androgen independence and bone metastasis.

Using a human prostate cancer coculture model, our laboratory has obtained evidence suggesting that nonrandom genetic changes occur in

the human bone stromal cell line MG-63, after coculture with the human androgen-independent prostate cancer cell line C4 to 2 (a lineage-derived LNCaP subline with growth and metastatic potential to lymph node and bone when injected subcutaneously or orthotopically in castrated mice) under 3-D conditions. The 3-D model is valuable for the evaluation of tumor-stroma interaction *in vitro*. The participation of stroma in tumor growth and progression suggests that when prostate cancer metastasizes to bone, there are complex and reciprocal cellular interactions between populations of tumor and host bone cells.

## Vicious Cycle Between Cancer and Bone Stroma

Whereas clinical human prostate cancer is predominantly osteoblastic, the established human prostate human cancer cell lines inoculated and grown in the bone of immune compromised mice yield both osteoblastic and osteolytic lesions. Apparently, prostate cancer cells can participate in the process of bone turnover by exhibiting properties similar to osteoblasts, the so-called "osteomimetic" properties of prostate cancer cells we reported earlier.[56,255] Much evidence supports this interesting phenotype of prostate cancer cells, in which they behave like osteoblasts. Prostate cancer cells express both soluble and membrane-bound RANK ligands, and were shown to participate directly in osteoclastogenesis.[285,296] Prostate cancer cells expressed a number of noncollagenous bone matrix proteins, such as osteocalcin, osteopontin, osteonectin, bone sialoprotein, alkaline phosphatase, and a key transcription factor, Runx 2 (cbfa1), that controls the transcription of osteocalcin and collagenous-3.[297,298] In addition, on exposure to mineralizing cell culture conditions, prostate cancer cells have been shown to form *bona fide* mineralized bone crystals as detected under electron microscope. These observations raise the possibility that soluble and/or matrix-associated molecules may be responsible for signaling between prostate cancer and bone stromal cells. Since bone-homing prostate cancer cells seek to adhere, colonize, and survive in bone, it is of pivotal importance to find out how prostate tumor and bone cells interact, with the hope of identifying novel therapeutic targets for the treatment of prostate cancer bone metastasis. One attractive hypothesis is that prostate cancer cells may behave like osteoblasts and functionally participate in bone turnover. By markedly increasing the basal rate of bone turnover, they may further enhance prostate cancer cell colonization in bone.[299,300] This hypothesis is supported by some clinical observations where bisphosphonates, an effective class of agents that slow down or inhibit bone resorption, have been shown to reduce cancer cell colonization in experimental models of prostate and breast can-

cers.[301,302] In men harboring prostate cancer, there is evidence that increased bone resorption occurs on castration. Whether these changes in bone turnover subsequent to hormonal manipulation or bisphosphonate treatment after prostate cancer cell colonization in bone affect the natural history of prostate cancer progression should be the subject of future thorough investigation.

## Factors Driving the Vicious Cycle Between Breast or Prostate Cancer and Bone Cells

Guise[303] and Mundy[304] presented the concept of a vicious cycle involving TGF$\beta$ produced by bone cells that promotes the production of PTHrP by tumor cells, which in turn stimulates bone turnover by enhancing osteolytic reaction in the bone. Increased release of TGF$\beta$ could result from rapid bone turnover and this triggers more PTHrP production by cancer cells. The production of PTHrP by tumor cells will induce osteolytic cells to express an increased level of RANK ligands. The increased RANK ligands will help promote osteoclast formation/ activation and subsequently increase bone resorption. The enhanced resorptive process by osteoblasts and osteoclasts leads to "bone pitting" and subsequent colonization by breast cancer cells in the skeleton, and associated bone destruction often observed in breast cancer patients. It is likely that the similar proposed "vicious cycle" between TGF$\beta$, PTHrP, RANK ligands and osteolytic breast cancer cells could also occur in prostate cancer. Interrupting the vicious cycle in breast cancer models using anti-PTHrP antibodies or osteoprogerin (OPG) has been shown to reduce colonization of breast cancer metastasis to bone and prevent prostate cancer growth in the skeleton.[305,306]

Patients with advanced prostate cancer bone metastases often have androgen-independent prostate cancer (AIPC) and are hormone refractory, hence bone-associated growth factors and cytokines preferentially stimulate the growth of hormonally independent prostate cancer cells. Several factors are regulated by prostate cancer in the bone, such as bFGF, IGF, PDGF, EGF, and TGF-$\alpha$,[62,255,307] which can reciprocally regulate prostate cancer invasion and survival in bone microenvironment.[255] However, some bone growth factors, such as TGF-$\beta$, can inhibit or stimulate the growth of prostate cancer cells, depending on their phenotype.[289] Other factors, such as CXCL12, may synergize the mitogenic effect of other growth factors, which suggests CXCL12 and its receptor (CXCR4) may play a role as prostate cancer bone metastasis homing signals.[308] The level of CXCR4 increases with the malignancy of prostate cancer cell lines by both RT-PCR and Western blot analysis, and

increased expression of CXCR4 also increased spreading to bone in animal studies. An *in vitro* study of cellular spreading in basement membrane indicates that spreading can be inhibited by CXCR4 antibody. These findings suggest that chemokine and its receptor could also be important in prostate cancer bone metastasis.

## Cancer Therapy and the Response of Stroma: Cotargeting Both Tumor and Stroma

### Radiation Therapy and the Response of the Microenvironment

Radiation therapy for cancer patients depends on killing cancer cells but not normal tissues. It is a widely used treatment for cancer, with over half of all cancer patients receiving radiation therapy during their course of treatment.[309] Recent experimental protocols for treating cancer combine cytotoxic chemotherapeutic agents with radiation.[310] The cytotoxicity of chemotherapeutic agents, however, is not limited to tumor cells because treatment of tumors with these agents can result in significant normal tissue toxicity. We will separate the discussion of the stromal effects of radiation and chemotherapy into two parts. The first part will mainly focus on ionizing radiation (IR) to the stromal compartment and the second will discuss stromal effects in chemotherapy.

IR kills cancer cells through many multicellular effects, indicating that other mechanisms than IR-caused DNA damage contribute to therapeutic response. In an intact organism, all cells are subject to complex regulatory mechanisms that depend on their interactions with other cells and cellular products that comprise their microenvironment. Therefore, the effects of IR should not just be considered in terms of isolated cells, but rather the entire tissue has a role in determining the response of any individual cell to regulatory or damaging signals. Once cells are exposed to radiation, DNA damage induces a stress response through activation or repression of distinct target proteins that primarily function to facilitate DNA repair and prevent the proliferation of damaged cells. Similar to the stress response program within cells, IR induces a multicellular program that orchestrates a response to damage at the tissue level. Such programs are executed by soluble signals such as cytokines, growth factors, and chemokines, which function on the stroma to modulate cell behaviors and phenotypes. IR can elicit an "activated" phenotype in some cells that promotes rapid, persistent stromal remodeling of the ECM. Remodeling of the ECM occurs through the induction of proteases and growth factors, and the chronic production of reactive oxygen species (ROS). Tissue

responses to IR seem to be directed toward limiting damage, inducing repair, and restoring tissue homeostasis. However, as with most tissue processes, this response can be disrupted by high doses of radiation, preexisting conditions such as previous exposure, and the genetic features of the individual.

IR damages both the tissue microenvironment and tumor/target cells, and each of these components has a different effect on tissue homeostasis. In target cells such as epithelial and hematopoietic stem cells, IR activates cell-cycle checkpoints and apoptotic programs. When these processes are ineffective and target cells survive, they can propagate chromosome abnormalities and mutations that lead to tumorigenesis. Concomitantly, cells in the microenvironment, such as fibroblasts and immune cells, respond to IR by altering their production of soluble growth factors, cytokines, ROS, and extracellular matrix proteins. These signals normally have effects on damaged target cells to limit neoplastic potential. However, alterations in these activities can promote tumor formation through the pathways such as permanent arrest in an activated state that continually generates growth factors and ROS, affecting the function of normal epithelial cells and hematopoietic stem cells and facilitating tumorigenesis by cells carrying genetic alterations. These signals from the microenvironment can persist for long periods and contribute additional damage which promotes malignant phenotypes.

In determining how the microenvironment is altered by IR exposure, one must consider how energy interacts with biological matter. The two primary mechanisms are direct effects, owing to deposition of energy within a macromolecule, and indirect effects, the interaction of energy with water to produce ROS. Indirect effects cause 60% of the damage from IR. The probability that IR functions on a sufficient number of similar proteins to elicit a biological response is very small. By contrast, the effects of ROS generation are rapidly amplified through their interactions with lipids, membranes and oxygen. In addition to their self-amplification, ROS are probably crucial mediators of changes in the microenvironment, because many proteins have built-in sensors for oxidative stress. So when an organism is exposed to IR, direct macromolecular damage might be dealt with quickly by tagging proteins for degradation by proteosomes, or by repairing DNA molecules, whereas indirect action through ROS can itself be a signal, can be amplified, and can be persistent.

***The Response of Tumor Microenvironment to Ionizing Radiation.*** Cells from the microenvironment can regulate the parenchyma by cell–cell contact with target cells and/or by secreting regulatory mole-

cules (such as hormone or cytokines around the microenvironment) that stimulate or inhibit target-cell proliferation and differentiation. IR also induced many cytokines in the surrounding tissues, such as epidermal growth factor,[311] pro-inflammatory growth factor,[312] and fibroblast growth factor.[313] Furthermore, activation of TGF$\beta$ is an early and persistent event in tissues that have been exposed to both high and low doses of IR.[314-316] TGF$\beta$1 is secreted in a latent complex[317] that is widely distributed throughout the microenvironment. A protein redox switch activates latent TGF$\beta$1, allowing it to function as an extra-cellular sensor of oxidative stress.[318] In addition to its role in homeostatic growth control, TGF$\beta$ has a more complex role in regulating tissue responses to damage, the failure of which could contribute to the development of cancer. The most intriguing of the recent mouse models of TGF$\beta$ function is a fibroblast-specific conditional knockout of TGF$\beta$ signaling created by Moses and colleagues. Mice with a fibroblast-specific knockout of the TGF$\beta$ type II receptor rapidly develop epithelial tumors.[319] The development of intraepithelial neoplasia in prostate tissues and invasive squamous-cell carcinoma of the forestomach were accompanied by an increased abundance of stromal cells. The authors suggest that this is partly owing to the dysregulation of hepatocyte growth factor production, but it is clear that TGF$\beta$ signaling functions both directly and indirectly to suppress tumorigenesis. Furthermore, studies using Tgf$\beta$1-knockout mice have shown that IR-induced epithelial apoptosis and phosphorylation of p53 are severely compromised.[320] This indicates that radiation-induced extracellular signaling has a direct and crucial impact on the cellular response to DNA damage.

Studies of irradiated tissues have shown that the stem-cell compartment is most sensitive to damage, as shown by the selective apoptosis of these cells in response to IR.[321] It has been postulated that this mechanism might serve to eliminate potentially neoplastic cells from the organism. However, in some tissues there is a regenerative recruitment of progenitor cells to re-establish the stem-cell compartment. How does the irradiated microenvironment contribute to the regulation of stem cells? In the intestine, TGF$\beta$ concentrations have been observed to increase in the proliferative zone where stem cells reside,[322] and this cytokine has been postulated to regulate the exit of cells in the intestinal crypt from the cell cycle and their subsequent differentiation.[323] Furthermore, treatment of the intestine with TGF$\beta$3 reduces cell loss in the sensitive stem-cell compartment following irradiation.[324] These data indicate that one function of radiation-induced TGF$\beta$ is to protect the stem-cell compartment. However, the effects of IR on the normal tissue microenvironment limit the radiation dose that can be applied to

tumors. Several experimental models, however, support the concept that IR-mediated toxicity might be decreased by limiting TGFβ signaling. Studies in rodents have shown that inhibition of TGFβ signaling can limit the amount of IR-induced damage that occurs in normal tissues.[325-327] Limiting the predominantly stromal production of TGFβ during radiotherapy seems to block the deleterious cytokine cascades that stimulate inflammation and stromal remodeling.[328]

## Chemotherapy and the Response of the Microenvironment

Since Farber and coworkers first demonstrated the antitumor activity of aminopterin (4-aminopteroyl-glutamic acid) in 1948, much effort has been spent on developing effective cancer chemotherapeutic agents. However, curative or survival benefits have been achieved only in a few selected tumor types.[329] Clinical drug resistance remains a major problem in most cancers, especially in adult solid tumors. Recent cell culture studies have defined three genetic mechanisms of drug resistance: (1) activation and/or overexpression of cell membrane drug efflux transporters, such as p-glycoprotein and other ATP-binding cassette transporter or multi-drug resistance-associated proteins, breast cancer resistance protein, and lung resistance-related protein[330-335]; (2) altered expression or activation of detoxifying enzymes such as glutathione S transferase,[336,337] or quantitative or qualitative alterations of drug targets[338-342]; and (3) defects in apoptosis regulatory proteins.[343-345] Despite promising preclinical data indicating therapeutic advantages to reversing these genetic resistance mechanisms, the clinical results of these experimental approaches have often been disappointing.[346] In this regard, there is growing evidence suggesting that epigenetic factors or proteins present in the tumor microenvironment also play important roles in clinical drug resistance.

An outstanding study by Teicher and coworkers[347] showed that repeatedly treating mice bearing mammary tumors with alkylating agents over a 6-month period produced drug resistant tumor phenotype subclones which showed cross-resistance to alkylating agents when implanted in other recipient mice. They further showed that this acquired resistance was exhibited only *in vivo* and not in tissue culture dishes of the single tumor cell culture,[348] which suggests that some factor(s) in the microenvironment mediated the expression of the drug resistant phenotype. Subsequent work has identified a number of soluble factors in the extracellular environment that can influence tumor chemoresistance. These factors, such as cytokines (GM-CSF, GMSF, IL-6, VEGF, nitric

oxide, and TGF-$\beta$), have been implicated in negatively regulating drug response.[349-352]

Recent studies have accumulated enough evidence to indicate that the tumor microenvironment's growth factors, cytokines, cell–cell and cell–matrix adhesion molecules, hypoxia, and stromal cells also protect tumors from therapeutic intervention. These influences may take place in soluble or contact forms. The soluble form involves production and secretion of certain factors by stromal cells contained in the tumor microenvironment. These soluble factors are then able to bind to cell surface receptors and influence tumor behavior. For example, a series of interleukins are produced and secreted by stromal cells of the bone marrow. These cytokine transducers signal by binding surface receptors and affect proliferation, differentiation, and tumor cell survival. In some cases, interleukins prevent stress-induced apoptosis, which may include drug-induced apoptosis. One particular interleukin, interleukin-6 (IL-6), is able to prevent apoptosis induced by either Fas or drugs.[353,354]

Recently, IL-6 has been implicated in the resistance of myeloma cells to a variety of apoptotic stimuli including cross-linking of the TNF-R family death receptor Fas (CD-95), as well as chemotherapeutic drugs.[355-357] It has been shown that IL-6, produced and secreted primarily by bone marrow stromal cells, is an essential cytokine involved in the growth and survival of myeloma cells.[358,359] In 1992, Lotem and Sachs reported that IL-6 and other growth factors, such as granulocyte macrophage colony-stimulating factor, inhibit apoptosis induced by several chemotherapeutic drugs.[350] In addition, IL-6 has been reported to prevent apoptosis induced by dexamethasone, vitamin D3, and Fas agonistic antibodies.[356,360-362] The signaling pathway by which IL-6 prevents apoptosis and induces cell proliferation has only recently been elucidated. IL-6 activation requires binding to IL-6 receptor (IL-6R) composed of 80- and 130-kDa subunits, the $\alpha$ and $\beta$ subunits, respectively. Following binding of IL-6 to the $\alpha$ subunit, the $\alpha$ subunit then hetero-dimerizes with the $\beta$ subunit and subsequently the $\beta$ subunit homo-dimerizes and stimulates signal trans-duction pathways.[363] Substantial evidence now exists demonstrating that the proliferation effects of IL-6 may be independent of the cell survival effects. This dissociation of the proliferative effects of IL-6 vis-à-vis the antiapoptotic effects may be important for therapeutic manipulation of IL-6 and drug-induced apoptosis. For example, blocking IL-6 binding to the IL-6R$\alpha$ will likely block both the proliferative and antiapoptotic effects of IL-6, and it may be necessary to interrupt only the downstream signaling events associated with antiapoptosis to enhance cytotoxic drug effects. After binding to the IL-6R$\alpha$ and homodimerization of the $\beta$

subunits, the signal transducing component of this receptor, two major pathways are activated: (1) the JAK/STAT pathway; and (2) ras and subsequently the MAPK cascade.[364] One of the MAPK pathways activated by the IL-6 receptor involves the stress-activated protein kinase (SAPK). It was shown that IL-6 inhibited Fas-induced apoptosis by inhibiting the JNK/SAPK and P38 MAPK pathways that were associated with Fas.[355,365]

Another explanation as to how IL-6 blocks apoptosis may be the activation of the JAK/STAT pathway, in particular the JAK2/STAT3 pathway.[365-367] Recent evidence has shown that IL-6 signaling results in STAT3 dimerization, which in turn upregulates the antiapoptotic protein, Bcl-xL. Tu and coworkers showed in both myeloma cell lines and human myeloma specimens that expression of Bcl-sL correlated with resistance to chemotherapy.[368] Schwarze and Hawley, using a mouse myeloma model, showed that aiIL-6 mediated suppression of apoptosis in IL-6-dependent B9 cells involved induction of endogenous Bcl-xL expression but not Bcl-2.[369] In this study, Catlett-Falcone and colleagues showed that IL-6 receptor signaling resulted in elevated levels of activated STAT3, which in turn increased levels of Bcl-xL. These investigators conclusively demonstrated that IL-6 activation of STAT3 was necessary to block Fas-induced apoptosis by interrupting STAT signaling at two different levels: (1) by inhibiting JAK2 phosphorylation using the tyrphostin, AG490; and (2) by using the naturally occurring dominant-negative STAT3$\beta$ gene. Both approaches blocked the STAT3 pathway, resulting in reduced Bl-xL mRNA and protein levels, and reversed resistance to Gas-mediated apoptosis. These studies indicate that both the SAPK pathway and the JAK/STAT pathway are involved in preventing Fas-induced apoptosis. It remains to be determined whether one or both pathways are involved in preventing drug-induced apoptosis, but blocking IL-6 signaling may enhance drug activity. Agents that block JAK phosphorylation and activation of STAT, such as the tryphostin AG-490, may be effective in enhancing cytotoxic drug activity or preventing the emergence of drug resistance. Similarly, agents that reduce STAT3 binding to DNA may reduce the expression of Bcl-xL and thereby enhance drug response. A genetic approach using the dominant negative gene, STAT3$\beta$, may be analogous to using wild-type P53 gene transfer to enhance apoptosis and drug sensitivity.

In contrast to the soluble factors, the insoluble part of the tumor microenvironment may also influence tumor cell behavior by direct contact. Tumor cells may adhere to other cells or components of the extracellular matrix (ECM) making up the tumor microenvironment.

Adhesive interactions between cells or cells and ECM can regulate apoptosis and cell survival in a wide variety of cell types. Durand and Sutherland were among the first to describe how intercellular interactions contribute to tumor cell survival during exposure to cytotoxic stresses such as radiation.[370] Similarly, tumor cell adhesion may influence cell survival and prevent drug-induced apoptosis. It has been well documented that certain drug-resistance mechanisms may only be functional *in vivo*, where tumor cells are able to interact with environmental factors such as ECM and cellular-counter receptors.[370] As mentioned above, Teicher and coworkers showed that mammary tumors resistant to alkylating agents *in vivo* were sensitized to chemotherapeutic drugs once the tumor cells were removed from the animal.[347] St. Croix demonstrated that adhesive interactions between some cell types could confer drug resistance.[371] Using EMT-6 mouse mammary tumor cells, St. Croix and coworkers found that when cells were grown as tightly adherent spheroids the tumor cells had a higher fraction in G1 phase and were more resistant to drugs and radiation than when cells were grown as a monolayer.[371] Although the cell surface molecules mediating this type of kinetic resistance were not identified, studies showed that when mouse tumor cells were gown as spheroids compared with monolayers, cells grew slower and expressed higher levels of the cyclin-dependent kinase inhibitor, p27ktp1. Using an antisense approach, these investigators were able to demonstrate a causal relationship between elevated levels of p27kip1 and drug resistance. This study shows that identifying how cells communicate and regulate expression of p27kip1 may have important implications for cancer chemotherapy. Further, it establishes p27kip1 as a new target to enhance cytotoxic drug activity and perhaps prevent drug resistance.

Recent studies in myeloma cells demonstrated that integrins also are important in mediating resistance to drug-induced apoptosis.[372-374] Experimental evidence has implicated the $\beta 1$ integrin and fibronectin interaction in apoptotic suppression and tumor cell survival.[374] Several studies demonstrated that stress induced Bcl-2 antiapoptotic signaling pathway through $\alpha v\beta 1$ and fibronectin interaction, the anti-$\beta 1$ antibodies or antisense oligonucleotides enhanced apoptosis process.[375,376] Damiano and coworkers showed that integrins such as $\alpha v\beta 1$ or $\alpha 5\beta 1$ are major receptors in response to drug resistance in a myeloma cell line.[372,373] These studies showed that when drug-sensitive myeloma cells expressed receptors to fibronectin and adhered to fibronectin, they became relatively resistant to the apoptotic effects of chemotherapy agents such as doxorubicin and melphalan. This integrin-induced drug resistance in cancer was also shown in solid tumors in a recent study of small cell lung cancer

(SCLC) demonstrating that the levels of collagen IV, fibronectin, and tenascin were elevated in most sections of SCLC that protect SCLC cells from chemotherapy-induced apoptosis.[377] Importantly, incubation with a function-blocking integrin $\beta$1 antibody or with protein tyrosine kinase inhibitors could inhibit these effects, demonstrating that apoptosis resistance was mediated through binding of the integrins by the ECM and implicating tyrosine phosphorylation downstream of integrin activation.

It is still unclear what signaling pathways are activated by ECM in response to drug resistance, but tissue architecture may be crucial in mediating apoptosis resistance. Weaver and coworkers showed that reconstituted basement membrane can lead to the formation of polarized structures which are essential in protecting these cells from chemotherapy-induced apoptosis in a breast cancer cell model.[378] Cell polarity resulting from the interaction of the basement membrane molecules in conditions where polarity could not be induced did not lead to resistance. As a clue to possible downstream signals that may result from these interactions, chemoresistance was accompanied by NF-kB activation, a transcription factor that has been involved in mediating survival signals.[379] Similarly, myeloma cells strongly induced NF-kB when adhered to the ECM component fibronectin, a treatment known to promote drug resistance.[380]

Experimental evidence has defined some of the resistance mechanisms, leading to the development of innovative approaches aiming at specific targets. Interactions between tumor and microenvironment-derived factors affect chemosensitivity or chemoresistance in two ways. First, these factors can modulate each other and act cooperatively on several levels, eg, regulation of expression of factors to induce environmental remodeling, cooperative activation between adhesion molecules and receptor tyrosine kinases, and cross-talk between downstream signaling pathways. Growth factors and cytokines can also change in adhesion molecules, and cell–cell or cell–matrix adhesion promoting expression of survival-conferring soluble factors. Interaction between adhesion molecules and receptor tyrosine kinases on the cell membrane regulate the downstream signaling pathways and cell survival in multiple experimental models.[153,374,380,381] In addition, N-cadhesin, which is upregulated to replace E-cadherin during EMT, is able to activate or augment the signaling of the stromal cell factors, such as the FGF system. Simultaneous upregulation of adhesion molecules and FGFR3 in tumor tissues obtained from advanced lung cancer patients after chemotherapy further suggests a common response of tumor- and microenvironment-derived factors to cytotoxic insults. Individual factors may also have direct and indirect effects on multiple levels. For example, in addition to triggering the

protective mechanisms in hypoxic cells, hypoxia initiates environment change by regulating the expression of certain growth factors, matrix components, and adhesion molecules, and thereby protects hypoxic tumor cells as well as the neighboring nonhypoxic cells from stress. These various interactions often confer survival advantage to tumor cells.

Second, there is a high degree of redundancy between the intracellular signaling pathways activated by receptors and adhesion molecules. Cross-talk between these pathways regulates the intensity and duration of the activation and plays a critical role in signaling differentiation. An example is the redundant intracellular signaling pathways of integrins and growth factors. The effects of redundant signaling are twofold. The activation of one factor can compensate for the blocking of the activation of the second factor, eg, EGF-mediated protection is attenuated when cells are adherent to extracellular matrix components. Furthermore, the redundant signaling provides more robust protection, making it more difficult to overcome the survival advantage by blocking only a single target.

## Laboratory and Clinical Observations

Because prostate cancer growth is highly susceptible to tumor–microenvironment interaction and experimentally can be promoted by stroma fibroblasts, it is reasonable to think that control of prostate tumor growth might be optimized by cotargeting both tumor and stroma. To explore this concept, we designed studies coculturing prostate cancer cells and bone stroma *in vitro*, establishing chimeric tumor models consisting of human prostate cancer cells and bone stroma. By introducing a "bystander" therapeutic gene, herpes simplex thymidine kinase (hsv-TK), to stromal cells only, we observed effective cell kill in tumor epithelium *in vitro* and shrinkage of tumor size *in vivo* on addition of a pro-drug, ganciclovir (GCV). Since there were no identifiable gap junctions between prostate tumor cells and bone stroma under the electron microscope, we concluded that there must be metabolic cooperation between tumor epithelium and bone stroma mediated by soluble factors and extracellular matrices. By interrupting this communication, and targeting both tumor and stroma, tumor growth and survival may be adversely affected. Conceptually, cotargeting tumor and stroma in prostate cancer bone metastasis is a rational approach to the vicious cycle constantly operating between tumor and stroma. Directly inducing cell-kill of tumor epithelium and starving cancer cells by disrupting tumor interaction with the stromal compartment could achieve the best possible tumor regression.

In our laboratory, we cotargeted tumor and stroma using an adenoviral vector in which therapeutic gene expression was controlled

by a tissue-specific and tumor restrictive promoter, such as osteocalcin, osteonectin, or bone sialoprotein. These have been shown to be highly effective in inducing long-term tumor regression, and even some cure in preestablished tumor in the skeleton, with administration of the adenovirus through the intravenous route.[382-384] This concept of bone targeting to improve therapeutic effects has received clinical support. Tu and colleagues[213] reported a significant prolongation of patient survival by targeting bone with strontium 89 and prostate tumors with chemotherapy.

## Molecular Therapy Cotargeting Both Tumor and Stroma

The bone microenvironment was depicted by Paget over a century ago as a specialized "soil" that favors the metastasis of certain selective cancer cell types ("seed").[385] Although the precise mechanism by which cancer cells home to bone is still unknown, several attractive ideas and hypotheses have been proposed. Bone must express certain chemoattractants that selectively retain circulating cancer cells, and cancer cells must express cognate ligands or receptors allowing them to attach to bone marrow-associated endothelial cells, marrow stromal cells or osteoblasts, and/or respond to bone-derived growth factors, cytokines/chemokines, or extracellular matrices. To metastasize to bone, cancer cells must be able to survive hostile circulatory compartments, including the blood and lymphatic channels. The mere detection of cancer cells in blood or marrow stromal compartments may not reflect the vitality of cancer cells. Solakoglu and coworkers[386] demonstrated that 81% of prostate cancer patients showed cytokeratin-postive tumor cells in their bone marrow.

From our use of prostate cancer cell lines as a model to study tumor–stroma interaction, we suggest that a switch of transcriptional factors must occur during the pathogenesis of prostate cancer. This biochemical switch could occur early, even when epithelial cells are still in the primary, since even then the expression of bone-like proteins such as osteocalcin, osteopontin, osteonectin, and bone sialoprotein was detected. Considering how osteocalcin promoter in prostate cancer cells is regulated, a vicious cycle could occur at the level of transcription factor activation, wherein the coordinated activation of transcription factors by known soluble factors and ECM-integrin signaling culminates in the ability of prostate cancer cells to proliferate and survive in bone. Numerous links have been established between the upregulation of transcription factors such as Runx-2 and the potential alteration of cellular behavior that could lead to increased cell growth and spread to bone.

Runx-2 is a potent and specific transcription factor that controls mesenchymal–epithelial interaction in tooth development.[256] Apparently, Runx-2 activation is controlled by soluble growth factors, and on activation it can regulate soluble growth factor secretion, which ultimately controls the growth and differentiation of enamel tooth epithelium. Based on this and other published data, we proposed that activation of similar transcription factors such as Runx-2 in prostate cancer cells could potentially enhance prostate cancer cell invasion and migration through the induction of collagenase (eg, collagenase 3) and other metalloproteinases. The concomitant induction of Runx-2, collagenase 3, and other growth and differentiation supportive factors could enhance prostate cancer survival and invasion. Similarly, the activation of the $\alpha V\beta 3$ and $\alpha 2V\beta 1$ integrin-ECM pathways may promote outside-in signals that result in enhanced cell migration and invasion.

We proposed earlier that prostate cancer metastasis to bone is not a random process. It involves the specific recognition of cancer cells by bone as "self" and the production of bone-like proteins by cancer cells. The expression of bone-like proteins by prostate cancer cells may allow them to adhere, proliferate, and survive in the bone microenvironment and participate in certain normal functions of bone cells, ie, bone resorption.

Cancer cells express a bone-like phenotype early, when they are still in the primary lesion. This raises the possibility that the expression of bone-like proteins by cancer cells and reactive stroma may serve as a prognostic biomarker for prostate cancer bone metastasis and possibly as a predictor for cancer survival. By combining the expression of bone-like proteins and the stromal reaction to epithelium, it is possible that novel molecular markers can be developed both at the gene expression and genetic level. Although the role of bone-like protein is unclear now, it is possible that the activation of these processes may occur at the transcription level. Transcriptional factor switching could be of fundamental importance in determining the phenotype of cancer cells and might influence the extent of the vicious cycle between tumor cells and bone stroma. It is possible that specific targeting of transcriptional factors could have benefit as cancer therapy. Interrupting the activation of bone-like proteins by in tumor epithelium and bone stroma may prevent prostate cancer cell adherence, proliferation, and survival in bone.

## REFERENCES

1. Sung SY, Chung LW. Prostate tumor-stroma interaction: molecular mechanisms and opportunities for therapeutic targeting. Differentiation 2002;70(9-10):506-21.

2. Moussa M, Kloth D, Peers G, Cherian MG, Frei JV, Chin JL. Metallothionein expression in prostatic carcinoma: correlation with Gleason grade, pathologic stage, DNA content and serum level of prostate-specific antigen. Clin Invest Med 1997;20(6):371-80.

3. Stanford JL, McDonnell SK, Friedrichsen DM, et al. Prostate cancer and genetic susceptibility: a genome scan incorporating disease aggressiveness. Prostate 2006;66(3):317-25.

4. Glinsky VV, Glinsky GV, Glinskii OV, et al. Intravascular metastatic cancer cell homotypic aggregation at the sites of primary attachment to the endothelium. Cancer Res 2003;63(13):3805-11.

5. Mundy GR. Mechanisms of bone metastasis. Cancer 1997;80(8):1546-56 (suppl).

6. Corey E, Arfman EW, Oswin MM, et al. Detection of circulating prostate cells by reverse transcriptase-polymerase chain reaction of human glandular kallikrein (hK2) and prostate-specific antigen (PSA) messages. Urology 1997;50(2):184-8.

7. del Regato JA. Pathways of metastatic spread of malignant tumors. Semin Oncol 1977;4(1):33-8.

8. Berezovskaya O, Schimmer AD, Glinskii AB, et al. Increased expression of apoptosis inhibitor protein XIAP contributes to anoikis resistance of circulating human prostate cancer metastasis precursor cells. Cancer Res 2005;65(6):2378-86.

9. Steeg PS. Tumor metastasis: mechanistic insights and clinical challenges. Nat Med 2006;12(8):895-904.

10. Witz IP. Tumor-microenvironment interactions: the selectin-selectin ligand axis in tumor-endothelium cross talk. Cancer Treat Res 2006;130:125-40.

11. Harlozinska A. Progress in molecular mechanisms of tumor metastasis and angiogenesis. Anticancer Res 2005;25(5):3327-33.

12. Thalmann GN, Sikes RA, Wu TT, et al. LNCaP progression model of human prostate cancer: androgen-independence and osseous metastasis. Prostate 2000;44(2):91-103.

13. Wu HC, Hsieh JT, Gleave ME, Brown NM, Pathak S, Chung LW. Derivation of androgen-independent human LNCaP prostatic cancer cell sublines: role of bone stromal cells. Int J Cancer 1994;57(3):406-12.

14. Rhee HW, Zhau HE, Pathak S, et al. Permanent phenotypic and genotypic changes of prostate cancer cells cultured in a three-dimensional rotating-wall vessel. In Vitro Cell Dev Biol Anim 2001;37(3):127-40.

15. Wang R, Xu J, Juliette L, et al. Three-dimensional co-culture models to study prostate cancer growth, progression, and metastasis to bone. Semin Cancer Biol 2005;15(5):353-64.

16. Olumi AF, Grossfeld GD, Hayward SW, Carroll PR, Tlsty TD, Cunha GR. Carcinoma-associated fibroblasts direct tumor progression of initiated human prostatic epithelium. Cancer Res 1999;59(19):5002-11.

17. Wong YC, Wang YZ. Growth factors and epithelial-stromal interactions in prostate cancer development. Int Rev Cytol 2000;199:65-116.

18. Bissell MJ, Labarge MA. Context, tissue plasticity, and cancer: are tumor stem cells also regulated by the microenvironment? Cancer Cell 2005;7(1):17-23.

19. Bissell MJ, Radisky D. Putting tumours in context. Nat Rev Cancer 2001;1(1):46-54.

20. Naishiro Y, Yamada T, Takaoka AS, et al. Restoration of epithelial cell polarity in

a colorectal cancer cell line by suppression of beta-catenin/T-cell factor 4-mediated gene transactivation. Cancer Res 2001;61(6):2751-8.

21. Chung LW, Baseman A, Assikis V, Zhau HE. Molecular insights into prostate cancer progression: the missing link of tumor microenvironment. J Urol 2005;173(1):10-20.

22. Hill R, Song Y, Cardiff RD, Van Dyke T. Selective evolution of stromal mesenchyme with p53 loss in response to epithelial tumorigenesis. Cell 2005;123(6):1001-11.

23. Nishimura K, Kitamura M, Miura H, et al. Prostate stromal cell-derived hepatocyte growth factor induces invasion of prostate cancer cell line DU145 through tumor-stromal interaction. Prostate 1999;41(3):145-53.

24. Sung SY, Kubo H, Shigemura K, et al. Oxidative stress induces ADAM9 protein expression in human prostate cancer cells. Cancer Res 2006;66(19):9519-26.

25. Tuxhorn JA, Ayala GE, Smith MJ, Smith VC, Dang TD, Rowley DR. Reactive stroma in human prostate cancer: induction of myofibroblast phenotype and extracellular matrix remodeling. Clin Cancer Res 2002;8(9):2912-23.

26. Kaminski A, Hahne JC, Haddouti el M, Florin A, Wellmann A, Wernert N. Tumour-stroma interactions between metastatic prostate cancer cells and fibroblasts. Int J Mol Med 2006;18(5):941-50.

27. Huang W-C, Chung LW. Invasive Prostate Cancer Cells Secrete Soluble Protein Factors That Upregulate Osteocalcin (OC) Promoter Activity: Implication to Stroma Desmoplastic Response and Cancer Metastasis. AUA Annual Conference 2003. Chicago, IL: Journal of Urology, 2003:154.

28. Iacobuzio-Donahue CA, Argani P, Hempen PM, Jones J, Kern SE. The desmoplastic response to infiltrating breast carcinoma: gene expression at the site of primary invasion and implications for comparisons between tumor types. Cancer Res 2002;62(18):5351-7.

29. Nemeth JA, Harb JF, Barroso U Jr, He Z, Grignon DJ, Cher ML. Severe combined immunodeficient-hu model of human prostate cancer metastasis to human bone. Cancer Res 1999;59(8):1987-93.

30. Aishima S, Taguchi K, Terashi T, Matsuura S, Shimada M, Tsuneyoshi M. Tenascin expression at the invasive front is associated with poor prognosis in intrahepatic cholangiocarcinoma. Mod Pathol 2003;16(10):1019-27.

31. Weber CK, Sommer G, Michl P, et al. Biglycan is overexpressed in pancreatic cancer and induces G1-arrest in pancreatic cancer cell lines. Gastroenterology 2001;121(3):657-67.

32. Gordon JN, Shu WP, Schlussel RN, Droller MJ, Liu BC. Altered extracellular matrices influence cellular processes and nuclear matrix organizations of overlying human bladder urothelial cells. Cancer Res 1993;53(20):4971-7.

33. Robbins SE, Shu WP, Kirschenbaum A, Levine AC, Miniati DN, Liu BC. Bone extracellular matrix induces homeobox proteins independent of androgens: possible mechanism for androgen-independent growth in human prostate cancer cells. Prostate 1996;29(6):362-70.

34. Untergasser G, Gander R, Lilg C, Lepperdinger G, Plas E, Berger P. Profiling molecular targets of TGF-beta1 in prostate fibroblast-to-myofibroblast transdifferentiation. Mech Ageing Dev 2005;126(1):59-69.

35. Ricciardelli C, Mayne K, Sykes PJ, et al. Elevated levels of versican but not decorin

predict disease progression in early-stage prostate cancer. Clin Cancer Res 1998;4(4):963-71.

36. Cross NA, Chandrasekharan S, Jokonya N, et al. The expression and regulation of ADAMTS-1, -4, -5, -9, and -15, and TIMP-3 by TGFbeta1 in prostate cells: relevance to the accumulation of versican. Prostate 2005;63(3):269-75.

37. Sakko AJ, Ricciardelli C, Mayne K, et al. Modulation of prostate cancer cell attachment to matrix by versican. Cancer Res 2003;63(16):4786-91.

38. Ayala G, Tuxhorn JA, Wheeler TM, et al. Reactive stroma as a predictor of biochemical-free recurrence in prostate cancer. Clin Cancer Res 2003;9(13): 4792-801.

39. Moinfar F, Man YG, Arnould L, Bratthauer GL, Ratschek M, Tavassoli FA. Concurrent and independent genetic alterations in the stromal and epithelial cells of mammary carcinoma: implications for tumorigenesis. Cancer Res 2000;60(9): 2562-6.

40. Xu J, Wang R, Xie ZH, et al. Prostate cancer metastasis: role of the host microenvironment in promoting epithelial to mesenchymal transition and increased bone and adrenal gland metastasis. Prostate 2006;66(15):1664-73.

41. Singer C, Rasmussen A, Smith HS, Lippman ME, Lynch HT, Cullen KJ. Malignant breast epithelium selects for insulin-like growth factor II expression in breast stroma: evidence for paracrine function. Cancer Res 1995;55(11):2448-54.

42. Chung LW. The role of stromal-epithelial interaction in normal and malignant growth. Cancer Surv 1995;23:33-42.

43. Ames BN, Gold LS, Willett WC. The causes and prevention of cancer. Proc Natl Acad Sci U S A 1995;92(12):5258-65.

44. Platz EA, De Marzo AM. Epidemiology of inflammation and prostate cancer. J Urol 2004;171(2 Pt 2):S36-40.

45. Nelson WG, De Marzo AM, DeWeese TL, Isaacs WB. The role of inflammation in the pathogenesis of prostate cancer. J Urol 2004;172(5 Pt 2):S6-11; discussion S-2.

46. De Marzo AM, Marchi VL, Epstein JI, Nelson WG. Proliferative inflammatory atrophy of the prostate: implications for prostatic carcinogenesis. Am J Pathol 1999;155(6):1985-92.

47. Zha S, Gage WR, Sauvageot J, et al. Cyclooxygenase-2 is up-regulated in proliferative inflammatory atrophy of the prostate, but not in prostate carcinoma. Cancer Res 2001;61(24):8617-23.

48. Gerstenbluth RE, Seftel AD, MacLennan GT, et al. Distribution of chronic prostatitis in radical prostatectomy specimens with up-regulation of bcl-2 in areas of inflammation. J Urol 2002;167(5):2267-70.

49. Bostwick DG, de la Roza G, Dundore P, Corica FA, Iczkowski KA. Intraepithelial and stromal lymphocytes in the normal human prostate. Prostate 2003;55(3): 187-93.

50. Liu D, Liao M, Zuo J, Henner WD, Fan F. The effect of chemical carcinogenesis on rat glutathione S-transferase P1 gene transcriptional regulation. Mol Biol Rep 2001;28(1):19-25.

51. Gasche C, Chang CL, Rhees J, Goel A, Boland CR. Oxidative stress increases frameshift mutations in human colorectal cancer cells. Cancer Res 2001;61(20): 7444-8.

52. Oda D, Nguyen MP, Royack GA, Tong DC. H2O2 oxidative damage in cultured

oral epithelial cells: the effect of short-term vitamin C exposure. Anticancer Res 2001;21(4A):2719-24.

53. Tuxhorn JA, Ayala GE, Rowley DR. Reactive stroma in prostate cancer progression. J Urol 2001;166(6):2472-83.

54. Bonkhoff H, Wernert N, Dhom G, Remberger K. Basement membranes in fetal, adult normal, hyperplastic and neoplastic human prostate. Virchows Arch A Pathol Anat Histopathol 1991;418(5):375-81.

55. Chung LW, Davies R. Prostate epithelial differentiation is dictated by its surrounding stroma. Mol Biol Rep 1996;23(1):13-9.

56. Chung LW, Huang WC, Sung SY, et al. Stromal-epithelial interaction in prostate cancer progression. Clin Genitourin Cancer 2006;5(2):162-70.

57. Cunha GR, Cooke PS, Kurita T. Role of stromal-epithelial interactions in hormonal responses. Arch Histol Cytol 2004;67(5):417-34.

58. Cunha GR, Hayward SW, Wang YZ. Role of stroma in carcinogenesis of the prostate. Differentiation 2002;70(9-10):473-85.

59. Chung LW, Cunha GR. Stromal-epithelial interactions. II. Regulation of prostatic growth by embryonic urogenital sinus mesenchyme. Prostate 1983;4(5):503-11.

60. Hsieh CL, Gardner TA, Miao L, Balian G, Chung LW. Cotargeting tumor and stroma in a novel chimeric tumor model involving the growth of both human prostate cancer and bone stromal cells. Cancer Gene Ther 2004;11(2):148-55.

61. Gleave M, Hsieh JT, Gao CA, von Eschenbach AC, Chung LW. Acceleration of human prostate cancer growth *in vivo* by factors produced by prostate and bone fibroblasts. Cancer Res 1991;51(14):3753-61.

62. Gleave ME, Hsieh JT, von Eschenbach AC, Chung LW. Prostate and bone fibroblasts induce human prostate cancer growth *in vivo*: implications for bidirectional tumor-stromal cell interaction in prostate carcinoma growth and metastasis. J Urol 1992;147(4):1151-9.

63. Zhau HE, Hong SJ, Chung LW. A fetal rat urogenital sinus mesenchymal cell line (rUGM): accelerated growth and conferral of androgen-induced growth responsiveness upon a human bladder cancer epithelial cell line *in vivo*. Int J Cancer 1994;56(5):706-14.

64. Chung LW. Prostate carcinoma bone-stroma interaction and its biologic and therapeutic implications. Cancer 2003;97(3):772-8 (suppl).

65. Mundy GR, Yoneda T, Hiraga T. Preclinical studies with zoledronic acid and other bisphosphonates: impact on the bone microenvironment. Semin Oncol 2001;28(2):35-44 (suppl 6).

66. Chirgwin JM, Mohammad KS, Guise TA. Tumor-bone cellular interactions in skeletal metastases. J Musculoskelet Neuronal Interact 2004;4(3):308-18.

67. Rowley DR. What might a stromal response mean to prostate cancer progression? Cancer Metastasis Rev 1998;17(4):411-9.

68. Yang F, Tuxhorn JA, Ressler SJ, McAlhany SJ, Dang TD, Rowley DR. Stromal expression of connective tissue growth factor promotes angiogenesis and prostate cancer tumorigenesis. Cancer Res 2005;65(19):8887-95.

69. Boddy JL, Fox SB, Han C, et al. The androgen receptor is significantly associated with vascular endothelial growth factor and hypoxia sensing via hypoxia-inducible factors HIF-1a, HIF-2a, and the prolyl hydroxylases in human prostate cancer. Clin Cancer Res 2005;11(21):7658-63.

70. Mabjeesh NJ, Willard MT, Frederickson CE, Zhong H, Simons JW. Androgens

stimulate hypoxia-inducible factor 1 activation via autocrine loop of tyrosine kinase receptor/phosphatidylinositol 3′-kinase/protein kinase B in prostate cancer cells. Clin Cancer Res 2003;9(7):2416-25.

71. Zhou Q, Liu LZ, Fu B, et al. Reactive oxygen species regulate insulin-induced VEGF and HIF-1{alpha} expression through the activation of p70S6K1 in human prostate cancer cells. Carcinogenesis 2007;28(1):28-37.

72. Burchardt M, Burchardt T, Chen MW, et al. Vascular endothelial growth factor-A expression in the rat ventral prostate gland and the early effects of castration. Prostate 2000;43(3):184-94.

73. Colavitti R, Pani G, Bedogni B, et al. Reactive oxygen species as downstream mediators of angiogenic signaling by vascular endothelial growth factor receptor-2/KDR. J Biol Chem 2002;277(5):3101-8.

74. Charames GS, Bapat B. Genomic instability and cancer. Curr Mol Med 2003;3(7):589-96.

75. Juliano RL, Varner JA. Adhesion molecules in cancer: the role of integrins. Curr Opin Cell Biol 1993;5(5):812-8.

76. Kornberg LJ. Focal adhesion kinase and its potential involvement in tumor invasion and metastasis. Head Neck 1998;20(8):745-52.

77. Cordes N. Integrin-mediated cell-matrix interactions for prosurvivaland antiapop-totic signaling after genotoxic injury. Cancer Lett 2006;242(1):11-9.

78. Zhang X, Li Y, Huang Q, et al. Increased resistance of tumor cells to hyperthermia mediated by integrin-linked kinase. Clin Cancer Res 2003;9(3):1155-60.

79. Edlund M, Miyamoto T, Sikes RA, et al. Integrin expression and usage by prostate cancer cell lines on laminin substrata. Cell Growth Differ 2001;12(2):99-107.

80. Zheng DQ, Woodard AS, Tallini G, Languino LR. Substrate specificity of alpha(v)beta(3) integrin-mediated cell migration and phosphatidylinositol 3-kinase/AKT pathway activation. J Biol Chem 2000;275(32):24565-74.

81. Zheng DQ, Woodard AS, Fornaro M, Tallini G, Languino LR. Prostatic carcinoma cell migration via alpha(v) beta3 integrin is modulated by a focal adhesion kinase pathway. Cancer Res 1999;59(7):1655-64.

82. Vellon L, Menendez JA, Lupu R. A bidirectional "alpha(v)beta(3) integrin-ERK1/ERK2 MAPK" connection regulates the proliferation of breast cancer cells. Mol Carcinog 2006;45(10):795-804.

83. Thamilselvan V, Basson MD. Pressure activates colon cancer cell adhesion by inside-out focal adhesion complex and actin cytoskeletal signaling. Gastroenterology 2004;126(1):8-18.

84. Vellon L, Menendez JA, Lupu R. AlphaVbeta3 integrin regulates heregulin (HRG)-induced cell proliferation and survival in breast cancer. Oncogene 2005;24(23):3759-73.

85. Dow JK, DeVere White RW. Fibroblast growth factor 2: its structure and property, paracrine function, tumor angiogenesis, and prostate-related mitogenic and onco-genic functions. Urology 2000;55(6):800-6.

86. Giri D, Ropiquet F, Ittmann M. Alterations in expression of basic fibroblast growth factor (FGF) 2 and its receptor FGFR-1 in human prostate cancer. Clin Cancer Res 1999;5(5):1063-71.

87. Wu X, Jin C, Wang F, Yu C, McKeehan WL. Stromal cell heterogeneity in fibroblast growth factor-mediated stromal-epithelial cell cross-talk in premalignant prostate tumors. Cancer Res 2003;63(16):4936-44.

88. Kwabi-Addo B, Ozen M, Ittmann M. The role of fibroblast growth factors and their receptors in prostate cancer. Endocr Relat Cancer 2004;11(4):709-24.

89. Doll JA, Reiher FK, Crawford SE, Pins MR, Campbell SC, Bouck NP. Thrombospondin-1, vascular endothelial growth factor and fibroblast growth factor-2 are key functional regulators of angiogenesis in the prostate. Prostate 2001;49(4): 293-305.

90. West AF, O'Donnell M, Charlton RG, Neal DE, Leung HY. Correlation of vascular endothelial growth factor expression with fibroblast growth factor-8 expression and clinico-pathologic parameters in human prostate cancer. Br J Cancer 2001;85(4):576-83.

91. Claffey KP, Abrams K, Shih SC, Brown LF, Mullen A, Keough M. Fibroblast growth factor 2 activation of stromal cell vascular endothelial growth factor expression and angiogenesis. Lab Invest 2001;81(1):61-75.

92. Yan G, Fukabori Y, McBride G, Nikolaropolous S, McKeehan WL. Exon switching and activation of stromal and embryonic fibroblast growth factor (FGF)-FGF receptor genes in prostate epithelial cells accompany stromal independence and malignancy. Mol Cell Biol 1993;13(8):4513-22.

93. Sitaras NM, Sariban E, Bravo M, Pantazis P, Antoniades HN. Constitutive production of platelet-derived growth factor-like proteins by human prostate carcinoma cell lines. Cancer Res 1988;48(7):1930-5.

94. Schatteman GC, Morrison-Graham K, van Koppen A, Weston JA, Bowen-Pope DF. Regulation and role of PDGF receptor alpha-subunit expression during embryogenesis. Development 1992;115(1):123-31.

95. Ikuno Y, Hibino S, Bando H, Kawasaki Y, Nakamura T, Tano Y. Retinal glial cells stimulate microvascular pericyte proliferation via fibroblast growth factor and platelet-derived growth factor *in vitro*. Jpn J Ophthalmol 2002;46(4):413-18.

96. Bostrom H, Gritli-Linde A, Betsholtz C. PDGF-A/PDGF alpha-receptor signaling is required for lung growth and the formation of alveoli but not for early lung branching morphogenesis. Dev Dyn 2002;223(1):155-62.

97. Ishiwata I, Tokieda Y, Kiguchi K, Sato K, Ishikawa H. Effects of embryotrophic factors on the embryogenesis and organogenesis of mouse embryos *in vitro*. Hum Cell 2000;13(4):185-95.

98. Khachigian LM, Collins T. Early growth response factor 1: a pleiotropic mediator of inducible gene expression. J Mol Med 1998;76(9):613-6.

99. Fudge K, Wang CY, Stearns ME. Immunohistochemistry analysis of platelet-derived growth factor A and B chains and platelet-derived growth factor alpha and beta receptor expression in benign prostatic hyperplasias and Gleason-graded human prostate adenocarcinomas. Mod Pathol 1994;7(5):549-54.

100. Vlahos CJ, Kriauciunas TD, Gleason PE, et al. Platelet-derived growth factor induces proliferation of hyperplastic human prostatic stromal cells. J Cell Biochem 1993;52(4):404-13.

101. Greco C, D'Agnano I, Vitelli G, et al. c-MYC deregulation is involved in melphalan resistance of multiple myeloma: role of PDGF-BB. Int J Immunopathol Pharmacol 2006;19(1):67-79.

102. Ferrer FA, Miller LJ, Andrawis RI, et al. Vascular endothelial growth factor (VEGF) expression in human prostate cancer: *in situ* and *in vitro* expression of VEGF by human prostate cancer cells. J Urol 1997;157(6):2329-33.

103. Hanahan D. Signaling vascular morphogenesis and maintenance. Science 1997;277(5322):48-50.
104. Jackson MW, Roberts JS, Heckford SE, et al. A potential autocrine role for vascular endothelial growth factor in prostate cancer. Cancer Res 2002;62(3):854-9.
105. Soker S, Kaefer M, Johnson M, Klagsbrun M, Atala A, Freeman MR. Vascular endothelial growth factor-mediated autocrine stimulation of prostate tumor cells coincides with progression to a malignant phenotype. Am J Pathol 2001;159(2): 651-9.
106. Arbiser JL, Petros J, Klafter R, et al. Reactive oxygen generated by Nox1 triggers the angiogenic switch. Proc Natl Acad Sci U S A 2002;99(2):715-20.
107. Comoglio PM, Tamagnone L, Boccaccio C. Plasminogen-related growth factor and semaphorin receptors: a gene superfamily controlling invasive growth. Exp Cell Res 1999;253(1):88-99.
108. Brunelleschi S, Penengo L, Lavagno L, et al. Macrophage stimulating protein (MSP) evokes superoxide anion production by human macrophages of different origin. Br J Pharmacol 2001;134(6):1285-95.
109. Rampino T, Collesi C, Gregorini M, et al. Macrophage-stimulating protein is produced by tubular cells and activates mesangial cells. J Am Soc Nephrol 2002;13(3):649-57.
110. Cowin AJ, Kallincos N, Hatzirodos N, et al. Hepatocyte growth factor and macrophage-stimulating protein are upregulated during excisional wound repair in rats. Cell Tissue Res 2001;306(2):239-50.
111. Comoglio PM, Trusolino L. Invasive growth: from development to metastasis. J Clin Invest 2002;109(7):857-62.
112. Parr C, Jiang WG. Expression of hepatocyte growth factor/scatter factor, its activator, inhibitors and the c-Met receptor in human cancer cells. Int J Oncol 2001;19(4):857-63.
113. Denda K, Shimomura T, Kawaguchi T, Miyazawa K, Kitamura N. Functional characterization of Kunitz domains in hepatocyte growth factor activator inhibitor type 1. J Biol Chem 2002;277(16):14053-9.
114. Nishimura K, Kitamura M, Takada S, et al. Regulation of invasive potential of human prostate cancer cell lines by hepatocyte growth factor. Int J Urol 1998;5(3):276-81.
115. Zhu X, Humphrey PA. Overexpression and regulation of expression of scatter factor/hepatocyte growth factor in prostatic carcinoma. Urology 2000;56(6): 1071-4.
116. Gmyrek GA, Walburg M, Webb CP, et al. Normal and malignant prostate epithelial cells differ in their response to hepatocyte growth factor/scatter factor. Am J Pathol 2001;159(2):579-90.
117. Davies G, Jiang WG, Mason MD. HGF/SF modifies the interaction between its receptor c-Met, and the E-cadherin/catenin complex in prostate cancer cells. Int J Mol Med 2001;7(4):385-8.
118. Davies G, Jiang WG, Mason MD. Matrilysin mediates extracellular cleavage of E-cadherin from prostate cancer cells: a key mechanism in hepatocyte growth factor/scatter factor-induced cell-cell dissociation and *in vitro* invasion. Clin Cancer Res 2001;7(10):3289-97.
119. Miura H, Nishimura K, Tsujimura A, et al. Effects of hepatocyte growth factor on

E-cadherin-mediated cell-cell adhesion in DU145 prostate cancer cells. Urology 2001;58(6):1064-9.

120. You X, Yu HM, Cohen-Gould L, et al. Regulation of migration of primary prostate epithelial cells by secreted factors from prostate stromal cells. Exp Cell Res 2003;288(2):246-56.

121. Gimbrone MA, Jr, Cotran RS, Leapman SB, Folkman J. Tumor growth and neovascularization: an experimental model using the rabbit cornea. J Natl Cancer Inst 1974;52(2):413-27.

122. Folkman J. How is blood vessel growth regulated in normal and neoplastic tissue? G.H.A. Clowes memorial Award lecture. Cancer Res 1986;46(2):467-73.

123. Auerbach W, Auerbach R. Angiogenesis inhibition: a review. Pharmacol Ther 1994;63(3):265-311.

124. Fidler IJ. The organ microenvironment and cancer metastasis. Differentiation 2002;70(9-10):498-505.

125. Carmeliet P, Jain RK. Angiogenesis in cancer and other diseases. Nature 2000;407(6801):249-57.

126. Jain RK. Molecular regulation of vessel maturation. Nat Med 2003;9(6):685-93.

127. Yancopoulos GD, Davis S, Gale NW, Rudge JS, Wiegand SJ, Holash J. Vascular-specific growth factors and blood vessel formation. Nature 2000;407(6801):242-8.

128. Ferrara N, Gerber HP, LeCouter J. The biology of VEGF and its receptors. Nat Med 2003;9(6):669-76.

129. Ke LD, Shi YX, Im SA, Chen X, Yung WK. The relevance of cell proliferation, vascular endothelial growth factor, and basic fibroblast growth factor production to angiogenesis and tumorigenicity in human glioma cell lines. Clin Cancer Res 2000;6(6):2562-72.

130. Zhang H, Issekutz AC. Growth factor regulation of neutrophil-endothelial cell interactions. J Leukoc Biol 2001;70(2):225-32.

131. Mandriota SJ, Seghezzi G, Vassalli JD, et al. Vascular endothelial growth factor increases urokinase receptor expression in vascular endothelial cells. J Biol Chem 1995;270(17):9709-16.

132. Prager GW, Breuss JM, Steurer S, Mihaly J, Binder BR. Vascular endothelial growth factor (VEGF) induces rapid prourokinase (pro-uPA) activation on the surface of endothelial cells. Blood 2004;103(3):955-62.

133. Ishikawa F, Miyazono K, Hellman U, et al. Identification of angiogenic activity and the cloning and expression of platelet-derived endothelial cell growth factor. Nature 1989;338(6216):557-62.

134. Bussolino F, Di Renzo MF, Ziche M, et al. Hepatocyte growth factor is a potent angiogenic factor which stimulates endothelial cell motility and growth. J Cell Biol 1992;119(3):629-41.

135. Risau W, Drexler H, Mironov V, et al. Platelet-derived growth factor is angiogenic *in vivo.* Growth Factors 1992;7(4):261-6.

136. McAlhany SJ, Ressler SJ, Larsen M, et al. Promotion of angiogenesis by ps20 in the differential reactive stroma prostate cancer xenograft model. Cancer Res 2003;63(18):5859-65.

137. Richard C, Kim G, Koikawa Y, et al. Androgens modulate the balance between VEGF and angiopoietin expression in prostate epithelial and smooth muscle cells. Prostate 2002;50(2):83-91.

138. Cascinu S, Graziano F, Catalano V, et al. Vascular endothelial growth factor and

p53 expressions in liver and abdominal metastases from colon cancer. Tumour Biol 2003;24(2):77-81.

139. Cascinu S, Graziano F, Catalano V, et al. Differences of vascular endothelial growth factor (VEGF) expression between liver and abdominal metastases from colon cancer. Implications for the treatment with VEGF inhibitors. Clin Exp Metastasis 2000;18(8):651-5.

140. Brigstock DR. The connective tissue growth factor/cysteine-rich 61/nephroblastoma overexpressed (CCN) family. Endocr Rev 1999;20(2):189-206.

141. Grotendorst GR, Lau LF, Perbal B. CCN proteins are distinct from and should not be considered members of the insulin-like growth factor-binding protein superfamily. Endocrinology 2000;141(6):2254-6.

142. Lau LF, Lam SC. The CCN family of angiogenic regulators: the integrin connection. Exp Cell Res 1999;248(1):44-57.

143. Bradham DM, Igarashi A, Potter RL, Grotendorst GR. Connective tissue growth factor: a cysteine-rich mitogen secreted by human vascular endothelial cells is related to the SRC-induced immediate early gene product CEF-10. J Cell Biol 1991;114(6):1285-94.

144. Ryseck RP, Macdonald-Bravo H, Mattei MG, Bravo R. Structure, mapping, and expression of fisp-12, a growth factor-inducible gene encoding a secreted cysteine-rich protein. Cell Growth Differ 1991;2(5):225-33.

145. O'Brien TP, Yang GP, Sanders L, Lau LF. Expression of cyr61, a growth factor-inducible immediate-early gene. Mol Cell Biol 1990;10(7):3569-77.

146. Martinerie C, Viegas-Pequignot E, Guenard I, et al. Physical mapping of human loci homologous to the chicken nov proto-oncogene. Oncogene 1992;7(12):2529-34.

147. Pennica D, Swanson TA, Welsh JW, et al. WISP genes are members of the connective tissue growth factor family that are up-regulated in wnt-1-transformed cells and aberrantly expressed in human colon tumors. Proc Natl Acad Sci U S A 1998;95(25):14717-22.

148. Chen MM, Lam A, Abraham JA, Schreiner GF, Joly AH. CTGF expression is induced by TGF- beta in cardiac fibroblasts and cardiac myocytes: a potential role in heart fibrosis. J Mol Cell Cardiol 2000;32(10):1805-19.

149. Frazier K, Williams S, Kothapalli D, Klapper H, Grotendorst GR. Stimulation of fibroblast cell growth, matrix production, and granulation tissue formation by connective tissue growth factor. J Invest Dermatol 1996;107(3):404-11.

150. Grotendorst GR, Okochi H, Hayashi N. A novel transforming growth factor beta response element controls the expression of the connective tissue growth factor gene. Cell Growth Differ 1996;7(4):469-80.

151. Igarashi A, Okochi H, Bradham DM, Grotendorst GR. Regulation of connective tissue growth factor gene expression in human skin fibroblasts and during wound repair. Mol Biol Cell 1993;4(6):637-45.

152. Duncan MR, Frazier KS, Abramson S, et al. Connective tissue growth factor mediates transforming growth factor beta-induced collagen synthesis: down-regulation by cAMP. FASEB J 1999;13(13):1774-86.

153. Chen Y, Abraham DJ, Shi-Wen X, et al. CCN2 (connective tissue growth factor) promotes fibroblast adhesion to fibronectin. Mol Biol Cell 2004;15(12):5635-46.

154. Fan WH, Pech M, Karnovsky MJ. Connective tissue growth factor (CTGF)

stimulates vascular smooth muscle cell growth and migration *in vitro*. Eur J Cell Biol 2000;79(12):915-23.

155. Babic AM, Chen CC, Lau LF. Fisp12/mouse connective tissue growth factor mediates endothelial cell adhesion and migration through integrin alphavbeta3, promotes endothelial cell survival, and induces angiogenesis *in vivo*. Mol Cell Biol 1999;19(4):2958-66.

156. Brigstock DR. Regulation of angiogenesis and endothelial cell function by connective tissue growth factor (CTGF) and cysteine-rich 61 (CYR61). Angiogenesis 2002;5(3):153-65.

157. Shimo T, Nakanishi T, Nishida T, et al. Connective tissue growth factor induces the proliferation, migration, and tube formation of vascular endothelial cells *in vitro*, and angiogenesis *in vivo*. J Biochem (Tokyo) 1999;126(1):137-45.

158. Frazier KS, Grotendorst GR. Expression of connective tissue growth factor mRNA in the fibrous stroma of mammary tumors. Int J Biochem Cell Biol 1997;29(1):153-61.

159. Koliopanos A, Friess H, di Mola FF, et al. Connective tissue growth factor gene expression alters tumor progression in esophageal cancer. World J Surg 2002;26(4):420-7.

160. Wenger C, Ellenrieder V, Alber B, et al. Expression and differential regulation of connective tissue growth factor in pancreatic cancer cells. Oncogene 1999;18(4):1073-80.

161. Kasaragod AB, Lucia MS, Cabirac G, Grotendorst GR, Stenmark KR. Connective tissue growth factor expression in pediatric myofibroblastic tumors. Pediatr Dev Pathol 2001;4(1):37-45.

162. Shakunaga T, Ozaki T, Ohara N, et al. Expression of connective tissue growth factor in cartilaginous tumors. Cancer 2000;89(7):1466-73.

163. Blom IE, Goldschmeding R, Leask A. Gene regulation of connective tissue growth factor: new targets for antifibrotic therapy? Matrix Biol 2002;21(6):473-82.

164. Takeichi M. Morphogenetic roles of classic cadherins. Curr Opin Cell Biol 1995;7(5):619-27.

165. Yagi T, Takeichi M. Cadherin superfamily genes: functions, genomic organization, and neurologic diversity. Genes Dev 2000;14(10):1169-80.

166. Birchmeier W, Behrens J. Cadherin expression in carcinomas: role in the formation of cell junctions and the prevention of invasiveness. Biochim Biophys Acta 1994;1198(1):11-26.

167. Vleminckx K, Vakaet L Jr, Mareel M, Fiers W, van Roy F. Genetic manipulation of E-cadherin expression by epithelial tumor cells reveals an invasion suppressor role. Cell 1991;66(1):107-19.

168. Perl AK, Wilgenbus P, Dahl U, Semb H, Christofori G. A causal role for E-cadherin in the transition from adenoma to carcinoma. Nature 1998;392(6672): 190-3.

169. Li G, Herlyn M. Dynamics of intercellular communication during melanoma development. Mol Med Today 2000;6(4):163-9.

170. Tomita K, van Bokhoven A, van Leenders GJ, et al. Cadherin switching in human prostate cancer progression. Cancer Res 2000;60(13):3650-4.

171. Hazan RB, Phillips GR, Qiao RF, Norton L, Aaronson SA. Exogenous expression of N-cadherin in breast cancer cells induces cell migration, invasion, and metastasis. J Cell Biol 2000;148(4):779-90.

172. Islam S, Carey TE, Wolf GT, Wheelock MJ, Johnson KR. Expression of N-cadherin by human squamous carcinoma cells induces a scattered fibroblastic phenotype with disrupted cell-cell adhesion. J Cell Biol 1996;135(6 Pt 1):1643-54.

173. Li G, Satyamoorthy K, Herlyn M. N-cadherin-mediated intercellular interactions promote survival and migration of melanoma cells. Cancer Res 2001;61(9): 3819-25.

174. Nieman MT, Prudoff RS, Johnson KR, Wheelock MJ. N-cadherin promotes motility in human breast cancer cells regardless of their E-cadherin expression. J Cell Biol 1999;147(3):631-44.

175. Edelman GM, Gallin WJ, Delouvee A, Cunningham BA, Thiery JP. Early epochal maps of two different cell adhesion molecules. Proc Natl Acad Sci U S A 1983;80(14):4384-8.

176. Hatta K, Takeichi M. Expression of N-cadherin adhesion molecules associated with early morphogenetic events in chick development. Nature 1986;320(6061):447-9.

177. Bolos V, Peinado H, Perez-Moreno MA, Fraga MF, Esteller M, Cano A. The transcription factor Slug represses E-cadherin expression and induces epithelial to mesenchymal transitions: a comparison with Snail and E47 repressors. J Cell Sci 2003;116(Pt 3):499-511.

178. Peschard P, Ishiyama N, Lin T, Lipkowitz S, Park M. A conserved DpYR motif in the juxtamembrane domain of the Met receptor family forms an atypical c-Cbl/Cbl-b tyrosine kinase binding domain binding site required for suppression of oncogenic activation. J Biol Chem 2004;279(28):29565-71.

179. Carter O, Bailey GS, Dashwood RH. The dietary phytochemical chlorophyllin alters E-cadherin and beta-catenin expression in human colon cancer cells. J Nutr 2004;134(12):3441S-4S (suppl).

180. Fujita Y, Krause G, Scheffner M, et al. Hakai, a c-Cbl-like protein, ubiquitinates and induces endocytosis of the E-cadherin complex. Nat Cell Biol 2002;4(3):222-31.

181. Doherty P, Walsh FS. CAM-FGF receptor interactions: a model for axonal growth. Mol Cell Neurosci 1996;8(2/3):99-111.

182. Suyama K, Shapiro I, Guttman M, Hazan RB. A signaling pathway leading to metastasis is controlled by N-cadherin and the FGF receptor. Cancer Cell 2002;2(4):301-14.

183. Cavallaro U, Niedermeyer J, Fuxa M, Christofori G. N-CAM modulates tumour-cell adhesion to matrix by inducing FGF-receptor signalling. Nat Cell Biol 2001;3(7):650-7.

184. Dejana E, Lampugnani MG, Martinez-Estrada O, Bazzoni G. The molecular organization of endothelial junctions and their functional role in vascular morphogenesis and permeability. Int J Dev Biol 2000;44(6):743-8.

185. Carmeliet P, Lampugnani MG, Moons L, et al. Targeted deficiency or cytosolic truncation of the VE-cadherin gene in mice impairs VEGF-mediated endothelial survival and angiogenesis. Cell 1999;98(2):147-57.

186. Esser S, Lampugnani MG, Corada M, Dejana E, Risau W. Vascular endothelial growth factor induces VE-cadherin tyrosine phosphorylation in endothelial cells. J Cell Sci 1998;111(Pt 13):1853-65.

187. Birchmeier C, Gherardi E. Developmental roles of HGF/SF and its receptor, the c-Met tyrosine kinase. Trends Cell Biol 1998;8(10):404-10.

188. Ponta H, Sherman L, Herrlich PA. CD44: from adhesion molecules to signalling regulators. Nat Rev Mol Cell Biol 2003;4(1):33-45.

189. Ponta H, Wainwright D, Herrlich P. The CD44 protein family. Int J Biochem Cell Biol 1998;30(3):299-305.

190. Herrlich P, Sleeman J, Wainwright D, et al. How tumor cells make use of CD44. Cell Adhes Commun 1998;6(2-3):141-7.

191. Orian-Rousseau V, Chen L, Sleeman JP, Herrlich P, Ponta H. CD44 is required for two consecutive steps in HGF/c-Met signaling. Genes Dev 2002;16(23):3074-86.

192. Yu WH, Woessner JF Jr, McNeish JD, Stamenkovic I. CD44 anchors the assembly of matrilysin/MMP-7 with heparin-binding epidermal growth factor precursor and ErbB4 and regulates female reproductive organ remodeling. Genes Dev 2002;16(3):307-23.

193. Bienz M, Clevers H. Linking colorectal cancer to Wnt signaling. Cell 2000;103(2):311-20.

194. Hay ED. An overview of epithelio-mesenchymal transformation. Acta Anat (Basel) 1995;154(1):8-20.

195. Veltmaat JM, Orelio CC, Ward-Van Oostwaard D, Van Rooijen MA, Mummery CL, Defize LH. Snail is an immediate early target gene of parathyroid hormone related peptide signaling in parietal endoderm formation. Int J Dev Biol 2000;44(3):297-307.

196. Ciruna B, Rossant J. FGF signaling regulates mesoderm cell fate specification and morphogenetic movement at the primitive streak. Dev Cell 2001;1(1):37-49.

197. Nieto MA. The early steps of neural crest development. Mech Dev 2001;105(1-2):27-35.

198. Markwald R, Eisenberg C, Eisenberg L, Trusk T, Sugi Y. Epithelial-mesenchymal transformations in early avian heart development. Acta Anat (Basel) 1996;156(3):173-86.

199. Thiery JP. Epithelial-mesenchymal transitions in tumour progression. Nat Rev Cancer 2002;2(6):442-54.

200. Briegel KJ. Embryonic transcription factors in human breast cancer. IUBMB Life 2006;58(3):123-32.

201. Lombaerts M, van Wezel T, Philippo K, et al. E-cadherin transcriptional down-regulation by promoter methylation but not mutation is related to epithelial-to-mesenchymal transition in breast cancer cell lines. Br J Cancer 2006;94(5):661-71.

202. Luo Y, He DL, Ning L, Shen SL, Li L, Li X. Hypoxia-inducible factor-1alpha induces the epithelial-mesenchymal transition of human prostatecancer cells. Chin Med J (Engl) 2006;119(9):713-8.

203. Rosano L, Spinella F, Di Castro V, et al. Endothelin-1 promotes epithelial-to-mesenchymal transition in human ovarian cancer cells. Cancer Res 2005;65(24):11649-57.

204. Wicki A, Lehembre F, Wick N, Hantusch B, Kerjaschki D, Christofori G. Tumor invasion in the absence of epithelial-mesenchymal transition: podoplanin-mediated remodeling of the actin cytoskeleton. Cancer Cell 2006;9(4):261-72.

205. Yauch RL, Januario T, Eberhard DA, et al. Epithelial versus mesenchymal phenotype determines *in vitro* sensitivity and predicts clinical activity of erlotinib in lung cancer patients. Clin Cancer Res 2005;11(24 Pt 1):8686-98.

206. Vincent-Salomon A, Thiery JP. Host microenvironment in breast cancer

development: epithelial-mesenchymal transition in breast cancer development. Breast Cancer Res 2003;5(2):101-6.

207. Thalmann GN, Anezinis PE, Chang SM, et al. Androgen-independent cancer progression and bone metastasis in the LNCaP model of human prostate cancer. Cancer Res 1994;54(10):2577-81.

208. Bates AW, Baithun SI. Secondary solid neoplasms of the prostate: a clinico-pathological series of 51 cases. Virchows Arch 2002;440(4):392-6.

209. Nelson JB, Nabulsi AA, Vogelzang NJ, et al. Suppression of prostate cancer induced bone remodeling by the endothelin receptor A antagonist atrasentan. J Urol 2003;169(3):1143-9.

210. Smith MR. Zoledronic acid to prevent skeletal complications in cancer: corroborating the evidence. Cancer Treat Rev 2005;31:19-25 (suppl 3).

211. Wu JD, Odman A, Higgins LM, et al. *In vivo* effects of the human type I insulin-like growth factor receptor antibody A12 on androgen-dependent and androgen-independent xenograft human prostate tumors. Clin Cancer Res 2005;11(8):3065-74.

212. Longoria RL, Cox MC, Figg WD. Antiangiogenesis: a possible treatment option for prostate cancer? Clin Genitourin Cancer 2005;4(3):197-202.

213. Tu SM, Millikan RE, Mengistu B, et al. Bone-targeted therapy for advanced androgen-independent carcinoma of the prostate: a randomised phase II trial. Lancet 2001;357(9253):336-41.

214. Boon T, van Baren N. Immunosurveillance against cancer and immunotherapy: synergy or antagonism? N Engl J Med 2003;348(3):252-4.

215. Dunn GP, Bruce AT, Ikeda H, Old LJ, Schreiber RD. Cancer immunoediting: from immunosurveillance to tumor escape. Nat Immunol 2002;3(11):991-8.

216. Zhang L, Conejo-Garcia JR, Katsaros D, et al. Intratumoral T cells, recurrence, and survival in epithelial ovarian cancer. N Engl J Med 2003;348(3):203-13.

217. Boon T, van der Bruggen P. Human tumor antigens recognized by T lymphocytes. J Exp Med 1996;183(3):725-9.

218. van der Bruggen P, Traversari C, Chomez P, et al. A gene encoding an antigen recognized by cytolytic T lymphocytes on a human melanoma. Science 1991;254(5038):1643-7.

219. Renkvist N, Castelli C, Robbins PF, Parmiani G. A listing of human tumor antigens recognized by T cells. Cancer Immunol Immunother 2001;50(1):3-15.

220. Jager E, Ringhoffer M, Altmannsberger M, et al. Immunoselection *in vivo*: independent loss of MHC class I and melanocyte differentiation antigen expression in metastatic melanoma. Int J Cancer 1997;71(2):142-7.

221. Ferrone S, Marincola FM. Loss of HLA class I antigens by melanoma cells: molecular mechanisms, functional significance and clinical relevance. Immunol Today 1995;16(10):487-94.

222. Garrido F, Ruiz-Cabello F, Cabrera T, et al. Implications for immunosurveillance of altered HLA class I phenotypes in human tumours. Immunol Today 1997;18(2):89-95.

223. Hicklin DJ, Marincola FM, Ferrone S. HLA class I antigen downregulation in human cancers: T-cell immunotherapy revives an old story. Mol Med Today 1999;5(4):178-86.

224. Marincola FM, Jaffee EM, Hicklin DJ, Ferrone S. Escape of human solid tumors

from T-cell recognition: molecular mechanisms and functional significance. Adv Immunol 2000;74:181-273.

225. Kammula US, Lee KH, Riker AI, et al. Functional analysis of antigen-specific T lymphocytes by serial measurement of gene expression in peripheral blood mononuclear cells and tumor specimens. J Immunol 1999;163(12):6867-75.

226. Lee KH, Panelli MC, Kim CJ, et al. Functional dissociation between local and systemic immune response during anti-melanoma peptide vaccination. J Immunol 1998;161(8):4183-94.

227. Panelli MC, Riker A, Kammula U, et al. Expansion of tumor-T cell pairs from fine needle aspirates of melanoma metastases. J Immunol 2000;164(1):495-504.

228. Pellegrini P, Berghella AM, Del Beato T, Cicia S, Adorno D, Casciani CU. Disregulation in TH1 and TH2 subsets of CD4+ T cells in peripheral blood of colorectal cancer patients and involvement in cancer establishment and progression. Cancer Immunol Immunother 1996;42(1):1-8.

229. Yoong KF, Adams DH. Interleukin 2 restores CD3-zeta chain expression but fails to generate tumour-specific lytic activity in tumour-infiltrating lymphocytes derived from human colorectal hepatic metastases. Br J Cancer 1998;77(7):1072-81.

230. Lee PP, Yee C, Savage PA, et al. Characterization of circulating T cells specific for tumor-associated antigens in melanoma patients. Nat Med 1999;5(6):677-85.

231. Pasche B. Role of transforming growth factor beta in cancer. J Cell Physiol 2001;186(2):153-68.

232. Khong HT, Restifo NP. Natural selection of tumor variants in the generation of "tumor escape" phenotypes. Nat Immunol 2002;3(11):999-1005.

233. Wang T, Niu G, Kortylewski M, et al. Regulation of the innate and adaptive immune responses by Stat-3 signaling in tumor cells. Nat Med 2004;10(1):48-54.

234. Parmiani G, Castelli C, Dalerba P, et al. Cancer immunotherapy with peptide-based vaccines: what have we achieved? Where are we going? J Natl Cancer Inst 2002;94(11):805-18.

235. Nagorsen D, Scheibenbogen C, Marincola FM, Letsch A, Keilholz U. Natural T cell immunity against cancer. Clin Cancer Res 2003;9(12):4296-303.

236. Nagorsen D, Keilholz U, Rivoltini L, et al. Natural T-cell response against MHC class I epitopes of epithelial cell adhesion molecule, her-2/neu, and carcinoembryonic antigen in patients with colorectal cancer. Cancer Res 2000;60(17):4850-4.

237. Hamann D, Baars PA, Rep MH, et al. Phenotypic and functional separation of memory and effector human CD8+ T cells. J Exp Med 1997;186(9):1407-18.

238. Scheibenbogen C, Letsch A, Schmittel A, Asemissen AM, Thiel E, Keilholz U. Rational peptide-based tumour vaccine development and T cell monitoring. Semin Cancer Biol 2003;13(6):423-9.

239. Friedl P, Wolf K. Tumour-cell invasion and migration: diversity and escape mechanisms. Nat Rev Cancer 2003;3(5):362-74.

240. Folgueras AR, Pendas AM, Sanchez LM, Lopez-Otin C. Matrix metalloproteinases in cancer: from new functions to improved inhibition strategies. Int J Dev Biol 2004;48(5-6):411-24.

241. Overall CM, Kleifeld O. Tumour microenvironment - opinion: validating matrix metalloproteinases as drug targets and anti-targets for cancer therapy. Nat Rev Cancer 2006;6(3):227-39.

242. Goswami S, Sahai E, Wyckoff JB, et al. Macrophages promote the invasion of

breast carcinoma cells via a colony-stimulating factor-1/epidermal growth factor paracrine loop. Cancer Res 2005;65(12):5278-83.

243. Balkwill F. Chemokine biology in cancer. Semin Immunol 2003;15(1):49-55.
244. Wlodarski KH. Properties and origin of osteoblasts. Clin Orthop Relat Res 1990;252:276-93.
245. Andre-Frei V, Chevallay B, Orly I, Boudeulle M, Huc A, Herbage D. Acellular mineral deposition in collagen-based biomaterials incubated in cell culture media. Calcif Tissue Int 2000;66(3):204-11.
246. Wiesmann HP, Meyer U, Plate U, Hohling HJ. Aspects of collagen mineralization in hard tissue formation. Int Rev Cytol 2005;242:121-56.
247. Moursi AM, Damsky CH, Lull J, et al. Fibronectin regulates calvarial osteoblast differentiation. J Cell Sci 1996;109(Pt 6):1369-80.
248. Bellahcene A, Bonjean K, Fohr B, et al. Bone sialoprotein mediates human endothelial cell attachment and migration and promotes angiogenesis. Circ Res 2000;86(8):885-91.
249. Burdick JA, Anseth KS. Photoencapsulation of osteoblasts in injectable RGD-modified PEG hydrogels for bone tissue engineering. Biomaterials 2002;23(22):4315-23.
250. Horton MA. Interactions of connective tissue cells with the extracellular matrix. Bone 1995;17(2):51S-3S (suppl).
251. Kostenuik PJ, Sanchez-Sweatman O, Orr FW, Singh G. Bone cell matrix promotes the adhesion of human prostatic carcinoma cells via the alpha 2 beta 1 integrin. Clin Exp Metastasis 1996;14(1):19-26.
252. O'Regan A, Berman JS. Osteopontin: a key cytokine in cell-mediated and granulomatous inflammation. Int J Exp Pathol 2000;81(6):373-90.
253. Rapuano BE, Wu C, MacDonald DE. Osteoblast-like cell adhesion to bone sialoprotein peptides. J Orthop Res 2004;22(2):353-61.
254. Decker S, van Valen F, Vischer P. Adhesion of osteosarcoma cells to the 70-kDa core region of thrombospondin-1 is mediated by the alpha 4 beta 1 integrin. Biochem Biophys Res Commun 2002;293(1):86-92.
255. Koeneman KS, Yeung F, Chung LW. Osteomimetic properties of prostate cancer cells: a hypothesis supporting the predilection of prostate cancer metastasis and growth in the bone environment. Prostate 1999;39(4):246-61.
256. D'Souza RN, Aberg T, Gaikwad J, et al. Cbfa1 is required for epithelial-mesenchymal interactions regulating tooth development in mice. Development 1999;126(13):2911-20.
257. Strayhorn CL, Garrett JS, Dunn RL, Benedict JJ, Somerman MJ. Growth factors regulate expression of osteoblast-associated genes. J Periodontol 1999;70(11):1345-54.
258. Termine JD. Non-collagen proteins in bone. Ciba Found Symp 1988;136:178-202.
259. Chellaiah MA, Kizer N, Biswas R, et al. Osteopontin deficiency produces osteoclast dysfunction due to reduced CD44 surface expression. Mol Biol Cell 2003;14(1):173-89.
260. Faccio R, Grano M, Colucci S, et al. Localization and possible role of two different alpha v beta 3 integrin conformations in resting and resorbing osteoclasts. J Cell Sci 2002;115(Pt 14):2919-29.
261. Zhou Z, Immel D, Xi CX, et al. Regulation of osteoclast function and bone mass by RAGE. J Exp Med 2006;203(4):1067-80.

262. Zhao H, Kitaura H, Sands MS, Ross FP, Teitelbaum SL, Novack DV. Critical role of beta3 integrin in experimental postmenopausal osteoporosis. J Bone Miner Res 2005;20(12):2116-23.

263. Bakewell SJ, Nestor P, Prasad S, et al. Platelet and osteoclast beta3 integrins are critical for bone metastasis. Proc Natl Acad Sci U S A 2003;100(24):14205-10.

264. Bossard MJ, Tomaszek TA, Thompson SK, et al. Proteolytic activity of human osteoclast cathepsin K. Expression, purification, activation, and substrate identification. J Biol Chem 1996;271(21):12517-24.

265. Sires UI, Schmid TM, Fliszar CJ, Wang ZQ, Gluck SL, Welgus HG. Complete degradation of type X collagen requires the combined action of interstitial collagenase and osteoclast-derived cathepsin-B. J Clin Invest 1995;95(5):2089-95.

266. Geoffroy V, Marty-Morieux C, Le Goupil N, et al. *In vivo* inhibition of osteoblastic metalloproteinases leads to increased trabecular bone mass. J Bone Miner Res 2004;19(5):811-22.

267. Guo LJ, Xie H, Zhou HD, Luo XH, Peng YQ, Liao EY. Stimulation of RANKL and inhibition of membrane-type matrix metalloproteinase-1 expression by parathyroid hormone in normal human osteoblasts. Endocr Res 2004;30(3):369-77.

268. Inoue K, Mikuni-Takagaki Y, Oikawa K, et al. A crucial role for matrix metalloproteinase 2 in osteocytic canalicular formation and bone metabolism. J Biol Chem 2006;281(44):33814-24.

269. Nemeth JA, Yousif R, Herzog M, et al. Matrix metalloproteinase activity, bone matrix turnover, and tumor cell proliferation in prostate cancer bone metastasis. J Natl Cancer Inst 2002;94(1):17-25.

270. Pelletier JP, Boileau C, Brunet J, et al. The inhibition of subchondral bone resorption in the early phase of experimental dog osteoarthritis by licofelone is associated with a reduction in the synthesis of MMP-13 and cathepsin K. Bone 2004;34(3):527-38.

271. Yu X, Huang Y, Collin-Osdoby P, Osdoby P. Stromal cell-derived factor-1 (SDF-1) recruits osteoclast precursors by inducing chemotaxis, matrix metalloproteinase-9 (MMP-9) activity, and collagen transmigration. J Bone Miner Res 2003;18(8):1404-18.

272. Kiviranta R, Morko J, Alatalo SL, et al. Impaired bone resorption in cathepsin K-deficient mice is partially compensated for by enhanced osteoclastogenesis and increased expression of other proteases via an increased RANKL/OPG ratio. Bone 2005;36(1):159-72.

273. Andersen TL, del Carmen Ovejero M, Kirkegaard T, Lenhard T, Foged NT, Delaiss JM. A scrutiny of matrix metalloproteinases in osteoclasts: evidence for heterogeneity and for the presence of MMPs synthesized by other cells. Bone 2004;35(5):1107-19.

274. Sundaram K, Nishimura R, Senn J, Youssef RF, London SD, Reddy SV. RANK ligand signaling modulates the matrix metalloproteinase-9 gene expression during osteoclast differentiation. Exp Cell Res 2007;313(1):168-78.

275. de Vries TJ, Schoenmaker T, Beertsen W, van der Neut R, Everts V. Effect of CD44 deficiency on *in vitro* and *in vivo* osteoclast formation. J Cell Biochem 2005;94(5):954-66.

276. Gray AW, Davies ME, Jeffcott LB. Generation and activity of equine osteoclasts *in vitro*: effects of the bisphosphonate pamidronate (APD). Res Vet Sci 2002;72(2):105-13.

277. Ross FP, Teitelbaum SL. alphavbeta3 and macrophage colony-stimulating factor: partners in osteoclast biology. Immunol Rev 2005;208:88-105.

278. Fu Q, Manolagas SC, O'Brien CA. Parathyroid hormone controls receptor activator of NF-kappaB ligand gene expression via a distant transcriptional enhancer. Mol Cell Biol 2006;26(17):6453-68.

279. Mandelin J, Li TF, Liljestrom M, et al. Imbalance of RANKL/RANK/OPG system in interface tissue in loosening of total hip replacement. J Bone Joint Surg Br 2003;85(8):1196-201.

280. Nakashima T, Kobayashi Y, Yamasaki S, et al. Protein expression and functional difference of membrane-bound and soluble receptor activator of NF-kappaB ligand: modulation of the expression by osteotropic factors and cytokines. Biochem Biophys Res Commun 2000;275(3):768-75.

281. Zou W, Amcheslavsky A, Bar-Shavit Z. CpG oligodeoxynucleotides modulate the osteoclastogenic activity of osteoblasts via Toll-like receptor 9. J Biol Chem 2003;278(19):16732-40.

282. Xing L, Venegas AM, Chen A, et al. Genetic evidence for a role for Src family kinases in TNF family receptor signaling and cell survival. Genes Dev 2001;15(2):241-53.

283. Kong YY, Yoshida H, Sarosi I, et al. OPGL is a key regulator of osteoclastogenesis, lymphocyte development and lymph-node organogenesis. Nature 1999;397(6717): 315-23.

284. Penno H, Silfversward CJ, Frost A, Brandstrom H, Nilsson O, Ljunggren O. Osteoprotegerin secretion from prostate cancer is stimulated by cytokines. in vitro. Biochem Biophys Res Commun 2002;293(1):451-5.

285. Zhang J, Dai J, Yao Z, Lu Y, Dougall W, Keller ET. Soluble receptor activator of nuclear factor kappaB Fc diminishes prostate cancer progression in bone. Cancer Res 2003;63(22):7883-90.

286. Mizuno A, Amizuka N, Irie K, et al. Severe osteoporosis in mice lacking osteoclastogenesis inhibitory factor/osteoprotegerin. Biochem Biophys Res Commun 1998;247(3):610-5.

287. Bucay N, Sarosi I, Dunstan CR, et al. osteoprotegerin-deficient mice develop early onset osteoporosis and arterial calcification. Genes Dev 1998;12(9):1260-8.

288. Rubens RD. Bone metastases: the clinical problem. Eur J Cancer 1998;34(2):210-3.

289. Orr FW, Lee J, Duivenvoorden WC, Singh G. Pathophysiologic interactions in skeletal metastasis. Cancer 2000;88(12):2912-8 (suppl).

290. Roodman GD. Mechanisms of bone metastasis. N Engl J Med 2004;350(16): 1655-64.

291. Yi B, Williams PJ, Niewolna M, Wang Y, Yoneda T. Tumor-derived platelet-derived growth factor-BB plays a critical role in osteosclerotic bone metastasis in an animal model of human breast cancer. Cancer Res 2002;62(3):917-23.

292. Prasad A, Fernandis AZ, Rao Y, Ganju RK. Slit protein-mediated inhibition of CXCR4-induced chemotactic and chemoinvasive signaling pathways in breast cancer cells. J Biol Chem 2004;279(10):9115-24.

293. Norton L, Massague J. Is cancer a disease of self-seeding? Nat Med 2006;12(8):875-8.

294. Cooper CR, Chay CH, Gendernalik JD, et al. Stromal factors involved in prostate carcinoma metastasis to bone. Cancer 2003;97(3):739-47 (suppl).

295. Romanenko A, Morell-Quadreny L, Ramos D, Nepomnyaschiy V, Vozianov A,

Llombart-Bosch A. Extracellular matrix alterations in conventional renal cell carcinomas by tissue microarray profiling influenced by the persistent, long-term, low-dose ionizing radiation exposure in humans. Virchows Arch 2006;448(5): 584-90.

296. Keller ET, Brown J. Prostate cancer bone metastases promote both osteolytic and osteoblastic activity. J Cell Biochem 2004;91(4):718-29.

297. Yeung F, Law WK, Yeh CH, et al. Regulation of human osteocalcin promoter in hormone-independent human prostate cancer cells. J Biol Chem 2002;277(4): 2468-76.

298. Jimenez MJ, Balbin M, Lopez JM, Alvarez J, Komori T, Lopez-Otin C. Collage-nase 3 is a target of Cbfa1, a transcription factor of the runt gene family involved in bone formation. Mol Cell Biol 1999;19(6):4431-42.

299. Garnero P, Buchs N, Zekri J, Rizzoli R, Coleman RE, Delmas PD. Markers of bone turnover for the management of patients with bone metastases from prostate cancer. Br J Cancer 2000;82(4):858-64.

300. Schneider A, Kalikin LM, Mattos AC, et al. Bone turnover mediates preferential localization of prostate cancer in the skeleton. Endocrinology 2005;146(4): 1727-36.

301. Berruti A, Dogliotti L, Tucci M, Tarabuzzi R, Fontana D, Angeli A. Metabolic bone disease induced by prostate cancer: rationale for the use of bisphosphonates. J Urol 2001;166(6):2023-31.

302. Smith MR. The role of bisphosphonates in men with prostate cancer receiving androgen deprivation therapy. Oncology (Williston Park) 2004;18(5):21-5 (suppl 3).

303. Chirgwin JM, Guise TA. Molecular mechanisms of tumor-bone interactions in osteolytic metastases. Crit Rev Eukaryot Gene Expr 2000;10(2):159-78.

304. Mundy GR. Metastasis: Metastasis to bone: causes, consequences and therapeutic opportunities. Nat Rev Cancer 2002;2(8):584-93.

305. Saito H, Tsunenari T, Onuma E, Sato K, Ogata E, Yamada-Okabe H. Humanized monoclonal antibody against parathyroid hormone-related protein suppresses os-teolytic bone metastasis of human breast cancer cells derived from MDA-MB-231. Anticancer Res 2005;25(6B):3817-23.

306. Zhang J, Dai J, Qi Y, et al. Osteoprotegerin inhibits prostate cancer-induced osteoclastogenesis and prevents prostate tumor growth in the bone. J Clin Invest 2001;107(10):1235-44.

307. Lee HL, Pienta KJ, Kim WJ, Cooper CR. The effect of bone-associated growth factors and cytokines on the growth of prostate cancer cells derived from soft tissue versus bone metastases in vitro. Int J Oncol 2003;22(4):921-6.

308. Taichman RS, Cooper C, Keller ET, Pienta KJ, Taichman NS, McCauley LK. Use of the stromal cell-derived factor-1/CXCR4 pathway in prostate cancer metastasis to bone. Cancer Res 2002;62(6):1832-7.

309. Cleeland CS, Gonin R, Hatfield AK, et al. Pain and its treatment in outpatients with metastatic cancer. N Engl J Med 1994;330(9):592-6.

310. Gottesman MM. Cancer gene therapy: an awkward adolescence. Cancer Gene Ther 2003;10(7):501-8.

311. Dent P, Yacoub A, Fisher PB, Hagan MP, Grant S. MAPK pathways in radiation responses. Oncogene 2003;22(37):5885-96.

312. McBride WH, Chiang CS, Olson JL, et al. A sense of danger from radiation. Radiat Res 2004;162(1):1-19.

313. Fuks Z, Persaud RS, Alfieri A, et al. Basic fibroblast growth factor protects endothelial cells against radiation-induced programmed cell death *in vitro* and *in vivo.* Cancer Res 1994;54(10):2582-90.

314. Anscher MS, Crocker IR, Jirtle RL. Transforming growth factor-beta 1 expression in irradiated liver. Radiat Res 1990;122(1):77-85.

315. Barcellos-Hoff MH, Derynck R, Tsang ML, Weatherbee JA. Transforming growth factor-beta activation in irradiated murine mammary gland. J Clin Invest 1994;93(2):892-9.

316. Wang J, Zheng H, Sung CC, Richter KK, Hauer-Jensen M. Cellular sources of transforming growth factor-beta isoforms in early and chronic radiation enteropathy. Am J Pathol 1998;153(5):1531-40.

317. Lawrence DA, Pircher R, Jullien P. Conversion of a high molecular weight latent beta-TGF from chicken embryo fibroblasts into a low molecular weight active beta-TGF under acidic conditions. Biochem Biophys Res Commun 1985;133(3):1026-34.

318. Barcellos-Hoff MH, Dix TA. Redox-mediated activation of latent transforming growth factor-beta 1. Mol Endocrinol 1996;10(9):1077-83.

319. Bhowmick NA, Chytil A, Plieth D, et al. TGF-beta signaling in fibroblasts modulates the oncogenic potential of adjacent epithelia. Science 2004;303(5659):848-51.

320. Ewan KB, Henshall-Powell RL, Ravani SA, et al. Transforming growth factor-beta1 mediates cellular response to DNA damage in situ. Cancer Res 2002;62(20):5627-31.

321. Booth C, Potten CS. Gut instincts: thoughts on intestinal epithelial stem cells. J Clin Invest 2000;105(11):1493-9.

322. Koyama SY, Podolsky DK. Differential expression of transforming growth factors alpha and beta in rat intestinal epithelial cells. J Clin Invest 1989;83(5):1768-73.

323. Barnard JA, Beauchamp RD, Coffey RJ, Moses HL. Regulation of intestinal epithelial cell growth by transforming growth factor type beta. Proc Natl Acad Sci U S A 1989;86(5):1578-82.

324. Potten CS, Booth D, Haley JD. Pretreatment with transforming growth factor beta-3 protects small intestinal stem cells against radiation damage *in vivo.* Br J Cancer 1997;75(10):1454-9.

325. Flanders KC, Major CD, Arabshahi A, et al. Interference with transforming growth factor-beta/ Smad3 signaling results in accelerated healing of wounds in previously irradiated skin. Am J Pathol 2003;163(6):2247-57.

326. Rabbani ZN, Anscher MS, Zhang X, et al. Soluble TGFbeta type II receptor gene therapy ameliorates acute radiation-induced pulmonary injury in rats. Int J Radiat Oncol Biol Phys 2003;57(2):563-72.

327. Xavier S, Piek E, Fujii M, et al. Amelioration of radiation-induced fibrosis: inhibition of transforming growth factor-beta signaling by halofuginone. J Biol Chem 2004;279(15):15167-76.

328. Barcellos-Hoff MH. How do tissues respond to damage at the cellular level? The role of cytokines in irradiated tissues. Radiat Res 1998;150(5):S109-20 (suppl).

329. Nygren P. What is cancer chemotherapy? Acta Oncol 2001;40(2-3):166-74.

330. Borges-Walmsley MI, McKeegan KS, Walmsley AR. Structure and function of efflux pumps that confer resistance to drugs. Biochem J 2003;376(Pt 2):313-38.

331. Gottesman MM, Fojo T, Bates SE. Multidrug resistance in cancer: role of ATP-dependent transporters. Nat Rev Cancer 2002;2(1):48-58.

332. Leonessa F, Clarke R. ATP binding cassette transporters and drug resistance in breast cancer. Endocr Relat Cancer 2003;10(1):43-73.

333. Litman T, Druley TE, Stein WD, Bates SE. From MDR to MXR: new understanding of multidrug resistance systems, their properties and clinical significance. Cell Mol Life Sci 2001;58(7):931-59.

334. Persidis A. Cancer multidrug resistance. Nat Biotechnol 1999;17(1):94-5.

335. Varadi A, Szakacs G, Bakos E, Sarkadi B. P glycoprotein and the mechanism of multidrug resistance. Novartis Found Symp 2002;243:54-65.

336. Hayes JD, Pulford DJ. The glutathione S-transferase supergene family: regulation of GST and the contribution of the isoenzymes to cancer chemoprotection and drug resistance. Crit Rev Biochem Mol Biol 1995;30(6):445-600.

337. Townsend DM, Tew KD. The role of glutathione-S-transferase in anti-cancer drug resistance. Oncogene 2003;22(47):7369-75.

338. Dingemans AM, Pinedo HM, Giaccone G. Clinical resistance to topoisomerase-targeted drugs. Biochim Biophys Acta 1998;1400(1-3):275-88.

339. Drukman S, Kavallaris M. Microtubule alterations and resistance to tubulin-binding agents (review). Int J Oncol 2002;21(3):621-8.

340. Orr GA, Verdier-Pinard P, McDaid H, Horwitz SB. Mechanisms of Taxol resistance related to microtubules. Oncogene 2003;22(47):7280-95.

341. Rasheed ZA, Rubin EH. Mechanisms of resistance to topoisomerase I-targeting drugs. Oncogene 2003;22(47):7296-304.

342. Sangrajrang S, Fellous A. Taxol resistance. Chemotherapy 2000;46(5):327-34.

343. Hersey P, Zhang XD. Overcoming resistance of cancer cells to apoptosis. J Cell Physiol 2003;196(1):9-18.

344. Reed JC. Bcl-2: prevention of apoptosis as a mechanism of drug resistance. Hematol Oncol Clin North Am 1995;9(2):451-73.

345. Tolomeo M, Simoni D. Drug resistance and apoptosis in cancer treatment: development of new apoptosis-inducing agents active in drug resistant malignancies. Curr Med Chem Anticancer Agents 2002;2(3):387-401.

346. Nygren P, Larsson R. Overview of the clinical efficacy of investigational anticancer drugs. J Intern Med 2003;253(1):46-75.

347. Teicher BA, Herman TS, Holden SA, et al. Tumor resistance to alkylating agents conferred by mechanisms operative only *in vivo*. Science 1990;247(4949 Pt 1):1457-61.

348. Hoffman RM. Orthotopic metastatic mouse models for anticancer drug discovery and evaluation: a bridge to the clinic. Invest New Drugs 1999;17(4):343-59.

349. Dias S, Choy M, Alitalo K, Rafii S. Vascular endothelial growth factor (VEGF)-C signaling through FLT-4 (VEGFR-3) mediates leukemic cell proliferation, survival, and resistance to chemotherapy. Blood 2002;99(6):2179-84.

350. Lotem J, Sachs L. Hematopoietic cytokines inhibit apoptosis induced by transforming growth factor beta 1 and cancer chemotherapy compounds in myeloid leukemic cells. Blood 1992;80(7):1750-7.

351. Teicher BA, Ikebe M, Ara G, Keyes SR, Herbst RS. Transforming growth

factor-beta 1 overexpression produces drug resistance *in vivo*: reversal by decorin. In Vivo 1997;11(6):463-72.

352. Xu W, Liu L, Smith GC, Charles G. Nitric oxide upregulates expression of DNA-PKcs to protect cells from DNA-damaging anti-tumour agents. Nat Cell Biol 2000;2(6):339-45.

353. Hodge DR, Hurt EM, Farrar WL. The role of IL-6 and STAT3 in inflammation and cancer. Eur J Cancer 2005;41(16):2502-12.

354. Wei LH, Kuo ML, Chen CA, et al. The anti-apoptotic role of interleukin-6 in human cervical cancer is mediated by up-regulation of Mcl-1 through a PI 3-K/Akt pathway. Oncogene 2001;20(41):5799-809.

355. Chauhan D, Kharbanda S, Ogata A, et al. Interleukin-6 inhibits Fas-induced apoptosis and stress-activated protein kinase activation in multiple myeloma cells. Blood 1997;89(1):227-34.

356. Lichtenstein A, Tu Y, Fady C, Vescio R, Berenson J. Interleukin-6 inhibits apoptosis of malignant plasma cells. Cell Immunol 1995;162(2):248-55.

357. Nagata S, Golstein P. The Fas death factor. Science 1995;267(5203):1449-56.

358. Kawano M, Hirano T, Matsuda T, et al. Autocrine generation and requirement of BSF-2/IL-6 for human multiple myelomas. Nature 1988;332(6159):83-5.

359. Klein B, Zhang XG, Lu ZY, Bataille R. Interleukin-6 in human multiple myeloma. Blood 1995;85(4):863-72.

360. Hardin J, MacLeod S, Grigorieva I, et al. Interleukin-6 prevents dexamethasone-induced myeloma cell death. Blood 1994;84(9):3063-70.

361. Puthier D, Bataille R, Barille S, et al. Myeloma cell growth arrest, apoptosis, and interleukin-6 receptor modulation induced by EB1089, a vitamin D3 derivative, alone or in association with dexamethasone. Blood 1996;88(12):4659-66.

362. Shiao RT, Miglietta L, Khera SY, Wolfson A, Freter CE. Dexamethasone and suramin inhibit cell proliferation and interleukin-6-mediated immunoglobulin secretion in human lymphoid and multiple myeloma cell lines. Leuk Lymphoma 1995;17(5-6):485-94.

363. Murakami M, Hibi M, Nakagawa N, et al. IL-6-induced homodimerization of gp130 and associated activation of a tyrosine kinase. Science 1993;260(5115):1808-10.

364. Kishimoto T, Akira S, Narazaki M, Taga T. Interleukin-6 family of cytokines and gp130. Blood 1995;86(4):1243-54.

365. Lutticken C, Wegenka UM, Yuan J, et al. Association of transcription factor APRF and protein kinase Jak1 with the interleukin-6 signal transducer gp130. Science 1994;263(5143):89-92.

366. Darnell JE Jr, Kerr IM, Stark GR. Jak-STAT pathways and transcriptional activation in response to IFNs and other extracellular signaling proteins. Science 1994;264(5164):1415-21.

367. Ihle JN. STATs: signal transducers and activators of transcription. Cell 1996;84(3):331-4.

368. Tu Y, Renner S, Xu F, et al. BCL-X expression in multiple myeloma: possible indicator of chemoresistance. Cancer Res 1998;58(2):256-62.

369. Schwarze MM, Hawley RG. Prevention of myeloma cell apoptosis by ectopic bcl-2 expression or interleukin 6-mediated up-regulation of bcl-xL. Cancer Res 1995;55(11):2262-5.

370. Durand RE, Sutherland RM. Effects of intercellular contact on repair of radiation damage. Exp Cell Res 1972;71(1):75-80.

371. St Croix B, Florenes VA, Rak JW, et al. Impact of the cyclin-dependent kinase inhibitor p27Kip1 on resistance of tumor cells to anticancer agents. Nat Med 1996;2(11):1204-10.

372. Damiano JS. Integrins as novel drug targets for overcoming innate drug resistance. Curr Cancer Drug Targets 2002;2(1):37-43.

373. Damiano JS, Dalton WS. Integrin-mediated drug resistance in multiple myeloma. Leuk Lymphoma 2000;38(1-2):71-81.

374. Holt RU, Baykov V, Ro TB, et al. Human myeloma cells adhere to fibronectin in response to hepatocyte growth factor. Haematologica 2005;90(4):479-88.

375. Damiano JS, Hazlehurst LA, Dalton WS. Cell adhesion-mediated drug resistance (CAM-DR) protects the K562 chronic myelogenous leukemia cell line from apoptosis induced by BCR/ABL inhibition, cytotoxic drugs, and gamma-irradiation. Leukemia 2001;15(8):1232-9.

376. Hazlehurst LA, Valkov N, Wisner L, et al. Reduction in drug-induced DNA double-strand breaks associated with beta1 integrin-mediated adhesion correlates with drug resistance in U937 cells. Blood 2001;98(6):1897-903.

377. Sethi T, Rintoul RC, Moore SM, et al. Extracellular matrix proteins protect small cell lung cancer cells against apoptosis: a mechanism for small cell lung cancer growth and drug resistance *in vivo.* Nat Med 1999;5(6):662-8.

378. Weaver VM, Lelievre S, Lakins JN, et al. beta4 integrin-dependent formation of polarized three-dimensional architecture confers resistance to apoptosis in normal and malignant mammary epithelium. Cancer Cell 2002;2(3):205-16.

379. Wang CY, Mayo MW, Baldwin AS Jr. TNF- and cancer therapy-induced apoptosis: potentiation by inhibition of NF-kappaB. Science 1996;274(5288):784-7.

380. Landowski TH, Olashaw NE, Agrawal D, Dalton WS. Cell adhesion-mediated drug resistance (CAM-DR) is associated with activation of NF-kappa B (RelB/p50) in myeloma cells. Oncogene 2003;22(16):2417-21.

381. Tlsty TD. Cell-adhesion-dependent influences on genomic instability and carcinogenesis. Curr Opin Cell Biol 1998;10(5):647-53.

382. Hsieh CL, Chung LW. New prospectives of prostate cancer gene therapy: molecular targets and animal models. Crit Rev Eukaryot Gene Expr 2001;11(1-3):77-120.

383. Hsieh CL, Yang L, Miao L, et al. A novel targeting modality to enhance adenoviral replication by vitamin D(3) in androgen-independent human prostate cancer cells and tumors. Cancer Res 2002;62(11):3084-92.

384. Matsubara S, Wada Y, Gardner TA, et al. A conditional replication-competent adenoviral vector, Ad-OC-E1a, to cotarget prostate cancer and bone stroma in an experimental model of androgen-independent prostate cancer bone metastasis. Cancer Res 2001;61(16):6012-9.

385. Paget S. The distribution of secondary growths in cancer of the breast. 1889. Cancer Metastasis Rev 1889;8(2):98-101.

386. Solakoglu O, Maierhofer C, Lahr G, et al. Heterogeneous proliferative potential of occult metastatic cells in bone marrow of patients with solid epithelial tumors. Proc Natl Acad Sci U S A 2002;99(4):2246-51.